ISSN 0021-9673

VOL. 596 NO. 1 APRIL 3, 1992

JOURNAL OF CHROMATOGRAPHY

INCLUDING ELECTROPHORESIS AND OTHER SEPARATION METHODS

ELSEVIER

JOURNAL OF CHROMATOGRAPHY

INCLUDING ELECTROPHORESIS AND OTHER SEPARATION METHODS

Scope. The *Journal of Chromatography* publishes papers on all aspects of chromatography, electrophoresis and related methods. Contributions consist mainly of research papers dealing with chromatographic theory, instrumental development and their applications. The section *Biomedical Applications*, which is under separate editorship, deals with the following aspects: developments in and applications of chromatographic and electrophoretic techniques related to clinical diagnosis or alterations during medical treatment; screening and profiling of body fluids or tissues with special reference to metabolic disorders; results from basic medical research with direct consequences in clinical practice; drug level monitoring and pharmacokinetic studies; clinical toxicology; analytical studies in occupational medicine.

Submission of Papers. Manuscripts (in English; *four* copies are required) should be submitted to: Editorial Office of *Journal of Chromatography*, P.O. Box 681, 1000 AR Amsterdam, Netherlands, Telefax (+31-20) 5862 304, or to: The Editor of *Journal of Chromatography, Biomedical Applications*, P.O. Box 681, 1000 AR Amsterdam, Netherlands. Review articles are invited or proposed by letter to the Editors. An outline of the proposed review should first be forwarded to the Editors for preliminary discussion prior to preparation. Submission of an article is understood to imply that the article is original and unpublished and is not being considered for publication elsewhere. For copyright regulations, see below.

Publication. The *Journal of Chromatography* (incl. *Biomedical Applications*) has 39 volumes in 1992. The subscription prices for 1992 are:

J. Chromatogr. (incl. *Cum. Indexes, Vols. 551–600*) + *Biomed. Appl.* (Vols. 573–611):
Dfl. 7722.00 plus Dfl. 1209.00 (p.p.h.) (total *ca.* US$ 4880.25)

J. Chromatogr. (incl. *Cum. Indexes, Vols. 551–600*) only (Vols. 585–611):
Dfl. 6210.00 plus Dfl. 837.00 (p.p.h.) (total *ca.* US$ 3850.75)

Biomed. Appl. only (Vols. 573–584):
Dfl. 2760.00 plus Dfl. 372.00 (p.p.h.) (total *ca.* US$ 1711.50).

Subscription Orders. The Dutch guilder price is definitive. The US$ price is subject to exchange-rate fluctuations and is given as a guide. Subscriptions are accepted on a prepaid basis only, unless different terms have been previously agreed upon. Subscriptions orders can be entered only by calender year (Jan.–Dec.) and should be sent to Elsevier Science Publishers, Journal Department, P.O. Box 211, 1000 AE Amsterdam, Netherlands, Tel. (+31-20) 5803 642, Telefax (+31-20) 5803 598, or to your usual subscription agent. Postage and handling charges include surface delivery except to the following countries where air delivery via SAL (Surface Air Lift) mail is ensured: Argentina, Australia, Brazil, Canada, China, Hong Kong, India, Israel, Japan*, Malaysia, Mexico, New Zealand, Pakistan, Singapore, South Africa, South Korea, Taiwan, Thailand, USA. *For Japan air delivery (SAL) requires 25% additional charge of the normal postage and handling charge. For all other countries airmail rates are available upon request. Claims for missing issues must be made within three months of our publication (mailing) date, otherwise such claims cannot be honoured free of charge. Back volumes of the *Journal of Chromatography* (Vols. 1–572) are available at Dfl. 217.00 (plus postage). Customers in the USA and Canada wishing information on this and other Elsevier journals, please contact Journal Information Center, Elsevier Science Publishing Co. Inc., 655 Avenue of the Americas, New York, NY 10010, USA, Tel. (+1-212) 633 3750, Telefax (+1-212) 633 3990.

Abstracts/Contents Lists published in Analytical Abstracts, Biochemical Abstracts, Biological Abstracts, Chemical Abstracts, Chemical Titles, Chromatography Abstracts, Clinical Chemistry Lookout, Current Contents/Life Sciences, Current Contents/Physical, Chemical & Earth Sciences, Deep-Sea Research/Part B: Oceanographic Literature Review, Excerpta Medica, Index Medicus, Mass Spectrometry Bulletin, PASCAL-CNRS, Pharmaceutical Abstracts, Referativnyi Zhurnal, Research Alert, Science Citation Index and Trends in Biotechnology.

See inside back cover for Publication Schedule, Information for Authors and information on Advertisements.

0021-9673/92/$05.00

Printed in the Netherlands

CONTENTS

(Abstracts/Contents Lists published in Analytical Abstracts, Biochemical Abstracts, Biological Abstracts, Chemical Abstracts, Chemical Titles, Chromatography Abstracts, Current Contents/Life Sciences, Current Contents/Physical, Chemical & Earth Sciences, Deep-Sea Research/Part B: Oceanographic Literature Review, Excerpta Medica, Index Medicus, Mass Spectrometry Bulletin, PASCAL-CRNS, Referativnyi Zhurnal, Research Alert and Science Citation Index)

REGULAR PAPERS

General

Column Liquid Chromatography

Gas Chromatography

Planar Chromatography

(Continued overleaf)

Contents (continued)

In articles with more than one author, the name of the author to whom correspondence should be addressed is indicated in the article heading by a 6-pointed asterisk (*).

Discover new solutions to your analysis problems

Capillary Electrophoresis

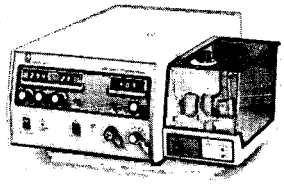

CE is a powerful new tool for separation and analysis of proteins, peptides, organic acids, nucleotides, and other sample mixtures. Isco's two CE systems give you femtomole detection sensitivity with nanoliter samples. One system is automated with computer data management; the other is a compact, affordable "personal CE".

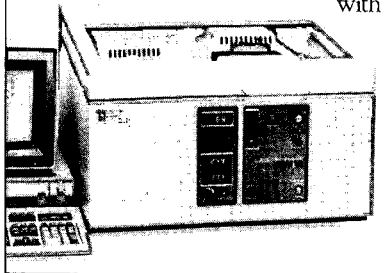

SFC

Add a supercritical fluid "front end" to your GC for greatly improved separations of waxes, tars, and other difficult polymer mixtures. Or get a complete Isco packed-column SFC system with UV-vis detection. Our modular approach makes it easy and affordable to get the SFC capabilities you need.

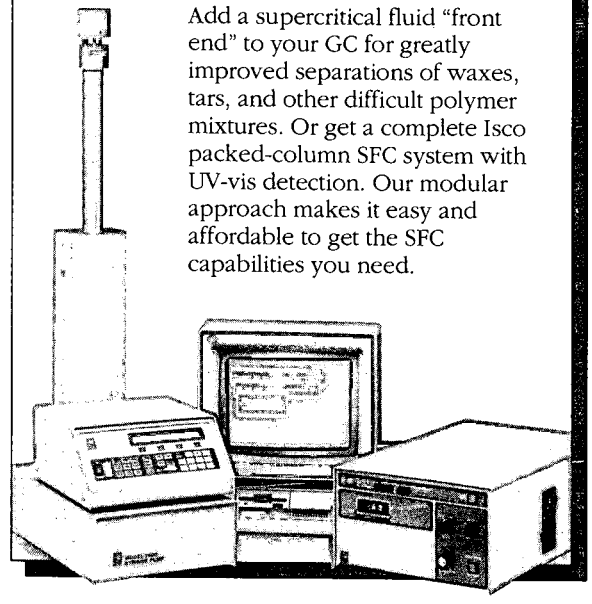

Microbore HPLC

If a tiny sample is all you have, microbore HPLC is what you need. Unique Isco systems are ideal for scarce and precious samples. They offer simple, direct interfacing to FAB-MS, and many-fold improvement in mass sensitivity and resolution. Pulseless syringe pumps include built-in gradient programming.

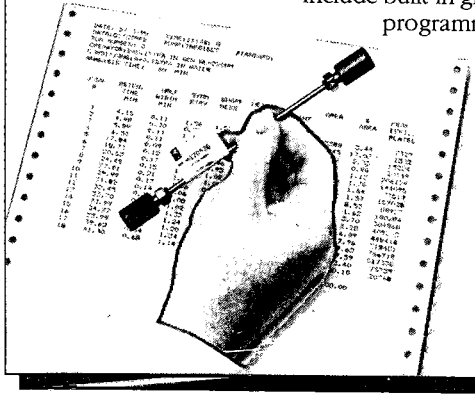

Low-pressure prep LC

Compact LC systems give you big capacity and features in a small bench space. Fractionate your proteins by time, drop count, or peak shape. Solve difficult separation problems with optional gradient programming. Scale up easily to liter/min flow rates. And forget about lost samples and coldroom troubles.

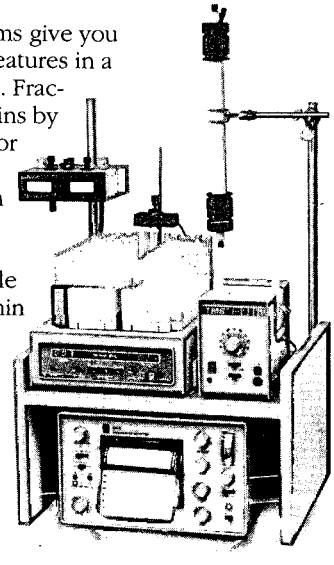

Call toll-free today for your copy of our big, 120-page catalog.

Isco, Inc., P.O. Box 5347
Lincoln NE 68505 U.S.A.
Tel. **(800)228-4250**

Isco Europe AG, Brüschstr. 17
CH8708 Männedorf, Switzerland
Fax **(41-1)920 62 08**

ISCO

Distributors • **Australia:** Australian Chromatography Co. • **Austria:** INULA • **Belgium:** N.V. Mettler-Toledo S.A. • **Canada:** Canberra-Packard Canada, Ltd. • **Denmark:** Mikrolab Aarhus • **Finland:** ETEK OY • **France:** Ets. Roucaire, S.A. • **Germany:** Colora Messtechnik GmbH • **Italy:** Analytical Control Italia s.p.a. • **Japan:** JSI Co. Ltd. • **Korea:** Sang Chung, Ltd. • **The Netherlands:** Beun-de Ronde B.V. • **Norway:** Dipl. Ing. Houm a.s. • **Spain:** VARIAN-CHEMICONTROL, S.L. • **Sweden:** SpectroChrom AB • **Switzerland:** IG Instrumenten-Gesellschaft AG • **U.K.:** Jones Chromatography Ltd. •

Physical Sciences Data Volume 2

Statistical Treatment of Experimental Data

by **J.R. Green** *and* **D. Margerison**

This book is primarily intended for researchers wishing to analyse experimental data using statistical methods. Statistical concepts and methods which may be employed to treat experimental data are explained, and the ideas and reasoning behind statistical methodology are clarified. Formal results are illustrated by many numerical worked examples mainly taken from the laboratory. Concepts, practical methodology, and worked examples are integrated in the text.

Consideration is given in this work to a large number of practical topics which are often omitted from standard texts. These include; obtaining an approximate confidence interval for a function of some unknown parameters; testing for outliers, stabilization of heterogeneous variances, and significant differences between means; estimation of parameters after performing tests; deciding what numbers of significant figures to quote for sample means and variances; straight-line and polynomial regression, through the origin or not, using weighted points, and testing the homogeneity of a set of such lines or curves. The numerous examples which are provided throughout the text will serve as models for the various problems encountered by the readers when employing statistical methods to treat experimental data. Neither a strong mathematical background nor a prior knowledge of probability or statistics is required in order to make use of this work. In addition to research workers in universities and industry, the book will be of use for first-year students of statistics, and would be expecially suitable as the basis of a graduate course in experimental sciences.

Contents:

1977 5th imp. 1988 x + 382 pages
Price: US $ 96.00 / Dfl. 168.00
ISBN 0-444-41725-7

Elsevier Science Publishers

P.O. Box 211, 1000 AE Amsterdam, The Netherlands
P.O. Box 882, Madison Square Station, New York, NY 10159, USA

JOURNAL OF CHROMATOGRAPHY

VOL. 596 (1992)

JOURNAL of CHROMATOGRAPHY

INCLUDING ELECTROPHORESIS AND OTHER SEPARATION METHODS

ELSEVIER

AMSTERDAM — LONDON — NEW YORK — TOKYO

0021-9673/92/$05.00

Printed in the Netherlands

Journal of Chromatography, 596 (1992) 1–13
Elsevier Science Publishers B.V., Amsterdam

CHROM. 23 977

Variance of a zone migrating in a non-uniform time-invariant linear medium

Leonid M. Blumberg* and Terry A. Berger

Hewlett-Packard Co., P.O. Box 900, Avondale, PA 19311-0900 (USA)

(First received May 13th, 1991; revised manuscript received December 29th, 1991)

ABSTRACT

A general model describing the evolution (expansion and contraction) of a zone migrating in a non-uniform (coordinate-dependent) chromatographic medium was developed. Equations for the spatial and temporal rates of change of variance of a zone were derived starting from the basic principle of mass balance in convective diffusion in a one-dimensional non-uniform medium. Also, the distinction between local and average values of many important quantities describing the evolution of a zone in a non-uniform medium such as velocity of a zone, plate height, chromatographic efficiency and was re-examined. It was shown that under certain conditions covering all practically important cases the chromatographic efficiency of a non-uniform medium cannot exceed that of a corresponding uniform medium. The study also produced unexpected results. It became apparent that a gradient of diffusivity affected the velocity of migration of an analyte in a column, and part of dispersion-related zone broadening could be recovered. It also became apparent that previous approaches for dealing with non-uniformity depended on unknown implicit conditions. Typically, these conditions were not satisfied in the cases considered. For example, many classical results deemed to be exact values must be viewed only as approximations. Hence, the known pressure correction factor for plate height in capillary gas chromatography with ideal gases is only an approximation to a still unknown correct value.

INTRODUCTION

Existing chromatographic theory has done an admirable job in predicting the performance of capillary columns under uniform and near uniform conditions. However, situations in which chromatographic conditions are not uniform throughout the column have been only partially addressed [*e.g.*, the effect of large pressure drops in gas chromatography (GC) with ideal carrier gases has been explained]. The general approach has been to develop theory for uniform conditions, then apply correction factors to account for non-uniformity. Such an approach is inherently limited to relatively small deviations from non-uniformity. In this paper, a general expression is developed which directly describes zone broadening under time-invariant, non-uniform conditions (zones traversing standing gradients). The intent is to lay a foundation for further work in which the effects of simultaneous time-variant and spatially non-uniform conditions on peak shape can be described.

Physical conditions often change from the inlet to the outlet of the column. A typical example of such a non-uniform (coordinate-dependent) chromatographic medium is the change in density of the carrier gas in GC caused by the pressure drop from the inlet to the outlet. With small-diameter capillary columns, the column inlet pressure can be many times the column outlet pressure. This pressure drop has an impact on chromatographic performance in terms of both speed and efficiency.

Non-uniformity of other conditions along the column can also affect chromatographic performance. Variations in column cross-sectional area, stationary phase film thickness and composition, mobile phase composition, etc., are further examples in GC. Other techniques such as liquid (LC) and supercritical fluid chromatography (SFC) and others are also affected by non-uniform conditions.

0021-9673/92/$05.00

Thus, non-uniform conditions are widely encountered in chromatography.

Analysis of a non-uniform chromatographic medium becomes significantly more complex when non-uniformity of a medium is combined with a sample overloading, a cause of non-linear effects, and/or with time variance of a medium such as in the case of temperature programming in GC or programming of solvent composition in LC and SFC. The scope of this paper is limited to analysis of a linear time-invariant (constant in time) medium.

In analytical chromatography, whenever possible, non-linearity is avoided by measures such as injection of a substantially small amount of a sample. Time variance, on the other hand, is an important component of many analytical techniques. The theory of non-uniformity combined with time variance is a subject of the next paper in this series.

The most widely used approach to the theoretical analysis of chromatography in a non-uniform time-invariant linear medium was outlined by Golay [1] in 1958. Specific results accounting for the compressibility of an ideal carrier gas in GC were published by Giddings and co-workers [2,3] in 1959–60. A more general treatment published by Giddings a few years later [4–6] is widely considered as the basis for the analysis of all types of non-uniformity in a chromatographic medium.

Unfortunately, these known theories have shortcomings. As the starting point, results are derived for a uniform medium, and corrections are applied to accommodate non-uniformity in further derivations. Hence the derivations rely on the implicit assumption of uniformity of chromatographic conditions within a zone of a migrating analyte.

For example, Golay suggested that non-uniformity should be treated in the following way. He wrote (ref. 1, p. 43) that the conclusions in that reference[a] "are applicable to columns of uniform cross-sections in which the input to exit pressure ratio is near unity. When there is a succession of varying cross-sections ..., we should *replace* the second moment [of density] u by the volumetric second moment U, the incremental value of which is: $dU = S^2 du$, where S represents the cross-section area of the column *at the point considered*". In a similar manner, Golay considers corrections for pressure drop and for combination of both types of non-uniformity. Substantial in that discussion are two factors: (a) the starting point of du (incremental variance of the zone) which was previously derived for *uniform* conditions, and (b) the correction by multiplying du by quantities such as S^2 *at the point considered.* If conditions within a zone of a non-zero width are substantially non-uniform it becomes unclear which is "*the point considered*", and the correction of an incremental variance by a single parameter (in this case S) becomes generally inappropriate.

Similarly, analysis developed by Giddings [5] starts by dividing a column into equal small segments. It was then assumed that the local conditions within each segment *approach uniformity*, and are represented with *any required precision* when the number of segments becomes sufficiently large. This is a common mathematical technique. However, in derivations for non-uniform chromatography, the size of a segment could not be meaningfully reduced below the width of a zone of analyte in the vicinity of a given location. Therefore, the logic fails if conditions remain substantially non-uniform *within* the zone. Therefore, for such derivations, the requirement of uniformity of conditions within a zone of a non-zero width is implicitly a *de facto* limitation even if not explicitly stated. Obviously, if time-invariant conditions are uniform within a zone at any position in a column, the entire column must be uniform, and analysis of non-uniformity becomes irrelevant. The analysis can and must be expected to yield practically accurate and reliable predictions if conditions within a zone are *almost* uniform. It must be recognized, however, that the predictions based on such an assumption are approximate.

For example, utilizing the aforementioned methodology, Stewart *et al.* [2] in 1959 and Golay [7] in 1963 arrived at the same value for what is now well known as Giddings' correction factor for the plate height in a compressible ideal carrier gas in GC [2]. Although in GC conditions as functions of coordinates typically do not change rapidly, nevertheless, they are not constant within the zone [1]. Therefore, it must be recognized that even in an ideal case, Giddings' correction factor is only an approximation to the still unknown correct value.

[a] All notations in this paragraph are the same as in the source [1] and are limited to this paragraph only.

Further, when a theory is based on the assumption of near uniformity of chromatographic conditions within a zone while actual conditions are substantially non-uniform, as can be the case in SFC [8], predictions of the theory become unreliable.

Hence non-uniform conditions are only superficially dealt with in chromatographic theory.

The purpose of this paper was to develop a general theory of chromatography in a non-uniform time-invariant linear medium. The topic of the paper was a study of evolution of variance of a zone of analyte migrating in the medium.

The model

It is important to base a general study of the process of a chromatographic separation in a non-uniform medium on a model which reduces all specifics of the process to a minimum set of independent factors.

Giddings [6] treated the process of a velocity-based chromatographic separation in a uniform column as a one-dimensional phenomenon described by the mass-balance equation of convective diffusion [6,9]:

$$\frac{\partial m}{\partial t} = D \cdot \frac{\partial^2 m}{\partial x^2} - v \cdot \frac{\partial m}{\partial x} \tag{1}$$

where all quantities m, D and v are cross-sectional averages, m is the amount of analyte per unit of column length, which will be referred to as the specific mass of analyte, D is the effective diffusivity (in brief, diffusivity) of analyte in the column, representing the cross-sectional average of all factors causing dispersion [10] of a zone, such as molecular diffusivity in the mobile phase and resistance to mass transfer, and v is the velocity of migration of analyte which could be described through a cross-sectional averaged velocity of the mobile phase, v_m, and a capacity factor of the analyte, k, as

$$v = v_m/(1 + k) \tag{2}$$

A chromatographic theory based on a mass-balance equation such as eqn. 1 provides a high level of generality, as it allows reduction of all the specifics of a chromatographic process (such as the thermodynamics of all internal interactions in a medium and statistics of migration of a sample [6,11,12] affected by such interactions) to only two parameters: the dispersivity and the velocity of migration of the sample in the medium.

Eqn. 1 and similar equations [13] are widely used for studies of chromatography in uniform media. In a non-uniform medium, both the velocity of the analyte and its dispersion at each specific location are functions of the coordinate of the location. Unfortunately, to adapt eqn. 1 and similar equations to a non-uniform medium, it is not enough simply to assume that both parameters, D and v, are functions of x. With that assumption, eqn. 1 is *not mass conservative*, *i.e.*, it does not represent the balance of mass in a non-uniform medium.

A more general equation of convective diffusion in a one-dimensional medium is

$$\frac{\partial m}{\partial t} = \frac{\partial}{\partial x}\left(D \cdot \frac{\partial m}{\partial x}\right) - \frac{\partial}{\partial x}(vm) \tag{3}$$

This equation is *mass conservative* even when D and v are functions of x and t (see Appendix). Eqn. 3 represents a one-dimensional version of a more general mass-conservative three-dimensional convective diffusion equation [9]:

$$\frac{\partial \rho}{\partial t} = \text{div}\,(D_m \,\text{grad}\,\rho) - \text{div}\,(\rho \mathbf{v}) \tag{4}$$

where ρ is the density of the migrating entity, D_m is its molecular diffusivity and $\mathbf{v}$ is a vector of velocity in the medium.

In eqn. 3, all coordinate-dependent properties of a non-uniform medium such as a variation in column diameter, thickness and composition of stationary phase are represented by the two functions of the coordinate, D and v. Obviously, when a medium is uniform, *i.e.*, $\partial D/\partial x = \partial v/\partial x = 0$ for any x, eqn. 3 could be rewritten as eqn. 1.

In this paper, eqn. 3 is the basic model for chromatography in a non-uniform medium.

Limitations within the model

The assumptions limiting the scope of the model in this paper can be summarized as follows.

C1. The medium is time invariant and linear, *i.e.*, the quantities $D = D(x)$ and $v = v(x)$ depend only on x.

Assumption of linearity (no dependence of D and v on m) allows one, among other simplifications, to

deal individually with each component of a complex mixture. Thus, only migration of a single-component analyte is studied. The assumption of time invariance (no dependence of D and v on t) avoids complications caused by interaction of variation of chromatographic conditions in space with their variation in time.

It is also assumed that the quantities D and v are finite within any bounded interval of the x-axis, and D is not negative. Further, derivatives $\partial v/\partial x$ and $\partial D/\partial x$ are limited when x approaches infinity. More accurately:

C2. $0 \leqslant D < \infty$ and $|v| < \infty$ when $|x| < \infty$;
$|\partial v/\partial x| < \infty$ and $|\partial D/\partial x| < \infty$ when $x \to \pm\infty$.

As for a zone of analyte, it is assumed that its second moment is always limited (limited width of the zone). That, together with the recognition of the fact that the specific mass, $m = m(x,t)$, of the zone is a non-negative function, could be formally expressed as:

$$\text{C3.} \quad \left| \int_{-\infty}^{\infty} x^2 m \mathrm{d}x \right| < \infty; \quad m \geqslant 0 \tag{5}$$

It is apparent that only condition C1 provides a significant limitation to the scope of the theory. The other two sets of conditions, C2 and C3, are almost unrestrictive.

The last two conditions could be combined for further use as follows. Inequalities 5 imply:

$$x^3 m \to 0 \text{ and } x^4 \cdot \frac{\partial m}{\partial x} \to 0 \text{ when } x \to \pm\infty \tag{6}$$

Combination of these relationships and conditions C2 provides

$$xDm \to 0,\ x^2 vm \to 0,\ x^2 D \cdot \frac{\partial m}{\partial x} \to 0 \text{ and } x^2 m \cdot \frac{\partial D}{\partial x} \to 0 \text{ when } x \to \pm\infty \tag{7}$$

Moments and other relevant relationships

As stated earlier, the purpose of this paper was to account for variations in D and v down the column, in calculations of the variance,

$$\sigma^2 = \int_{-\infty}^{\infty} (x - z)^2 m \mathrm{d}x \tag{8}$$

of specific mass in a zone, the second central moment of m. The variance is mathematically the most convenient representation of the width of a zone.

In eqn. 8, the quantity

$$z = \int_{-\infty}^{\infty} x m \mathrm{d}x \tag{9}$$

is the first moment of m which represents a coordinate of the center of mass of the zone. Both eqns. 8 and 9 assume that m is normalized so that the zone has a unity mass, *i.e.*,

$$\int_{-\infty}^{\infty} m \mathrm{d}x = 1 \tag{10}$$

Such normalization is possible owing to the mass-conservative nature of the model. It is also useful to note that eqn. 9 implies

$$\int_{-\infty}^{\infty} (x - z) m \mathrm{d}x = 0 \tag{11}$$

Several other relationships from the theory of chromatography in a uniform medium are relevant to further discussions.

Giddings [6] has shown that the diffusivity, D, in eqn. 1 could be expressed via the column plate height, H, as

$$D = Hv/2 \tag{12}$$

Relationships between a column plate height and other column parameters are known from the literature [1,6,14,15].

From another perspective, Golay's [1] expressions

$$\mathrm{d}\sigma^2/\mathrm{d}x = H \tag{13}$$

and

$$\mathrm{d}\sigma^2/\mathrm{d}t = Hv \tag{14}$$

allow interpretation of H in eqn. 13 as a spatial rate of dispersion of a zone while the quantity Hv in eqn. 14 and, therefore, the diffusivity, D, in eqn. 12 could be interpreted as a representative of the zone's temporal dispersion rate.

It is also interesting that eqn. 14 is a generalization of Einstein's [16,17] expression $\sigma^2 = 2Dt$ for Brownian motion in a stationary ($v = 0$) medium. In the differential form, the latter can be rewritten as

$$\mathrm{d}\sigma^2/\mathrm{d}t = 2D \tag{15}$$

which, together with eqn. 14, serves as another justification for eqn. 12.

Expressions 13–15 represent spatial and temporal rates of growth of σ^2 in uniform media. Similar equations for the evolution of σ^2 in a non-uniform medium are derived from eqn. 3 in the next section.

THEORY

Aggregate velocity of migration of a zone

As mentioned earlier, the subject of this paper is the derivation of the spatial and temporal rates of change of σ^2 in a non-uniform medium.

If the location of a zone in space is represented by its center of mass, z, then the spatial rate of changes of σ^2 is $d\sigma^2/dz$ and the temporal rate is $d\sigma^2/dt$. The two relate as

$$\frac{d\sigma^2}{dz} = \frac{dt}{dz} \cdot \frac{d\sigma^2}{dt} = \frac{1}{u_a} \cdot \frac{d\sigma^2}{dt} \tag{16}$$

where

$$u_a = dz/dt \tag{17}$$

is a temporal rate of displacement of the center of mass of the zone. This quantity can be viewed as an aggregate velocity of migration of the entire zone. In a non-uniform medium, u_a could be different from local velocities of elements of the zone.

It can be shown (see Appendix) that

$$u_a = \int_{-\infty}^{\infty} \left(v + \frac{\partial D}{\partial x}\right) m dx = \int_{-\infty}^{\infty} um dx \tag{18}$$

where

$$u = u(x) = v + \frac{\partial D}{\partial x} \tag{19}$$

The integral on the right-hand side of eqn. 18 represents the momentum of a zone and indicates that it is the quantity u (not v) which represents the net local velocity of migration of analyte in the medium. According to eqn. 19, the net velocity, u, consists of two components. Component $\partial D/\partial x$ represents the migration velocity caused by a gradient of diffusivity and exists *only* in a non-uniform medium. The other component, v, is the convective velocity of the analyte defined for a uniform medium as in eqn. 2 [1,6]. In a non-uniform medium, both v_m and k in eqn. 2 defining v could be functions of x, *i.e.*, $v_m = v_m(x)$, $k = k(x)$.

Rearranged equation of convective diffusion

Using the notation in eqn. 19, eqn. 3 can be rewritten (see Appendix) in the form

$$\frac{\partial m}{\partial t} = \frac{\partial^2}{\partial x^2}(Dm) - \frac{\partial}{\partial x}(um) \tag{20}$$

which is more convenient for analysis of evolution of variance of a zone (see below). Eqn. 20 is similar to what is known in physics as the Fokker–Planck equation [18]. Further developments are based on eqn. 20.

Evolution of variance of a zone

The temporal rate of change of variance of a zone, $d\sigma^2/dt$, could be expressed (see Appendix) as

$$\frac{d\sigma^2}{dt} = 2\int_{-\infty}^{\infty} Dm dx + 2\int_{-\infty}^{\infty} (x - z)um dx \tag{21}$$

and can be viewed as a generalization of Einstein's eqn. 15 applied to a convective dispersion in a one-dimensional non-uniform medium. Substitution of eqn. 21 in eqn. 16 yields an expression for the spatial rate of change of σ^2:

$$\frac{d\sigma^2}{dz} = \frac{2}{u_a}\int_{-\infty}^{\infty} Dm dx + \frac{2}{u_a}\int_{-\infty}^{\infty} (x - z)um dx \tag{22}$$

which can be further rewritten as

$$\frac{d\sigma^2}{dz} = \frac{1}{u_a}\int_{-\infty}^{\infty} Hum dx + \frac{2}{u_a}\int_{-\infty}^{\infty} (x - z)um dx \tag{23}$$

where similarly to eqn. 12,

$$H = H(x) = 2D/u \tag{24}$$

Eqn. 23 can be viewed as a generalization of Golay's eqn. 13 for non-uniform media with the quantity H playing the role of the local plate height. Further discussion of this topic is postponed until the next section.

Typically in chromatography, the column length rather than the retention time of an analyte is known *a priori*. This makes the spatial rate, $d\sigma^2/dz$, more convenient than the temporal rate, $d\sigma^2/dt$, for calculation of the variance of a zone at the column outlet. Therefore, greater attention in further developments is given to the former.

Approximation of the spatial rate of zone variance

Eqns. 21–23 describe the evolution of variance of

a zone migrating in a one-dimensional linear time-invariant non-uniform medium under practically unrestrictive conditions (C2 and C3). The condition s allow even for a random non-uniformity where the velocity, u, and diffusivity, D, of the analyte can change so rapidly that the gradients, $\partial v/\partial x$ and $\partial D/\partial x$, can change signs several times within the zone.

Chromatographically, this might include variations in conditions such as a completely random variation in the column inside diameter, stationary phase film thickness or particle size of a packing material in a column.

Typically in chromatography, zones of analytes are so narrow relative to the column length that

C4. gradients, $\partial v/\partial x$ and $\partial D/\partial x$, are nearly constant within a zone.

It is important to emphasize that these conditions require no limit on the degree of change of u or D within the zone, or along the entire column. The conditions only limit the degree of the change of gradients of those quantities within the zone. However, even the gradients are allowed to have large changes along the entire column. Examples include locally nearly constant density gradients in GC and SFC.

Except for special cases, eqns. 21–23 are difficult to solve. However, under condition C4, they could be replaced by simplified approximations. Thus, if condition C4 is valid with a required precision, eqn. 23 can be reduced to the ordinary differential equation (see Appendix) for $\sigma^2 = \sigma^2(z)$:

$$(\sigma^2)' = H + 2\sigma^2 \cdot \frac{u'}{u} \text{ or } (\sigma^2)' = H + \sigma^2 \cdot \frac{(u^2)'}{u^2} \quad (25)$$

where the prime serves as an abbreviation for a derivative by z. Obviously, for media with a uniform velocity ($u' = 0$), this equation becomes Golay's eqn. 13.

To solve eqn. 25, one may introduce a quantity

$$\tau^2 = \sigma^2/u^2 \quad (26)$$

which represents a measure of variance of a zone in time units. Eqn. 25 could be rearranged as

$$(\tau^2)' = (\sigma^2/u^2)' = H/u^2 \quad (27)$$

and

$$\tau^2 = \frac{\sigma^2}{u^2} = \frac{\sigma^2(0)}{u^2(0)} + \int_0^z \frac{H}{u^2} \cdot dx \quad (28)$$

where $\sigma^2(0)$ and $u^2(0)$ are, respectively, the variance and the velocity of the zone at the beginning of its path (column inlet).

If $\sigma^2(0) = 0$, then

$$\tau^2 = \int_0^z \frac{H}{u^2} \cdot dx \quad \text{and} \quad \sigma^2 = u^2 \int_0^z \frac{H}{u^2} \cdot dx \quad (29)$$

Further, under typical chromatographic conditions,

C5. $\left|\frac{\partial D}{\partial x}\right| \ll |v|$

In that case, owing to eqn. 19, eqns. 27 and 29 could be reduced respectively to

$$(\tau^2)' = (\sigma^2/v^2)' = H/v^2 \quad (30)$$

and

$$\tau^2 = \int_0^z \frac{H}{v^2} \cdot dx \quad \text{and} \quad \sigma^2 = v^2 \int_0^z \frac{H}{v^2} \cdot dx \quad (31)$$

Eqn. 30 reflects Golay's [1] approach to accounting for non-uniformity in a medium. Also, eqns. 30 and 31 reflect Giddings' idea [4,6] of additivity of local $d\tau^2$ values in their contribution to the total τ^2 value of a zone of analyte at any location along its path. This discussion continues in the next section.

Finally, for a uniform medium, the latter expressions yield

$$\sigma^2 = Hz \quad (32)$$

which, after substitution of eqn. 24 and $z = ut$, takes the form of Einstein's relationship $\sigma^2 = 2Dt$.

DISCUSSION

Local and aggregate plate height and diffusivity

Earlier, a quantity H (eqn. 24) was introduced. Comparison of eqn. 24 with Giddings' eqn. 12 shows that in uniform media, the quantity H in eqn. 24 defines a chromatographic plate height. A similar conclusion follows from comparison of eqns. 14 and 15.

To interpret the quantity H in a non-uniform medium, consider eqn. 23 and an extremely narrow zone with a center of mass z. When the variance of the zone approaches zero, its specific mass, m, as a

function of x approaches Dirac's delta-function $\delta(x - z)$. The latter conclusion comes from an examination of eqn. 8. When m converges to the delta-function, the first term in eqn. 23 converges to H and the second term vanishes. Thus, the entire expression converges to $d\sigma^2/dz = H(z)$, which is similar to Golay's eqn. 13 and indicates that in a non-uniform medium, the quantity H is a local plate height. A similar conclusion could be derived from assuming $\sigma^2 = 0$ in eqn. 25.

The concept of a local plate height helps in further interpretation of the first term on the right-hand side of eqn. 23. Note first that the quantity

$$f_u = f_u(x,t) = um \tag{33}$$

represents a local mass flow (in brief, a flow) due to migration of analyte[a]. The zeroth moment, M_0, of f_u is the same as an aggregate velocity of the zone. Indeed, from eqns. 33 and 18:

$$M_0 = \int_{-\infty}^{\infty} f_u dx = \int_{-\infty}^{\infty} um dx = u_a \tag{34}$$

Eqns. 33 and 34 allow the first term on the right-hand side of eqn. 23 to be rewritten as

$$H_a = H_a(z) = \frac{1}{u_a} \int_{-\infty}^{\infty} Hum dx = \frac{1}{M_0} \int_{-\infty}^{\infty} Hf_u dx \tag{35}$$

indicating that H_a is a flow-weighted average plate height, and could be referred to as an aggregate plate height of the zone. Unlike a local plate height, the aggregate plate height is no longer a property of the medium alone, but also depends on spatial distribution of the flow of analyte. Of course, if the plate height is uniform (H is constant), eqn. 35 becomes $H_a = H$. In other words, if the local plate height in a medium is uniform, its aggregate plate height is everywhere the same as the local plate height.

The first term on the right-hand side of eqn. 21 could be interpreted in a similar manner. Indeed, a quantity

$$D_a = D_a(z) = \int_{-\infty}^{\infty} Dm dx \tag{36}$$

could be introduced which is a specific-mass-weighted average of the diffusivity, and can be referred to as an aggregate diffusivity of a zone (a combined property of a medium and a zone).

Comparison of the first terms on the right-hand side of eqns. 22 and 23 with notations 35 and 36 suggests that

$$H_a = 2D_a/u_a \tag{37}$$

a relationship similar to that in eqn. 24 for local quantities.

Further, in a uniform chromatographic medium, a plate height is a spatial rate of growth of variance of a zone (eqn. 13) while the quantity $2D$ can be interpreted as a temporal rate of growth of variance of the zone (eqn. 15). In a non-uniform medium, the analogy remains. A local plate height and a local diffusivity represent, respectively, a local spatial rate and half of a local temporal rate of growth of variance of a zone. Similarly, an aggregate plate height and an aggregate diffusivity represent, respectively, an aggregate spatial rate and half of an aggregate temporal rate of growth of variance of a zone.

In spite of many similarities between the aggregate plate height and diffusivity, there is an important difference. A specific mass, m, and a migration flow, f_u, of an analyte could be viewed as static and dynamic distributions of a zone, respectively. Therefore, an aggregate diffusivity, being a specific-mass-weighted average (eqn. 36), can be viewed as a static average of a local diffusivity. The aggregate plate height, on the other hand, is a flow-weighted average (eqn. 35), and can be viewed as a dynamic average of local plate height.

This discussion could be summarized as follows. It is an accepted practice in the chromatographic literature to view a zone migrating in a non-uniform medium as a lump entity subjected to dispersion with a single spatial dispersion rate equal to a local plate height, H, at the center of mass of the zone. This is a convenient logical concept. However, as the previous discussion suggests, that single spatial dispersion rate is an aggregate plate height, H_a, which is also a function of the coordinate of the center of mass of the zone but might be different from the local plate height there. Similar conclusions are valid for local and aggregate diffusivities in a non-uniform medium.

[a] This does not include a component, $-\partial/\partial x\,(Dm)$, of a local mass flow due to the zone dispersion in the medium.

Gradient of diffusivity

All the results discussed so far were derived from eqn. 20, which along with notation 19 indicates that the gradient, $\partial D/\partial x$, of the diffusivity behaves as a component of velocity of an analyte. This was not previously known in the chromatographic literature.

The appearance of the quantity $\partial D/\partial x$ as a part of velocity indicates that a positive $\partial D/\partial x$ increases and a negative $\partial D/\partial x$ reduces the velocity of analyte.

Recognition of the fact that the gradient of diffusivity behaves as a component of velocity helped significantly in deriving eqns. 21–23 and in understanding the mechanisms of evolution of a zone in a non-uniform medium.

Comparison with known results

As was mentioned earlier, eqn. 30 reflects Golay's [1] approach to accounting for non-uniformity in a medium. Golay recommended a similar approach as a corrective measure against such sources of non-uniformity as pressure drop in GC with an ideal carrier gas, non-uniformity of column diameter and combinations of both. Here, eqn. 30 has been derived for a combination of any non-uniformities.

It was also mentioned before that eqns. 30 and 31 reflect Giddings' heuristic assumption [4,6] of additivity of local $d\tau^2$ values in their contribution to the total τ^2 value of a zone of analyte at any location along its path.

It must be noted, however, that the treatment of non-uniformity in the aforementioned references relies on the implicit assumption that all chromatographic conditions within the zone are nearly uniform. A more detailed discussion was presented in the Introduction.

Here, eqns. 21–23 for evolution of variance of a zone have been derived under no limits to non-uniformity in a medium.

A simplified version (eqn. 25) and its modifications (eqns. 27, 28 and 29) do impose some limits to non-uniformity, namely both gradients, $\partial v/\partial x$ and $\partial D/\partial x$, must be nearly constant within the zone. Still, no limits to the rate or degree of change of D and/or v is required. In short, eqn. 25 can be applied to a wider class of non-uniform media and allow more relaxed conditions than previous treatments of non-uniformity.

For typical chromatographic conditions, eqn. 25 can be further reduced to eqns. 30 and 31. Special cases of these equations are known from the literature [1,4,6]. However, again, in this paper, eqns. 30 and 31 are shown to be applicable to a wider class of non-uniform media and allow more relaxed conditions than previous treatments.

APPLICATION OF THE THEORY

Erosion of chromatographic efficiency

It can be argued that a positive gradient of velocity of a zone can reduce efficiency as it causes extra expansion of the zone. Alternatively, when a zone of analyte suffers significant deceleration it contracts. It can be argued, therefore, that creating a negative gradient of velocity in a column can improve chromatographic efficiency. Such statements are examined in this section.

To simplify mathematical expressions in this section, a quantity

$$\phi = \phi(x) = 1/u \tag{38}$$

is introduced where ϕ is measured in units of time per unit length and could be interpreted as a spatial rate of delay, or delay rate of an analyte: the greater the delay rate at some coordinate of a medium, the longer the analyte remains in the vicinity of that coordinate. Utilizing the delay rate, the retention time, t_r, at $x = L$ could be expressed as

$$t_r = \int_0^L \phi \mathrm{d}x \tag{39}$$

A chromatographic efficiency, N, is defined as $N = t_r^2/\tau^2(L)$ with $\sigma^2(0) = 0$. Substituting here eqns. 29 and 39, and taking into account notation 38, one has

$$N = \frac{\left(\int_0^L \phi \mathrm{d}x\right)^2}{\int_0^L H\phi^2 \mathrm{d}x} \tag{40}$$

A similar expression for apparent plate height was derived earlier by Giddings [4]. Introducing notations

$$N_\Sigma = \int_0^L \frac{\mathrm{d}x}{H} \quad \text{and} \quad \varepsilon^2 = \frac{\left(\int_0^L H\phi^2 \mathrm{d}x\right)\int_0^L \frac{\mathrm{d}x}{H}}{\left(\int_0^L \phi \mathrm{d}x\right)^2} \tag{41}$$

one has

$$N = N_\Sigma/\varepsilon^2 \tag{42}$$

The quantity $1/H$ in the integrals in eqn. 41 represents a local specific efficiency (efficiency per unit length at a given location) of a medium (a column). Therefore, the quantity N_Σ in eqn. 41 is the sum of all local efficiencies and can be referred to as a cumulative efficiency of a non-uniform medium (a column). If the velocity of a zone was uniform, and only the column plate height was not uniform, the efficiency of the column would have been N_Σ.

For the quantity ε^2, it can be shown (see Appendix) that

$$\varepsilon^2 \geqslant 1 \tag{43}$$

Thus, from eqn. 42, the chromatographic efficiency of a non-uniform medium cannot exceed its cumulative efficiency (standing gradients cannot improve efficiency). Giddings [4] came to the same conclusion for the special case when only the velocity of the analyte could vary along a column while the local plate height remained the same everywhere. The derivation of inequality 43 employed here did not require such a limitation.

Quantities ε^2 and ε represent, respectively, the degree of erosion of efficiency and resolution due to non-uniformity within a medium and can be referred to as erosion factors of those quantities.

Re-examination of the introductory statements of this section provide further interpretation of the erosion factor.

Note first that eqn. 42 gives the same result whether the velocity of analyte (inverse of the delay rate) increases or decreases down its path. This means that both types of non-uniformity are equally damaging to efficiency.

Indeed, when a zone of analyte accelerates down its path owing to the positive velocity gradient and broadens, the loss from the zone expansion is partially compensated for by the accompanying gain from faster migration of the zone. The compensation, however, is not large enough to prevent a net erosion of efficiency. GC represents a typical example of a medium with positive velocity gradients. Similarly, when a zone decelerates down its path due to the negative velocity gradient and narrows, the gain from the zone contraction is smaller than the accompanying loss from the zone's slower migration. The net result is erosion of efficiency. SFC represents a typical example of a medium with the negative velocity gradients [19]. In either case, the net result of non-uniformity is erosion of efficiency and resolution.

Still, there is one favorable aspect from this net unfavorable outcome. As the erosion is a result of two competing effects (such as the gain from a zone contraction and the loss from its deceleration), a large degree of the erosion ($\varepsilon \gg 1$) could be considered as an exception rather than the rule. This observation is confirmed by experimental data [20].

Consider now a medium where the plate height is uniform (H is constant) but the delay rate varies down the column. Examples include cases with a large pressure drop in GC and SFC where local plate height changes not nearly as much as a local velocity of an analyte. In these media, the cumulative efficiency (eqn. 41) has a more familiar form:

$$N_\Sigma = L/H \tag{44}$$

and the eqn. 42 can be reduced to

$$\varepsilon^2 = \frac{L\int_0^L \phi^2 \mathrm{d}x}{\left(\int_0^L \phi \mathrm{d}x\right)^2} = 1 + \frac{L^{-1}\int_0^L \Delta\phi^2 \mathrm{d}x}{\phi_{av}^2} \tag{45}$$

where (Fig. 1) $\phi_{av} = L^{-1}\int_0^L \phi \mathrm{d}x$ is a column length averaged delay rate and $\Delta\phi = \phi - \phi_{av}$ is a local variation of the delay rate (a deviation of a delay rate from its average). Obviously, $\Delta\phi$ has a zero average. The numerator on the right-hand side of eqn. 45 represents an average "energy" of the variation in delay rate. Therefore, the erosion factor, ε^2, deviates from unity by the ratio of the average "energy" of variation of the delay rate to the square of the average delay rate. The above "energy" is always positive as long as the delay rate is not uniform. Therefore, when the delay rate is not uniform the erosion factor is always larger than unity. On the other hand, drastic non-monotonic variations of delay rate down the path might be required in order to cause a significant difference between the "energy" and the square of the area under the function $\phi(x)$. Therefore, monotonic changes in the velocity of the analyte along the column (even orders of magnitude changes) might cause only a slight ero-

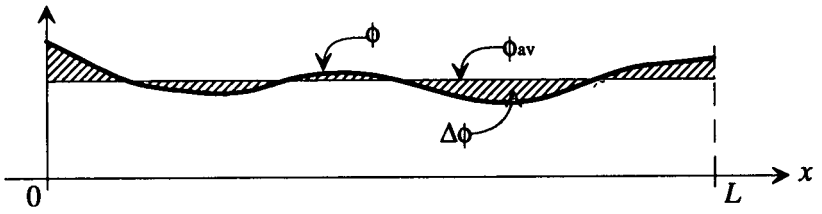

Fig. 1. Non-uniform delay rate. The shaded area represents the variation, $\Delta\phi$, of the delay rate, ϕ, relative to its average, ϕ_{av}. In the case of a uniform plate height, the decrease in chromatographic efficiency due to the non-uniformity of the delay rate is proportional to the ratio of the average "energy" of $\Delta\phi$ to ϕ_{av}^2.

sion of efficiency. This interpretation helps to explain the experimental SFC data [20] where even large deceleration of analytes caused only the small erosion of efficiency.

An example of a weak influence of a zone acceleration on efficiency is GC with compressible carrier gas. It has been shown by Stewart *et al.* [2] and it directly follows from eqn. 45 that for non-retained peaks in GC using an ideal carrier gas

$$\varepsilon^2 = \frac{9(p^4 - 1)(p^2 - 1)}{8(p^3 - 1)^2} \tag{46}$$

where p is the inlet-to-outlet pressure ratio across the column. It also represents an outlet-to-inlet velocity ratio of the analyte. From eqn. 46, it follows that even for large ratios of outlet-to-inlet velocity, the erosion of column efficiency could not exceed 12.5%.

It must be pointed out, however, that eqn. 46 is based on the *approximate* eqn. 25 (conditions C4). Therefore, eqn. 46 *cannot be viewed as the exact expression* for the erosion of efficiency in GC with an ideal carrier gas; it is only the first approximation of that quantity. This important theoretical fact has not been recognized before.

CONCLUSIONS

A general model (eqn. 3) for chromatography based on convective diffusion has been proposed. The model can be applied to a chromatographic medium which can be non-uniform, time-varying and non-linear, or have any combination of these properties. Such a model has not previously been found in the chromatographic literature.

In this paper, the model was utilized for the analysis of non-uniform time-invariant linear media. The main subject of this paper was the derivation of variance of a zone of analyte migrating in such a medium. Results of the derivation are applicable to any type of non-uniformity regardless of its cause, be it variation in the density of an ideal or non-ideal carrier gas, in the column diameter, in the thickness or in the composition of the stationary phase, etc.

It has been found that a special form of the model known as the Fokker–Planck equation is the most convenient for moment analysis in such a medium, and can be used in other moment-based studies of chromatography. The Fokker–Planck equation has not previously been utilized in the chromatographic literature.

Exact eqns. 21, 22 and 23 for temporal and spatial derivatives of variance of a zone have been derived. These are the first exact expressions for the general case of non-uniformity.

The expressions could be further reduced to a first-order ordinary linear differential equation (eqn. 25) if gradients of diffusivity and velocity in the medium are locally nearly constant (changes can be large but nearly linear). Such a general equation for a zone variance in a non-uniform medium was not known before. Further, the conditions under which eqn. 25 was valid are less restrictive than those known from the literature. Previous implicit or explicit conditions were more restrictive yet were developed for narrower cases.

It has been shown that regardless of the type of non-uniformity, chromatographic efficiency cannot be improved. This statement is more general than a similar statement published before. On the other hand, a simple graphical concept based on the newly introduced delay rate in a non-uniform medium has been developed to demonstrate that in many instances even significant non-uniformity can cause only minor decreases in efficiency. Roughly, it is impossible to gain extra efficiency via non-uni-

formity, but significant losses are unlikely unless the medium becomes very lumpy.

It has also been shown that in a non-uniform medium, a gradient of diffusivity affects the local velocity of migration of the analyte. Although for typical chromatographic conditions the addition is virtually insignificant, recognition of the fact is theoretically important. References to the phenomenon have not been found in the literature. Several new parameters of a non-uniform chromatographic medium were also introduced.

SYMBOLS

D local effective diffusivity in a medium (length^2/time)
D_a aggregate diffusivity of a zone of analyte (length^2/time)
D_m molecular diffusivity (length^2/time)
f_u local mass flow due to migration of analyte (mass/time)
H local plate height (length)
H_a aggregate plate height of a zone of analyte (length)
k capacity factor
L length of a path of a zone (length)
m specific mass of a migrating analyte (mass/length)
N_Σ cumulative chromatographic efficiency
N chromatographic efficiency
p ratio of inlet to outlet pressure on a column
t time (time)
t_r retention time of a zone (time)
u net local velocity of an analyte (length/time)
u_a aggregate velocity of a zone (length/time)
v local convective velocity of analyte (length/time)
v_m local velocity of a mobile phase (length/time)
x spatial coordinate (length)
z center of mass (first moment) of a zone (length)
ε erosion factor
ϕ delay rate of an analyte (time/length)
ϕ_{av} average delay rate of an analyte (time/length)
$\Delta\phi$ variation of delay rate (time/length)
ρ density (mass/length^3)
σ^2 variance (second central moment) of a zone (length^2)
τ^2 time measure of variance of a zone ($\tau^2 = \sigma^2/u^2$) (time^2)

APPENDIX

Mass balance of convective diffusion in a non-uniform medium

The total mass of a zone migrating in a unbounded medium could be expressed as $\int_{-\infty}^{\infty} m\mathrm{d}x$. Its derivative $\frac{\mathrm{d}}{\mathrm{d}t}\int_{-\infty}^{\infty} m\mathrm{d}x$ reflects the variation of the total mass with time, and must be zero if the total mass is to be conserved. Taking account of eqn. 3, one has

$$\frac{\mathrm{d}}{\mathrm{d}t}\int_{-\infty}^{\infty} m\mathrm{d}x = \int_{-\infty}^{\infty}\frac{\partial m}{\partial t}\mathrm{d}x = \int_{-\infty}^{\infty}\left[\frac{\partial}{\partial x}\left(D\cdot\frac{\partial m}{\partial x}\right) - \frac{\partial}{\partial x}(vm)\right]\mathrm{d}x = \left(D\cdot\frac{\partial m}{\partial x} - vm\right)\Bigg|_{-\infty}^{\infty} = 0$$

The last transaction to zero becomes valid under the following practically unrestrictive assumptions (see C2 and C3 in the main text): $m \to 0$, $|\partial D/\partial x| < \infty$ and $|v| < \infty$ when $x \to \pm\infty$.

Derivation of aggregate velocity, $\mathrm{d}z/\mathrm{d}t$, of a zone

Taking account of eqns. 17, 9 and 3, then integrating by parts one has

$$u_a = \frac{\mathrm{d}z}{\mathrm{d}t} = \frac{\mathrm{d}}{\mathrm{d}t}\int_{-\infty}^{\infty} xm\mathrm{d}x = \int_{-\infty}^{\infty}\frac{\partial}{\partial t}(xm)\mathrm{d}x = \int_{-\infty}^{\infty} x\cdot\frac{\partial m}{\partial t}\mathrm{d}x = \int_{-\infty}^{\infty} x\left[\frac{\partial}{\partial x}\left(D\cdot\frac{\partial m}{\partial x}\right) - \frac{\partial}{\partial x}(vm)\right]\mathrm{d}x =$$

$$\int_{-\infty}^{\infty} x\mathrm{d}\left(D\cdot\frac{\partial m}{\partial x} - vm\right) = xD\cdot\frac{\partial m}{\partial x}\Bigg|_{-\infty}^{\infty} - \int_{-\infty}^{\infty} D\cdot\frac{\partial m}{\partial x}\mathrm{d}x - xvm\Bigg|_{-\infty}^{\infty} + \int_{-\infty}^{\infty} vm\mathrm{d}x = \int_{-\infty}^{\infty} vm\mathrm{d}x - \int_{-\infty}^{\infty} D\cdot\frac{\partial m}{\partial x}\cdot\mathrm{d}x$$

The last transaction here was based on the properties 7 securing $xD(\partial m/\partial x)\Big|_{-\infty}^{\infty} = 0$, $xvm\Big|_{-\infty}^{\infty} = 0$. When properties 7 are accounted for again, integration by parts for the second integral in the last right-hand side yields

$$u_a = \int_{-\infty}^{\infty} vm\mathrm{d}x - Dm\Big|_{-\infty}^{\infty} + \int_{-\infty}^{\infty} \frac{\partial D}{\partial x} \cdot m\mathrm{d}x = \int_{-\infty}^{\infty} vm\mathrm{d}x + \int_{-\infty}^{\infty} \frac{\partial D}{\partial x} \cdot m\mathrm{d}x = \int_{-\infty}^{\infty} \left(v + \frac{\partial D}{\partial x}\right) m\mathrm{d}x \tag{47}$$

Modification of the equation for convective diffusion

Eqn. 3 can be modified in the following way. After adding a quantity $m(\partial D/\partial x)$ within both derivatives of its right-hand side, one has

$$\frac{\partial m}{\partial t} = \frac{\partial}{\partial x}\left(D \cdot \frac{\partial m}{\partial x} + m \cdot \frac{\partial D}{\partial x}\right) - \frac{\partial}{\partial x}\left(vm + m \cdot \frac{\partial D}{\partial x}\right) = \frac{\partial^2}{\partial x^2}(Dm) - \frac{\partial}{\partial x}\left[\left(v + \frac{\partial D}{\partial x}\right) m\right]$$

After introduction of a variable u by eqn. 19, the last equation becomes

$$\frac{\partial m}{\partial t} = \frac{\partial^2}{\partial x^2}(Dm) - \frac{\partial}{\partial x}(um)$$

Derivation of $\mathrm{d}\sigma^2/\mathrm{d}t$

This derivation is based on the modified equation of convective diffusion derived above. Starting with eqn. 8, and repeating integration by parts similar to that employed for derivation of $\mathrm{d}z/\mathrm{d}t$ above, one has

$$\frac{\mathrm{d}\sigma^2}{\mathrm{d}t} = \frac{\mathrm{d}}{\mathrm{d}t}\int_{-\infty}^{\infty} (x - z)^2 m\mathrm{d}x = -\int_{-\infty}^{\infty} 2z(x - z) \cdot \frac{\mathrm{d}z}{\mathrm{d}t} \cdot m\mathrm{d}x + \int_{-\infty}^{\infty} (x - z)^2 \cdot \frac{\partial m}{\partial t} \cdot \mathrm{d}x = -2u_a z \int_{-\infty}^{\infty} (x - z)m\mathrm{d}x +$$

$$\int_{-\infty}^{\infty} (x - z)^2 \left(\frac{\partial^2}{\partial x^2}(Dm) - \frac{\partial}{\partial x}(um)\right)\mathrm{d}x = -2u_a z \int_{-\infty}^{\infty} (x - z)m\mathrm{d}x + \int_{-\infty}^{\infty} (x - z)^2 \mathrm{d}\left(\frac{\partial}{\partial x}(Dm) - um\right)$$

Owing to eqn. 11, the first integral in the last sum vanishes. Integrating the second integral by parts, one further has

$$\frac{\mathrm{d}\sigma^2}{\mathrm{d}t} = (x - z)^2 \left(\frac{\partial}{\partial x}(D\rho) - um\right)\Big|_{-\infty}^{\infty} - 2\int_{-\infty}^{\infty} (x - z)\left(\frac{\partial}{\partial x}(Dm) - um\right)\mathrm{d}x$$

Eqns. 7 nullify the value of $(x - z)^2\left(\frac{\partial}{\partial x}(Dm) - vm\right)\Big|_{-\infty}^{\infty}$. Integrating the remaining integral by parts again, one further has

$$\frac{\mathrm{d}\sigma^2}{\mathrm{d}t} = -2\int_{-\infty}^{\infty} (x - z)\left(\frac{\partial}{\partial x}(Dm) - um\right)\mathrm{d}x = -2\int_{-\infty}^{\infty} (x - z)\mathrm{d}(Dm) + 2\int_{-\infty}^{\infty} (x - z)um\mathrm{d}x = -2(x - z)Dm\Big|_{-\infty}^{\infty} +$$

$$2\int_{-\infty}^{\infty} Dm\mathrm{d}x + 2\int_{-\infty}^{\infty} (x - z)um\mathrm{d}x$$

With the first member of the last right-hand side nullified by eqns. 7 again, the entire expression finally becomes

$$\frac{d\sigma^2}{dt} = 2\int_{-\infty}^{\infty} Dm\,dx + 2\int_{-\infty}^{\infty} (x - z)um\,dx$$

Derivation of ordinary differential equation for σ^2

At any x-coordinate of a medium, both u and D could be expressed via their linear terms and the second-order remainders as:

$$u = u(z) + u'(z)(x - z) + O_u; \quad O_u = O_u(x,z)$$

$$D = D(z) + D'(z)(x - z) + O_D; \quad O_D = O_D(x,z)$$

If both the second-order remainders, O_u and O_D, in these expressions are substantially small within a zone of analyte, then the above expressions could be replaced with their respective linear approximations:

$$u = u(z) + u'(z)(x - z) \tag{48}$$

$$D = D(z) + D'(z)(x - z) \tag{49}$$

Owing to eqns. 48 and 11, the aggregate velocity from eqn. 18 becomes

$$u_a = u(z) \tag{50}$$

Finally, recalling eqns. 11, 8 and 24 and substituting eqns. 48, 49 and 50 into eqn. 22, one has

$$\frac{d\sigma^2}{dz} = H(z) + \frac{2\sigma^2}{u(z)} \cdot \frac{du}{dz}$$

Lower bound for the erosion factor

As H is positive, new functions

$$f = \phi\sqrt{H}, \quad g = \frac{1}{\sqrt{H}}$$

could be introduced to rewrite eqn. 41 as

$$\varepsilon^2 = \frac{\left(\int_0^L H\phi^2 dx\right)\int_0^L \frac{dx}{H}}{\left(\int_0^L \phi dx\right)^2} = \frac{\left(\int_0^L f^2 dx\right)\int_0^L g^2 dx}{\left(\int_0^L fg\,dx\right)^2}$$

According to the Cauchy–Schwarz inequality

$$\varepsilon^2 \geqslant 1.$$

REFERENCES

1 M. J. Golay, in D. H. Desty (Editor), *Gas Chromatography*, Butterworths, London, 1958, pp. 36–53.
2 J. H. Stewart, S. L. Seager and J. C. Giddings, *Anal. Chem.*, 31 (1959) 1738.
3 J. C. Giddings, S. L. Seager, L. R. Stucki and G. H. Stewart, *Anal. Chem.*, 32 (1960) 867.
4 J. C. Giddings, *Anal. Chem.*, 35 (1963) 353.
5 J. C. Giddings, *J. Gas Chromatogr.*, 2 (1964) 167.
6 J. C. Giddings, *Dynamics of Chromatography, Part I, Principles and Theory*, Marcel Dekker, New York, 1965.
7 M. J. E. Golay, *Nature (London)*, 200 (1963) 776.
8 U. van Wasen and G. M. Schneider, *Chromatographia*, 8 (1975) 274.
9 V. G. Levich, *Physicochemical Hydrodynamics*, Prentice-Hall, Englewood Cliffs, NJ, 1962.
10 G. Taylor, *Proc. R. Soc. London, Ser. A*, 219 (1953) 186.
11 S. G. Weber, *Anal. Chem.*, 56 (1984) 2104.
12 D. M. Scott and J. S. Fritz, *Anal. Chem.*, 56 (1984) 1561.
13 J. Å. Jönsson, in J. Å. Jönsson (Editor), *Chromatographic Theory and Basic Principles*, Marcel Dekker, New York, Basle, 1957, pp. 27–102.
14 J. H. Knox and P. H. Scott, *J. Chromatogr.*, 282 (1983) 297.
15 J. J. van Deemter, F. J. Zuiderweg and A. Klinkenberg, *Chem. Eng. Sci.*, 5 (1956) 271.
16 A. Einstein, *Ann. Phys. (Leipzig)*, 17 (1905) 549.
17 A. Einstein, *Ann. Phys. (Leipzig)*, 19 (1906) 371.
18 E. Zauderer, *Partial Differential Equations of Applied Mathematics*, Wiley, New York, 2nd ed., 1989.
19 H.-G. Janssen, H. M. J. Snijders, J. A. Rijks, C. A. Cramers and P. J. Schoenmakers, *J. High Resolut. Chromatogr.*, 14 (1991) 438.
20 T. A. Berger and J. F. Deye, *Chromatographia*, 31 (1991) 529.

Journal of Chromatography, 596 (1992) 15–25
Elsevier Science Publishers B.V., Amsterdam

CHROM. 23 967

Preparative liquid chromatography

II. Existence of optimum injection conditions for overloaded gradient elution separations

G. Crétier*, M. El Khabchi and J. L. Rocca

Laboratoire des Sciences Analytiques (UA CNRS 435), Université Claude Bernard Lyon I, Bât. 308, 43 Boulevard du 11 novembre 1918, 69622 Villeurbanne Cedex (France)

(First received May 30th, 1991; revised manuscript received December 17th, 1991)

ABSTRACT

The effect of injection conditions on overloaded gradient elution separations in liquid chromatography was studied theoretically from simulated chromatograms. The simulation algorithm was based on the Craig machine. The separation of binary mixtures having both constant and non-constant separation factors with changing modulator concentration was examined. It appears that there is a general parallelism between gradient elution and isocratic elution under overload conditions: the injection concentration has to be optimized in order to maximize the recovered amount and the optimum injection conditions depend on the column efficiency.

INTRODUCTION

Gradient elution is widely used in preparative-scale liquid chromatography, especially to recover, in a single run, pure solutes from a complex mixture whose components exhibit a broad range of retentivity. In the gradient elution mode, the initial injection step is carried out under strong retention conditions, after which the eluent strength is increased continuously during the chromatographic run by progressive modification of the mobile phase composition. Because of the very low eluent strength of the initial mobile phase, immediately following sample injection, the solutes are retained in a very thin slice of the column inlet where their mobile phase concentration is very high, their distribution isotherm is very non-linear and the degree of interference between them is very strong. Consequently, the profile of solute bands at the column inlet is very distorted and, intuitively, decreasing the injected concentration could result in less band broadening and better resolution between two successive elution bands.

The influence of input concentration on the degree of separation has been studied in overloaded isocratic elution [1–4]. However, none of the recent attempts to model overloaded gradient elution separations for multi-component samples [3,5–12] dealt with this issue; all these studies, regardless of the role of injection conditions, assumed that only the magnitude of the sample load has to be taken into account.

The goal of preparative liquid chromatography is to recover, from a mixture, the largest amount of certain components with a specified purity, and in this work we investigated the effect of the sample concentration on the recovered amounts for binary mixtures of various compositions, chromatographed under linear-strength (LSS) gradient elution conditions [13,14] and having both constant and non-constant separation factors with changing mobile phase composition. The influence of column efficiency on the optimization of the injection conditions was also considered. This work is based on the use of our new approach using the Craig model,

0021-9673/92/$05.00

CRAIGSIM [4], that we first tested under analytical gradient conditions, *i.e.*, in gradient elution with a linear isotherm, in order to verify that it matches the LSS theory.

THEORY

Simulation

The CRAIGSIM software was detailed in Part I [4].

Elution conditions

In our simulation experiments, we consider only linear forms for the gradient profile and there is no system dwell volume, *i.e.*, the variation of the modifier concentration φ in the mobile phase at the column inlet against the eluted volume V is written as

$$\varphi = \varphi_0 \qquad V \leqslant V_i \tag{1}$$

$$\varphi = \varphi_0 + G(V - V_i) \qquad V > V_i \tag{2}$$

where φ_0 is the modifier concentration in the eluent before the start of the gradient run, V_i is the injection volume and G is the gradient steepness.

Characteristics of sample mixtures

In overloaded chromatography and for a two-component mixture, the equilibrium concentration of a solute j ($j = 1$ or 2) in the stationary phase depends on its own equilibrium concentration in the phase mobile and on the equilibrium mobile phase concentration of the other solute. Assuming a mixed Langmuir isotherm model for the solute distribution, the equilibrium concentrations of solutes 1 and 2 in the stationary phase, $C_{s,1}$ and $C_{s,2}$, and in the mobile phase, $C_{m,1}$ and $C_{m,2}$, are related by

$$C_{s,1} = \frac{a_1 C_{m,1}}{1 + b_1 C_{m,1} + b_2 C_{m,2}} \tag{3}$$

$$C_{s,2} = \frac{a_2 C_{m,2}}{1 + b_2 C_{m,2} + b_1 C_{m,1}} \tag{4}$$

where the isotherm coefficients a_j and b_j ($j = 1$ or 2) depend on the mobile phase composition φ. a_j is related to the isocratic capacity factor, k'_j, of the solute by means of the total porosity ε of the column packing according to $a_j = \varepsilon k'_j/(1 - \varepsilon)$ and, in reversed-phase chromatography, the variation of a_j with φ can usually be described by the empirical relationship

$$a_j = a_{0,j} \cdot 10^{-m_j \varphi} \tag{5}$$

where $a_{0,j}$ is the a_j value for pure water as mobile phase and m_j is a constant that depends on both the solute and the organic modifier used in the organic–water mobile phase. On the assumption that the saturation concentration of the stationary phase, a_j/b_j, is a constant $C_{s,0}$ independent of both the solute and the mobile phase composition, the isotherm coefficient of non-linearity, b_j, is given by

$$b_j = \frac{a_{0,j}}{C_{s,0}} \cdot 10^{-m_j \varphi} \tag{6}$$

Fig. 1 shows the three different types of sample mixture that can be distinguished. For mixture type A, the m_1 and m_2 values are equal, the $\log a_j$ *versus* φ plots are parallel (Fig. 1a) and, consequently, the separation factor defined by

$$\frac{a_2}{a_1} = \frac{a_{0,2}}{a_{0,1}} \cdot 10^{-(m_2 - m_1)\varphi} \tag{7}$$

is kept constant as the mobile phase composition φ is changing. For the two other mixture types, m_1 and m_2 differ and the separation factor a_2/a_1 is non-constant while changing the modifier concentration. For mixture type B ($m_1 > m_2$) the $\log a_i$ *versus* φ plots are divergent and a_2/a_1 increases with increase in φ (Fig. 1b). For mixture type C ($m_1 < m_2$), the $\log a_i$ *versus* φ plots are convergent and a_2/a_1 decreases with increase in φ (Fig. 1c). As suggested by Antia and Horváth [11], the three mixture types A, B and C are denoted parllel, divergent and convergent solutes, respectively.

LSS theory

According to the linear solvent strength theory [13], under analytical gradient conditions, the retention volume $V_{R,j}$ of a component j and the standard deviation expressed in volume units, σ_j, of its peak are given by

$$V_{R,j} = V_M + \frac{1}{m_j G} \cdot \log\left[1 + 2.3 m_j G V_M \cdot \frac{(1 - \varepsilon)}{\varepsilon} \cdot a_{0,j} \cdot 10^{-m_j \varphi_0}\right] \tag{8}$$

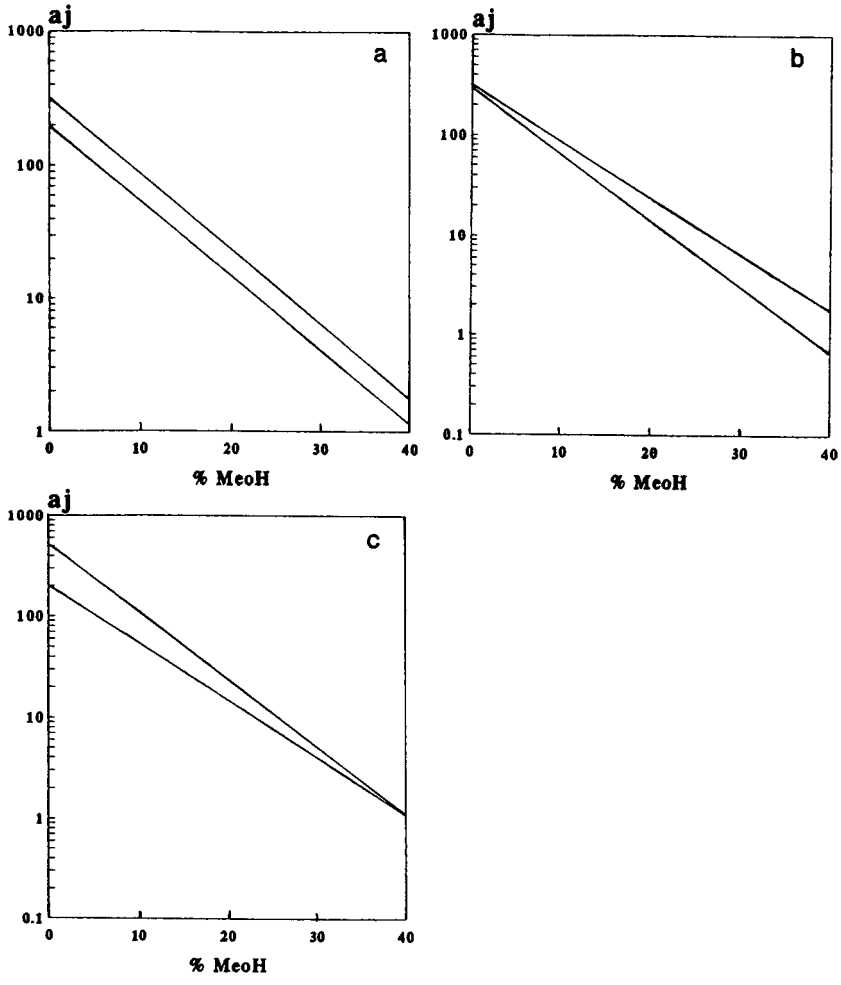

Fig. 1. Log a_j *vs.* φ plots corresponding to the various mixture types (see Table I). (a) Mixture type A (parallel solutes); (b) mixture type B (divergent solutes); (c) mixture type C (convergent solutes).

and

$$\sigma_j = \frac{gV_M}{\sqrt{N_j}}\left(1 + \frac{\frac{1-\varepsilon}{\varepsilon}\cdot a_{0,j}\cdot 10^{-m_j\varphi_0}}{1 + 2.3m_jGV_M\cdot\frac{1-\varepsilon}{\varepsilon}\cdot a_{0,j}\cdot 10^{-m_j\varphi_0}}\right) \tag{9}$$

where V_M is the column dead volume, g is the band compression factor defined by

$$g = \frac{\sqrt{1 + p + p^{2/3}}}{1 + p} \tag{10}$$

with

$$p = \frac{2.3m_jGV_M\cdot\frac{1-\varepsilon}{\varepsilon}\cdot a_{0,j}\cdot 10^{-m_j\varphi_0}}{1 + \frac{1-\varepsilon}{\varepsilon}\cdot a_{0,j}\cdot 10^{-m_j\varphi_0}} \tag{11}$$

and N_j is the column plate number. N_j can be measured under isocratic conditions selected to be equivalent to those in gradient elution (see discussion in ref. 14), *i.e.*, under isocratic conditions for which the capacity factor k'_j is equal to the median capacity factor during the gradient run $\overline{k'_j}$ (value of

the capacity factor when the band has migrated half way along the column). $\overline{k'_j}$ is given by

$$\overline{k'_j} = \frac{\frac{1-\varepsilon}{\varepsilon} \cdot a_{0,j} \cdot 10^{-m_j\varphi_0}}{1 + 1.15 m_j G V_M \cdot \frac{1-\varepsilon}{\varepsilon} \cdot a_{0,j} \cdot 10^{-m_j\varphi_0}} \quad (12)$$

In a simulated isocratic separation, the column plate number N_j is equal to $(n_c + 1)[(1 + k'_j)/k'_j]$, where n_c is the stage number of the Craig machine [15]. Similarly, in a simulated gradient run, N_j is assumed to be related to n_c by the following equation [12]

$$N_j = (n_c + 1)\frac{1 + \overline{k'_j}}{\overline{k'_j}} \quad (13)$$

Reduced production rate

The production rate of solute j, $R_{H,j}$, is defined as amount of solute j recovered with the required purity level, $Q_{r,j}$, divided by the run time, T:

$$R_{H,j} = \frac{Q_{r,j}}{T} \quad (14)$$

The run time in our study extends from the start of the injection to the point where the last traces of the second component elute:

$$T = \frac{V_{E,2}}{D} \quad (15)$$

where D is the elution flow rate and $V_{E,2}$ is the elution volume when the eluted concentration of solute 2 is equal to 10^{-8} mol/l.

We define the reduced production rate of solute j, $r_{H,j}$, as production rate of the solute j, $R_{H,j}$, divided by the elution flow rate, D. Substitution of eqn. 15 in eqn. 14 gives

$$r_{H,j} = \frac{R_{H,j}}{D} = \frac{Q_{r,j}}{V_{E,2}} \quad (16)$$

EXPERIMENTAL

Equipment, materials and procedures were the same as in Part I [4]. The simulated column was 150 mm × 5 mm I.D. with a total porosity ε of 0.8; hence its dead volume V_M was 2.36 ml. The column plate number N_j was varied by changing the number of stages n_c in the Craig machine.

The gradient profile simulated corresponded to $\varphi_0 = 0$ and $G = 0.015$ ml^{-1}. Table I summarizes the retention characteristics of the various sample mixtures studied. The analytical resolution is identical for each of these three samples owing to the equal values of $(V_{R,j} - V_M)/V_M$ for $j = 1$ and $j = 2$, respectively. Plots of log a_j *versus* φ are shown in Fig. 1.

RESULTS AND DISCUSSION

Comparison between CRAIGSIM results and LSS theory for analytical gradient separations

Fig. 2 shows the chromatograms of the sample mixture of type A at a relative composition of 1:1, obtained under analytical injection conditions and simulated for stage numbers of 200 and 600. The accuracy of the CRAIGSIM algorithm previously demonstrated in preparative isocratic elution [4] is

TABLE I

CHARACTERISTICS OF THE VARIOUS MIXTURE TYPES CONSIDERED

Mixture type	Solute	$a_{0,j}$	m_j	$C_{s,0}$ (mol/l)	$\frac{V_{R,j} - V_M}{V_M}$	$\overline{k'_j}$
A (parallel solutes)	1	200	5.65	10	6.90	4.00
	2	320	5.65		7.89	4.12
B (divergent solutes)	1	300	6.65	10	6.88	3.53
	2	320	5.65		7.89	4.12
C (convergent solutes)	1	200	5.65	10	6.90	4.00
	2	520	6.65		7.88	3.60

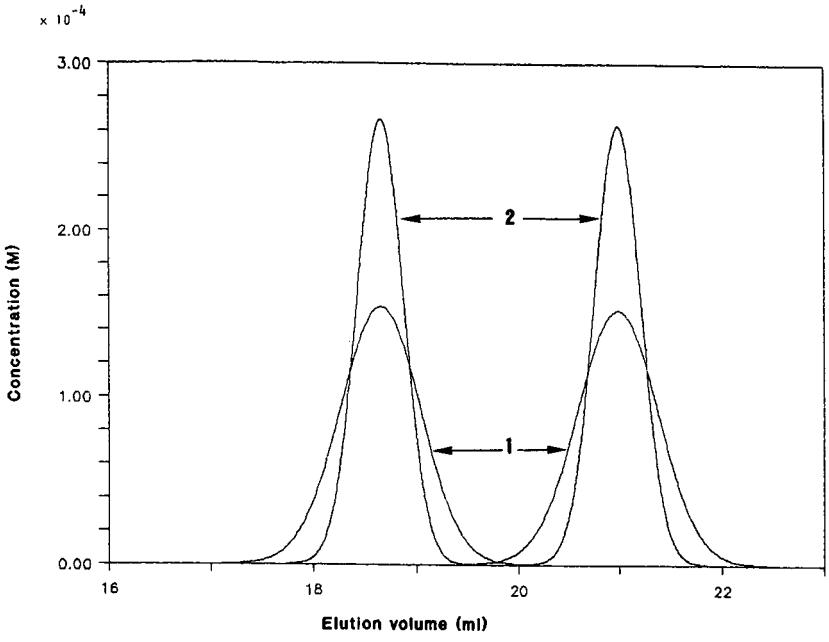

Fig. 2. Analytical chromatograms of the sample mixture of type A. Relative mixture composition: 1:1. Injection conditions: $C_i = 2.5 \cdot 10^{-2}$ mol/l; $Q_i = 3 \cdot 10^{-7}$ mol. Elution conditions: $\varphi_0 = 0$; $G = 0.015\ \mathrm{ml}^{-1}$. Curves: (1) $n_c = 200$ ($N_1 = 251$, $N_2 = 250$); (2) $n_c = 600$ ($N_1 = 751$, $N_2 = 747$).

confirmed in analytical gradient elution by comparing the values of the retention volumes and the peak standard deviations measured from simulated chromatograms in Fig. 2 with those calculated from the LSS theory, eqns. 8 and 9 (Table II). The values measured from CRAIGSIM simulations match those predicted by the LSS theory, within 0.05% for the retention volume and 1.5% for the peak standard deviation.

TABLE II

COMPARISON OF THE RETENTION VOLUMES AND PEAK STANDARD DEVIATIONS MEASURED FROM CRAIGSIM SIMULATIONS AND CALCULATED FROM LSS THEORY EQUATIONS

Mixture type: parallel solutes (A). Mixture composition: 1:1.

Solute	n_c	N_j[a]	$V_{R,j}$ (ml)		σ_j (ml)	
			Measured[b]	Calculated[c]	Measured[d]	Calculated[e]
1	200	251	18.65	18.65	0.395	0.390
	600	751	18.65	19.65	0.226	0.225
2	200	250	20.98	20.97	0.401	0.395
	600	747	20.97	20.97	0.229	0.228

[a] Calculated by eqn. 13.
[b] Elution volume of the peak maximum on the simulated chromatogram.
[c] Value calculated by eqn. 8.
[d] Half-width of the band measured at 0.607 of the peak height on the simulated chromatogram.
[e] Value calculated by eqn. 9.

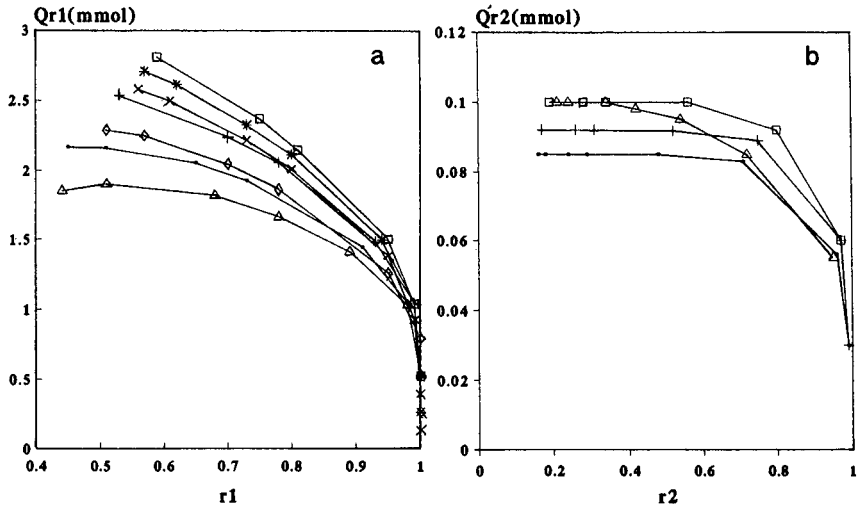

Fig. 3. Plot of the recovered amount at 99% purity *versus* the recovery yield for different sample concentrations. Mixture: relative composition = 9:1, type A (see Table I). n_c = 200 (N_1 = 251, N_2 = 250). C_i: ■ = 0.1; + = 0.2; ✳ = 0.4; □ = 1.7; × = 12.5; ◇ = 25; △ = 50 mol/l. (a) Component 1; (b) component 2.

Optimization of sample size and sample concentration for preparative gradient runs

The effect of the sample load Q_i and the sample concentration C_i on the recovery ratios, r_1 and r_2, and the recovered amounts, $Q_{r,1}$ and $Q_{r,2}$, of components 1 and 2, respectively, at 99% purity was studied for three different relative compositions, 9:1, 1:1 and 1:9, of the three binary sample mixtures mentioned in Table I. The results are qualitatively similar whatever the sample composition and we have only reported the results obtained with the 9:1 mixtures, for which the trends are much more pronounced.

Mixture of parallel solutes. Fig. 3 illustrates the effect of increasing sample size at constant injected concentration and plots the evolution of the re-

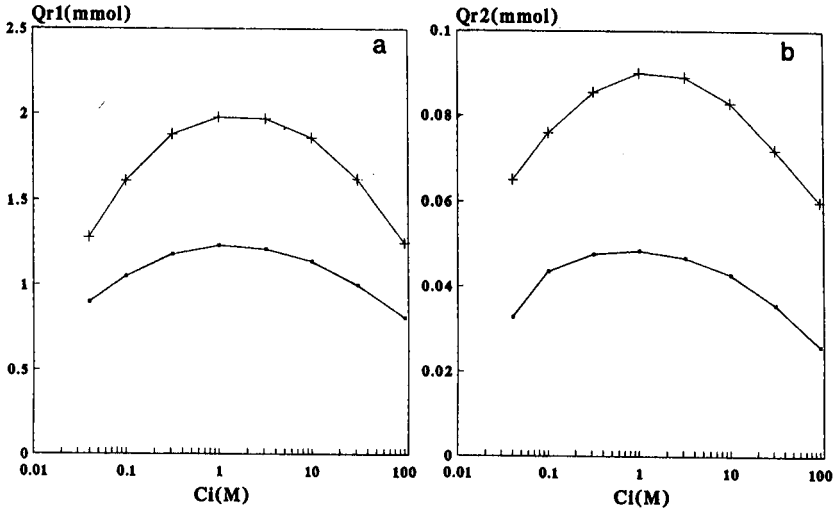

Fig. 4. Plot of the recovered amount at 99% purity *versus* the sample concentration for different recovery ratios. Mixture: relative composition = 9:1, type A (see Table I). n_c = 200 (N_1 = 251, N_2 = 250). r_j: (■) 98%; (+) 85%. (a) Component 1; (b) Component 2.

covered amount at 99% purity $Q_{r,j}$ *versus* the recovery yield r_j for different sample concentrations C_i. By increasing the sample amount, the chromatogram changes from Gaussian peaks (under analytical conditions) to touching bands and, finally, to overlapping bands. The recovery ratio remains nearly constant and equal to 100% for all sample concentrations up to a certain injected amount. Under these conditions, the band overlap is small and all the injected solute amounts can be recovered with 99% purity. Beyond this point, the bands overlap too much, the recovery of the whole injected amount is no longer possible and the recovery ratio falls more or less rapidly, depending on both the sample concentration injected and the solute considered.

The study of the variation of the recovered solute amount against the injected sample concentration for a specified solute recovery ratio shows that there is an optimum sample concentration giving the highest recovered amount (Fig. 4). For solute 1, this optimum is more and more critically defined with decreasing recovery ratio. In contrast, for solute 2, the maximum of the recovered amount is sharper with increasing recovery ratio. However, for each solute, the optimum injection concentration seems to be independent of the fixed recovery ratio. Fig. 4 also illustrates that, in preparative chromatography, the fact of allowing as certain loss of product is very advantageous: it is possible to recover about 1.5–2 times as much 99% pure solute with a recovery of 85% as with a recovery of 98%.

The influence of the column efficiency on the optimum injection conditions is shown in Fig. 5, which plots, for different column plate numbers, the variation of the recovered amount $Q_{r,j}$ of 99% pure solute 1 against both the sample concentration C_i and the reduced injection volume V_i/σ_1 (ratio of the injection volume to the standard deviation of the Gaussian peak observed at infinite dilution). The larger the column plate number, the higher is the recovered amount and the more concentrated the sample has to be injected to recover the maximum amount. In contrast, the optimum value of the reduced injection volume seems not to be affected by the column efficiency.

All the preceding observations parallel those found for the case of isocratic overlapping band separation [4]. This confirms the essential similarity of the overloaded separations in isocratic or gradient elution, which was mentioned previously [8,10,12]. Figs. 6 and 7 also demonstrate that the phenomena explaining the existence of optimum injection conditions in gradient elution are the same as in isocratic elution. Fig. 6 superposes the band profiles corresponding to injection of the 9:1 mixture

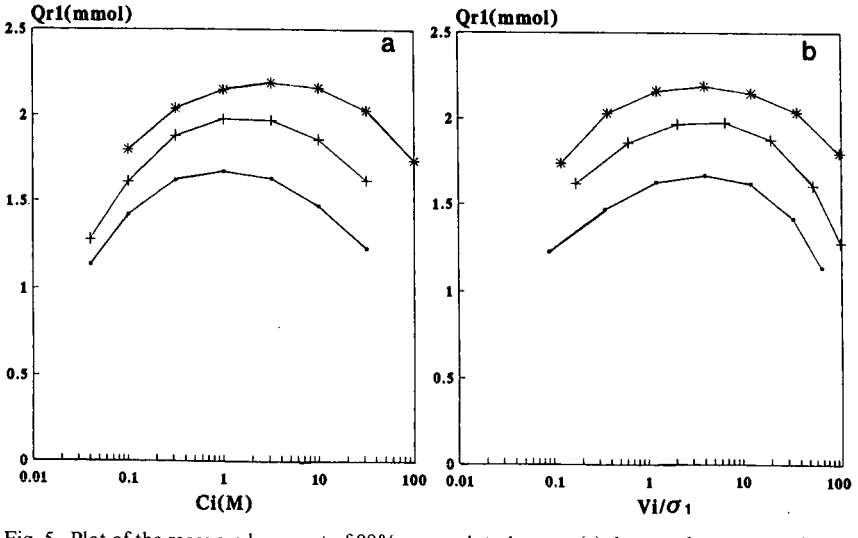

Fig. 5. Plot of the recovered amount of 99% pure solute 1 *versus* (a) the sample concentration and (b) the reduced injection volume for different column efficiencies. Mixture: relative composition = 9:1, type A (see Table I). r_1 = 85%. (□) n_c = 100 (N_1 = 126, N_2 = 126); (+) n_c = 200 (N_1 = 251, N_2 = 250); (*): n_c = 600 (N_1 = 751, N_2 = 747).

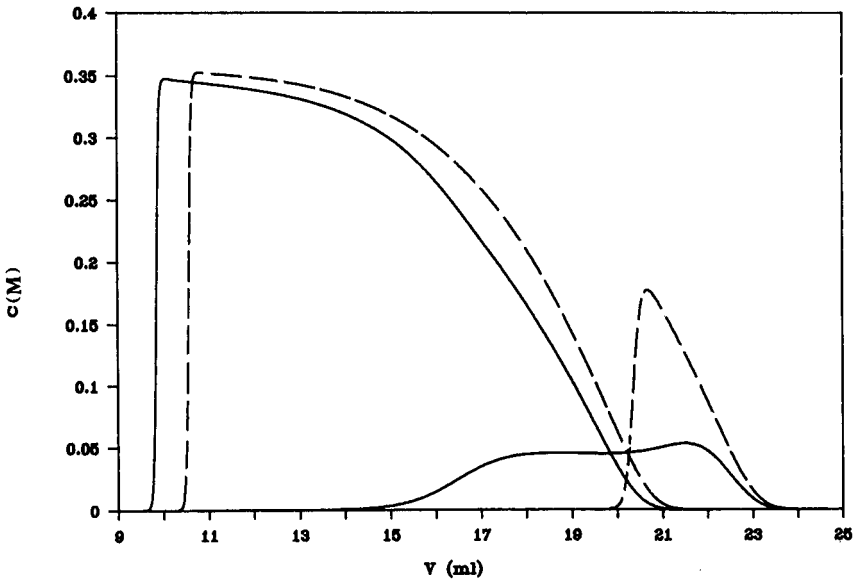

Fig. 6. Chromatograms obtained by (solid line) direct injection of the mixture and (dashed line) superposition of the band profiles corresponding to the equivalent amounts of single solutes. Q_i = 2.96 mmol; C_i = 1.7 mol/l. Mixture: relative composition = 9:1, type A (see Table I). n_c = 200 (N_1 = 251, N_2 = 250).

A (full line) and to injection of the equivalent amounts of single solutes (dashed line). Clearly, there are displacement and tag-along effects for overload separations in the gradient elution mode, as already seen in the isocratic elution mode (compare with Fig. 2 in ref. 4). However, in contrast to the right triangle appearance of the isocratic bands, the rounded shape of the more heavily overloaded band (solute 1) reflects the fact that the band tail in gradient elution always travels in a stronger mobile phase. Fig. 7 compares three chromatograms corresponding to the same amount injected at three different concentrations (this figure should be compared with Figs. 11 and 12 in Part I [4]). The injected sample amount was kept constant at 2.96 mmol. The elution profiles 1, 2 and 3 were obtained for injected concentrations of 0.1, 1.7 and 27.8 mol/l, respectively. The corresponding recovery ratios of 99% pure first component are 72.6, 81.0 and 72.3%. Hence the elution profile 2, which corresponds to the optimum injection concentration for the recovery of the first-eluted solute, results from a compromise between two simultneous phenomena: when the injected concentration is increased and the injected volume is decreased (the injected amount being constant), classically the peak width is decreased (comparison of elution profiles 1 and 2) and consequently the first component recovery ratio is increased; however, for a high injection concentration, owing to the tag-along effect, the front base of the second component peak is attracted under the first component peak (comparison of elution profiles 2 and 3). This additional band broadening is responsible for the decrease in the first component recovery ratio for high injected concentrations. In contrast to isocratic elution (Figs. 11 and 12 in ref. 4), the rear portion of the second component which does not overlap with the first component does not exhibit a plateau, but forms a hump because the compressive effect of the gradient acts to concentrate it.

Like the recovered amount, the production rate for given conditions of column, flow-rate, recovery ratio and purity (*i.e.*, the reduced production rate) also depends on the injection concentration. Fig. 8 shows that both recovered amount and reduced production rate are maximum for certain values of the sample concentration, but the optimum sample concentration for the reduced production rate is larger than that for the recovered amount. The

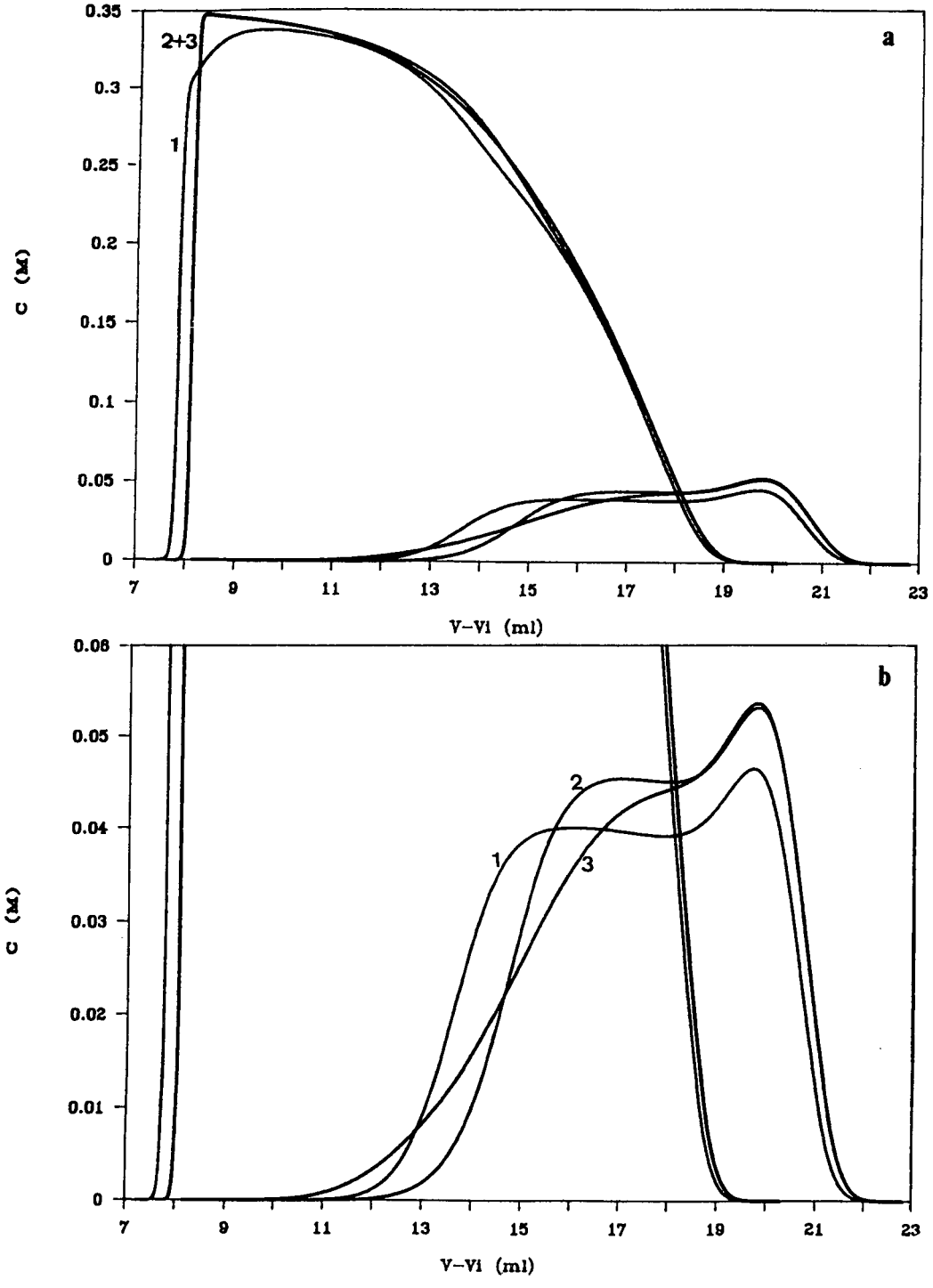

Fig. 7. Three chromatograms corresponding to the same injected amount, Q_i = 2.96 mmol. Mixture: relative composition = 9:1, type A (see Table I). n_c = 200 (N_1 = 251, N_2 = 250). (1) C_i = 0.1 mol/l; (2) C_i = 1.7 mol/l; (3) C_i = 27.8 mol/l (the elution volume is adjusted by subtracting the injection volume). (a) Global chromatograms: (b) enlargement of the seconds peaks.

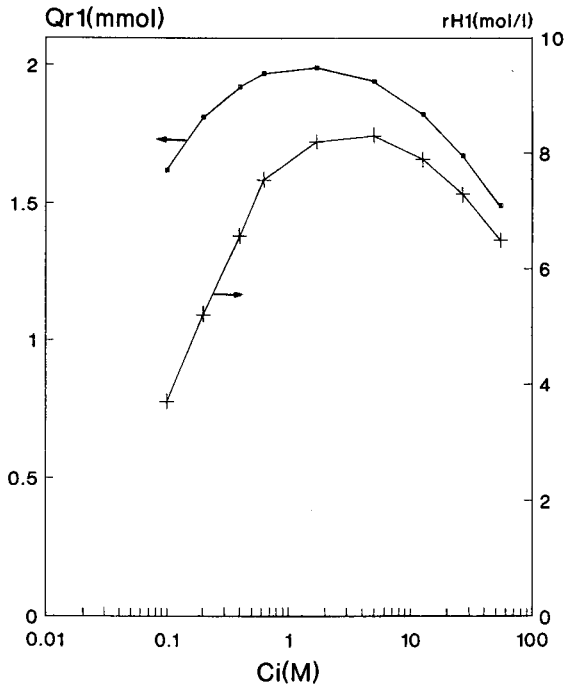

Fig. 8. Dependence of the recovered amount and reduced production rate for 99% pure solute 1 as a function of sample concentration. Mixture: relative composition = 9:1, type A (see Table I). r_i = 85%. n_c = 200 (N_1 = 251, N_2 = 250).

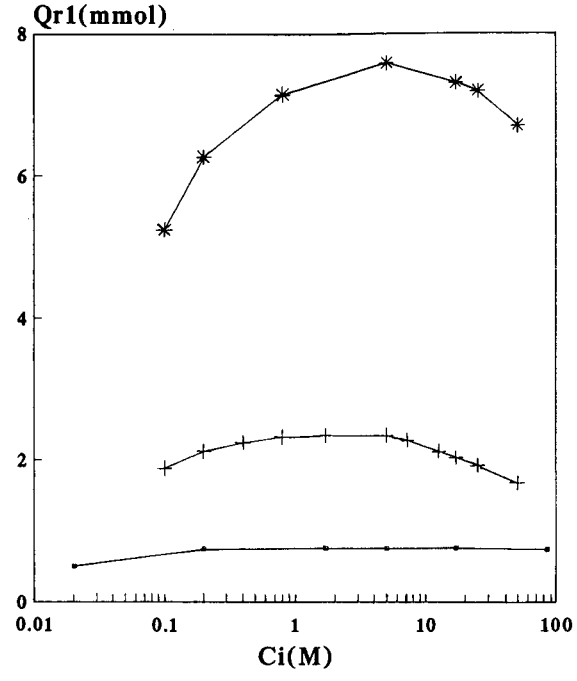

Fig. 9. Plot of the recovered amount of 99% pure solte 1 *versus* the sample concentration for different mixture types. Relative mixture composition: 9:1. r_1 = 75%. n_c = 200 (N_1 = 251, N_2 = 250). + = Mixture type A (parallel solutes): ■ = mixture type B (divergent solutes); ✳ = mixture type C (convergent solutes).

reason is that the run time varies as a function of injection concentration: when the injection concentration is decreased, the injected volume is increased; hence the feed time, the delay before the gradient is introduced at the column inlet and consequently the run-time are increased.

Mixtures with non-constant separation factor. Comparison of the behaviours of parallel, divergent and convergent solute pairs having the same resolution in analytical gradient elution is shown in Fig. 9, which plots the first component amount recovered at 99% purity with a yield of 75% against the sample injection concentration for each mixture type (see Table I). As demonstrated by Snyder *et al.* [10,12], the maximum recovered amount and, consequently, the injectable sample load are increased when we successively consider mixtures of divergent, parallel and convergent solutes. Fig. 9 also shows that the optimum injection concentration is more critically defined for convergent solutes (compared with parallel solutes) and much less marked for divergent solutes. This results from two opposite effects. On the one hand, the injection volume corresponding to the beginning of the column volume overload is independent of the sample size and the corresponding injection concentration decreases with decreasing sample size. On the other hand, as the sample size decreases, the tag-along effect becomes weaker [16] and band broadening of the front base of the second-eluted component appears for higher injected concentrations. This explains why the recovered amount from divergent solute mixtures remains nearly constant within a broad range of injected concentrations.

CONCLUSIONS

We have studied gradient elution under overload conditions for binary mixtures. The findings parallel those deduced from overloaded isocratic elution. For given preparative specifications of recovery ratio and purity level, the maximum amount re-

covered is obtained for certain injection conditions. These optimum injection conditions are critically defined for mixtures of convergent solutes. These cases also correspond to larger samples that can be separated and it is important to optimize accurately the injection conditions with such mixtures. The column efficiency also influences the optimum injection conditions. The optimum injection volume corresponding to the maximum amount recovered is directly proportional to the standard deviation of the Gaussian peak observed at infinite dilution.

SYMBOLS

a_j initial slope of the Langmuir isotherm of solute j (j = 1 or 2)
$a_{0,j}$ value of a_j for φ = 0 (eqn. 5)
b_j coefficient of non-linearity of Langmuir isotherm of solute j (j = 1 or 2)
C_i sample concentration
$C_{m,j}$ equilibrium concentration of solute j in mobile phase (j = 1 or 2)
$C_{s,0}$ value of the saturation concentration of the stationary phase for solute 1 or 2 and whatever the mobile phase composition
$C_{s,j}$ equilibrium concentration of solute j in stationary phase (j = 1 or 2)
D elution flow-rate
g band compression factor (eqn. 10)
G linear rate of change of modulator concentration with elution volume
k'_j capacity factor of solute j under isocratic conditions (j = 1 or 2)
$\overline{k'_j}$ median capacity factor during the gradient run (eqn. 12)
m_j parameter that measures change in a_j value with change in φ (eqn. 5)
n_c stage number of the Craig machine
N_j column plate number under corresponding isocratic conditions
p parameter defined by eqn. 11
Q_i sample amount
$Q_{r,j}$ recovered amount of solute j at a certain purity (j = 1 or 2)
$r_{H,j}$ reduced production rate of solute j (j = 1 or 2) (eqn. 16)
r_j recovery ratio of solute j (j = 1 or 2)
$R_{H,j}$ production rate of solute j (j = 1 or 2)
T run time
V elution volume
$V_{E,2}$ end-point of the chromatogram; elution volume when the eluted concentration of solute 2 is equal to 10^{-8} mol/l
V_i injected volume of sample
V_M column dead volume
$V_{R,j}$ retention volume of solute j under analytical gradient conditions (j = 1 or 2)
ε total porosity of the chromatographic bed
φ modifier concentration in the mobile phase
φ_0 modifier concentration at the start of the gradient
σ_j standard deviation expressed in volume units of the Gaussian peak observed under analytical gradient conditions (j = 1 or 2)

REFERENCES

1 G. Crétier and J. L. Rocca, *Sep. Sci. Technol.*, 23 (1987) 1881.
2 A. Katti and G. Guiochon, *Anal. Chem.*, 61 (1989) 982.
3 V. Svoboda, *J. Chromatogr.*, 464 (1989) 1.
4 G. Crétier, L. Macherel and J. L. Rocca, *J. Chromatogr.*, 590 (1992) 175.
5 J. E. Eble, R. L. Grob, P. E. Antle and L. R. Snyder, *J. Chromatogr.*, 405 (1987) 51.
6 L. R. Snyder, G. B. Cox and P. E. Antle, *J. Chromatogr.*, 444 (1988) 303.
7 G. B. Cox, P. E. Antle and L. R. Snyder, *J. Chromatogr.*, 444 (1988) 325.
8 G. B. Cox, L. R. Snyder and J. W. Dolan, *J. Chromatogr.*, 484 (1989) 409.
9 L. R. Snyder, J. W. Dolan, D. C. Lommen and G. B. Cox, *J. Chromatogr.*, 484 (1989) 425.
10 L. R. Snyder, J. W. Dolan and G. B. Cox, *J. Chromatogr.*, 484 (1989) 437.
11 F. D. Antia and Cs. Horváth, *J. Chromatogr.*, 484 (1989) 1.
12 L. R. Snyder, J. W. Dolan and G. B. Cox, *J. Chromatogr.*, 540 (1991) 21.
13 L. R. Snyder, in Cs. Horváth (Editor), *High Performance Liquid Chromatography—Advances and Perspectives*, Vol. 1, Academic Press, New York, 1980, p, 208.
14 L. R. Snyder and M. A. Stadalius, in Cs. Horváth (Editor), *High Performance Liquid Chromatography—Advances and Perspectives*, Vol. 4, Academic Press, New York, 1987, p. 195.
15 B. L. Karger, L. R. Snyder and Cs. Horváth, *An Introduction to Separation Science*, Wiley-Interscience, New York, 1973, p. 110.
16 S. Golshan-Shirazi and G. Guiochon, *Anal. Chem.*, 62 (1990) 217.

Journal of Chromatography, 596 (1992) 27–41
Elsevier Science Publishers B.V., Amsterdam

CHROM. 23 978

Ion- and ligand-exchange chromatography of proteins using porous zirconium oxide supports in organic and inorganic Lewis base eluents

John A. Blackwell*

3M Company, Specialty Adhesives and Chemicals Division, Group Analytical Laboratory, 236-2B-11, 3M Center, St. Paul, MN 55144-1000 (USA)

Peter W. Carr

Department of Chemistry and Institute for Advanced Studies in Bioprocess Technology, University of Minnesota, 207 Pleasant St. S.E., Minneapolis, MN 55455 (USA)

(First received October 16th, 1991; revised manuscript received December 17th, 1991)

ABSTRACT

The applicability of an eluotropic scale pertaining to the desorption of low molecular weight Lewis base solutes from zirconium oxide is examined for its ability to rationalize the retention of proteins on this substrate. The strongest Lewis base eluents (phosphate and fluoride) are able to bring about elution of nearly all proteins provided that their initial mobile phase concentration almost saturates the eluent's adsorption isotherm. In contrast, weaker Lewis bases such as borate, sulfate and bromide are able to elute only those proteins which are retained primarily by ionic interactions. In weak eluents, proteins that contain a large number of accessible Lewis base sites are not eluted from the support. The effect of ionic strength and a variety of Lewis base eluents were also examined.

INTRODUCTION

Early attempts in this laboratory to separate proteins on zirconium oxide based supports were unsuccessful [1]. Conventional protein ion-exchange elution strategies, consistent with the anticipated amphoteric ion-exchange nature of zirconia, failed to effectively elute many proteins. Elution of a few robust proteins was achieved by use of very high pH values. The resulting peaks were poorly shaped and the proteins were only marginally resolved despite large differences in their isoelectric points and sizes.

Subsequent work showed that proteins could be eluted with good selectivity and efficiency from "phosphated" zirconia supports [1–4]. Treatment of the native metal oxide with boiling phosphoric acid formed a surface coating of zirconium phosphate. This material was found to be very biocompatible and gave very well shaped chromatographic peaks for proteins, but it acted only as a cation exchanger for proteins that have rather high isoelectric points. Such proteins were well retained and could be eluted with ionic strength gradients. By and large, acidic proteins were unretained.

The bio-incompatibility of native zirconia supports is due to Lewis base interactions between protein and exposed Lewis acid (zirconium ion) sites on the particle surface. We have shown that these sites strongly bind those solutes which have accessible Lewis base moieties [5–8]. The "irreversible" binding of many proteins to bare zirconia is a consequence of these acid–base interactions [6,7].

We have shown that fluoride interacts very strongly with these Lewis acid sites, and at an appropriate concentration it can prevent "irreversible" protein adsorption [6,7]. When the fluoride

0021-9673/92/$05.00

concentration in the eluent suffices to nearly saturate the support's Lewis base adsorption isotherm, the residual ligand-exchange interactions between the surface and a protein results in well shaped peaks. Moreover, the balance of cation-exchange and ligand-exchange character of the support formed by this adsorptive surface modification provides unique chromatographic selectivity for the separation of proteins. In many ways, the retention mechanism of proteins on Lewis base modified zirconia surfaces is analogous to that of calcium hydroxyapatite. That is, on hydroxyapatite ligand exchange occurs on exposed calcium sites, and cation exchange takes place on ionized surface hydroxyl and phosphate groups [9–11].

For many proteins, fluoride competes much too strongly and retention is low. The main problem in achieving retention of acidic proteins is the ease of saturation of the fluoride adsorption isotherm [5,7]. Relatively low levels of fluoride block the ligand-exchange interactions and displace acidic proteins [6,7]. As a result, there is not much leeway for modulating the strength of the competitive ligand-exchange interaction through adjustments of the fluoride concentration. This results in a nearly an "on/off" retention process where the protein is either strongly retained or not retained at all. Obviously, adjusting selectivity and resolution is extremely difficult under these circumstances.

We now know that the addition of a very wide variety of inorganic and organic Lewis bases to the eluent can attenuate the interactions of low-molecular-weight solute with the surface [8,12,13]. Carboxylate groups on proteins are the main sites for ligand exchange with Lewis acid sites on zirconia.

In the above studies, a number of competing bases were evaluated in terms of their ability to cause elution of a series of low-molecular-weight carboxylic acids. This led to an eluotropic strength scale for some 30 different Lewis bases [13]. This ranking should be useful in predicting the effect of eluent Lewis bases on the retention of other types of Lewis base solutes in the absence of other strong interactions with the support. The applicability of this eluotropic series to the elution of proteins is the subject of this investigation.

EXPERIMENTAL

Chemicals

N-Tris (hydroxymethyl)methyl-3-aminopropanesulfonic acid (TAPS), 2-(N-morpholino)ethanesulfonic acid (MES) and all proteins were obtained from Sigma (St. Louis, MO, USA). Sodium acetate was from Aldrich (Milwaukee, WI, USA). Hydrochloric acid, acetic acid and sodium fluoride were from Mallinckrodt (St. Louis, MO, USA). Sodium sulfate was obtained from EM Science (Gibbstown, NJ, USA) and 50% sodium hydroxide solution was obtained from CMS Scientific (Houston, TX, USA). Particle pretreatment and solution fluoride measurements were as described in detail earlier [1–7]. All chemicals were reagent grade or better.

Chromatographic supports

The porous zirconium oxide spherules were provided by the Ceramic Technology Center of the 3M Company and were described earlier [1–8, 12–14]. The particles used in this investigation had a nominal diameter of 5.3 μm ± 1.3 μm, an average pore diameter of 308 Å by mercury porosimetry and an average BET surface area of 30.5 m^2/μ. They were suspended in isopropanol and packed at 4500 p.s.i. into 50 × 4.6 mm I.D. columns by the upward slurry method. Titanium screens (2 μm) were used instead of frits to minimize protein losses [15] and to minimize contamination of the column by solubilized metal ions. Whenever the buffer was changed, the column was regenerated by flushing it with approximately 50 ml of 0.1 *M* sodium hydroxide solution followed by 50 ml of freshly boiled (carbon dioxide free) deionized water. This treatment is essential since it removes all irreversibly bound solutes from the zirconia and reproducibly prepares the surface for equilibration in the next buffer [5,7]. The zirconia particles are not damaged at all by this treatment. Some columns of zirconia have been subjected to over fifty cycles of such washes with alkali without any damage to the column.

Chromatographic systems

Chromatographic studies were carried out with a Hewlett-Packard (Avondale, PA, USA) Model 1090M liquid chromatograph equipped with a DR5 ternary solvent delivery system and a diode array detector. This system was outfitted with a 50 × 4.6

mm I.D. pre-column filled with 10–20-μm zirconia particles. This pre-column was placed before the injection valve to remove any contaminants in the buffer. The optional expanded pH range kit as well as ultrahigh-molecular-weight polyethylene piston seals (UPC-10) obtained from Bal Seal Engineering (Santa Ana, CA, USA) were installed. Data were processed using a Hewlett-Packard 9000/Series 300 computer with ChemStation software.

RESULTS AND DISCUSSION

Lewis base gradients at low ionic strength

A variety of proteins were chosen to cover a wide range in molecular weights and isoelectric points. A list of these proteins and their relevant properties is given in Table I [16,17]. These proteins were separated using Lewis base gradients. The results are shown in Table II. Phosphate is known to be the strongest Lewis base of the four shown in Table II [7,13]. It is, therefore, not surprising that most proteins are unretained in this medium. Because adsorption of phosphate is so strong and phosphate desorbs so slowly from zirconia that the surface is not fully equilibrated with the mobile phase before the start of the next gradient, many of the surface Lewis acid sites are occupied even when the eluent phosphate concentration is only 10 m*M*. Although these sorbed phosphate ions strongly inhibit the interaction of proteins with Lewis acid sites, they do provide additional sites for cation exchange by virtue of their ionized hydroxyl groups [2–4, 9–11].

The contribution of cation exchange to the retention of proteins on zirconium oxide in phosphate media is shown by the rather high retention of the cationic proteins (see Table II). Cytochrome *c*, α-chymotrypsin, ribonuclease and lysozyme have very high capacity factors (k') despite the high

TABLE I

PHYSICAL PARAMETERS FOR SELECTED PROTEINS

Values are taken from refs. 16 and 17.

Protein	Abbrev.	Type	p*I*	Molecular weight
Albumin	BSA	Bovine serum	4.7, 4.9	65 400
Albumin	HSA	Human serum	4.6–5.3	69 000
Apotransferrin	ATRH	Human	5.9, 6.0	80 000
Catalase	CAT	Bovine liver	5.8	247 000
Cellulase	CELL	*Asp. niger*	3.9, 4.2, 4.5	52 000
α-Chymotrypsin	αCHY	Bovine pancreas	8.8	21 600
Concanavalin A	CONA	*Can ensiformis*	4.5–5.5	71 000
Cytochrome *c*	CYTC	Horse heart	9.0, 9.4	12 360
Glucose oxidase	GLOX	*Asp. niger*	4.2	186 000
β-Glucuronidase	βGLU	Bovine liver	5.1, 5.9	290 000
Hemoglobin	HEMO	Human blood	6.9–7.4	64 500
Hexokinase	HEXO	Baker's yeast	4.9, 5.3	102 000
Holotransferrin	HTRH	Human		80 000
Laccase	LACC	*Pyr. oryzae*		
β-Lactoglobulin	βLAC	Bovine milk	5.2, 5.3	35 000
Lectin	LEC	Wheat germ		36 000
Lipase	LIP	Porcine pancreas	5.2, 5.5	60 000
Lysozyme	LYS	Chicken egg white	11.0	14 306
Mucin	MUC	Porcine stomach		40 000
Myoglobin	MYO	Equine muscle	6.8, 7.3	17 500
Ovalbumin	OVA	Egg white	4.7	43 500
Pepsin	PEP	Porcine mucosa	2.2, 2.8	33 000
Phosphatase, alk.	ALKP	Chicken intestine	5.7	140 000
Ribonuclease A	RNA	Bovine pancreas	9.3	13 683
Ribonuclease B	RNB	Bovine pancreas	9.3	14 700
Trypsin inhibitor	TINH	Soybean	4.5	20 091

TABLE II

CAPACITY FACTORS FOR VARIOUS PROTEINS WITH LEWIS BASE GRADIENTS AT LOW IONIC STRENGTH

Linear gradient from 2% to 100% B in 30 min then back to 2% B in 15 min followed by a 15 min-equilibration period. Injections were 10 μl of a 10 mg/ml protein in buffer A solution. Detection was at 280 and 410 nm. – = Elution not observed.
Buffer A = 20 m*M* MES at pH 6.1 or 20 m*M* TAPS at pH 8.4.
Gradient I: B = 0.5 *M* sodium phosphate in 20 m*M* MES (pH 6.1) or 20 m*M* TAPS (pH 8.4).
Gradient II: B = 0.5 *M* sodium fluoride in 20 m*M* MES (pH 6.1) or 20 m*M* TAPS (pH 8.4).
Gradient III: B = 0.5 *M* sodium sulfate in 20 m*M* MES (pH 6.1) or 20 m*M* TAPS (pH 8.4).
Gradient IV: B = 0.5 *M* sodium borate in 20 m*M* MES (pH 6.1) or 20 m*M* TAPS (pH 8.4).

Protein	*k'*							
	Gradient I		Gradient II		Gradient III		Gradient IV	
	pH 6.1	pH 8.4	pH 6.1	pH 8.4	pH 6.1	pH 8.4	pH 6.1	pH 8.4
Pepsin	−0.3	−0.3	–	−0.3	–	–	–	−0.3
Cellulase	−0.2	−0.2	–	−0.3	–	–	–	−0.3
Glucose oxidase	−0.3	−0.3	–	−0.3	–	–	–	−0.3
Trypsin inhibitor	−0.3	−0.2	0.2	5.8	–	–	–	4.3
Bovine albumin	−0.3	−0.3	–	4.1	–	–	–	−0.3
Human albumin	−0.3	−0.3	–	3.5	–	–	–	−0.3
Concanavalin A	–	−0.3	–	–	–	–	–	8.3
Hexokinase	0.3	−0.3	0.6	3.9	2.9	–	4.1	3.7
β-Lactoglobulin	−0.3	−0.3	–	−0.3	–	–	–	4.4
Lipase	0.3	−0.2	0.6	2.2	2.9	1.9	3.5	3.7
β-Glucuronidase	−0.1	−0.3	0.8	3.4	3.1	–	4.1	4.1
Phosphatase, alk.	−0.3	−0.3	0.2	−0.3	3.0	0.2	4.1	0.1
Catalase	−0.3	−0.3	–	4.5	–	–	–	−0.3
Apotransferrin	8.3	−0.3	25.5	–	–	–	–	4.7
Myoglobin	9.3	0.0	24.1	5.9	–	–	–	5.7
Hemoglobin	25.1	−0.3	–	3.8	–	–	–	3.8
α-Chymotrypsin	22.0	11.0	22.8	23.2	–	–	–	3.8
Cytochrome	–	22.3	–	–	–	–	–	–
Ribonuclease A	20.9	8.6	23.7	21.0	–	20.6	–	–
Ribonuclease B	14.2	5.7	13.1	13.2	–	20.7	–	–
Lysozyme	15.9	7.9	11.9	14.9	–	17.8	–	–
Holotransferrin	8.5	−0.3	–	–	–	–	–	4.5
Laccase	0.1	−0.1	0.1	–	–	–	–	–
Lectin	−0.2	−0.2	–	–	–	–	–	–
Mucin	−0.2	−0.2	0.6	3.9	3.2	3.0	4.0	4.3

eluent ionic strength at the point of elution (approximately 0.35 *M* phosphate). Ligand-exchange interactions between the protein and the surface Lewis acid sites are still possible, but they are attenuated at this high phosphate concentration. This, however, does not preclude changes in selectivity due to minor contributions from ligand-exchange interactions. Fig. 1 shows that closely related proteins can be well resolved using strong phosphate eluents. In this case, commercial ribonuclease preparations are well resolved into the A and B sub-types which differ only in their degree of glycosylation.

The elution behavior of the acidic proteins in fluoride media at pH 6.1 (see Table II) is quite different from that observed in our previous studies [6,7]. This is because the initial fluoride concentrations were very different. In the earlier studies [6,7], the initial fluoride concentration was about 20 m*M*. This is sufficient to nearly saturate the fluoride adsorption isotherm and provides very strong competition for the incoming proteins. The net effect was to make protein retention quite weak, since Lewis base solutes are readily displaced by fluoride [5–7, 13].

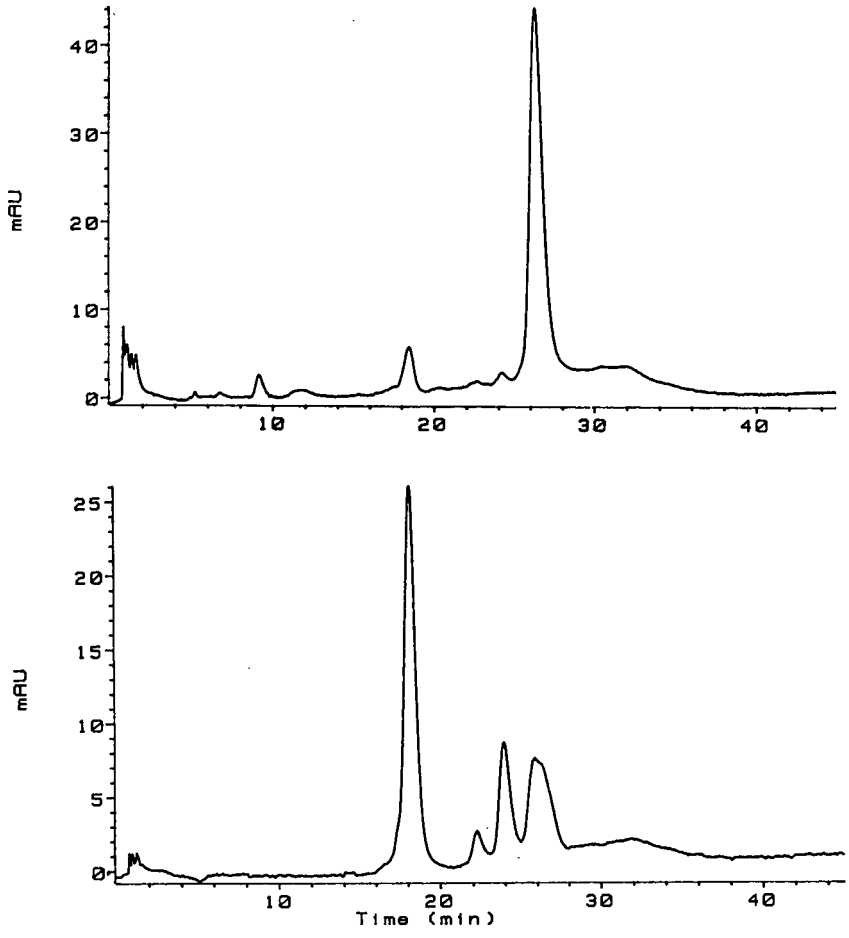

Fig. 1. Separation of commercial preparations of ribonuclease A (top) and ribonuclease B (bottom) from bovine pancreas. Linear gradient elution from 98% A (20 m*M* MES pH 6.1) to 100% B (0.5 *M* sodium phosphate, 20 m*M* MES pH 6.1) in 30 min, then back to 98% A in 15 min with a 15-min equilibration pertiod. Injections were 10-μl volumes of 10 mg/ml solutions in buffer A. Flow-rate was 0.5 ml/min at 35°C.

In the present experiment (Table II), the initial fluoride concentration was reduced to only 10 m*M*. This low concentration of fluoride relative to that used in prior work (20 m*M*) leaves a substantial number of Lewis acid sites available for interaction with Lewis base solutes. Thus proteins "stick" very strongly to the Lewis acid sites, and are not as readily displaced as when the an initially higher fluoride concentration is used. We believe that once one site on a polyvalent Lewis base is sorbed, additional Lewis sites on the same molecule then readily interact with unblocked Lewis acid sites on the support. One can view this as a local concentration effect or as an entropic effect related to the chelate effect. The result is that retention and elution are very strongly dependent on the number of available (unblocked) Lewis acid surface sites at the start of the gradient. Most likely, such multiply-coordinated solutes desorb rather slowly upon an increase in the fluoride concentration. This effect should be much more pronounced for acidic proteins and especially for those proteins containing proximal carboxylic acid groups capable of forming chelates with the surface.

We believe that the presence of proximal acidic amino acids in a protein plays an important role in determining the strength of the eluent needed to desorb a protein. Table III indicates the number and location of the acidic amino acids for some of

TABLE III

LOCATION OF ACIDIC AMINO ACID RESIDUES IN TEST PROTEINS

Taken from ref. 18.

Protein	Acidic residues
Cytochrome *c* (horse)	Asp(2), Glu(4), Glu(21), Asp(50), Glu(61), Glu(62), Glu(66), Glu(69), Glu(90), Glu(92), Asp(93), Glu(104)t[a]
Lysozyme (egg)	Glu(7), Asp(18), Glu(35), Asp(48), Asp(52), Asp(66), Asp(87), Asp(101), Asp(103), Asp(119)
Ribonuclease A (bovine)	Glu(2), Glu(9), Asp(14), Asp(38), Asp(53), Asp(83), Glu(86), Glu(111), Asp(121)

[a] t = Terminal residue

the proteins used in this study [18]. Many amino acids with ionized side chains are present on a protein's surface and may be available for interaction with a stationary phase. Lysozyme is retained on zirconium oxide in the presence of fluoride mainly by electrostatic interactions [6,7]. The amino acid content of lysozyme shows that 10 of its 129 amino acids are acidic [18]. However, most of these acidic residues are separated by other amino acids and offer little chance to form chelates on the zirconia surface. The aspartic acid residues at positions 101 and 103 may show some strengthening of the ligand exchange interaction due to their proximity, however, studies with small solutes have shown that the importance of chelation decreases rapidly as the ring size increases (*cf.* succunic acid *vs.* iminodiacetic acid [7,13]). As a result, lysozyme does not show any strong ligand exchange character.

Cytochrome *c* behaves quite differently. Table II shows that it is hard to elute cytochrome *c*, even when strong Lewis bases such as phosphate and fluoride are used. Its amino acid sequence suggests that this may be due to the presence of many (12 out of 104) proximal acidic amino acid residues. Ribonuclease A behaves similarly to lysozyme in that it shows little ligand-exchange character. This may be due to either a lower proportion of acidic amino acids (9/124) or the spatial separation of the acidic residues.

Weaker Lewis bases, such as sulfate and borate, are less effective in displacing proteins which are strongly retained by ligand exchange. This is especially true at eluent concentrations below the point of isotherm saturation. The result is "irreversible" binding of most proteins with no clear elution pattern (see solutes denoted as "−" in Table II).

When the same study was conducted at a higher pH, a few notable changes in the elution pattern were observed. These results are also shown in Table II. Most elution changes can be predicted based on the isoelectric points of the proteins. At higher pH values, the anion charge density on the stationary phase increases as the surface hydroxyl groups and bound phosphate groups become more ionized. This should increase retention for cationic proteins. However, this effect is offset by the increased competition by hydroxyl ions for the Lewis acid sites. The net result for a given protein is due to the relative contributions of cation and ligand-exchange to retention.

In phosphate media the retention of all proteins decreased upon increasing the pH. The same is true in sulfate media. However, in fluoride media the retention of hexokinase, lipase and mucin increased upon increasing the pH. In borate the retention of lipase and mucin increase, but only slightly, when the pH was raised. The decrease in retention is due to two factors. First, at higher pH the hydroxide concentration is greater. Hydroxide is the strongest known Lewis base towards zirconia and thus it is a very powerful displacing agent. Second, at higher pH the proteins are less positively charged and therefore are held less strongly by cation exchange. Clearly, pH is an important variable that can be used to elute proteins once the Lewis acid sites on the surface are moderated by use of a competing Lewis base in the eluent.

Lewis base gradients at high ionic strength

The study reported in Table II was repeated using a higher ionic strength to attenuate ion-exchange contributions to retention; the results are shown in Table IV. The ionic strength was increased by adding 0.5 *M* sodium chloride, since chloride is a very weak Lewis base towards zirconia [19]. The major trend observed in Table IV is that the retention of almost all proteins that were well retained (k' greater than 1) at low ionic strength (Table II) decreased

TABLE IV

CAPACITY FACTORS FOR VARIOUS PROTEINS WITH LEWIS BASE GRADIENTS AT HIGH IONIC STRENGTH

Conditions as in Table II except buffer A contained 0.5 *M* sodium chloride in addition to the MES or TAPS. – = Elution not observed.

Protein	*k'*							
	Gradient I		Gradient II		Gradient III		Gradient IV	
	pH 6.1	pH 8.4	pH 6.1	pH 8.4	pH 6.1	pH 8.4	pH 6.1	pH 8.4
Pepsin	0.0	−0.1	–	0.1	–	–	–	4.3
Cellulase	0.0	0.0	–	0.1	–	0.1	–	4.2
Glucose oxidase	0.0	0.0	–	–	–	–	–	–
Trypsin inhibitor	0.1	0.0	0.2	–	–	–	–	4.7
Bovine albumin	0.0	−0.1	–	–	–	–	–	4.5
Human albumin	0.0	−0.1	–	–	–	–	–	4.6
Concanavalin A	–	3.1	–	–	–	–	–	–
Hexokinase	0.1	0.0	0.2	2.5	2.4	0.1	1.9	4.1
β-Lactoglobulin	–	0.0	–	0.1	–	0.1	–	4.4
Lipase	0.1	0.1	0.2	1.3	2.5	0.7	1.7	4.0
β-Glucuronidase	0.1	0.0	–	0.1	2.6	0.1	3.1	4.5
Phosphatase, alk.	0.1	0.0	0.2	0.1	2.5	0.1	3.1	0.1
Catalase	0.1	0.0	–	0.1	–	0.1	–	4.9
Apotransferrin	0.8	0.0	–	22.2	–	–	–	4.7
Myoglobin	1.4	0.1	11.6	5.3	–	18.1	–	4.3
Hemoglobin	10.0	0.0	15.4	13.2	–	–	–	4.2
α-Chymotrypsin	3.2	1.3	12.4	6.9	25.6	18.0	–	6.4
Cytochrome *c*	35.1	11.5	13.9	–	–	–	–	–
Ribonuclease A	5.1	0.9	7.6	4.3	–	5.47	–	4.7
Ribonuclease B	1.4	0.4	0.9	4.6	–	5.2	–	4.5
Lysozyme	0.9	0.3	0.7	1.4	–	3.2	9.4	2.7
Holotransferrin	1.4	0.0	–	–	–	–	–	5.2
Laccase	0.0	0.0	0.1	–	–	–	–	–
Lectin	0.0	0.0	–	–	–	–	–	–
Mucin	0.0	0.0	60.2	2.5	3.0	0.1	3.5	4.9

upon increasing the ionic strength. This trend was followed by virtually all proteins at both pH values in phosphate media. There are a few significant exceptions most notably concanavalin A. For example, at pH 8.4 its k' is 3.1 at high ionic strength (Table IV) but drops to −0.3 at low ionic strength (Table II).

The changes in retention with ionic strength in fluoride buffer are similar to those in phosphate media except that almost all proteins are more retained in fluoride. Note that a few changes in the elution sequence do take place.

Not much was learned in sulfate and borate buffer because even upon increasing the ionic strength most of the proteins still did not elute. However, where proteins were eluted the changes in retention upon increasing the ionic strength were not as large as the effect in phosphate and fluoride media. Those proteins which do elute in these buffers show some decrease in retention suggesting that there are some ionic contributions to retention but that ligand exchange interactions are dominant.

Retention in borate media is clearly rather unusual. At low pH, only a few proteins elute at either low or high ionic strength. This indicates that the retention process is not ionic. "Irreversible" retention occurs for both acidic and basic proteins. Even more curious are the retentive properties at pH 8.4. Those proteins that are weakly retained at high pH and low ionic strength, such as pepsin through human albumin, actually show an increase in retention upon increasing ionic strength. This is very

strange behavior for an ion-exchange separation, but vaguely reminiscent of hydrophobic interaction chromatography. At low ionic strength, the borate system acts like a cation exchanger. This is consistent with studies which show that adsorption of borate reaches a maximum at a pH near borate's first pK_a (9.24) [20]. This results in a higher surface coverage by borate at pH 7.4 relative to pH 6.1. Borate is also more ionized at the higher pH, thereby generating a higher negative charge. Some acidic proteins are excluded, the others are retained by non-ligand-exchange interactions. Neutral proteins behave like the acidic proteins, but not all basic proteins are eluted under these conditions.

Upon decreasing the ionic interactions (Table IV), the residual retention of acidic, neutral and basic proteins appear to be similar. Most proteins are eluted at nearly the same borate buffer concentration. This effect may indicate non-specific adsorptive processes. Additional experiments in borate media are given below.

Retention of tightly bound proteins

A number of proteins are very well retained despite the use of very strong elution conditions (see Table V). In gradient I (see Table V for conditions) only a few proteins are retained. This may be due to any of three factors. First, the ionic strength is very high throughout the gradient (1.5 *M*). Second, the initial fluoride concentration (30 m*M*) virtually completely saturated the Lewis acid site adsorption isotherm, thereby strongly attenuating the ligand-exchange interactions. Finally, the starting conditions (0.5 *M* sulfate) also served to saturate the Lewis acid adsorption isotherm.

In gradient II, most proteins were retained. This

TABLE V

ELUTION OF TIGHTLY BOUND PROTEINS USING VARIOUS ELUTION STRATEGIES: CAPACITY FACTORS AT pH 6.1

Linear gradient elution at 0.5 ml/min and 35°C was used. Gradients were from 2% B to 100% B in 30 min then back to 2% B in 15 min followed by a 15-min equilibration period. Injections were 20 µl of 10 mg/ml solution of protein in 0.5 *M* K_2SO_4 20 m*M* MES pH 6.1. – = Elution not observed. Buffers were as follows:
Gradient I: A = 0.5 *M* K_2SO_4, 20 m*M* MES, pH 6.1; B = 1.5 *M* KF, 20 m*M* MES, pH 6.1.
Gradient II: A = 1.5 *M* KCl, 20 m*M* MES, pH 6.1; B = 1.5 *M* KF, 20 m*M* MES, pH 6.1.
Gradient III: A = 1.5 *M* KCl, 20 m*M* MES, pH 6.1; B = 0.5 *M* K_2SO_4, 20 m*M* MES, pH 6.1.
Gradient IV: A = 0.5 *M* K_2SO_4, 20 m*M* MES, pH 6.1; B = 50 m*M* KF, 0.5 *M* K_2SO_4, 20 m*M* MES, pH 6.1.

Protein	p*I*	Mol. wt.	*k'*			
			Gradient			
			I	II	III	IV
Albumins:						
ovalbumin	4.7	43 500	1.5	6.4	–	–
human serum	4.6–5.3	68 460	0.1	8.3	–	15.1
bovine serum	4.7, 4.9	65 400	0.1	6.4	–	16.2
bovine (maltosyl)			0.1	6.4	–	16.2
sheep serum			0.1	7.1	–	14.4
horse serum		68 600	0.1	8.0	–	15.7
pig serum			0.2	8.2	–	16.2
β-Lactoglobulin	5.1, 5.3	17 500	0.3	6.7	–	15.0
Hemoglobin	6.9–7.4	16 000	0.1	0.2	–	0.8
Alcohol dehydrogenase	8.7–9.3	41 000	0.2	6.1	–	7.4
Creatine phosphokinase	6.6–6.9	40 000	0.4	3.4	–	11.8
Transferrins:						
human, apo	5.9	80 000	0.0	1.8	–	6.9
human, holo			0.1	1.9	–	8.1
bovine, apo			0.1	6.3	–	14.1

clearly shows the effect of the higher Lewis basicity of sulfate compared to chloride since the same ionic strength was used in both gradients. Comparison of the retention data under gradients I and II demonstrates that, although the Lewis acid sites were nearly saturated by fluoride, the presence of sulfate obviously had a strong effect on retention. In gradient II most of the albumins had capacity factors of about 7, however, some selectivity between variants is evident. More dramatic differences in retention were observed with the apotransferrin variants. Human and bovine variants are well separated despite very minor differences in their amino acid compositions.

As shown by the data obtained in gradient III (which did not contain any fluoride) sulfate gradients cannot induce the tightly bound proteins to elute. The initial low concentration of sulfate (10 m*M*) does not saturate the adsorption isotherm and the lower binding constant of sulfate with zirconium ion, relative to fluoride [19], combine to preclude elution.

Gradient IV is a modification of the first gradient. These data demonstrate that only a small amount of fluoride is needed to bring about elution of the tightly bound proteins once ligand-exchange interactions have been attenuated by other species. The initial fluoride concentration was only 4 m*M*, which is far below the amount needed to saturate the adsorption isotherm. We conlude that sulfate must be responsible for some attenuation of the ligand-exchange interactions. Higher fluoride concentrations cover more Lewis acid sites. Most proteins elute when the concentration of fluoride is approximately 20 m*M* (isotherm saturation); since fluoride's formation constant with Zr(IV) is so much larger than the other competing bases it is by far the more important Lewis base. In gradient IV, as in gradient II, a fair degree of selectivity between variants was obtained for the albumins and the transferrins.

These results demonstrate some important operational aspects of controlling the ligand-exchange interactions between proteins and zirconia surfaces. As is also true with hydroxyapatite supports, adsorption and desorption do not correspond to the reversal of the same process [9–11]. Unless the strength of the Lewis acid sites are initially attenuated by addition of a competing ligand prior to loading the sample, these sites will cause very strong adsorption of proteins as described above. These observations are in good agreement with the hypothesis of Van Oss *et al.* [21] concerning protein binding processes. Adsorption, which is driven by long range interactions such as Coulombic and Van der Waals interactions, may be accentuated by other attractive interactions. Once long range interactions have drawn the attracting bodies into close proximity, short range interactions augment the attraction between these two bodies. In this work, the ligation of a single Lewis base to a Lewis acid site promotes further Lewis interactions. In addition, hydrogen bonding, which is normally masked in aqueous solutions, is facilitated by the close proximity of bonding groups. The result is that a very strong adsorptive interaction can take place once a single ligating bond is formed. Therefore, to overcome the deleterious effects of strong binding on chromatographic efficiency, the ligand-exchange interaction must be labilized as much as possible.

A final comment concerning the effect of the various displacing ligands on protein selectivity is in order. When only fluoride is used to desorb the tenaciously bound proteins, the elution pattern is different from when fluoride is used to displace proteins which are not tightly bound. In gradient II, bovine albumin was more retained than its maltosyl derivative. However, the change in retention mechanism in gradient IV allows the maltosyl derivative to be more retained than the underivatized albumin.

Retention of acidic proteins

A dozen acidic proteins were examined at pH 6.1 and 8.4 using linear Lewis base gradients under conditions of nearly constant ionic strength. Table VI shows the results using four Lewis base eluents ranging in strength from fluoride to acetate. Based on the acidic proteins tested here, fluoride is the strongest competitive ligand. All of the acidic proteins can be eluted at low pH, although some proteins are rather well retained. This high retention did not correlate with the protein's isoelectric point or molecular weight. Presumably, the high retention is due to the spatial arrangement of Lewis bases on the protein surface.

We also note that the pH effects are not simple. For some proteins, retention increased with pH

TABLE VI

ACIDIC PROTEIN RETENTION VERSUS LEWIS BASE STRENGTH: CAPACITY FACTORS

Linear gradient elution at 0.5 ml/min and 35°C from 2% to 100%B in 30 min followed by a return to 2% B in 15 min. A 15-min equilibration period followed each gradient run. Injections were 20 μl of 10 mg/ml solutions of protein in buffer A. Detection was at 280 and 410 nm. – = Elution not observed.
Gradient I: A: 1 *M* NaCl, 20 m*M* MES, pH 6.1; B: 1 *M* KF, 20 m*M* MES, pH 6.1.
Gradient II: A: 1 *M* NaCl, 20 m*M* MES, pH 6.1; B: 0.33 *M* Malic acid, 20 m*M* MES, pH 6.1.
Gradient III: A: 1 *M* NaCl, 20 m*M* MES, pH 6.1; B: 0.33 *M* Na_2SO_4, 20 m*M* MES, pH 6.1.
Gradient IV: A: 1 *M* NaCl, 20 m*M* MES, pH 6.1; B: 1 *M* Sodium acetate, 20 m*M* MES, pH 6.1.

Protein	*k'*							
	Gradient I		Gradient II		Gradient III		Gradient IV	
	pH 6.1	pH 8.4	pH 6.1	pH 8.4	pH 6.1	pH 8.4	pH 6.1	pH 8.4
Fetuin	4.0	–	–	–	–	–	–	–
Cellulase	0.2	–	0.3	0.1	1.8	3.7	2.4	3.5
Trypsin inhibitor	17.1	0.0	–	0.4	–	1.4	–	1.5
Ovalbumin	18.3	25.6	–	–	–	–	–	–
Bovine albumin	2.6	–	–	–	–	–	–	–
Human albumin	27.3	–	–	–	–	–	–	–
β-Lactoglobulin	24.7	–	0.1	–	–	–	–	–
Insulin	20.1	4.9	–	2.6	–	–	–	25.9
Peroxidase	0.5	2.5	0.2	0.3	2.0	1.9	2.8	8.4
Phosphatase, acid	0.2	0.3	0.3	0.4	1.7	4.3	2.2	2.1

whereas in other studies (Table II and IV) the general trend was for retention to decrease with an increase in pH. This suggests that acidic proteins can behave quite distinctly from neutral and basic proteins in these chromatographic systems. While this greatly complicates understanding the mechanism of retention it suggests that the separation chemistry exhibited by zirconia in Lewis base media offers great promise for unique selectivities.

Lewis bases that are weaker than fluoride leave many strongly retained proteins bound to the support. Some proteins which were weakly retained in fluoride buffers are eluted by the weaker bases. The capacity factors are, however, higher. This increase in capacity factor for these proteins closely follow the eluotropic strength of each of the Lewis bases as established in our study of the retention of benzoic acid derivatives. Deviations from this eluotropic sequence were not observed, except for horseradish peroxidase in malate buffer. This agreement occurs despite the many other types of interactions between proteins and the support.

Fig. 2 shows a correlation of the capacity factor for acidic proteins with eluotropic strength (denoted *E*). *E* is arbitrarily defined as the capacity factor for paracyanobenzoic acid in 20 m*M* Lewis base–20 m*M* MES at pH 6.1 [12,13]. The "levelling" of the

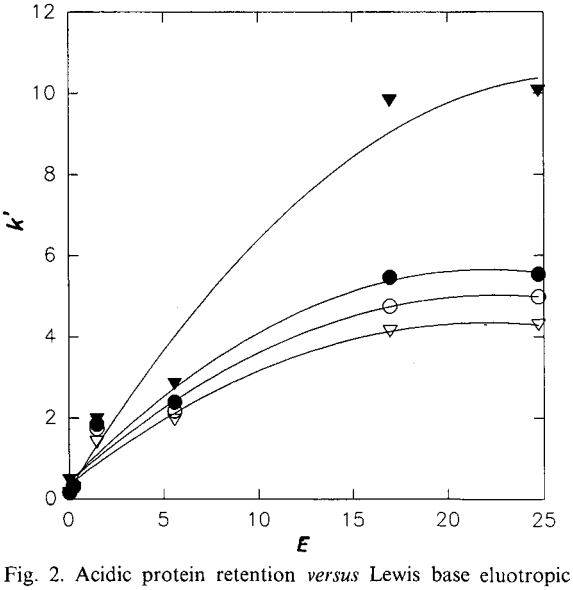

Fig. 2. Acidic protein retention *versus* Lewis base eluotropic strength. ▼ = Horseradish peroxidase; ● = cellulase; ○ = acid phosphatase; ▽ = hexokinase. Elution was a linear Lewis base gradient at 0.5 ml/min and 35°C. See Table II for gradient details.

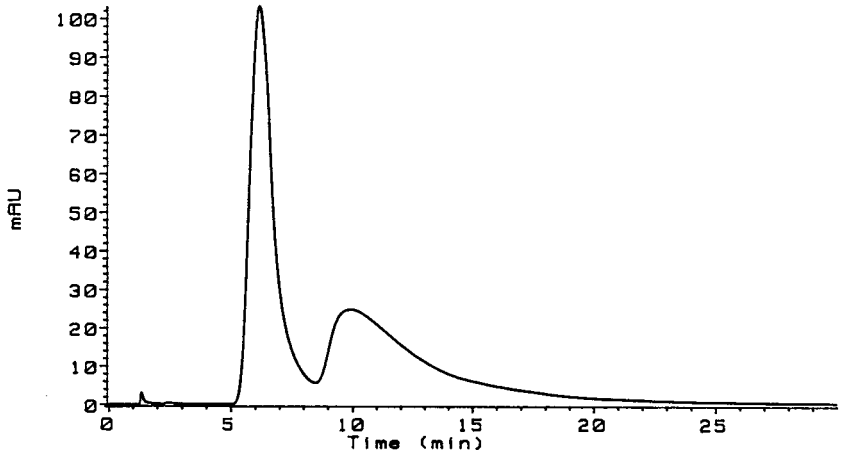

Fig. 3. Separation of hexokinase (baker's yeast) proteins PI and PII. Linear gradient elution from 98% A (1 *M* sodium chloride, 20 m*M* MES pH 6.1) to 100% B (1 *M* sodium bromide, 20 m*M* MES pH 6.1) in 30 min, then back to 98% A in 15 min with a 15-min equilibration period. Injections were 10-μl volumes of 10 mg/ml solutions in buffer A. Flow-rate was 0.5 ml/min at 35°C.

capacity factor at high *E* (low eluotropic strength) is due to the effect of the MES buffer. The sulfonic acid group on the MES molecule is a Lewis base which is stronger than either bromide or chloride, but weaker than the other bases. Therefore, the resulting eluotropic strength of the buffer is dominated by this buffer and not by the added ligand (bromide, chloride).

This does not mean that the weak displacing anion is of no importance. Fig. 3 shows that the hexokinase sub-types (PI and PII) are readily separated by a gradient from chloride to bromide. All other aspects of the weak and strong buffers were identical. Although the peak shapes are not satisfying, this separation shows that even weak Lewis base gradients can be useful. It should be noted that isocratic elution of the same sample in the chloride buffer failed to elute the second protein and when a bromide eluent was used the peaks were not resolved.

Ionic strength gradients

Based on the above, it is clear that gradient elution with changes in the concentration of the Lewis base are chemically and chromatographically very complex. In order to study the differential effect of a chemically wide variety of Lewis bases under the simplest possible conditions the experiment described in Table VII was implemented. In this study, the Lewis base concentration was held constant throughout the gradient and the ionic strength was increased by varying the concentration of sodium chloride.

The data in phosphate media show that many proteins are not affected by the changes in the gradient. The acidic proteins, which are not retained to any significant extent, remain relatively unretained. However, cationic proteins (*e.g.* β-lactoglobulin, apotransferrin, ribonuclease, etc.) all show significantly higher capacity factors relative to the conditions in Table II. This is not surprising since these proteins are primarily retained by cation exchange and the chloride gradient used in Table VII has a lower ionic strength than the phosphate gradient used in Table II. Additional retention probably results from ligand-exchange interactions. Since these proteins do show some ligand-exchange character, this retention process will be accentuated at a low, constant Lewis base concentration compared to conditions where the gradient rapidly swamps the ligand-exchange equilibria.

The results in the fluoride buffer are also interesting. A higher ionic strength was used here than in Table II. Given this, it is interesting to note that some proteins are more retained in this experiment than that described in Table II. Once again, the changes in retention do not correlate with protein isoelectric point or molecular weight. More likely, the differences are due to the complex balance of ligand- and ion-exchange contributions to retention in the systems reported here.

TABLE VII

PROTEIN RETENTION WITH IONIC STRENGTH GRADIENTS AND CONSTANT LEWIS BASE CONCENTRATIONS

Linear gradient elution from 2% B to 100% B in 30 min, then back to 2% B in 15 min with a 15-min equilibration period. Flow-rate was 0.5 ml/min at 35°C. Injections were 10 μl volumes of 10 mg/ml solutions of protein in 20 m*M* TAPS at pH 8.4. Detection was at 280 and 410 nm. Buffer A: 20 m*M* Lewis base in 20 m*M* TAPS at pH 8.4; buffer B: buffer A with 1 *M* sodium chloride. – = Elution not observed. Lewis bases: A = sodium phosphate; B = sodium fluoride; C = boric acid; D = citric acid; E = aspartic acid; F = tartaric acid; G = iminodiacetic acid; H = aminomethylphosphonic acid; I = ethylphosphonic acid; J = O-phospho-DL-serine.

Protein	*k'*									
	Gradient									
	A	B	C	D	E	F	G	H	I	J
PEP	−0.3	−0.3	−0.3	−0.3	−0.3	−0.3	−0.3	−0.3	−0.3	−0.3
GLOX	−0.3	–	−0.3	−0.3	1.2	−0.3	–	−0.3	−0.3	−0.3
TINH	−0.2	0.1	0.1	0.0	0.2	0.0	0.2	0.0	−0.2	−0.2
OVA	−0.2	–	–	−0.2	–	0.2	–	−0.2	−0.2	−0.2
HSA	−0.3	–	−0.3	−0.3	−0.3	−0.3	–	−0.3	−0.3	−0.3
HEXO	−0.2	1.6	1.9	0.5	1.3	1.3	3.0	0.1	−0.3	0.1
βLAC	–	–	–	–	–	–	–	−0.3	−0.3	−0.2
LIP	0.2	1.2	1.3	0.5	1.3	1.3	2.2	0.1	0.5	0.1
ATRH	12.0	–	–	0.1	–	0.0	–	−0.1	−0.2	−0.2
MYO	11.6	14.5	13.4	1.1	26.9	3.8	–	0.3	0.7	0.1
HEMO	19.4	20.0	14.4	−0.1	–	−0.1	–	−0.1	−0.2	−0.1
αCHY	13.8	–	–	12.5	22.5	14.5	–	6.3	14.2	8.8
CYTC	23.4	–	–	23.3	–	26.2	–	11.3	26.4	16.5
RNA	15.1	13.0	13.2	9.9	14.1	11.0	18.8	6.6	11.3	7.4
RNB	11.1	12.8	13.0	8.5	13.7	9.7	18.9	3.8	9.5	6.2
LYS	10.9	9.4	11.2	10.5	12.8	10.2	12.6	5.9	15.1	8.1

Retention in borate buffers is comparable to that in fluoride media. Proteins which are more retained in borate media rely more on ligand-exchange interactions than ionic interactions. However, slight differences in selectivity are apparent between fluoride and borate buffers, indicating that secondary interactions (hydrogen bonding, etc.) between the proteins and the bound Lewis bases may be important.

Lewis base buffers which contain more than one Lewis base functional group per molecule (*e.g.* citrate) stick much more tightly to the surface than do monovalent buffer Lewis bases (*e.g.* acetate). One consequence of this effect is that the adsorption isotherm for polyvalent Lewis bases will saturate at much lower buffer concentrations than those of monovalent bases. Therefore, lower concentrations of these species can be used to promote the elution of Lewis base solutes. This can also help promote elution by reducing the mean number of available Lewis acid sites.

To determine the effect that these polyvalent organic Lewis bases have on protein retention, a number of proteins were examined in such systems. The results of this study are shown in Table VII. According to our previously developed eluotropic scale, the displacing strength of the bases should be: citric acid > aspartic acid > tartaric acid > iminodiacetic acid. This trend was observed for many of the proteins studied here. Proteins such as hexokinase, lipase and ribonuclease A followed clear trends, while some proteins showed a different pattern of retention.

Acidic proteins, in general, were not well retained in polyvalent Lewis base buffers. The eluent base simply out-competed the protein for the Lewis acid sites on the surface. Basic proteins, on the other hand, may be retained by cation exchange in the absence of strong ligand-exchange contributions to retention.

Glucose oxidase was slightly retained in the aspartic acid buffer, but not in any other buffer, other than iminodiacetic acid. The elution strength of imi-

nodiacetic acid may not be sufficient to overcome ligand-exchange interactions. Aspartic acid is probably bound to the surface via its two carboxylate groups. The amino functional group is fully protonated at this pH and should be available for ionic interactions with solutes. This anion-exchange capacity would allow anionic proteins to be retained. Myoglobin, α-chymotrypsin, ribonuclease and lysozyme all show this interesting retention pattern in the aspartic acid buffer.

In contrast to the results obtained with monovalent bases, protein retention in polyvalent base eluents is not in good agreement with the eluotropic scale (*E*) described above. Based on the *E* scale fluoride should be a stronger competitor than any of the organic ligands. Many proteins did not elute in fluoride media but do elute in citrate, aspartate and tartrate eluents.

Secondary interactions are a second major source of differences in the behavior of polyvalent bases. As in the case of aspartic acid, the non-chelating portion of the buffer Lewis base is free to interact with the solutes. This can result in additional ionic and hydrophobic interactions with the solute.

It is often necessary to use very strong buffer Lewis bases to elute proteins from zirconium oxide. Phosphate and fluoride both suffice, but both produce more or less the same selectivity. An approach to inducing significant changes in selectivity while still maintaining high eluotropic strength is to use ligands with phosphate or phosphonic acid groups. This idea was tested by studying retention in eluents containing organophosphonates (see Table VII). Most of the acidic proteins were not well retained. The phosphate portion of the ligand competes too well for the available ligand-exchange sites and residual electrostatic interactions only serve to promote elution. Low retention is observed despite the presence of cationic amino groups on aminomethylphosphonic acid and O-phospho-DL-serine.

Basic proteins were well retained in these buffers. Secondary interactions, however, caused some significant changes in elution patterns among these proteins. All proteins which were retained had their greatest retention in the ethylphosphonic acid buffer. O-phospho-DL-serine is the next stronger Lewis base buffer, however, myoglobin was less retained in it than in aminomethylphosphonate. Aminomethylphosphonic acid is the strongest buffer and offers the greatest selectivity between ribonuclease A and B. This is no doubt due to the secondary interactions between the support and proteins.

Borate buffers

There were clear signs in the data of Tables II and IV that borate is an unusual eluent towards proteins. Blesa *et al.* [20] have shown that the driving force for adsorption of borate on zirconia is different from that of other Lewis bases. Most adsorbed borate is present in the form of esters of hydroxyl groups on the surface of zirconia. The remainder is present as ionized esters with tightly bound counterions. Such species can act to sterically block the Lewis acid sites, however, additional interactions between borate and the Lewis acid sites are possible.

Table VIII shows the retention of a variety of

TABLE VIII

PROTEIN RETENTION IN BORATE BUFFERS: CAPACITY FACTORS

Linear gradient at 1.00 ml/min and 35°C from 100% A to 100% B in 30 min followed by a return to 100% A in 15 min. Equilibration period was 15 min between runs. Injections were 10 μl of 1 mg/ml solutions of proteins in 20 m*M* MES pH 6. Detection was at 280 and 410 nm. – = Elution not observed.
Gradient I: A: 0.5 *M* H_3BO_3, pH 5.5; B: 0.5 *M* H_3BO_3, 1.5 *M* NaCl, pH 5.5.
Gradient II: A: 0.5 *M* H_3BO_3, pH 5.5; B: 0.5 *M* H_3BO_3, 0.5 *M* Na_2SO_4, pH 5.5.
Gradient III: A: 0.5 *M* H_3BO_3, pH 5.5; B: 0.5 *M* H_3BO_3, 0.5 *M* NaCl, pH 5.5.
Gradient IV: A: 0.5 *M* H_3BO_3, pH 7.0; B: 0.5 *M* H_3BO_3, 0.5 *M* NaCl, pH 7.0.

Protein	*k'*			
	Gradient			
	I	II	III	IV
Ovalbumin	–	–	–	−0.3
Bovine serum albumin	–	–	–	−0.3
Human serum albumin	–	–	–	−0.3
Transferrin	–	–	–	4.4
Myoglobin	–	–	–	13.8
Hemoglobin	–	–	–	27.3
Alcohol dehydrogenase	–	–	–	−0.3
α-Chymotrypsin	29.5	0.3	–	35.1
Cytochrome *c*	52.0	–	–	–
Ribonuclease A	20.9	25.9	48.7	30.7
Ribonuclease B	20.8	25.0	–	26.3
Lysozyme	19.7	28.0	52.6	30.0

proteins in highly concentrated borate buffers. At low pH, borate is scarcely ionized and the surface esters are likely uncharged. Acidic and neutral proteins are not eluted. Cationic proteins were well retained in both gradients I and II. Because both gradients employed were of equal ionic strength, differences in capacity factor cannot be attributed to differences in ionic interactions. The fact that sulfate (gradient II) proves to be a weaker eluent than chloride (gradient I) suggests that Lewis acid site interactions are not responsible for retention. The non-elution of the acidic proteins is inexplicable.

At higher pH values, the borate esters are more ionized. Anionic proteins are eluted at pH 7.0 (gradient IV), but not at lower pH values. Neutral proteins are reasonably well retained at pH 7.0. Cationic proteins are strongly retained. However, they are not as well retained as at the lower pH. The net effect of a change to higher pH is the conversion of this medium from an adsorbent to a cation exchanger. It should be noted that the surface coverage with borate must be quite high since very high ionic strengths are required to elute the proteins at pH 7.0

This unique elution behavior may be due to two effects. First, Hingston *et al.* [22] found that the adsorption capacity of Lewis bases on metal oxides was maximal at pH values near their pK_a. The first ionization constant of borate is 9.24, so at pH 7.0, a higher surface loading of borate is anticipated. This could help to displace the acidic proteins bound to Lewis acid sites. Secondly, the unionized borate surface might act as a non-specific adsorbent for proteins. When this surface becomes ionized at high pH, electrostatic interactions may dominate the adsorptive interactions and cause elution by ion exchange. This explanation is highly speculative, but it does account for the borate buffer results given in Tables II and IV.

CONCLUSIONS

A wide variety of acidic, neutral and basic proteins can be chromatographically separated on porous zirconium oxide particles, provided that an appropriate concentration of a strong hard Lewis base is present in the eluent. The proteins are retained by a complex balance of ion-exchange (on anionic sites) and ligand-exchange (on surface Lewis acid) sites. Elution can be initiated by increasing the concentration of the Lewis base or by increasing the ionic strength. The most critical parameter in achieving acceptable retention and peak shape is the initial concentration of the Lewis base in the eluent. The retention mechanism is analogous to that of calcium hydroxyapatite, but the selectivites are quite different and depend very strongly on the type of Lewis base used for elution.

Most proteins did not show a clear correlation between displacing ligand strength and protein capacity factor. This is not entirely surprising, since neutral and basic proteins have significant cation-exchange contributions to retention once the ligand-exchange mechanism has been attenuated. Acidic proteins, however, showed a fairly high degree of correlation between retention and Lewis base displacing strength since ligand exchange is the main retention mode for these proteins. Overall, the selectivity was not unlike calcium hydroxyapatite. However, this support is far superior to hydroxyapatite in chemical and physical stability.

The most important finding is that a fairly strong buffer Lewis base must be present, in sufficient concentration to nearly saturate the adsorption isotherm, for any of the proteins to be fully eluted from the phase. In practice, phosphate, fluoride, polyvalent organic ligands and organosphosphate ligands proved most suitable for the successful attenuation of the Lewis acid sites at low concentrations.

The complex Lewis bases proved most interesting as modulators of the ligand-exchange process. Not only were the slow desorption kinetics and strong binding properties advantageous in effectively blocking the Lewis acid sites, but the complex structures allowed secondary interactions between the protein and the Lewis base to occur. This resulted in different selectivities which were not predictable based on electrostatic or ligand-exchange interactions.

ACKNOWLEDGEMENTS

J. A. B. acknowledges financial support from Specialty Adhesives and Chemicals Division and the Leading Edge Academic Program at 3M. This work was also supported in part by grants from the Institute for Advanced Studies in Bioprocess Tech-

nology and the National Institues of Health and the National Science Foundation.

REFERENCES

1 M. P. Rigney, *Ph.D. Thesis*, University of Minnesota, Minneapolis, MN, 1988.
2 W. A. Schafer, *MS Thesis*, University of Minnesota, Minneapolis, MN, 1990.
3 W. A. Schafer and P. W. Carr, *J. Chromatogr.*, 587 (1991) 149–160.
4 W. A. Schafer, P. W. Carr, E. F. Funkenbusch and K. A. Parson, *J. Chromatogr.*, 587 (1991) 137–147.
5 J. A. Blackwell and P. W. Carr, *J. Chromatogr.*, 549 (1991) 43–57.
6 J. A. Blackwell and P. W. Carr, *J. Chromatogrt.*, 549 (1991) 59–75.
7 J. A. Blackwell, *Ph. D. Thesis*, University of Minnesota, Minneapolis, MN, 1991.
8 J. A. Blackwell and P. W. Carr, *J. Liq. Chromatogr.*, 14 (1991) 2875–2889.
9 M. J. Gorbunoff, *Anal. Biochem.*, 136 (1984) 425–432.
10 M. J. Gorbunoff, *Anal. Biochem.*, 136 (1984) 433–439.
11 M. J. Gorbunoff and S. N. Timasheff, *Anal. Biochem.*, 136 (1984) 440–445.
12 J. A. Blackwell and P. W. Carr, *Anal. Chem.*, in press.
13 J. A. Blackwell and P. W. Carr, *Anal. Chem.*, in press.
14 M. P. Rigney, E. F. Funkenbusch and P. W. Carr, *J. Chromatogr.*, 499 (1990) 291–304.
15 P. C. Sadek, P. W. Carr, L. D. Bowers and L. C. Haddad, *Anal. Biochem.*, 144 (1985) 128–131.
16 D. Malamud and J. W. Drysdale, *Anal. Biochem.*, 86 (1978) 620–647.
17 P. G. Righetti and T. Caravaggio, *J. Chromatogr.*, 127 (1976) 1–28.
18 H. A. Sober, *Handbook of Biochemistry*, CRC Press, Cleveland, OH, 2nd ed., 1970.
19 L. G. Sillen and A. E. Martell, *Stability Constants of Metal Ion Complexes*, Chemical Society, London, 1964.
20 M. A. Blesa, A. J. G. Maroto and A. E. Regazzoni, *J. Coll. Int. Sci.*, 99 (1984) 32–40.
21 C. J. van Oss, R. J. Good and M. K. Chaudhury, *J. Chromatogr.*, 376 (1986) 111–119.
22 F. J. Hingston, R. J. Atkinson, A. M. Posner and J. P. Quirk, *Nature (London)*, 215 (1967) 1459–1461.

Journal of Chromatography, 596 (1992) 43–49
Elsevier Science Publishers B.V., Amsterdam

CHROM. 23 931

Cation-exchange liquid chromatography of choline and acetylcholine on free shielded silanols of silica-based reversed-phase stationary phases

Jaroslav Šalamoun*,☆

Institute of Analytical Chemistry, Veveri 97, 611 42 Brno (Czechoslovakia)

Phuc Trung Nguyen and Jörg Remien

Walther-Straub Institute of Pharmacology and Toxicology, Nussbaumstrasse 26, W-8000 Munich 2 (Germany)

(First received October 14th, 1991; revised manuscript received November 19th, 1991)

ABSTRACT

Free anionic functions present on the surface of reversed-phase packing materials were used for the selective cation-exchange preconcentration and separation of the neurotransmitters choline and acetylcholine from a biological matrix. The cation-exchange behaviour of different reversed-phase packing materials in the neat aqueous mobile phase, the properties of an end-capped column, the dependence of capacity factors and peak shape on the concentration of counter ions, ionic strength, pH and the addition of acetonitrile and optimum conditions for enzymatic conversion of solutes to hydrogen peroxide were studied. The studied reversed-phase columns exhibit better pH stability and longer lifetimes than normal silica-based cation exchangers. Acetylcholine is an effective and sensitive test sample for the measurement of adsorption on silica support. A large sample volume was injected onto a precolumn inserted instead of an injection valve and after injection the solutes were focused and separated on an analytical column with a mobile phase containing tetramethylammonium perchlorate as the counter ion.

INTRODUCTION

Acetylcholine [$CH_3COOCH_2CH_2N(CH_3)_3^+$, ACH] and choline [$HOCH_2CH_2N(CH_3)_3^+$, CH] are endogenous substances with a tetramethylammonium group present in very low concentrations in biological materials. A number of high-performance liquid chromatographic (HPLC) methods have been published [1–7] on the determination of these substances, using mainly packed-bed reactors with the immobilized enzymes acetylcholinesterase and cholinoxidase. The released hydrogen peroxide is then detected by an electrochemical detector with a platinum electrode. Cation-exchange chromatography [3,5] or the ion-pair technique on reversed-phase columns [1,2,4,6] was the most often used technique for the separation of both compounds. Reversed-phase liquid chromatographic (RPLC) separation on an octadecyl column without the addition of an ion-pairing reagent to the mobile phase was reported, suggesting a reversed-phase mechanism of the separation [7].

Many RPLC methods are performed by using porous silica chemically modified with alkyl groups bonded to the surface hydroxyl groups. About half or about 4 μmol/m^2 of the available silanols can be substituted even after end-capping because of steric hindrance [8–10]. The high concentration of the remaining surface silanols significantly influences the behaviour of many solutes and can cause

☆ Present address: Walther-Straub Institute of Pharmacology and Toxicology, Nussbaumstrasse 26, W-8000 Munich 2, Germany.

0021-9673/92/$05.00

irregular retention and peak broadening [11,12]. This undesirable effect of silanols is usually partly eliminated by adding a silanol blocking agent such as amines or tetraalkylammonium salts to the mobile phase or by varying the pH, ionic strength, etc. [13,14].

The pK_a of silica ($\equiv SiO^- \rightleftharpoons \equiv SiOH$) has been determined [15] to be 7.1. Iler [16] noted that the pK_a varies from 6.5 at 0% neutralization to about 9.5 at 50%. The silica surface is more strongly acidic than monosilicic acid, which has a pK_a of 9.8. As a weak acid, silica exhibits properties typical of weakly acidic cation exchangers.

The behaviour of basic amino compounds on silica and silica reversed phases has been reported and the contribution of the cation-exchange properties of silica matrix has been demonstrated [17,18]. Weber and Tramposch [19] studied Spherisorb ODS and reported that it has properties similar to a strong cation exchanger of low capacity and that the pK_a of silanols vary with the degree of neutralization, salt concentration and the microenvironment.

Scott and Simpson [20] showed that the "brush-type" reversed phases are slow to come to equilibrium with pure water, and in contact with water it would appear that the hydrocarbon chains dispersively interact with themselves and are lying almost flat on the surface.

We used the remaining shielded silanol functions of the RPLC materials for the cation-exchange chromatographic separation of CH and ACH. The samples were pretreated on a larger volume precolumn inserted instead of an injection loop and packed with coarser RPLC material. The mobile phase composition was evaluated with regard to the function of the precolumn, column and reactor.

EXPERIMENTAL

ACH iodide, CH chloride and tetramethylammonium (TMA) perchlorate were obtained from Sigma (Deisenhofen, Germany) and ethylenediaminotetraacetic (EDTA) sodium salt from Merck (Darmstadt, Germany). All other chemicals were of analytical-reagent grade.

Chromatographic separations were performed at ambient temperature on a Gynkothek (Munich, Germany) Model 600/200 liquid chromatograph equipped with a Gynkothek 20- or 50-μl six-port injection valve and with a Model EP 30 electrochemical detector set at 0.45 V (Biometra, Göttingen, Germany). A 30 × 2.1 mm I.D. cartridge with immobilized acetylcholinesterase and cholin-oxidase from Biometra was used for the detection of CH and ACH. A CGC column (150 × 3 mm I.D.) packed with LiChrosorb RP-18, particle diameter, d_p = 5 μm (Merck) was used for the study of its cation-exchange behaviour. The other analytical columns used were Hamilton PRP-X 200 (250 × 4.1 mm I.D.) packed with polymer-based strong cation exchanger, d_p = 10 μm, 250 × 4 mm I.D. packed with Supelcosil LC-8, d_p = 5 μm (Supelco, Bellefonte, PA, USA) and LiChroCART (125 × 2 mm I.D.) packed with Superspher 60 RP-Select B, d_p = 5 μm (Merck). A Supelguard LC-8, d_p = 5 μm, precolumn (20 × 4.6 mm I.D.) was used in conjunction with the Supelcosil LC-8 column. A Pelliquard LC-8, d_p = 40 μm column (20 × 4.6 mm I.D.) was used in conjunction with LiChrosorb RP-18 columns and large volumes of the sample were injected on to the precolumn inserted instead of an injection valve. The void volume of the precolumn was 250 μl and that of the LiChrosorb RP-18 column was 1 ml. The precolumn was equilibated with 0.005 *M* sodium phosphate buffer (pH 7.4) and volumes of sample up to 250 μl were injected. The precolumn was then washed with 250 μl of 0.005 *M* sodium phosphate buffer and all the contents of the precolumn were injected into the analytical column. The mobile phase for the analytical column was of 0.1 *M* sodium phosphate buffer (pH 7.4.) containing 1 m*M* TMA and 0.1 m*M* EDTA.

Brain and heart tissues were mixed with 2 ml of 6% trichloroacetic acid homogenized for 10 min at 0°C and kept for 10 min in an ice-cold bath. The homogenate was mixed with 2 ml of 0.1 *M* sodium phosphate buffer (pH 7.4) and after 10 min in an ice-cold bath was centrifuged for 25 min at 30 000 *g*. The supernatant was diluted tenfold with 0.1 *M* sodium phosphate buffer (pH 7.4) and 50 μl were injected on to the Supelcosil LC-8 column.

A 10-μl volume of erythrocytes was mixed with 10 μl of 3 *M* trichloroacetic acid and 180 μl of 0.1 *M* sodium phosphate buffer (pH 7.4) were added. The mixture was centrifuged for 10 min at 10 000 *g* and the supernatant, after further dilution, was injected on to the precolumn.

RESULTS AND DISCUSSION

The number of silanol groups accessible and their contribution to the retention in RPLC depend on the size and chemical character of the compounds to be analysed. CH and ACH are polar compounds containing a tetramethylammonium moiety. These small ionic molecules can easily penetrate silanol or other ionic groups hidden under the bonded layer of a reversed-phase stationary phase and interact with them on the cation-exchange principle. Not only the chromatographic behaviour but also the enzyme reactions are functions of many variables and experimental conditions. All these variables should eventually be considered whenever one wishes to utilize immobilized enzyme reactors in HPLC.

Influence of TMA on retention

We studied whether the mechanism of retention is based on hydrophobic or cation-exchange interactions. Optimum conditions for the separation of CH and ACH were established by varying the concentration of TMA. An increasing salt concentration in the mobile phase results in increased retention of hydrophobic solutes in RPLC. On the other hand, the capacity factor (k') in ion-exchange chromatography is a function of the selectivity coefficient or equilibration constant (K_A^B), total ion-exchange capacity (Q) and counter ion concentration in the mobile phase (c) [21]:

$$k' = V_s/V_m(K_A^B)^{1/a}Q^{b/a}c^{-b/a} = (V_s/V_m)K_D \qquad (1)$$

where V_s and V_m are the volumes of stationary and mobile phase in the column, respectively, a and b are charges of the counter ion in the mobile phase and solute, respectively, and K_D is the distribution constant. The logarithmic dependence of the capacity factor on the concentration of an eluted ion is linear, the slope of which is determined mainly by the ratio of the charges of the chromatographed and counter ions. The dependence for CH and ACH on LiChrosorb RP-18 is shown in Fig. 1. The higher the TMA concentration, the lower is the retention. The dependence is linear in accord with the suggested cation-exchange mechanism. A pure ion-exchange mechanism should give a slope of unity. The slopes of these plots are in fact 0.191 for CH and 0.226 for ACH. This shows that a mixed ion-exchange and reversed-phase mechanism is responsible for the chromatographic behaviour of CH and ACH in this system.

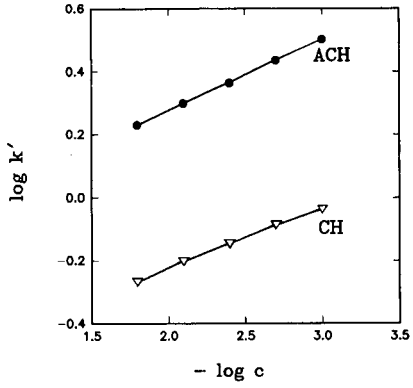

Fig. 1. Dependence of the capacity factor (k') of CH (▽) and (●) ACH on molar concentrations of TMA by cation-exchange chromatography on LiChrosorb RP-18. Mobile phase, 0.1 *M* phosphate buffer (pH 7.4) containing 0.1 m*M* EDTA. For other conditions, see Experimental.

A decrease in TMA concentration in the mobile phase to <2 m*M* results in significant peak tailing (the asymmetry factor at 10% of the ACH peak height is 3.3 for 1 m*M* TMA; see Fig. 2). This indicates that TMA inhibits the activity of strong cation-exchange sites. The activity of these groups is suppressed at higher concentrations of TMA when these high-activity sites are saturated with TMA, whereas the less reactive anionic sites remain for the cation-exchange chromatography of ACH and CH.

Linear range of ACH response

The dependence of the ACH response on the amount of ACH injected is linear up to about 1 nmol for the LiChrosorb RP-18 column. This value is significantly lower than that usually found in RPLC. Higher amounts decrease the retention time and result in peak asymmetry (see Fig. 2). The peak asymmetry factor is in the range 1.3–1.6, depending on the batch of the column used up to 1 nmol of ACH injected. For the injection of 10 and 200 nmol ACH, the peak asymmetry factor was 2.0 and 2.75 and the capacity factor decreased from the normal value of 2.35 to 2.30 and 1.8, respectively. This means that we work in the linear part of a convex absorption isotherm only at low concentrations of ACH. However, it is sufficient in the trace analysis of CH and ACH to have a linear range of three orders of magnitude.

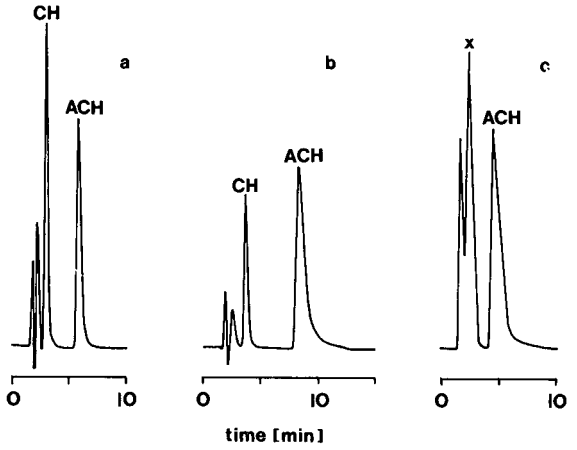

Fig. 2. Peak broadening in cation-exchange chromatography of ACH on LiChrosorb RP-18. (a) Mobile phase, 0.1 *M* sodium phosphate buffer (pH 7.4) containing 4 m*M* TMA and 0.1 m*M* EDTA; amount of ACH injected, Q = 400 pmol; detector range = 80 nA full-scale. (b) Mobile phase as in (a), containing 1 m*M* TMA; Q = 400 pmol; detector range = 160 nA full-scale. (c) Mobile phase as in (a); Q = 200 nmol; detector range = 8 μA full-scale. × = Unknown.

Influence of TMA on detection sensitivity

The dependence of ACH response on TMA concentration in the mobile phase is shown in Fig. 3. The higher the TMA concentration, the lower is the response. TMA is not only a competitor of ACH for the active sites on silica surface but also inhibits enzyme activity in the enzyme bioreactor. The advantage of reversed-phase low-capacity cation exchangers is that a lower concentration of TMA in the mobile phase (4 m*M*) can be used in comparison with normal cation exchangers (7 m*M*), resulting in higher response.

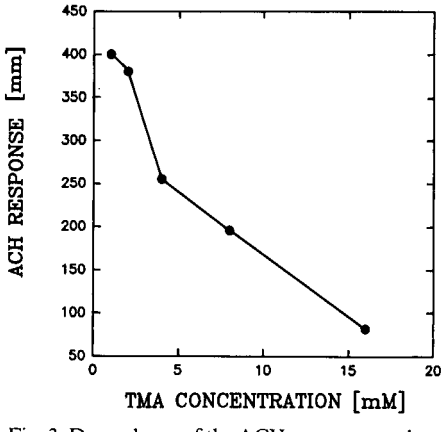

Fig. 3. Dependence of the ACH response on the concentration of TMA. Conditions as in Fig. 1.

Influence of sodium phosphate buffer concentration

The concentration of sodium phosphate buffer in the mobile phase was 0.1 mol l^{-1}. A tenfold decrease in Na^+ concentration had only a slight influence on the increase in ACH retention and did not affect its peak shape. The diameter of the solvated sodium ion is comparable to that of TMA. Anyway, the methyl groups present in the TMA molecule make TMA more hydrophobic than the solvated sodium ion [22], and it can easily penetrate through the hydrophobic layer and interact effectively with remaining silanols.

Influence of EDTA

The silica surface can be enriched by a number of metal oxide impurities. Twenty metals in the ppm range and fifteen in ppb range have been reported [12]. These metal impurities can cause both increases and decreases in enzyme activity. In our experience, a new column, even if preconditioned consecutively with methanol, water and buffer, brings about degradation of the enzyme reactor activity after the immediate application of the mobile phase. The EDTA present in the mobile phase complexes the metal impurities, making the silanol surface free, and protects not only both enzymes from inactivation but also the hydrogen peroxide from metal-catalyzed decomposition.

Influence of pH on retention

At lower pH of the mobile phase the silanol groups lose their ionic character and, as a result, the capacity of the column and also the capacity factor decrease. The influence of pH on the capacity factor of ACH is illustrated in Fig. 4. The retention of CH and ACH decreased only gradually, with no clear break in the pH range studied, which is in accord with the theory that the silanol groups behave like a polyelectrolyte [16].

Influence of pH on column lifetime

A major drawback of silica-based cation exchangers is a very short lifetime under the assay conditions (pH 7.4–8). Silica is dissolved at alkaline pH. Silica in a reversed-phase stationary phase is

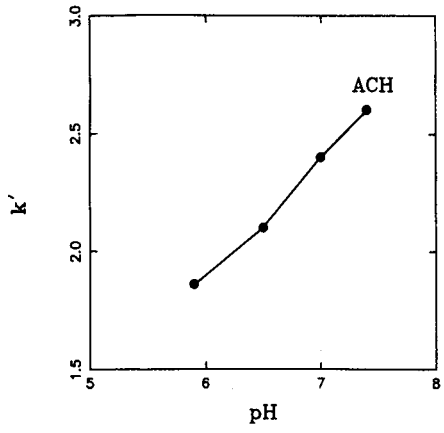

Fig. 4. Dependence of the capacity factor (k') of ACH on the pH of the mobile phase. Conditions as in Fig. 1; the mobile phase contained 4 mM TMA.

protected from intensive contact with the mobile phase by hydrophobic chains because the penetration of water molecules into the bonded layer is unfavourable [10,20]. This significantly prolongs the lifetime of the column from several days for normal silica-based cation exchangers [5] to several months for reversed-phase materials.

Effect of shielded anionic groups

The hydrophobic phase influences not only the pH stability of the column but also its deterioration by the sample matrix. The Supelcosil LC-8 column has been used in our laboratory for the determination of CH and ACH in heart and brain tissues and during 6 months hundreds of unextracted homogenate samples have been injected with the efficiency of the column gradually decreasing from 3000 to 2000 theoretical plates. In comparison, the Hamilton cation-exchange column was not able to separate ACH completely from biological components in the same samples because active sites soon deteriorate owing to the compounds present in the sample matrix. The active groups on the surface of RPLC packings have a net negative charge, causing ion exclusion, and moreover are hardly accessible to large negatively charged macromolecules because of size exclusion.

Performance of cation-exchange columns

The performance of the analytical columns used for the separation of CH and ACH was relatively low for all cation exchangers [5] and also for ion-pair RPLC [4]. The efficiency of our RPLC column was 3000 theoretical plates for ACH and the 25 × 0.4 cm I.D. Supelcosil LC-8 column and 1300–2000 for the 15 × 0.3 cm I.D. LiChrosorb RP-18 column. This is approximately the same efficiency as for silica-based cation exchangers [5]. The solutes diffuse to the surface silanols through the bonded layer with all the silica-based columns and the effect of stationary phase mass transfer contributes to the decrease in efficiency.

Influence of acetonitrile

Acetonitrile molecules at a low concentration in the eluent penetrate into the bonded layer and can cause rearrangement of the bonded layer structure [10]. The addition of 3% of acetonitrile to the mobile phase caused a decrease in the ACH capacity factor from 2.6 to 1.6. This behaviour can be explained by the competing adsorption of acetonitrile on accessible silanol groups by the polar part. Anyway, the low concentration of acetonitrile present in the mobile phase causes gradual damage to the immobilized enzyme reactor.

Sample focusing

Large-volume injections of very dilute samples in a non-eluting solvent have been successfully applied in conventional RPLC [23] and in microbore HPLC [24–26]. We applied this technique to the preconcentration of solutes on the precolumn and the top of the analytical column. The solutes were at first adsorbed on the precolumn silanols. With the injection of the precolumn eluent (*i.e.*, diluted buffer containing no TMA which, if used as the mobile phase on the chromatographic column, would lead to very long retention times), the top of the analytical column was conditioned. Simultaneously, the mobile phase enters the precolumn and CH and ACH are eluted in a sharp gradient on to the analytical column. Consequently, an increase in retention volume equal to the precolumn volume was observed. This technique allows one to vary the sample injection volume and preseparate the solutes from the non-retained sample matrix without any extra-column band broadening. The recovery of CH and ACH for erythrocytic samples was more than 95%.

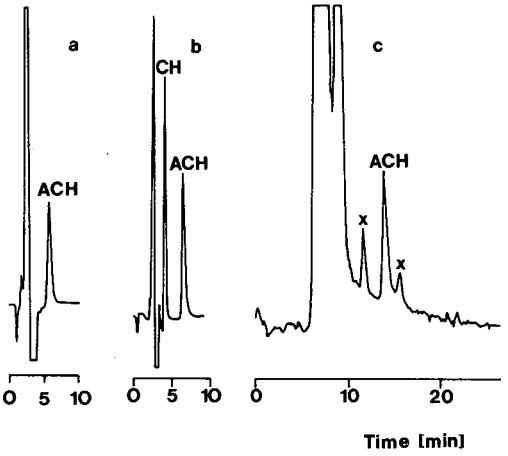

Fig. 5. Cation-exchange chromatography of CH and ACH on different RPLC columns. (a) Chromatogram of ACH standard solution on Superspher 60 RP-select B. Mobile phase, 0.1 *M* phosphate buffer (pH 7.4) containing 1 m*M* TMA and 0.1 m*M* EDTA; flow-rate, 0.1 ml/min; amount of ACH injected, Q = 84 pmol. (b) 200 μl of erythrocytic homogenate separated on LiChrosorb RP-18 column. Q = 423 pmol of ACH; mobile phase, 0.1 *M* phosphate buffer (pH 7.4) containing 4 m*M* TMA and 0.1 m*M* EDTA; flow-rate, 0.5 ml/min. For other conditions, see Experimental. (c) 50 μl of heart homogenate separated on a Supelcosil LC-8 column. Q = 17 pmol of ACH; conditions as in (b). × = Unknown.

Behaviour of other RPLC columns

Superspher 60 RP-select B, the column suggested for the separation of basic compounds, showed a considerably lower ability to retain CH and ACH. The concentration of TMA in the mobile phase had to be decreased to 1 m*M* to reach a capacity factor of 1.7 for ACH. The Supelcosil LC-8 column gave the same capacity factors as the LiChrosorb RP-18 column.

Chromatograms of some samples on these three columns are shown in Fig. 5. The detection limit of acetylcholine was 60 fmol on the LiChrosorb RP-18 column. The reproducibility of the retention time was better than 1% within day and better than 2.5% day to day.

CONCLUSIONS

Although it is widely recognized that interactions of basic or ionic substances with anionic sites of reversed-phase column occur, the magnitude of such effects is not always fully appreciated. This study is an example of the usefulness of these interactions. The present mode of cation-exchange chromatography of CH and ACH has several advantages over the conventional silica-based cation-exchange chromatography: better pH stability, shielded active sites, lower capacity of anionic groups allowing better optimization of the composition of the mobile phase for enzymatic reactions. The present results also show how incomplete the elimination of these interactions with silanols by addition of TMA to the mobile phase can be. The method involves very low concentrations of small and charged solute molecules and their detection in a packed-bed reactor system with immobilized enzymes and neat aqueous mobile phase. It also permits a better study of the behaviour of RPLC materials. ACH is an effective and sensitive test sample for the measurement of adsorption on silica supports. Apparently ACH is an even more sensitive probe than other basic compounds, because it is smaller and sterically more able to interact with surface silanol groups that are shielded by alkyl ligands.

ACKNOWLEDGEMENTS

We thank Hans-Joachim Kuss for providing the Superspher 60 RP-Select B column. This study was supported by BMVg grant In San I 0888-V-4890.

REFERENCES

1 P. E. Potter, J. L. Meek and N. H. Neff, *J. Neurochem.*, 41 (1983) 188.
2 C. Eva, M. Hadjiconstantinou, N. H. Neff and J. L. Meek, *Anal. Biochem.*, 143 (1984) 320.
3 H. Stadler and T. Nesselhut, *Neurochem. Int.*, 9 (1986) 127.
4 A. W. Teelken, H. F. Schuring, W. B. Trieling and G. Damsma, *J. Chromatogr.*, 529 (1990) 408.
5 E. Haen, H. Hagenmaier and J. Remien, *J. Chromatogr.*, 537 (1991) 514.
6 N. M. Barnes, B. Costall, A. F. Fell and R. J. Naylor, *J. Pharm. Pharmacol.*, 39 (1987) 727.
7 I. Wessler and J. Werhand, *Naunyn-Schmiedeberg's Arch. Pharmacol.*, 341 (1990) 510.
8 P. Roumeliotis and K. K. Unger, *J. Chromatogr.*, 149 (1978) 211.
9 M. Holik and B. Matejkova, *J. Chromatogr.*, 213 (1981) 33.
10 S. M. Staroverov and A. Yu. Fadeev, *J. Chromatogr.*, 544 (1991) 77.
11 J. Kohler and J. J. Kirkland, *J. Chromatogr.*, 385 (1987) 125.
12 H. Engelhardt, H. Löw and W. Götzinger, *J. Chromatogr.*, 544 (1991) 371.
13 W. A. Moats, *J. Chromatogr.*, 366 (1986) 69.

14 M. A. Stadalius, J. S. Berus and L. R. Snyder, *LC · GC*, 6 (1988) 494.
15 M. L. Hair and W. Hertl, *J. Phys. Chem.*, 74 (1970) 91.
16 R. K. Iler, *The Chemistry of Silica*, Wiley-Interscience, New York, 1979, p. 660.
17 K. Sugden, G. B. Cox and C. R. Loscombe, *J. Chromatogr.*, 149 (1978) 377.
18 G. B. Cox and R. W. Stout, *J. Chromatogr.*, 384 (1987) 315.
19 S. G. Weber and W. G. Tramposch, *Anal. Chem.*, 55 (1983) 1771.
20 R. P. W. Scott and C. F. Simpson, *J. Chromatogr.*, 197 (1980) 11.
21 P. Jandera and J. Churacek, *J. Chromatogr.*, 91 (1974) 207.
22 J. Dvorak and J. Koryta, *Elektrochemie*, Academia, Prague, 1983, p. 214.
23 P. R. Guineabault, M. Broquaire and R. A. Braithwaite, *J. Chromatogr.*, 204 (1981) 329.
24 M. Krejci, K. Slais, D. Kourilova and M. Vespalcova, *J. Pharm. Biomed. Anal.*, 2 (1984) 197.
25 K. Slais, *J. Chromatogr.*, 469 (1989) 223.
26 M. Janecek, J. Salamoun and K. Slais, *Chromatographia*, 32 (1991) 61.

Journal of Chromatography, 596 (1992) 51–58
Elsevier Science Publishers B.V., Amsterdam

CHROM. 23 972

Simultaneous purification of the neuroproteins synapsin I and synaptophysin

Isabel Llona☆, Wim G. Annaert and Werner P. De Potter*

Laboratory of Neuropharmacology, Department of Medicine, University of Antwerp (UIA), Universiteitsplein 1, 2610 Wilrijk (Belgium)

(First received October 24th, 1991; revised manuscript received December 22nd, 1991)

ABSTRACT

A procedure for the simultaneous purification of synapsin I and synaptophysin from calf brain was developed. Demyelinated membranes were extracted with 2% Triton X-100 and 2 *M* KCl. The extracted proteins were separated by weak cation-exchange chromatography on carboxymethyl-Sepharose Fast Flow. Synaptophysin was finally purified by preparative sodium dodecyl sulphate–polyacrylamine gel electrophoresis and synapsin I by affinity chromatography using a calmodulin-Sepharose column. The recovery obtained was 40 μg/g in brain for synaptophysin and 25 μg/g in brain for synapsin I.

INTRODUCTION

During the 1980s, enormous progress was made in the isolation and characterization of small synaptic vesicles (SSV) from mammalian brain and Torpedo electrical organ [1,2]. Several membrane proteins of SSV have been identified [3–7], of which the synapsin family (synapsin Ia and b, IIa and b) and synaptophysin are structurally and functionally the best characterized [8,9].

Synapsin I was discovered by Johnson *et al.* [10] in 1972 as an endogenous substrate for protein kinases. The protein has been extensively studied [11,12]. It is exclusively present in neuronal tissue, where it is localized on SSV. Owing to its ability to bind different elements of the cytoskeleton and by the other hand synaptic vesicles, it is believed to play a major role in the regulation of neurotransmitter release [13,14].

Synaptophysin is the most abundant integral membrane protein of SSV [15–17]. The protein was identified by means of the monoclonal antibody SY 38, produced by immunization with intrinsic membrane proteins of SSV from mammalian brain. It is present in virtually all nerve terminals and it has also been associated with vesicles of neuroendocrine cells. However, synaptophysin is not present in other cell types [18].

The currently available procedures for purifying synapsin I involve a series of time-consuming chromatographic steps, generally resulting in low recoveries. In this paper we describe a simplified method that allows the simultaneous purification of synapsin I and synaptophysin, both with high recoveries.

EXPERIMENTAL

Materials

All reagents were of analytical-reagent grade. Phenylmethylsulphonyl fluoride (PMSF) was purchased from Sigma (St. Louis, MO, USA). All chromatographic media used in the isolation procedure were purchased from Pharmacia (Uppsala, Sweden). Goat anti-rabbit immunoglobulin G (IgG) alkaline phosphatase conjugate was obtained from Bio-Rad Labs. (Richmond, CA, USA). [^{125}I]Protein A was purchased from ICN Biomedicals (Ir-

☆ On leave from the Catholic University of Chile.

0021-9673/92/$05.00

vine, CA, USA). For the immunodetection of synaptophysin we used the commercial monoclonal antibody from Boehringer (Mannheim, Germany). The antiserum against synapsin I was kindly provided by Dr. P. De Camilli (New Haven, CT, USA) and Dr. P. Greengard (New York, NY, USA).

Isolation of proteins

The procedure described was designed using published methods [19–21] as guidelines. The purification procedure is outlined schematically in Fig. 1. Calf brain was obtained from the local slaughterhouse. The cortex was cleaned, cut into small pieces and frozen in liquid nitrogen prior to transport to the laboratory. The day after, the tissue (ca. 250 g wet weight) was thawed, minced and homogenized with a glass–PTFE homogenizer in ice-cold buffer A, 320 m*M* sucrose–5 m*M* NaH_2PO_4 (pH 7.0)–1 m*M* [ethylenebis(oxyethylenenitrilo)]tetraacetic acid (EGTA)–0.3 m*M* PMSF. All subsequent steps

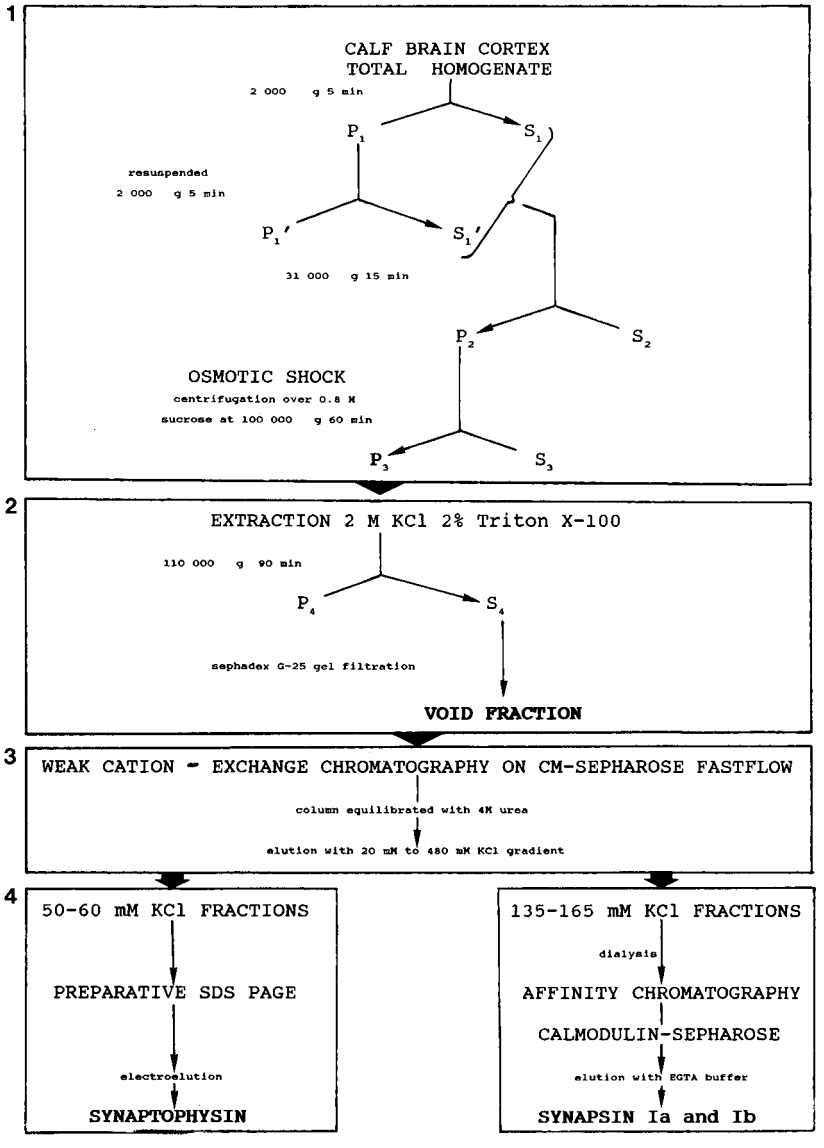

Fig. 1. Scheme of the isolation procedure for synapsin I and synaptophysin.

were performed at 4°C. The homogenate was diluted 1:8 (w/v) and centrifuged at 2000 *g* for 5 min. The pellet (P_1) was resuspended and centrifuged again. The combined supernatants (S_1 + S_1') were pelleted at 31 000 *g* for 15 min. The synaptosomal pellet (P_2) obtained was subjected to hyposmotic lysis by resuspension in buffer B [5 m*M* NaH_2PO_4 (pH 7.0)–1 m*M* EGTA–0.3 m*M* PMSF]. Subsequently, the suspension was centrifuged over a cushion of 0.8 *M* sucrose in buffer B at 100 000 *g* for 60 min. The pellet (P_3) was extracted with buffer C [5 m*M* NaH_2PO_4 (pH 7.2)–2 *M* KCl–2% (v/v) Triton X-100–0.3 m*M* PMSF] for 30 min at 37°C and centrifuged at 110 000 *g* for 90 min. The supernatant (S_4) was collected and subjected to chromatography on a Sephadex G-25 column (60 × 3 cm I.D.) equilibrated with buffer D [5 m*M* NaH_2PO_4 (pH 8.0)–20 m*M* KCl–0.1% Tween 20]. The void volume fraction was collected, diluted with one volume of 8 *M* urea and applied to a carboxymethyl-Sepharose Fast Flow column (16 × 1.6 cm I.D.), previously equilibrated with buffer D plus 4 *M* urea. After washing the unbound material with buffer D, bound proteins were eluted with a gradient from 20 to 480 m*M* KCl in buffer D.

Synaptophysin was highly enriched in the fractions eluting between 50 and 60 m*M* KCl. Final purification was achieved by subjecting these fractions to preparative sodium dodecyl sulphate polyacrylamide gel electrophoresis (SDS-PAGE) (see below).

The fractions eluting between 135 and 165 m*M* KCl were pooled and dialysed extensively against buffer E [5 m*M* 4-(2-hydroxyethyl)-1-piperazineethanesulphonic acid (HEPES) (pH 7.2)–0.1 m*M* EGTA–0.1 m*M* dithiothreitol (DTT)–100 m*M* KCl]. $CaCl_2$ was added to the dialysed material to give a final concentration of 1 m*M*. Subsequently, it was applied to a calmodulin-Sepharose column (10 × 0.9 cm I.D.) equilibrated with buffer F [5 m*M* HEPES (pH 7.2)–1 m*M* $CaCl_2$–0.1 m*M* DTT–100 m*M* KCl]. The column was washed with six to seven bed volumes of buffer F, followed by ten bed volumes of buffer F but containing 500 m*M* KCl. Finally, synapsin I was eluted with buffer F containing 5 m*M* EGTA instead of 1 m*M* $CaCl_2$.

Quantification of synapsin I and synaptophysin in the different steps of purification was achieved by quantitative immunoblotting. Samples were separated by SDS-PAGE and proteins transferred to nitrocellulose membranes. The latter were incubated overnight with synapsin I and synaptophysin antibodies. The immunocomplexes were detected using [^{125}I]protein A (0.1 μCi/ml). After autoradiography, the labelled bands were cut and counted in a gamma scintillation counter (Packard, Cobra 5005). Curved relating the radioactivity bound to synapsin I and synaptophysin with the amount of protein loaded were constructed. From the slopes of the linear graphs the relative concentration of synapsin I and synaptophysin per milligram of protein was calculated for each sample.

Miscellaneous procedures

Proteins were measured by the method of Bradford [22]. With detergent-containing samples, the bicinchoninic acid (BCA) kit from Pierce (Rockford, IL, USA) was used. Bovine serum albumin was used as a standard.

Protein samples from each step were separated by SDS-PAGE using 12.5% gels according to the procedure of Laemmli [23]. Gels were stained with Coomassie Brilliant Blue (CBB) (Serva, Heidelberg, Germany). In preparative SDS-PAGE, protein bands were made visible by copper staining according to Lee *et al.* [24]. The stained protein band was cut out and the piece of gel destained by incubation in 0.25 *M* Tris (pH 9)–0.25 *M* EDTA. Synaptophysin was electroeluted using a Centrilutor from Amicon (Lexington, MA, USA). Immunoblotting was performed according to established procedures [25]. Prior to the incubation with the antibodies, the nitrocellulose membranes were stained reversibly with Ponceau S [26]. After destaining, the membranes were incubated with antibodies overnight. Alkaline phosphatase-conjugated second antibodies were used for immunodetection.

RESULTS AND DISCUSSION

The expression of synapsin I and synaptophysin has been reported to correlate with the period of synapse formation [27–30]. Therefore, calf brain cortex was chosen as a starting material for the purification procedure. It is known that both synapsin I and synaptophysin are highly sensitive to degradation by calcium-dependent proteases [19]. For this reason, EGTA and PMSF were included in all buffers to control proteolytic degradation.

The isolation procedure consists of four main steps (Fig. 1): (1) preparation of a demyelinated membrane faction (P_3); (2) extraction of proteins with 2 *M* KCl and 2% Triton X-100; (3) separation of the extracted proteins by weak cation-exchange chromatography on carboxymethyl-Sepharose (CM-Sepharose FF); and (4) final purification of each protein.

The first step allows the removal of myelin-enriched membranes, which float as a white dense layer on the 0.8 *M* sucrose cushion. Myelin basic proteins are major contaminants in synapsin I preparations [19].

Second, the demyelinated membranes were extracted with a combination of high ionic strength (2 *M* KCl) and a non-ionic detergent (2% Triton X-100) containing buffer. Because synapsin I is a peripheral membrane protein and synaptophysin is an integral membrane protein of SSV, both proteins can be extracted simultaneously using this buffer. The extracted material (S_4) was immediately desalted by gel filtration on Sephadex G-25. We chose this procedure to avoid degradation of the proteins by a long period of dialysis.

Owing to its high isoelectric point (10.5), synapsin I can be bound to the weak cation-exchange column (CM-Sepharose FF) at pH 8.0, whereas most of the contaminating proteins remain unbound at the given pH. Synaptophysin also binds to the column but the nature of the interaction with the gel matrix is not clear, as the isoelectric point of synaptophysin is 4.8 [13]. Perhaps urea denatures the protein, exposing highly positive groups, which allows the binding to CM-Sepharose FF. Fig. 2A

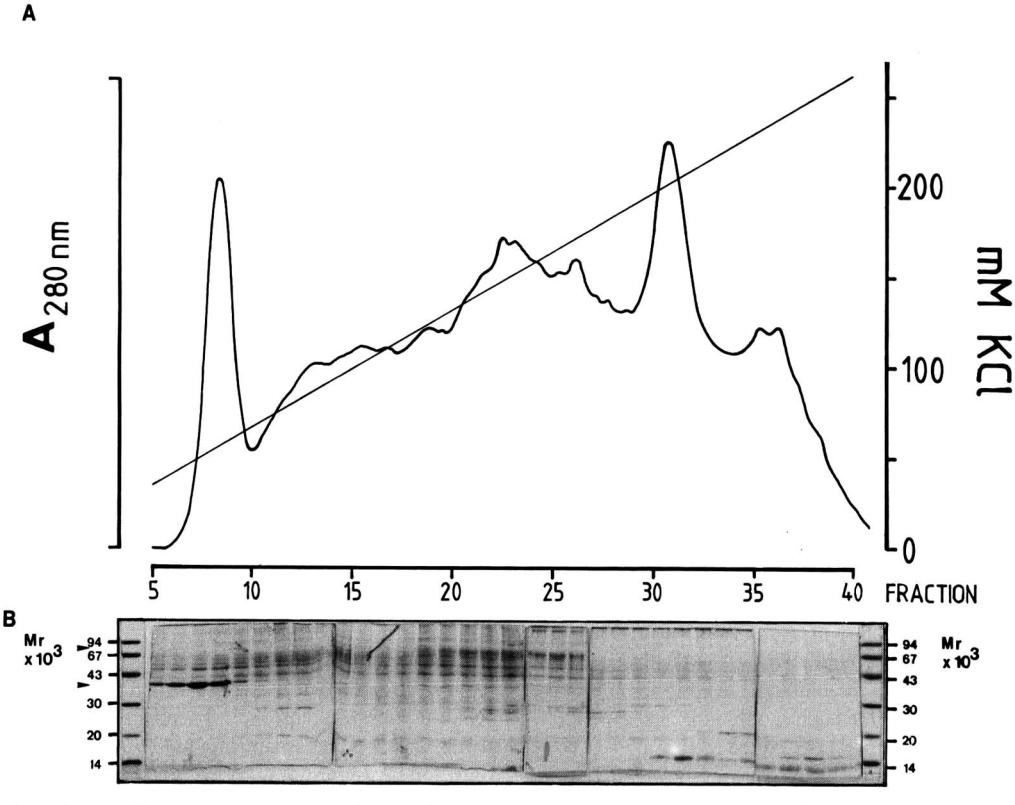

Fig. 2. Weak cation-exchange chromatography. (A) Elution profile (absorbance at 280 nm) of the CM-Sepharose FF column. The bound material was eluted with a gradient from 20 to 480 m*M* KCl. (B) Corresponding SDS-PAGE of the different fractions eluted from the column. Arrowheads point to the positions of synapsin I (M_r = 80 000–85 000) and synaptophysin (M_r = 38 000).

shows the elution profile for the column using a salt gradient from 20 to 480 m*M* KCl. The SDS-PAGE pattern from the different fractions is shown in Fig. 2B. Using polyclonal anti-synapsin I and monoclonal anti-synaptophysin antibodies, the two proteins could be identified. The corresponding immunoblots are shown in Fig. 3A and B, respectively. The binding of synaptophysin to the CM-Sepharose FF is weak because synaptophysin was eluted from the column at low ionic strength (between 50 and 60 m*M* KCl). As reflected by SDS-PAGE, synaptophysin is almost pure after CM-Sepharose FF chromatography (Fig. 2B, fractions 5–9). The final purification was achieved by preparative SDS-PAGE, followed by electroelution of the protein. The protein band at M_r 38 000 was excised and used for raising polyclonal antibodies in rabbits.

On the other hand, synapsin I-containing fractions (Fig. 2B, fractions 25–30) are still contaminated by several proteins. In contrast, Krebs *et al.* [21] purified synapsin I using a similar gel (CM-52 from Whatman). In addition to this gel type we also tested CM-Sephadex. At least in our hands, both gel types gave unsatisfactory results. Therefore, an additional purification step had to be developed. Synapsin I was identified as a Ca^{2+}-dependent calmodulin-binding protein by Okabe and Sobue [20]. Taking advantage of this property of synapsin I, we achieved the final purification of the protein using calmodulin affinity chromatography. Fig. 4A shows the elution profile of the calmodulin-Sepharose column. The first peak corresponds to the Ca^{2+}-independent bound proteins that were eluted at high ionic strength. Synapsin I was eluted by chelating Ca^{2+} ions with EGTA. As shown in Fig. 4B, the CBB pattern of pure synapsin I resembles the corresponding immunoblot fairly well, but there are some differences (see below).

Table I summarizes the protein recovery and the enrichment factor for the different fractions obtained during the purification procedure. Synaptophysin was enriched 386 times over total homogenate in the peak fraction eluted from the CM-Sepharose FF. A similar value has been reported by Navone *et al.* [18] using affinity chromatography with an anti-synaptophysin monoclonal antibody. The recovery was *ca.* 40 μg of synaptophysin per gram of brain. On the other hand, synapsin I was

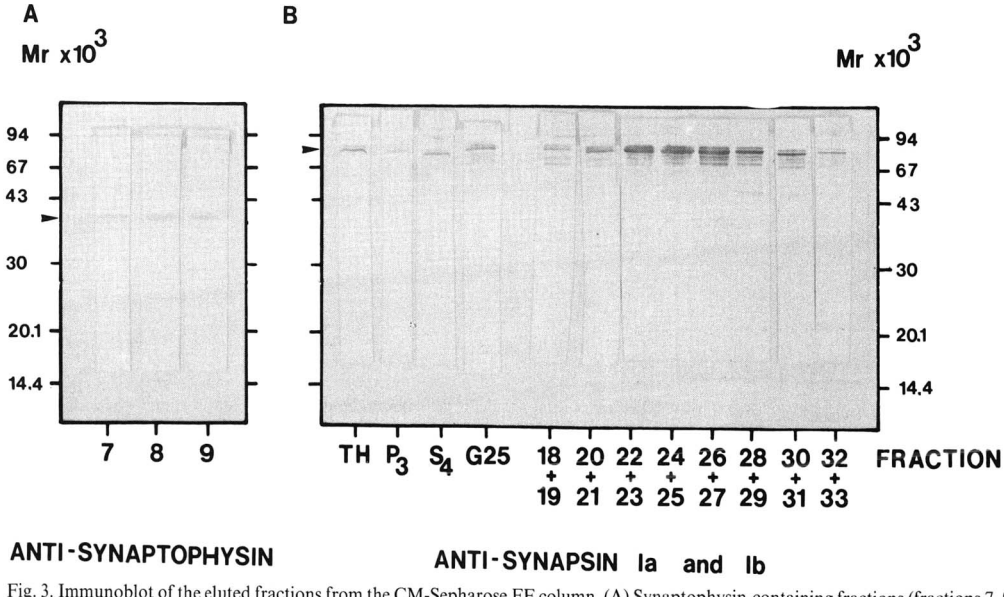

Fig. 3. Immunoblot of the eluted fractions from the CM-Sepharose FF column. (A) Synaptophysin-containing fractions (fractions 7–9); (B) synapsin I-containing fractions (fractions 20–30).

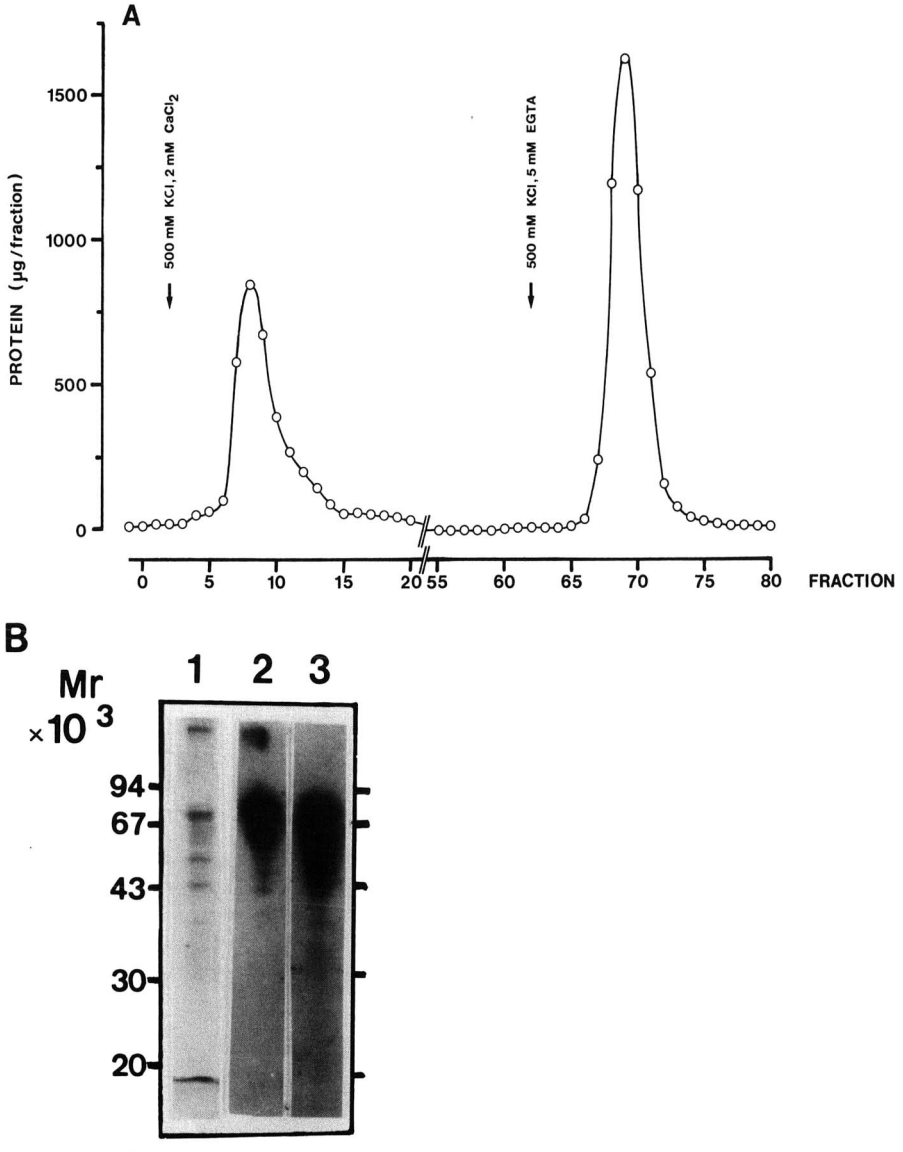

Fig. 4. Calmodulin affinity chromatography. (A) Protein elution profile of the column. Non-specific bound material was washed with buffer F plus 500 m*M* KCl. Synapsin I was eluted with buffer F plus 1 m*M* EGTA. (B) SDS-PAGE and corresponding immunoblot using [^{125}I]protein A for immunodetection. Lanes: 1 = CBB staining; 2 = 6 h exposure; 3 = 18 h exposure (5 µg of protein loaded per lane).

enriched only 87 times over total homogenate in the peak fraction eluting from the calmodulin column. The recovery was 25 µg of synapsin I per gram of brain. The original method of Ueda and Greengard [31] for the purification of synapsin I involved several chromatographic steps resulting in a low recov-

TABLE I

PROTEIN RECOVERY AND RELATIVE ENRICHMENT OF SYNAPSIN I AND SYNAPTOPHYSIN IN THE VARIOUS FRACTIONS OBTAINED IN THE COURSE OF THE PURIFICTION PROCEDURE

	Protein (%)	Enrichment factor[a]	
		Synapsin I	Synaptophysin
Total homogenate	100	1.00	1.00
S_1	57.5	0.91	0.90
P_2	27.2	0.83	1.42
P_3	19.1	1.62	1.31
Sephadex G-25	5.8	2.73	1.38
CM-Sepharose FF total bound	0.37	N.D.[d]	N.D.
CM-Sepharose FF fraction:			
7	0.027[b]	N.D.	84.7
8		N.D.	355.3
9		N.D.	386.2
10		N.D.	138.7
26	0.056[c]	25.6	N.D.
27		26.3	N.D.
28		40.0	N.D.
29		32.8	N.D.
30		29.8	N.D.
Calmodulin-Sepharose peak fraction	0.031	87.0	N.D.

[a] Enrichment factors for synapsin I and synaptophysin were calculated as described under Experimental. The values correspond to a typical experiment that was repeated at least four times with similar results.
[b] Percentage of protein recovered in fractions 7–10.
[c] Percentage of protein recovered in fractions 26–30.
[d] N.D. = Not determined.

ery (0.4 μg/g brain). Later, the method was modified by Schiebler *et al.* [32] and Bähler and Greengard [14], giving ten times higher recoveries (ca. 4 μg/g brain). A similar approach was used by Baines and Bennett [33] but with recoveries 5–6 times higher (20–23 μg/g brain). In 1986, Krebs *et al.* [21] published a rapid and simple method for the purification of synapsin I. Their recovery (80 μg/g brain) was much higher than any of the previous published methods. However, we were not able to reproduce the method with similar recoveries. If we assume that synapsin I comprises 0.5% of the total brain membrane protein [19], we recovered *ca.* 14% of the initial synapsin I. This low recovery can be atributed to several factors. First, synapsin I is a very "sticky" protein and adsorbs on tubes and surfaces, giving underestimates of protein measurements. Second, the presence of Ca^{2+} ions faciliates degradation of purified synapsin I [34]. As we eluted the calmodulin column with 5 m*M* $CaCl_2$, this degradation is inevitable. Breakdown products can be recognized in the immunoblots after longer incubation periods. Probably this also explains why the CBB staining does not match completely with the corresponding immunoblot (Fig. 4B). Some of the degradation products probably are not recognized by the polyclonal antibody. Degradation of synapsin I has also been reported *in vivo* in nerve terminals originating from sciatic nerve [35]. Moreover, recently it has been shown *in vitro* that synapsin I phosphorylated by Ca^{2+},calmodulin-dependent protein kinase II is able to self-degrade [36].

With the present method of purification, the recovery (25 μg of synapsin I per gram of brain) is similar to that reported by Bennett *et al.* [19] (20–23 μg/g brain). The additional advantage of this method is the simultaneous purification of synaptophysin with a high recovery (40 μg of synaptophysin per gram of brain). Until now, the methods for the purification of synapsin I consisted in the extraction of the protein starting from demyelinated membranes, followed by chromatography on carboxymethylcellulose [19]; a major contaminant protein has M_r = 38 000. This protein is also present in our chromatography on the CM-Sepharose FF column. However, we were able to identify this protein as synaptophysin. This positive identification of synaptophysin enables us to purify both the proteins synapsin I and synaptophysin simultaneously with a high recovery in a shorter time using a fairly simple method.

ACKNOWLEDGEMENTS

I.L. and W.G.A. have contributed equally to this article. This work was supported by a grant from the Queen Elizabeth Medical Foundation. We thank Dr. R. Jahn for fruitful discussions at his laboratory and Dr. P. Greengard and Dr. P. De Camilli for the generous gift of synapsin I antiserum. We thank M. Vandoolaeghe and M. De Donker for technical assistance, E. Coen for a critical review of the manuscript, and F. Jordaens and I. Bats for photographic work. W.G.A. holds an IWONL grant.

REFERENCES

1 E. Floor, S. F. Schaeffer, B. E. Feist and S. E. Leeman, *J. Neurochem.*, 50 (1988) 1588.
2 V. P. Whittaker, *Ann. N.Y. Acad. Sci.*, 493 (1987) 77.
3 E. Floor and S. E. Leeman, *J. Neurochem.*, 50 (1988) 1597.
4 M. Baumert, P. R. Maycox, F. Navone, P. De Camilli and R. Jahn, *EMBO J.*, 8 (1989) 379.
5 M. Baumert, K. Takei, J. Hartinger, P. M. Burger, G. Fisher von Mollard, P. R. Maycox, P. De Camilli and R. Jahn, *J. Cell Biol.*, 110 (1990) 1285.
6 S. Fournier and J. M. Trifaró, *J. Neurochem.*, 50 (1988) 27.
7 M. Bähler, R. L. Klein, J. K. T. Wang, F. Benfenati and P. Greengard, *J. Neurochem.*, 57 (1991) 423.
8 T. C. Südhof and R. Jahn, *Neuron*, 6 (1991) 665.
9 P. De Camilli and R. Jahn, *Annu. Rev. Physiol.*, 52 (1990) 625.
10 E. M. Johnson, T. Ueda, H. Maeno and P. Greengard, *J. Biol. Chem.*, 247 (1972) 5650.
11 E. J. Nestler and P. Greengard, *Prog. Brain Res.*, 69 (1986) 323.
12 T. C. Südhof, A. J. Czernik, H. Kao, K. Takei, P. A. Johnston, A. Horiuchi, S. D. Kanazir, M. A. Wagner, M. S. Perin, P. De Camilli and P. Greengard, *Science (Washington, D.C.)*, 245 (1989) 1474.
13 N. Hirokawa, K. Sobue, A. Harada and H. Yorifuji, *J. Cell Biol.*, 108 (1989) 111.
14 M. Bähler and P. Greengard, *Nature (London)*, 326 (1987) 704.
15 B. Wiedenmann and W. Franke, *Cell*, 41 (1985) 1017.
16 R. Jahn, W. Schiebler, C. Ouimet and P. Greengard, *Proc. Natl. Acad. Sci. U.S.A.*, 82 (1985) 4137.
17 H. Rehm, B. Wiedenmann and H. Betz, *EMBO J.*, 5 (1986) 535.
18 F. Navone, R. Jahn, G. Di Gioia, H. Stukenbrok, P. Greengard and P. De Camilli, *J. Cell Biol.*, 103 (1986) 2511.
19 V. Bennett, A. J. Baines and J. Davis, *Methods Enzymol.*, 134 (1986) 55.
20 T. Okabe and K. Sobue, *FEBS Lett.*, 213 (1987) 184.
21 K. E. Krebs, I. S. Zagon and S. R. Goodman, *Brain Res. Bull.*, 17 (1986) 237.
22 M. M. Bradford, *Anal. Biochem.*, 72 (1976) 248.
23 U. K. Laemmli, *Nature (London)*, 227 (1970) 680.
24 C. Lee, A. Levin and D. Branton, *Anal. Biochem.*, 166 (1987) 308.
25 H. Towbin, T. Staehelin and J. Gordon, *Proc. Natl. Acad. Sci. U.S.A.*, 76 (1979) 4350.
26 R. H. Aebersold, J. Laevitt, R. A. Saavedra, L. E. Hood and S. B. H. Kent, *Proc. Natl. Acad. Sci. U.S.A.*, 84 (1987) 6970.
27 S. M. Lohmann, T. Ueda and P. Greengard, *Proc. Natl. Acad. Sci. U.S.A.*, 75 (1978) 4037.
28 P. Knaus, H. Betz and H. Rehm, *J. Neurochem.*, 47 (1986) 1302.
29 C. A. Haas and L. J. De Gennaro, *J. Cell Biol.*, 106 (1988) 195.
30 N. Leclerc, P. W. Beesley, I. Brown, M. Colonnier, J. W. Gurd, T. Paladino and R. Hawkes, *J. Comp. Neurol.*, 280 (1989) 197.
31 T. Ueda and P. Greengard, *J. Biol. Chem.*, 252 (1977) 5155.
32 W. Schiebler, R. Jahn, J. P. Doucet, J. Rothlein and P. Greengard, *J. Biol. Chem.*, 261 (1986) 8383.
33 A. Baines and V. Bennett, *Nature (London)*, 315 (1985) 410.
34 R. Jahn, personal communication.
35 S. Bööj, P.-A. Larsson, A.-G. Dahllöf and A. Dahlström, *Acta Physiol. Scand.*, 128 (1986) 155.
36 A. N. Gubin and S. E. Severin, *FEBS Lett.*, 289 (1991) 11.

Journal of Chromatography, 596 (1992) 59–66
Elsevier Science Publishers B.V., Amsterdam

CHROM. 23 930

Optimization of the separation of the Rp and Sp diastereomers of phosphate-methylated DNA and RNA dinucleotides

A. J. J. M. Coenen, L. H. G. Henckens, Y. Mengerink and Sj. van der Wal*

DSM Research, Department FA-CO, P.O. Box 18, 6160 MD Geleen (Netherlands)

P. J. L. M. Quaedflieg, L. H. Koole and E. M. Meijer

Department of Organic Chemistry, Eindhoven University of Technology, Eindhoven (Netherlands)

(First received July 5th, 1991; revised manuscript received November 27th, 1991)

ABSTRACT

The separation by reversed-phase high-performance liquid chromatography of Rp and Sp diastereomers of phosphate-methylated DNA and RNA dinucleotides was studied with respect to pH, organic modifier type and concentration and reversed-phase packing material. Drylab G was used to deduce optimum conditions. On the basis of the observed discrepancies between the computer predictions and experimental results, the gradient operation procedure with volatile buffers was improved. By repetitive chromatography on a 250 × 22 mm I.D. reversed-phase column, fourteen diastereomeric pairs were obtained in at least 97% purity and 60% yield, in amounts of 10–100 mg.

INTRODUCTION

Phosphate-methylated 2′-deoxyribodinucleotides and 2′-O-methylphosphate-methylated ribodinucleotides (Fig. 1) show interesting structural properties [1–4]. Study of these structures using high-field proton NMR requires separation of the two diastereomeric forms present in the synthesis product. Several groups have analysed similar compounds. Cadet and Voituriez [5] used Nucleosil C_{18} and methanol–water (30:70) to separate dTp(OC_2H_5CN)T diastereomers. The separation of some O-isopropyl phosphate triesters and methyl phosphonates was performed by Stec *et al.* [6] with a volatile acetonitrile–triethylammonium acetate buffer system (pH 7). Recently Weinfeld *et al.* [7] purified O-ethylphosphate triesters on a reversed-phase system with methanol–water as an unbuffered mobile phase. These investigations all involved the isolation of the particular compounds and no optimization of the high-performance liquid chromatography (HPLC) system was carried out. Stec *et al.* [6] cautioned against predicting even the order of elution in these types of separations, let alone the relative separation factors. This means that each separation has to be optimized empirically.

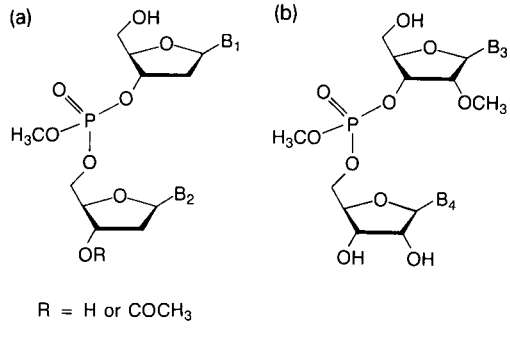

R = H or $COCH_3$

Naturally, it is of practical value if one can limit the number of phase systems to those with the largest orthogonality in selectivity. We therefore investigated the effect of the type and concentration of the organic modifier, the pH and the stationary phase to expedite the isolation of 0.01–0.1-g amounts of the Rp and Sp diastereomers of phosphate-methylated dinucleosides for study by high-resolution proton and phosphorus NMR.

EXPERIMENTAL

The isolation of 10–100-mg amounts of the diastereomers was effected in essentially three stages: (1) determination of suitable isocratic conditions using an analytical gradient system; (2) repetitive preparative separations on 10–20 mg of the analytes and collection of fractions; and (3) analysis of each fraction to assess its Rp and Sp diastereomer content. By repeating steps 2 and 3 on part of the fractions all diastereomers of d(CpG), d(GpC), d(ApC), d(ApA)ac, d(ApT)ac, d(CpC)ac, d(TpC), d(TpT), r(ApC), r(ApG), r(CpG), r(CpC), r(CpU) and r(ApU) were obtained in at least 97% purity.

The separation of the diastereomers was developed on an HP 1090 or HP 1050 (Hewlett-Packard, Waldbronn, Germany) gradient HPLC system using a built-in diode-array detector to locate the phosphate-methylated dinucleotides between highly absorbing N-(9-fluorenyl methoxycarbonyl) (Fmoc) derivatives and other reaction impurities, or using a Linear (Reno, NV, USA) Model 204 absorbance detector set at 270 nm. Preparative chromatography was performed on a high-performance liquid chromatograph consisting of a Waters (Milford, MA, USA) Model M590 solvent delivery system equipped with a solvent-selection valve module for sample introduction, an RSil C_{18} (10 μm particle size) column (250 × 22 mm I.D.) (Alltech, Deerfield, IL, USA) and a Waters Model 480 absorbance detector. Fractions were collected with an LKB (Bromma, Sweden) Model 2211 Superrac fraction collector and checked for purity on an analytical HPLC system consisting of a Spark (Emmen, Netherlands) SPH125 autosampler, an HP 1050 (Hewlett-Packard) or a Gilson (Villiers-le-Bel, France) Model 302 pump, a 250 × 4 mm I.D. Nucleosil 120-3 C_{18} reversed-phase column (Macherey–Nagel, Düren, Germany) and a linear UV-203 absorbance detector that monitored the eluate at 260 nm.

Other reversed-phase columns used for development were a 125 × 4 mm I.D. LiChrospher C_{18} (5 μm) (Merck, Darmstadt, Germany) and a 100 × 4.6 mm I.D. Microspher C_{18} (3 μm) column (Chrompack, Middelburg, Netherlands). The mobile phases were acetonitrile (gradient grade, Merck) or methanol (LiChrosolv, Merck) as organic modifiers and 0.1% (v/v) formic or acetic acid (analytical-reagent grade, Merck), 100–200 μl/l triethylamine (zur Synthese, Merck) in water purified with a Milli-Q water purification system, adjusted to the desired pH with ammonia solution (Baker Analysed Reagent, 25%, aqueous; Baker, Deventer, Netherlands).

RESULTS AND DISCUSSION

Phase system selectivity

Ribonucleotide derivatives of C and A with C, G and U were run in shallow acetonitrile and methanol gradients at pH 2.7 and 5.4 (see Table I). These are the extremes of a pH range encompassing the expected pK_a values of C and A nucleotides of 4.3 and 3.8, respectively, and well within the range of stability of reversed-phase silica-based columns, a prerequisite for preparative HPLC.

From Table I, isocratic phase systems can be calculated with the help of DryLab to compare the selectivity in a 15-min separation for the diastereomers with respect to modifier and pH (see Table II). For the r(CpG) sample a 10-min separation time was chosen, as the selectivity trend observed in Fig. 6 (and discussed below) decreases ($\alpha - 1$) rapidly on lowering the modifer concentration to obtain a 15-min separation.

It is possible that the optimum pH for separation is near the pK_a of a base owing to a slight difference in pK_a between the diastereomers, the more so if the capacity factor changes dramatically at the pK_a [6]. The variation of retention and selectivity with pH is shown in Figs. 2a and b, respectively, for some analyte pairs.

The retention of the Rp diastereomer is generally more sensitive to increase in pH and decrease in modifier concentration than that of the Sp diastereomer, so that in general the Rp diastereomer is eluted last at neutral pH and at low acetonitrile con-

TABLE I

RETENTION TIMES OF RIBONUCLEOTIDE DERIVATIVES UNDER GRADIENT CONDITIONS

Column: Microspher C_{18} (100 × 4.6 mm I.D.). Mobile phase: (A1) 0.1% formic acid–0.01% triethylamine (pH 2.7); (A2) 0.1% formic acid–0.2% triethylamine (pH 5.4); (B) acetonitrile. Gradient I: 5 → 15% B, 2 ml/min, temperature 25°C. Gradient II: 20 → 40% methanol in A1, 1 ml/min. Gradient III: 15 → 25% methanol in A2, 1 ml/min.

Compound	Gradient I								Gradient II				Gradient III			
	pH 2.7, 20 min		pH 2.7, 40 min		pH 5.4, 10 min		pH 5.4, 20 min		pH 2.7, 20 min		pH 2.7, 40 min		pH 5.4, 20 min		pH 5.4, 40 min	
	1[a]	2[a]	1	2	1	2	1	2	1	2	1	2	1	2	1	2
r(CpC)	7.00	7.40	8.59	9.17	4.09	4.29	5.43	5.75	7.70	7.78	8.20	8.32	8.75	9.50	9.97	10.95
r(CpG)	7.37	7.83	9.90	10.48	3.88	4.06	5.33	5.68	7.13	7.74	7.18	7.91	8.44	9.26	9.44	10.69
r(CpU)	8.37	8.62	11.35	11.86	4.45	4.70	5.95	6.51	7.86	7.86	8.54	8.54	8.94	10.06	10.09	11.80
r(ApC)	9.90	10.39	13.37	14.35	7.00	7.00	10.62	10.78	10.72	11.45	12.07	13.02	18.61	19.42	25.51	27.07
r(ApG)	9.19	10.33	13.70	15.07	6.85	7.26	10.90	11.65	8.92	10.00	9.85	11.39	20.17	21.59	28.52	31.04

[a] 1 and 2 denote the first and last eluting diastereomer, respectively.

TABLE II

DRYLAB PREDICTIONS FOR ISOCRATIC SEPARATIONS, BASED ON DATA IN TABLE I

Compound	Acetonitrile modifier						Methanol modifier					
	pH 2.7			pH 5.4			pH 2.7			pH 5.4		
	Modifier (%)	k'_2	$\alpha - 1$	Modifier (%)	k'_2	$\alpha - 1$	Modifier (%)	k'_2	$\alpha - 1$	Modifier (%)	k'_2	$\alpha - 1$
r(CpC)	4.5	29.8	0.09[a]	4.5	32.3	0.09	12	13.7	0.05[a]	14.5	13.6	0.13
r(CpG)	6	21.9	0.09[a]	5	32.9	0.22	5[b]	9.7	0.41[a]	14	15.1	0.26
r(CpU)	6	28.0	0.10	5	31.6	0.36				15	13.7	0.28
r(ApC)	6.5	30.4	0.15	7	35.5	0.13	20	14.2	0.10	21	13.5	0.11
r(ApG)	7	27.8	0.24	8	28.7	0.31	18	14.9	0.27	22	14.2	0.21

[a] Elution order: Rp, Sp.

[b] Separation is better at smaller k' than with a 15-min separation time (see Discussion of Fig. 6).

centrations (*i.e.*, $k' > 5$). The elution order of r(CpC) reverses at pH 3.1, below which the Rp diastereomer elutes first (see Fig. 3). Also, the elution order of d(CpG) and r(CpG) changes with pH of the mobile phase (Fig. 4a and b); similar chromatograms to those in Fig. 4a and b can be obtained with 15% methanol instead of 4–6% acetonitrile (*e.g.*, compare Fig. 4b and c). For d(CpC)ac, a maximum in resolution is found at pH 3.5 with a Nucleosil 120-3 C_{18} column and small capacity factors, and for r(CpC) at pH 4.0 with a Microspher C_{18} column (see Fig. 2b).

Overall, acetonitrile as a modifier and neutral pH appear to be a good choice in terms of selectively. We prefer acetronitrile to methanol owing to comparable selectivity, comparable expense at the modifier concentration used, the relatively low UV background at 200 nm and the low back-pressure generated. A disadvantage of the use of pH 2.7 is that the peaks of positively charged analytes show

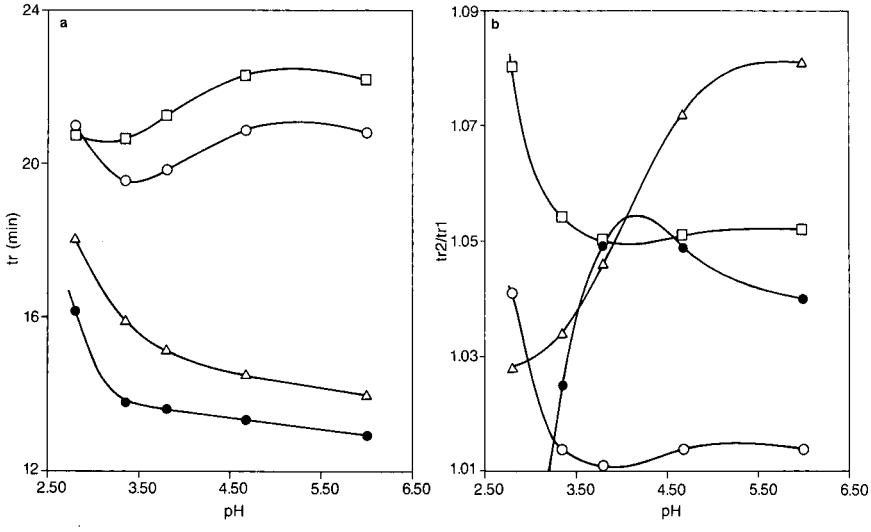

Fig. 2. Dependence of (a) retention time (tr) and (b) retention ratio of diastereomers on the pH of the mobile phase for some phosphate-methylated ribodinucleotides. Column, Microspher C_{18} (100 × 4.6 mm I.D.). Mobile phase: (A) 0.1% (v/v) formic acid–100 µl/l triethylamine adjusted to the required pH with 25% ammonia solution; (B) acetonitrile; gradient, 2–15% B in 33 min; flow-rate, 2 ml/min. Analytes: ● = r(CpC); △ = r(CpU); ○ = r(ApC); □ = (ApG).

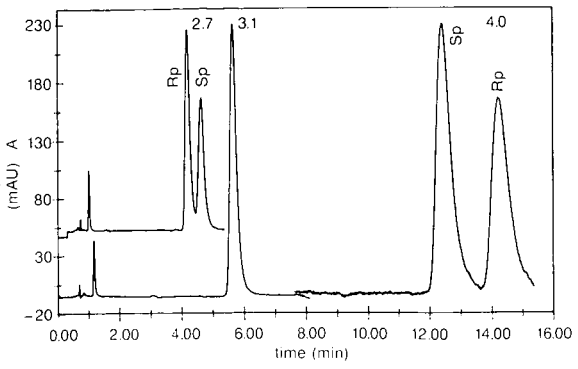

Fig. 3. Elution order reversal of r(CpC) with pH (2.7, 3.1, 4.0). Column, Microspher C_{18}; mobile phase, 6% acetronitrile–0.1% formic acid–60 μl/l triethylamine, adjusted to required pH; flow-rate, 2 ml/min.

tailing. Tailing can be decreased by increasing the ionic strength and the concentration of triethylamine as a competitive base. As shown in Fig. 5b, the capacity factors of the Sp diastereomers tend to decrease more than those of the Rp diastereomers with increasing triethylamine concentration, so that the diastereomeric selectivity at pH 2.7 increases for r(CpU) and decreases for r(CpC) and r(CpG) because at pH 2.7 the Rp diastereomers of r(CpC) and r(CpG) elute before the Sp diastereomers, and the Rp diastereomer of r(CpU) later than its Sp diastereomer (see Table II).

The selectivity of three types of reversed-phase columns was tested. On Nucleosil 120-5 C_{18} and LiChrospher 100 RP-18 the Rp diastereomers are more retained relative to the Sp diastereomers than on Microspher C_{18}, so the elution order reversal of r(CpC), r(CpG) and d(CpG) and the maximum in selectivity for r(CpC) occur at a pH that is lower (by *ca.* 0.4) on LiChrospher and Nucleosil than on Microspher. Apparently the last packing creates a more acidic environment for the analytes than the others; little effect on stereoselectivity was observed on testing packing materials having a different pore size, surface area, coverage or end-capping.

The most difficult separation, r(ApU), can be performed on a short Nucleosil 120-5 C_{18} column with a low acetonitrile concentration and at pH 4.5–6. The selectivity for r(ApU) on Nucleosil is then slightly better than that on LiChrospher and superior to that on Microspher.

There is a general trend to less retention of the Rp

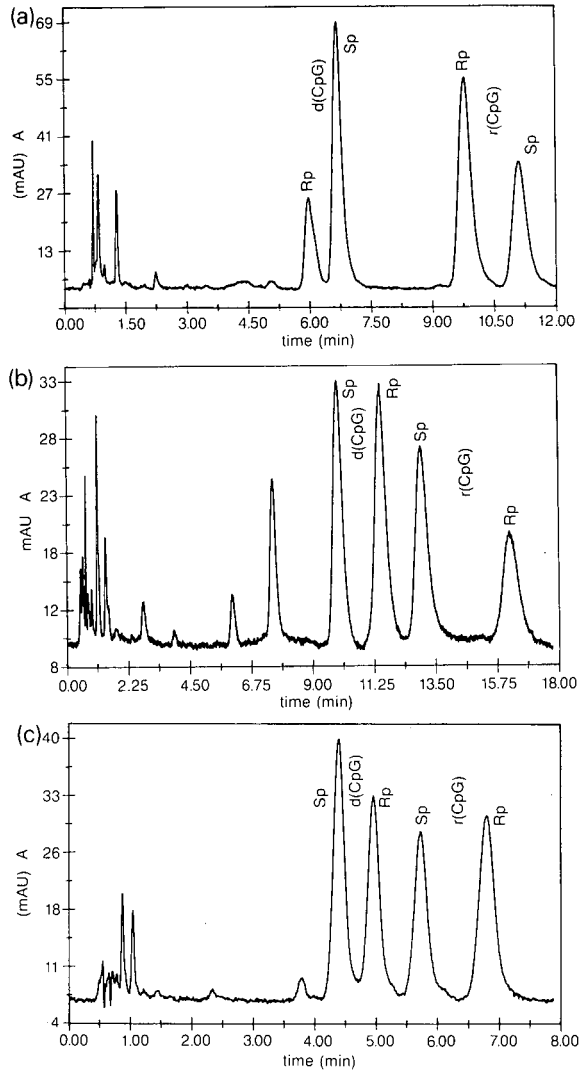

Fig. 4. Separation of d(CpG) and r(CpG) diastereomers. Column, Microspher C_{18}; flow-rate, 2 ml/min. Mobile phase: (a) 6% acetonitrile–0.1% formic acid–60 μl/l triethylamine (pH 2.7); (b) 4% acetonitrile–0.1% acetic acid–60μl/l triethylamine, adjusted to pH 5.2; (c) 15% methanol–0.1% acetic acid–60μl/l triethylamine, adjusted to pH 5.2

diastereomer relative to that of the Sp diastereomer at higher modifier concentrations. This is illustrated in Fig. 6, where for r(CpG) the selectivity factor increases with acetonitrile concentration when the Rp diastereomer is eluting first. The replacement of acetonitrile with methanol at concentration giving the same retention times for a given column and

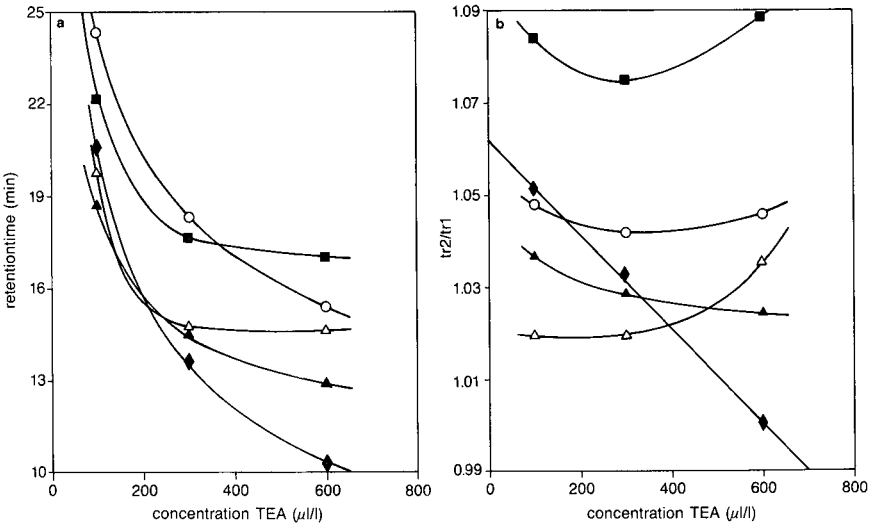

Fig. 5. Dependence of (a) retention time and (b) retention time ratio of diastereomers of phosphate-methylated ribodinucleotides on triethylamine (TEA) concentration. Column, Microspher C_{18}; flow-rate, 2 ml/min. Mobile phase: (A) 0.1–0.2% formic acid–100–600μl/l triethylamine; (B) acetonitrile; gradient, 2–14% B in 33 min. Analytes: ◆ = r(CpC); △ = r(CpU); ○ = r(ApC); ■ = r(ApG); ▲ = r(CpG).

back-pressure usually means that a much higher methanol concentration is needed. A general neat effect of the type of modifier in the experiments performed cannot be observed and often an acetonitrile concentration and pH can be found that give the same selectivity as is observed when using methanol (*cf.*, Table II and Fig. 4b and c). It can be predicted, however, that r(ApU) will be best separated in the order Rp–Sp on a Microspher C_{18} column at a low pH using methanol as a modifier (experimentally: $k' = 9.0$, $\alpha = 1.09$).

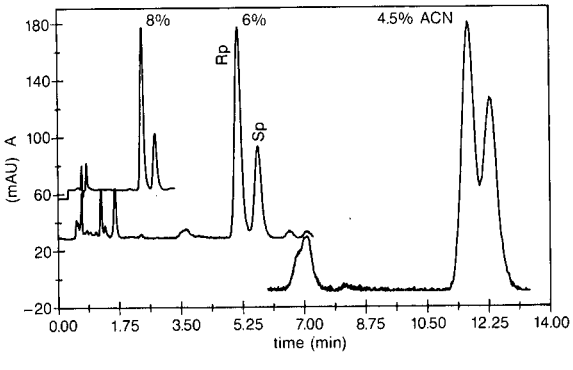

Fig. 6. Increasing resolution with modifier concentration for the separation of r(CpG). Column, Microspher C_{18}; flow-rate, 2 ml/min. Mobile phase: (a) 8% acetonitrile (ACN)–0.2% formic acid–60 μl/l triethylamine (pH 2.7); (b) 6% acetonitrile–0.2% formic acid–60 μl/l triethylamine (pH 2.7); (c) 4.5% acetonitrile–0.2% formic acid–60 μl/l triethylamine (pH 2.7).

Gradient operation

The data in Table I can be used for calculation of an optimum gradient system for a mixture that contains more than one pair of diastereomers; this is not the case with the present dimers, but more complex mixtures are obtained for larger oligomers. We used Drylab G to calculate such a gradient for the mixture of r(CpC), r(CpG), r(CpU), r(ApC) and r(ApG). The retention times of the experimental run were within 0–3% of the calculated values for the optimum gradient (see Table III). The authors of Drylab pointed out several factors that can contribute to errors in computer simulation amounting to 1–3% of the retention time [8]. This would mean additional fine tuning of the final gradient, but can be considered to be still acceptable for difficult separations. In the present case the major cause of discrepancy was not among the causes found by Dolan *et al.* [8]. Our studies were performed with a volatile buffer system to facilitate the transfer to preparative scale HPLC. The largest error turns out to be a drift

TABLE III

COMPARISON OF A CALCULATED AND EXPERIMENTAL OPTIMUM GRADIENT RESULTS FOR THE SEPARATION OF A COMPLEX TEST MIXTURE

Column: Microspher C_{18} (100 × 4.6 mm I.D.). Mobile phase: (A) 0.1% formic acid–0.01% triethylamine (pH 2.7). Gradient: 2 → 14% acetonitrile in A in 33 min, 2 ml/min.

Compound	Retention time (t_r) (min)		Δt_r (%)	ΔpH[a]
	Experimental	Calculated		
r(CpC)	14.45	13.97	3.4	0.05
	15.04	14.55	3.4	0.05
r(CpG)	15.91	15.97		
	16.39	16.38		
r(CpU)	17.13	17.13		
	17.61	17.60		
r(ApC)	18.80	18.66	0.8	0.05
	19.87	19.55	1.7	0.05
r(ApG)	19.03	19.11		
	20.29	20.21		

[a] Difference in experimental and calculated pH based on Fig. 2a. Only calculated for r(CpC) and r (ApC) owing to their strong dependence.

of 0.05 in the pH of the mobile phase over a period of 1 day. This meant that in order to use the computer program in such a way as to obtain even more accurate results we had to improve our operation with volatile buffers.

HPLC systems are to some extent sensitive to out-gassing. To eliminate bubble formation problems, the solvents are usually degassed with helium prior to use and sparged with helium during operation. From the solubility curves of gases in several solvents it seems clear that the high concentration of dissolved carbon dioxide in the organic solvent causes the problem [9]. By using three reservoirs, two with water containing different concentrations of volatile buffer, without helium sparging, and the other with pure organic modifier with helium degassing, the pH of an ammonium formate buffer of pH 4.3 (capacity = 0.005 *M* [10]) could be maintained within 0.02 over a 16-h period of use, keeping the discrepancy between calculated and experimental retention times within 1.4% (*cf.*, Fig. 2a). The two aqueous buffer solutions are very convenient for adjusting the absorbance when working at lower wavelengths (for maximum sensitivity) or for applying a slight pH gradient.

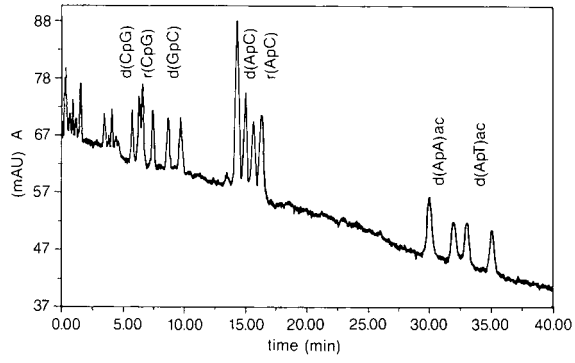

Fig. 7. Separation of a mixture of phosphate-methylated dinucleotides. Column, LiChrospher 100 RP-18 (125 × 4 mm I.D.). Mobile phase: (A) 0.1% formic acid–100 μl/l triethylamine adjusted to pH 5.3; (B) acetonitrile; gradient, 4–14% B in 40 min; flow-rate, 5 ml/min; starting pressure, 320 atm.

To demonstrate the overall separation capabilities of HPLC for the phosphate-methylated dinucleotides, a mixed organic modifier gradient separation is shown in Fig. 7.

Considering the complex dependence of selectivity on the combination of type and concentration of modifier, pH, ionic strength and competing base and stationary phase, the only sensible way to optimize such a separation is by a chemometric method with the help of a computer. Such a method is at present not available in our laboratories but it is expected to be commercially available soon and may prove invaluable for the separation of the more complex tetranucleotides that will be the next generation of modified oligonucleotides to be separated.

Preparative HPLC

After method development on an analytical scale to maximize the selectivity factor for the diastereomers, 10–100 mg amounts of the analyte mixtures were diluted with 2 ml of a solution consisting of the aqueous part of the mobile phase, containing at most half of the percentage of organic modifier to be used in preparative chromatography. By on-column concentration, volumes of 250 ml can be introduced on a 250 × 22 mm I.D. preparative column with the aid of a solvent-selection valve without much detrimental effect on the separation due to volume overloading. Mass overloading and, in particular, solubility in the injection solvent appear to be the limiting conditions.

TABLE IV

CONDITIONS AND RESULTS FOR ANALYTICAL AND SEMI-PREPARATIVE HPLC OF PHOSPHATE-METHYLATED RIBODINUCLEOTIDES

Analytical HPLC						Semi-preparative HPLC					
Compound	Mobile phase		k'_{Rp}	$\alpha_{Sp,Rp}$	$R_{Sp,Rp}$	Sample	Mobile phase		Purity (%)	Yield (%)
	Acetonitrile (%)	pH					Acetonitrile (%)	pH		
r(ApC)	10	4.5	10.0	1.10	2.1	r(ApC) 1			99.5	85
r(ApG)	12	2.5	1.9	1.33	3.8	2	8	4.5	97.5	77
r(CpG)	7	2.5	1.8	1.19	2.9	r(CpG) 1	4	2.5	99.8	86
r(CpC)	8	5.0	4.1	1.15	3.0	2	3	5.8	99.7	93
r(CpU)	8	5.0	3.4	1.12	2.0	r(CpC) 1	4	4.0	99.4	60
r(ApU)	12	4.7	3.0	1.07	1.1	2			99.5	75

The 4,4′-dimethoxytrityl-d( )methylphosphonate-( )-3′-menthoxycarbonates [where ( ) are the respective bases] were separated by Katti and Agarwal [11] using silica by virtue of the 3′-menthyl group. These derivatives are even less soluble in aqueous media, so normal-phase HPLC has to be used for isolation. Employing normal-phase HPLC we obtained recoveries of less than 50% for similar compounds, although the selectivities (but not efficiency) were much higher than with reversed-phase HPLC.

The type of reversed-phase column used for preparative HPLC (RSil-C_{18} HL, 10 μm) was different from that used in the analytical separations as it was not available at that time. The optimum conditions for analysis were therefore not always optimum for preparative HPLC [1]. The purities and yields of a few methylated ribodinucleotide pairs achieved by using 2–4% less acetonitrile and overlapping band fractionation are given in Table IV. Optimum conditions for most of the phosphate-methylated deoxyribunocleotides are given in Table I in ref. 1.

REFERENCES

1 L. H. Koole, H. M. Moody, N. L. H. L. Broeders, P. J. L. M. Quaedflieg, W. H. A. Kuijpers, M. H. P. van Genderen, A. J. J. M. Coenen, Sj. van der Wal and H. M. Buck, *J. Org. Chem.*, 54 (1989) 1657.
2 P. J. L. M. Quaedflieg, A. P. van der Heiden, L. H. Koole, M. H. P. van Genderen, A. J. J. M. Coenen, Sj. van der Wal and H. M. Buck, *Proc. K. Ned. Akad. Wet.*, 93, No. 1 (1990) 33.
3 P. J. L. M. Quaedflieg, L. H. Koole, M. H. P. van Genderen and H. M. Buck, *Recl. Trav. Chim. Pays-Bas*, 108 (1989) 421.
4 P. J. L. M. Quaedflieg, N. L. H. L. Broeders, L. H. Koole, M. H. P. van Genderen and H. M. Buck, *J. Org. Chem.*, 55 (1990) 122.
5 J. Cadet and L. Voituriez, *J. Chromatogr.*, 178 (1979) 337.
6 W. J. Stec, G. Zon and B. Uznanski, *J. Chromatogr.*, 326 (1985) 263.
7 M. Weinfeld, A. F. Drake, R. Kuroda and D. C. Livingston, *Anal. Biochem.*, 178 (1989) 93.
8 J. W. Dolan, D. C. Lommen and L. R. Snyder, *J. Chromatogr.*, 485 (1989) 91.
9 S. R. Bakalyar, M. P. T. Bradley and R. Honganen, *J. Chromatogr.*, 158 (1978) 277.
10 B. L. Karger, J. N. LePage and N. Tanaka, in Cs. Horváth (Editor), *High-performance Liquid Chromatography*, Vol. 2, Academic Press, New York, 1980, p. 113.
11 S. B. Katti and K. Agarwal, *Tetrahedron Lett.*, 27 (1986) 5327.

Journal of Chromatography, 596 (1992) 67–71
Elsevier Science Publishers B.V., Amsterdam

CHROM. 23 984

Determination of nitroxynil in cow milk by reversed-phase high-performance liquid chromatography with dual-electrode coulometric detection

Kazue Takeba* and Masao Matsumoto

Department of Food Hygiene and Nutrition, Tokyo Metropolitan Research Laboratory of Public Health, Tokyo 169 (Japan)

Hiroyuki Nakazawa

Department of Pharmaceutical Sciences, National Institute of Public Health, Tokyo 108 (Japan)

(First received September 24th, 1991; revised manuscript received December 31st, 1991)

ABSTRACT

A sensitive and specific method is described for the determination of nitroxynil (fasciolicide) residues in cow milk. The milk samples were extracted with acetone and acetonitrile, following clean-up using a simple liquid–liquid extraction step. Nitroxynil was separated from the matrix peaks by reversed-phase high-performance liquid chromatography and detected using dual-electrode coulometric detection. The mobile phase was a mixture (20:80, v/v) of acetonitrile and 0.05 *M* potassium dihydrogenphosphate with the pH adjusted to 4.0. The flow-rate was 1 ml/min at 40°C. The applied potentials of detectors 1 and 2 were maintained at −0.7 and +0.2 V, respectively. Average recoveries ($n = 5$) of nitroxynil from milk samples spiked at concentrations of 0.01 and 0.1 μg/ml were found to be 92.0% and 97.0% with coefficients of variation of 6.2% and 2.2%, respectively. The detection limit of nitroxynil in milk was 0.7 ng/ml. During the analysis of 30 raw cow milk and 140 market milk samples, nitroxynil was detected at a level of 4 ng/ml in one raw cow milk sample.

INTRODUCTION

Nitroxynil (4-hydroxy-3-iodo-5-nitrobenzonitrile) is an anthelmintic that controls fascioliasis caused by *Fasciola hepatica* in cattle. When compared with other fasciolicides, this compound shows high activity against both adult and immature liver flukes [1–4]. Infected cattle are injected subcutaneously with 10 mg/kg nitroxynil in the form of an aqueous solution of its N-alkylglucamine salt.

However, this compound is known to be excreted as a long-lasting residue in milk [5–11]. In Japan, milk for human consumption must not be taken from cows which have been fed or injected with medicine that has an effect on milk during the period when the medicine remains in the milk [12]. This has led to the need to developing a simple, sensitive and specific method of monitoring residual levels of nitroxynil in cow milk.

Most of the methods reported for determining residual levels of nitroxynil in milk involve polarography [5,10,13], gas chromatography [6,8,9,14] and high-performance liquid chromatography (HPLC) [11]. In this paper, a simple, sensitive and specific method for the determination of nitroxynil in milk using reversed-phase HPLC with electrochemical (dual-electrode coulometric) detection is described.

EXPERIMENTAL

Instrumentation

The HPLC system consisted of a Model LC-6A pump (Shimadzu, Kyoto, Japan) with a 20-μl sam-

0021-9673/92/$05.00

ple loop injector (Rheodyne, Cotati, CA, USA), a series of Model 870-UV UV monitors (Jasco, Tokyo, Japan), a Model Coulochem 5100A coulometric detector comprising a solid-state analytical cell (Model 5010), containing dual coulometric working electrodes made from porous graphite, and a guard cell (Model 5020) (ESA International, Bedford, USA). The applied potentials of the guard cell, detector 1 and detector 2 of the coulometric detector were maintained at −0.7, −0.7 and +0.2 V, respectively, at ambient temperature. The guard cell was directly connected to detector 1. The sensitivity of detector 2 was maintained with gain 10 × 40 and response time 10 s. The UV monitor was set at a wavelength of 270 nm with 0.08 a.u.f.s. LiChroCART LiChrospher 100 RP-18 (5 μm particle size, 250 × 4 mm I.D.) was used as an analytical column. The mobile phase consisted of acetonitrile–0.05 *M* potassium dihydrogenphosphate (20:80, v/v), adjusted to pH 4.0 with 10% (w/v) phosphoric acid. The flow-rate of the recycled mobile phase was 1.0 ml/min at 40°C with bubbling by nitrogen gas throughout the HPLC analysis.

Standard and chemicals

Nitroxynil was obtained from Rhone-Poulenc-Rorer (Dagenham, UK) through Kyowa Hakko Kôgyo (Tokyo, Japan). The structure of the compound is shown in Fig. 1. Nitroxynil was dissolved in acetonitrile and the working standard was diluted with the mobile phase. All other reagents and organic solvents used were of special and HPLC grade.

Sample preparation

A 10-ml sample of cow milk was mixed with 10 ml of acetonitrile and 10 ml of acetone in a 50-ml glass centrifuge tube. The mixture was shaken well and centrifuged at 2000 *g* for 10 min. The supernatant was transferred into a 100-ml separation funnel and extracted with 20 ml of dichloromethane. The organic phase was evaporated to dryness under reduced pressure. The wet residue was dissolved in 5 ml of 1% (w/v) sodium hydrogencarbonate and acidified by the addition of 1 ml of concentrated hydrochloric acid, to a final pH of 2–3. The acidified solution was transferred into a 100-ml separation funnel and extracted with 10 ml of dichloromethane. The organic phase was washed with 10 ml of distilled water. The extract was evaporated to dryness. A 1-ml aliquot of the mobile phase was added to the residue. This solution was filtered through a 0.2-μm membrane filter, and 5 μl of the sample were injected into the HPLC system.

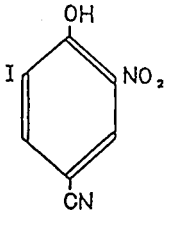

Fig. 1. Structure of nitroxynil (4-hydroxy-3-iodo-5-nitrobenzonitrile).

RESULTS AND DISCUSSION

To develop a sensitive and specific method for determining nitroxynil, electrochemical detection was evaluated because nitroxynil has a phenol group in its structure, as shown in Fig. 1. Although nitroxynil was oxidized above a potential of +0.8 V, this potential gave almost the same sensitivity as UV detection at 270 nm. In order to improve the sensitivity, the electrochemical behaviour of the nitro group at the reductive and oxidative area was investigated.

The effects of the applied potentials on the electrochemical response of nitroxynil at different pH values of the mobile phase are shown in Fig. 2, and the relationship between the capacity factor (k') and the pH is shown in Fig. 3. The applied potential of the guard cell and detector 1 was fixed at −0.7 V, and that of detector 2 was varied from +0.7 V to lower voltages.

The higher the applied potential of detector 2 and the lower the pH of the mobile phase, the higher the electrochemical response obtained. Nitroxynil in a mobile phase of pH 3.0 showed the highest electrochemical response, while the nitroxynil capacity factor (k') was 15.8 (retention time *ca.* 24 min), unsuitable for HPLC analysis. Therefore, from this current–voltage curve, the mobile phase was adjusted to pH 4.0 ($k' = 5.7$). The applied potential of detector 2 was adjusted to +0.2 V, resulting in the most stable baseline.

Secondly, the effect of the reductive applied potential of the guard cell and detector 1 on the elec-

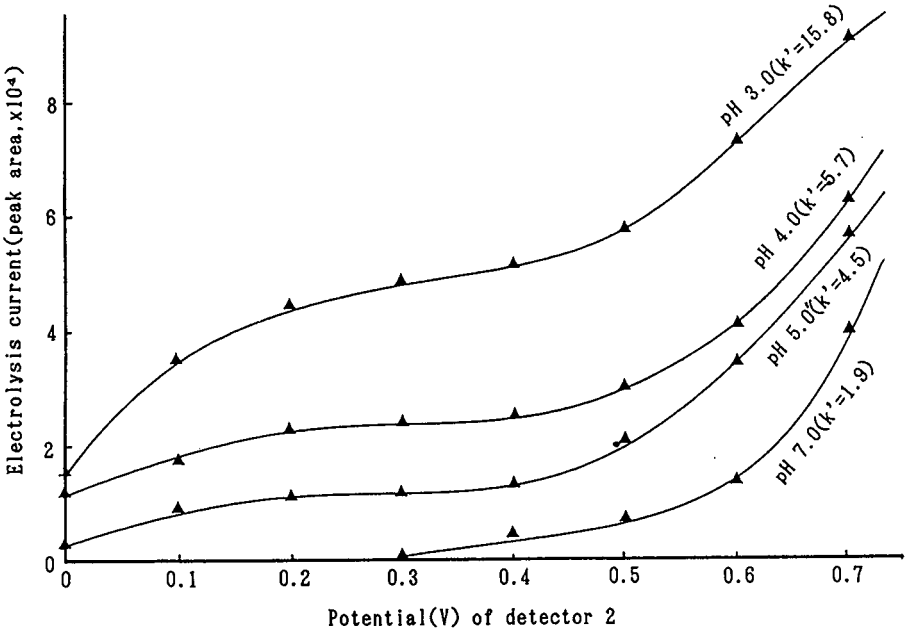

Fig. 2. Effects of the potential of detector 2 on the electrolysis current determining nitroxynil at different pH values (3.0, 4.0, 5.0, 7.0) of the mobile phase. Conditions of coulometric detection: guard cell, −0.7 V, detector 1, −0.7 V; detector 2, +0.7–0.0 V; gain, 10 × 40; response time, 10 s.

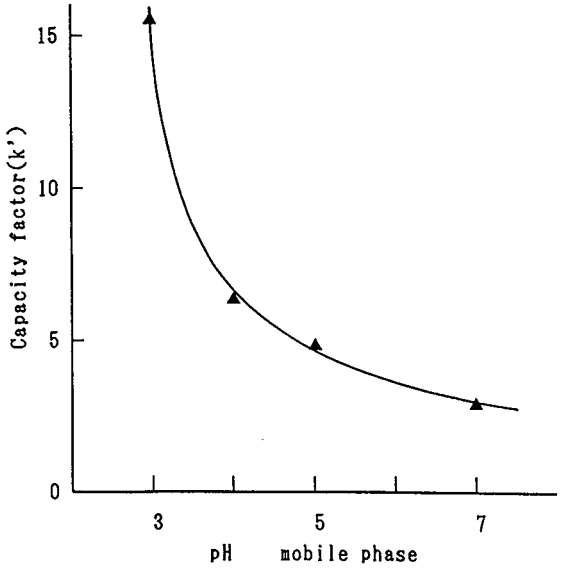

Fig. 3. Effects of the pH of the mobile phase on the capacity factor (k') of nitroxynil. Conditions of coulometric detection: guard cell, −0.7 V; detector 1, −0.7 V, detector 2, +0.7–0.0 V; gain, 10 × 40; response time, 10 s.

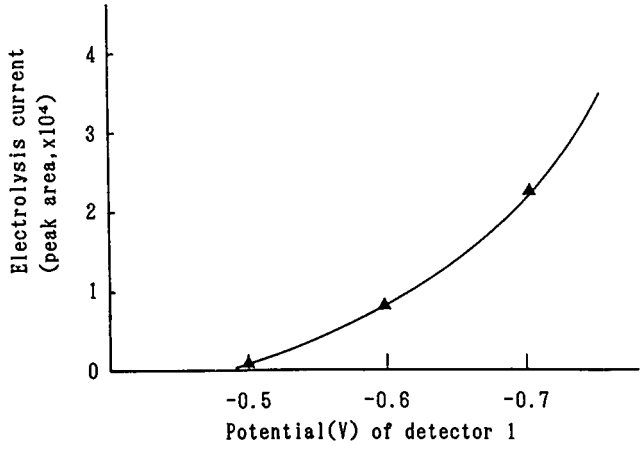

Fig. 4. Current–voltage curve of nitroxynil. Conditions of coulometric detection: guard cell, −0.7–0.5 V; detector 1, −0.7–0.5 V; detector 2, +0.2 V; gain, 10 × 40; response time, 10 s.

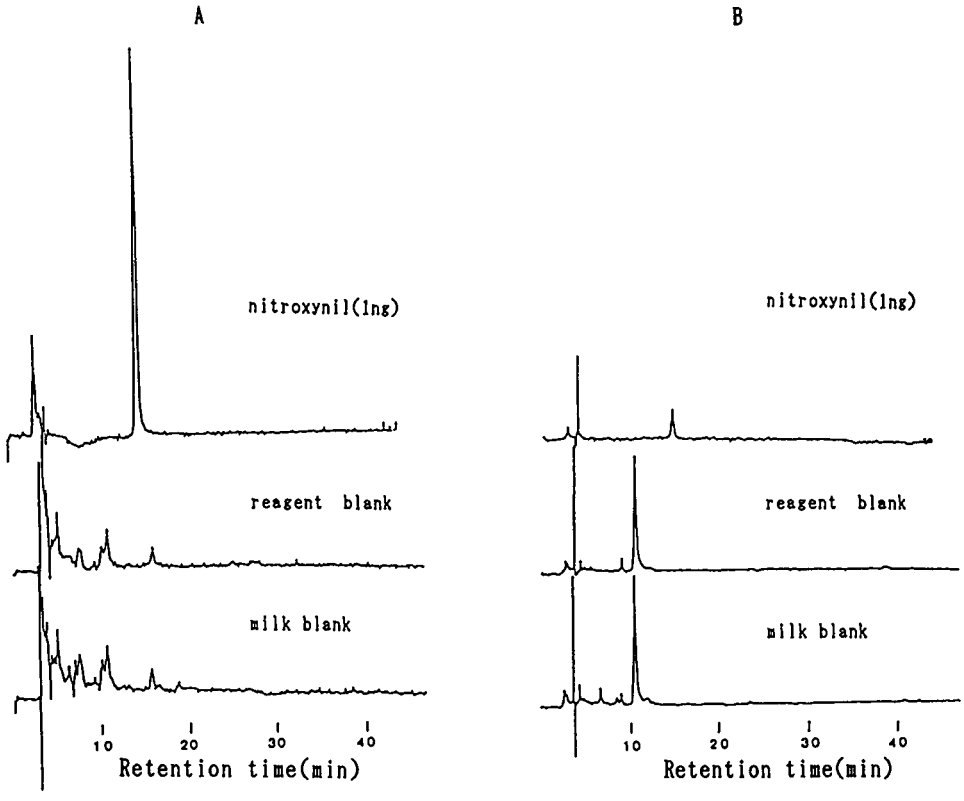

Fig. 5. High-performance liquid chromatograms of nitroxynil with electrochemical (A) and ultraviolet spectrophotometric (B) detection. HPLC conditions: column, LiChrospher 100 RP-18 (5 μm, 250 × 4 mm I.D.); mobile phase, acetonitrile–0.05 *M* potassium dihydrogenphosphate (20:80, v/v), pH 4.0; flow-rate, 1 ml/min at 40°C. Coulometric detection: guard cell, −0.7 V; detector 1, −0.7 V; detector 2, +0.2 V; gain, 10 × 40; response time, 10 s. UV: 270 nm; 0.08 a.u.f.s.

trochemical response of nitroxynil was evaluated. The current–voltage curve is shown in Fig. 4. The applied potential of detector 2 was fixed at +0.2 V and that of the guard cell and detector 1 was varied from −0.7 V to lower voltages. As is evident from Fig. 4, the applied potential of the guard cell and detector 1 at −0.7 V resulted in the highest electrochemical reduction. The applied potential of the guard cell and detector 1 was adjusted to −0.7 V.

Fig. 5 shows typical chromatograms of nitroxynil, a cow milk blank and a reagent blank. There are no peaks interfering with the matrix peaks. The detection limit of electrochemical determination was 15-fold higher than the UV detection limits.

The calibration curve of nitroxynil was linear in the range 1.0–10.0 ng. Average recoveries (n = 5) of nitroxynil from milk samples spiked at concentrations of 0.01 and 0.1 μg/ml were found to be 92.0% and 97.0% with coefficients of variation of 6.2% and 2.2%, respectively.

The recovery and detection limits with a concentration of nitroxynil as low as 0.7 ng/ml at a signal-to-noise ratio of 3:1 were satisfactory for the monitoring of residual nitroxynil in milk. This resulted in a 3- to 140-fold increase in the detection limit compared with other reported methods [5,10–12].

When the method was applied to 30 raw cow milk and 140 market milk samples, nitroxynil was detected at a level of 4 ng/ml in one sample, as shown in Fig. 6.

In conclusion, the proposed method is sensitive and specific and is applicable to the routine analysis of nitroxynil in milk.

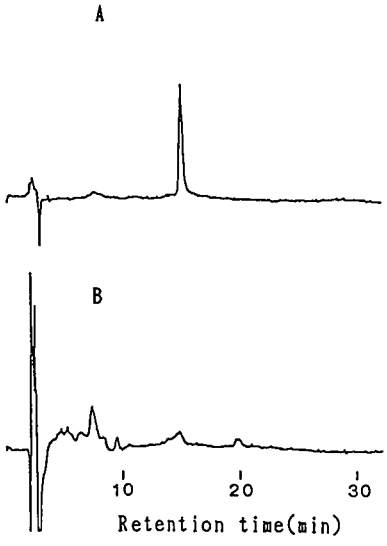

Fig. 6. High-performance liquid chromatograms. (A) Nitroxynil standard; (B) nitroxynil in raw milk sample. HPLC conditions: column, LiChrospher 100 RP-18 (5 μm, 250 × 4 mm I.D.); mobile phase, acetonitrile–0.05 *M* potassium dihydrogenphosphate (20:80, v/v), pH 4.0; flow-rate, 1 ml/min at 40°C. Coulometric detector: guard cell, −0.7 V; detector 1, −0.7 V; detector 2, +0.7 V; gain, 10 × 40; response time, 10 s.

REFERENCES

1 M. Davis, J. M. S. Lucas, J. Rosenbaum and D. E. Wright, *Nature (London)*, 211 (1966) 882.
2 J. M. S. Lucas, *Br. Vet. J.*, 123 (1967) 198.
3 J. R. Corbett and J. Goose, *Biochem. J. (Proc.)*, 3 (1971) 41.
4 J. C. Boray and A. Happich, *Austr. Vet. J.*, 44 (1968) 72.
5 M. J. Parnell, *Pestic. Sci.*, 1 (1970) 138.
6 W. Heeschen, A. Tolle and A. Bluthgen, *Arch. Lebensmittelhyg.*, 23 (1972) 1.
7 International Dairy Federation, *Bull. Int. Dairy Fed.*, No. 113 (1979) 30.
8 Y. Takeshita, K. Kishi, M. Seki, K. Fujiyama, G. Otsuka and K. Ahiko, *Milchwissenschaft*, 35 (1980) 133.
9 A. Bluthgen, W. Heeschen and H. Nijhuis, *Milchwissenschaft*, 37 (1982) 206.
10 L. G. Esktrom and P. Slanina, *Acta Vet. Scand.*, 23 (1989) 313.
11 W. J. Blanchflower and D. G. Kennedy, *Analyst*, 114 (1989) 1013.
12 Veterinary Sanitation Division, Environmental Health Bureau, Ministry of Health and Welfare, *Ministerial Ordinance Concerning Compositional Standards, etc. for Milk and Milk Products*, Japan Food Hygiene Association, Tokyo, 1990.
13 M. J. Parnell, *Pestic. Sci.*, 3 (1972) 685.
14 M. Kazacos and V. Mok, *Austr. J. Dairy Technol.*, June/September (1986) 82.

Journal of Chromatography, 596 (1992) 73–78
Elsevier Science Publishers B.V., Amsterdam

CHROM. 23 983

Reversed-phase high-performance liquid chromatography of several metal–8-quinolinethiol complexes

Takashi Yasui, Akio Yuchi, Hiroko Wada* and Genkichi Nakagawa

Laboratory of Analytical Chemistry, Department of Applied Chemistry, Nagoya Institute of Technology, Showa, Nagoya 466 (Japan)

(First received October 11th, 1991; revised manuscript received December 30th, 1991)

ABSTRACT

The reversed-phase high-performance liquid chromatography of 8-quinolinethiol (Hqt) complexes of Fe, Co, Ni, Cu, Zn, Hg and Pb on an octadecyl-bonded silica gel stationary phase was examined. The Pb complex dissociated in the column. The retention and separation of other complexes depended on the composition of the mobile phase. EDTA as an additive displaced the Zn complex and eliminated its peak. All the other metal complexes and also Hqt and its disulphide were separated in 23 min by using methanol–water (82:18, v/v) as the mobile phase. The complexes formed by the reaction of Co(II) and Hqt gave three peaks, which were assigned as *fac*(*S*)-$Co^{III}(qt)_3$, *mer*(*S*)-$Co^{III}(qt)_3$ and $Co^{II}(qt)_2$, respectively. This method is applicable to the simultaneous determination of Fe, Co, Ni, Cu and Hg.

INTRODUCTION

8-Quinolinethiol (Hqt), which preferentially reacts with soft metal ions, has been used as a reagent in spectrophotometry, spectrofluorimetry and solvent extraction [1]. The compositions of the resulting complexes have been studied by various methods, such as solvent extraction, precipitation, mass spectrometry, infrared spectrometry and polarography [2–8], and reported to be $M(qt)_2$ for Ni(II), Cu(II), Zn(II), Hg(II) and Pb(II) and $M(qt)_3$ for Fe(III). For some of them, the crystal structures have also been determined by X-ray crystallography [9]. In the extraction of Co(II) with Hqt into benzene, the complexes formed were diamagnetic and a major species was assigned as *mer*(*S*)-$Co^{III}(qt)_3$ by ^{13}C NMR [2].

König *et al.* [10] studied the thin-layer chromatographic behaviour of seventeen metal complexes with Hqt on silica gel and alumina plates. Using the same reagent, they also examined the separation of Fe, Co and Ni with a silica gel column by high-performance liquid chromatography (HPLC); however, the peaks were not resolved satisfactorily [11].

In this work, we studied the reversed-phase HPLC behaviour of Hqt complexes of Fe, Co, Ni, Cu, Zn, Hg and Pb on an octadecyl-bonded silica gel column. Metal complexes except those of Zn and Pb, excess of Hqt and the oxidation product [diquinolyl disulphide (Ds)] were separated. The elution order of the complexes is discussed in terms of their extractability with chloroform. The chromatographic behaviour of 2-methyl-8-quinolinethiol (Hmqt) complexes was also examined for comparison.

EXPERIMENTAL

Apparatus

The HPLC system (JASCO, Tokyo, Japan) consisted of a Model 880-PU intelligent pump, a Model 860-CO column oven and a MULTI-330 photodiode-array detector (wavelength range 200–800 nm; flow cell 4 μl; 1 mm I.D.; optical path length 5 mm) equipped with an NEC personal computer. An SVI-6U7 sample injector (dead volume 2 μl, sample loop 8 μl) (Sanuki Kogyo, Tokyo, Japan) and a Shim-pack CLC-ODS column (150 mm ×

0021-9673/92/$05.00

6.0 mm I.D.; particle diameter 5 μm) (Shimadzu, Kyoto, Japan) were used.

Reagents

8-Quinolinethiol and its 2-methyl derivative were prepared as described [12] and were stored as their disulphides.

Each disulphide (1 g) was dissolved in a mixture of phosphinic acid (15 ml) and hydrochloric acid (1 ml) and the solution was refluxed under a nitrogen atmosphere for 1 h. After the solution had been neutralized with aqueous ammonia, precipitated Hqt was extracted three times with 20 ml of chloroform. After dilution to 100 ml, the chloroform solution was back-extracted with the same volume of 6 *M* hydrochloric acid. The quinolinethiol hydrochloride solution thus obtained was stored in a refrigerator and used within 1 week.

Copper(II) and zinc(II) solutions were prepared from the analytical reagent-grade metals by dissolution in dilute nitric acid. An iron(III) solution was prepared from ammonium iron(III) sulphate dodecahydrate and other metal ion solutions from the sulphates or the nitrates. These solutions were standardized against an ethylenediamine-N,N,N′,N′-tetraacetate (EDTA) solution.

Chloroform was purified by shaking successively three times with concentrated sulphuric acid, 4 *M* sodium hydroxide solution and distilled water. The chloroform was stored in a refrigerator and used within 1 week.

Preparation of metal–Hqt complex solution

A 5-ml portion of $2.0 \cdot 10^{-5}$–$1.0 \cdot 10^{-3}$ *M* metal ion solution was placed in a 50-ml centrifuge tube with a screw-cap and mixed with 1 ml of $1.0 \cdot 10^{-2}$ *M* Hqt solution in hydrochloric acid. By adding 4 ml of 2.5% aqueous ammonia and 5 ml of 60% sodium acetate solution, the pH of the solution was adjusted to 5.5–6.5 to form precipitates of metal complexes. The suspension was shaken with chloroform (5 ml) for 20 min. The complexes were quantitatively extracted into chloroform.

Chromatographic procedure

An aliquot (10 μl) of the chloroform solution pre-

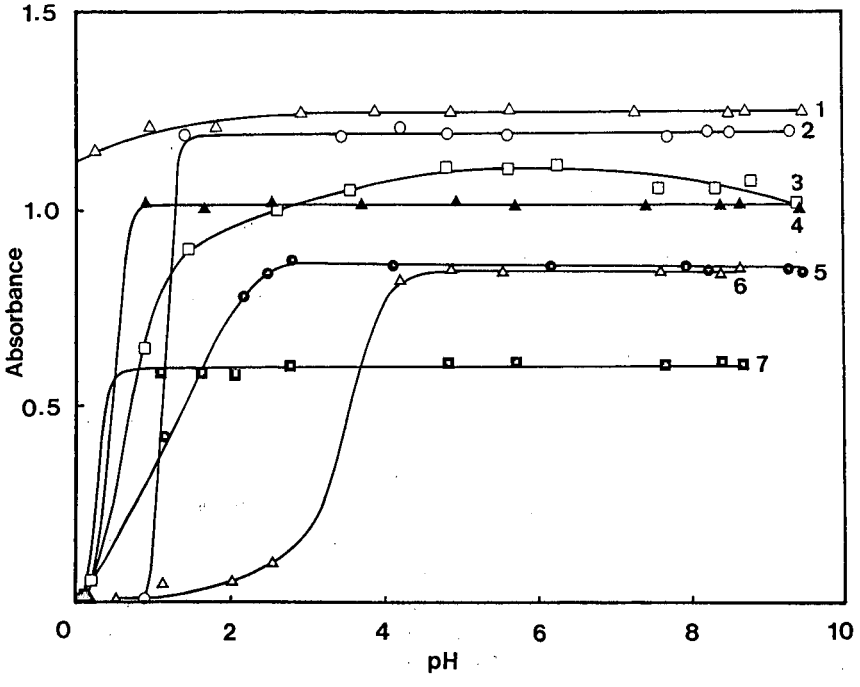

Fig. 1. Effect of pH on the extraction of Hqt complexes. $C_M = 1.0 \cdot 10^{-4}$ *M*, 5 ml; $C_{Hqt} = 1.0 \cdot 10^{-2}$ *M*, 1 ml; buffer, 5 ml; chloroform, 5 ml. Curves: 1 = Hg; 2 = Co; 3 = Fe; 4 = Cu; 5 = Zn; 6 = Pb; 7 = Ni.

pared above was placed on the column via an injection valve. In order to prevent contamination from metal ions from the microsyringe, the sample solution was introduced into the sample loop of the injector by suction. The mobile phase [methanol–water (82:18, v/v)] containing $5 \cdot 10^{-5}$ *M* EDTA was pumped at a flow-rate of 0.8 ml min^{-1}. Elution of metal complexes, excess of Hqt and Ds was monitored at 350–600 nm. The column void volume for calculation of the capacity factors was determined using sodium nitrite.

RESULTS AND DISCUSSION

Extraction conditions

The effect of pH on the extraction of the metal complexes was studied (Fig. 1). The extractability order judged from the half-extraction pH values is Hg > > Cu ≈ Ni > Fe > Co > Zn > Pb. At pH 5–6.5, all the metal ions were quantitatively extracted by shaking for 20 min. Back-extraction of the metals once extracted into chloroform was examined by shaking with a buffer or dilute hydrochloric acid for 20 min. Lead(II) was back-extracted at pH < 4 without EDTA and at pH < 9 with EDTA (10^{-3} *M*), whereas zinc(II) was not back-extracted at pH > 1 without EDTA or at pH > 3 with EDTA. Iron(III), Copper(II), nickel(II) and mercury (II) were not back-extracted with <1 *M* hydrochloric acid. Cobalt complexes were stable even against 5 *M* hydrochloric acid.

Detection wavelength and column temperature

Absorption spectra of Hqt complexes (Fe, Co, Ni, Cu, Hg) obtained using the HPLC system are shown in Fig. 2. The absorption maxima of all the chelates are in the range 350–600 nm, which was employed for detection.

The column temperature was varied from 25 to 45°C. The capacity factors of the complexes decreased by 22–33% with increase in temperature in this range. The temperature of the column oven was kept at 40°C in the subsequent experiments in order to maintain a reasonable flow-rate.

Retention and extractability of Hqt complexes

A solution containing Hqt complexes (Co, Pb, Zn, Fe, Cu, Ni and Hg) was injected into the column and eluted with mobile phase [methanol–water–chloroform (75:20:5, v/v/v)] containing $1 \cdot 10^{-3}$ *M* Hqt. All the peaks were observed for the complexes and excess of Hqt as shown in Fig. 3A.

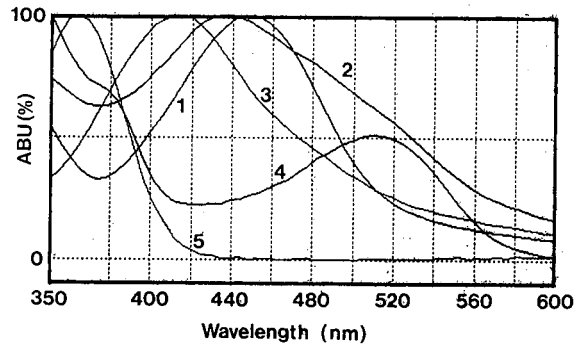

Fig. 2. Absorption spectra of Hqt complexes. (1) *mer*(*S*)-$Co^{III}(qt)_3$; (2) $Fe(qt)_3$; (3) $Cu(qt)_2$; (4) $Ni(qt)_2$; (5) $Hg(qt)_2$. The ordinate (ABU) represents absorbance in arbitrary units.

The retention order of the complexes in reversed-phase HPLC, which is the opposite of that in normal-phase TLC or HPLC [10,11], was the same as the order of extractability into chloroform. It is characteristic that square-planar complexes, $Ni(qt)_2$ and $Cu(qt)_2$, are strongly retained in this system.

Effects of mobile phase composition

The peak for Pb was absent without Hqt in the mobile phase and was appreciably lower than those for the others even in the presence of Hqt. Addition of Hqt to the mobile phase led to an unstable background and less reproducible chromatograms, probably owing to the oxidation of excess of Hqt. Thereafter, Hqt was not added to the mobile phase.

When only a chloroform solution of Hqt was injected as a sample, a large peak was obtained for Zn in addition to those for Hqt and Ds. To avoid contamination with Zn from the column and/or stainless-steel tubing, EDTA was added to the mobile phase. In the presence of more than $2 \cdot 10^{-5}$ *M* EDTA, no peaks for Zn and Pb were observed. In subsequent studies, $5 \cdot 10^{-5}$ *M* EDTA was added to the mobile phase. The dissociative nature of Zn and Pb complexes in the chromatographic system corresponds well with the results of back-extraction of these complexes as described above.

Various mixtures of organic solvents such as acetonitrile–water, ethanol–water, ethanol–chloro-

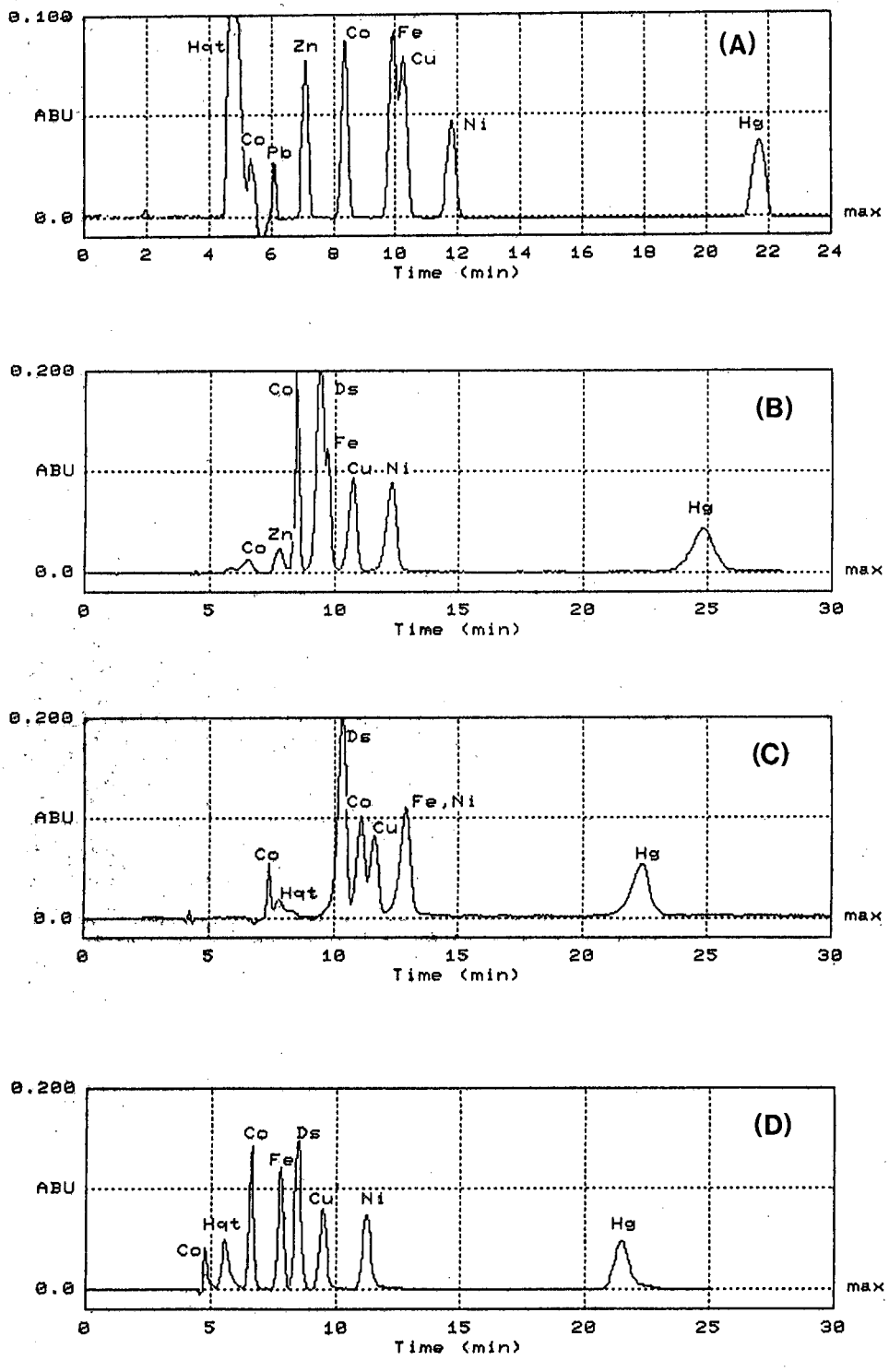
0.100
ABU
0.0
Hqt
Co
Pb
Zn
Co
Fe
Cu
Ni
Hg
(A)
max
0 2 4 6 8 10 12 14 16 18 20 22 24
Time (min)
0.200
ABU
0.0
Co
Zn
Co
Ds
Fe
Cu
Ni
Hg
(B)
max
0 5 10 15 20 25 30
Time (min)
0.200
ABU
0.0
Co
Hqt
Ds
Co
Cu
Fe,Ni
Hg
(C)
max
0 5 10 15 20 25 30
Time (min)
0.200
ABU
0.0
Co
Hqt
Co
Fe
Ds
Cu
Ni
Hg
(D)
max
0 5 10 15 20 25 30
Time (min)

Fig. 3.

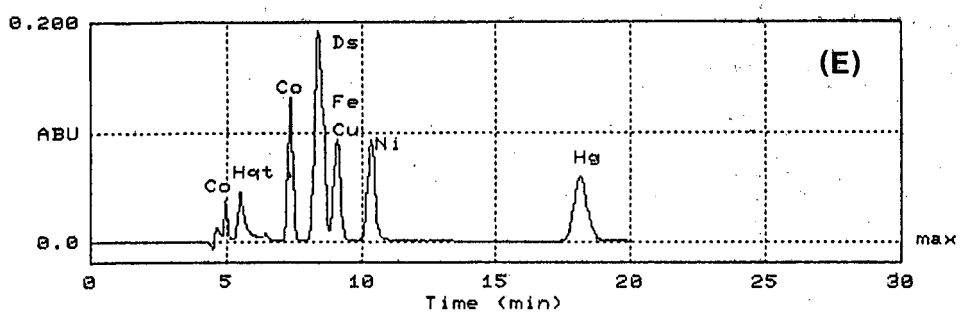

Fig. 3. Chromatogram of Hqt complexes. Mobile phase (A) methanol–water–chloroform (75:20:5, v/v/v) containing 1.0×10^{-3} *M* Hqt; (B) ethanol–water (65:35); (C) ethanol–water–chloroform (60:35:5); (D) methanol–water (82:18); (E) methanol–water–chloroform (77:18:5); mobile phases B–E contained 5×10^{-5} *M* EDTA. Flow-rate: (A,D,E) 0.8; (B,C) 0.6 ml min^{-1}. Amounts of metal injected: Co, 0.12; Pb, 0.41; Zn, 0.13; Fe, 0.11; Cu, 0.13; Ni, 0.12; Hg, 0.40 μg.

form–water, methanol–water and methanol–chloroform–water were examined as eluents. Typical chromatograms are shown in Fig. 3B–E. With acetonitrile–water, all the peaks broadened, whereas alcohol–water mixtures gave sharp peaks. The effects of methanol and ethanol content on the capacity factors are shown in Fig. 4A and B, respectively. The separation between Ds and the Fe complex was not good with ethanol–water. With methanol–water, better resolution was obtained in a shorter time. A methanol content of 82% (v/v) gave the best resolution and reasonable retention times. When 5% chloroform was added to methanol–water or ethanol–water, the Co and Fe complexes were retained stronger, whereas the retention of the Hg complex decreased (see Figs. 3C and E).

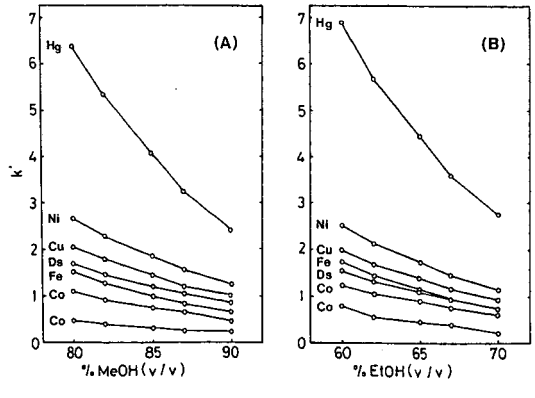

Fig. 4. Effect of alcohol content on capacity factors (*k'*). Mobile phase: (A) methanol (MeOH)–water; (B) ethanol (EtOH)–water. Flow-rate: (A) 0.8, (B) 0.6 ml min^{-1}.

With Hmqt, the complexes of Co(II), Ni(II), Zn (II) and Cd(II) were extracted into chloroform. In HPLC, however, only small peaks were observed for Co, Ni and Zn.

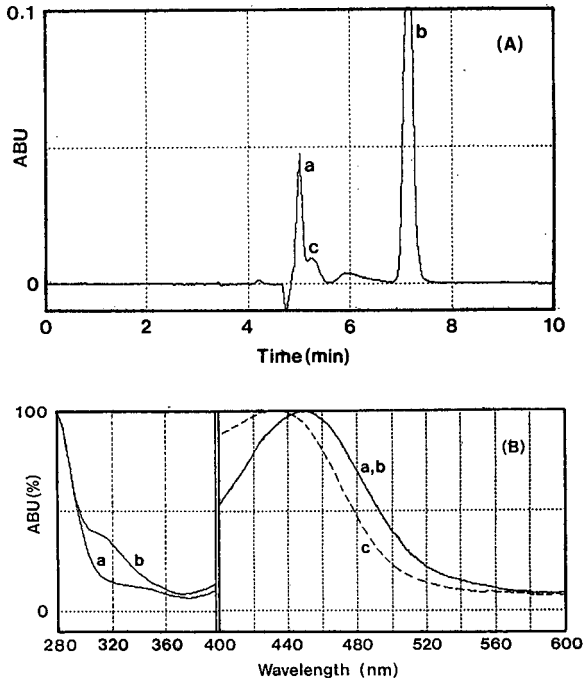

Fig. 5. (A) Chromatogram of cobalt–Hqt complexes and (B) their absorption spectra. Complex: (a) *fac*(*S*)-$Co^{III}(qt)_3$; (b) *mer* (*S*)-$Co^{III}(qt)_3$; (c) $Co^{II}(qt)_2$. Wavelength, 448 nm; mobile phase, methanol–water (80:20, v/v).

Complexes formed in Co–Hqt system

The chloroform extracts of Co complexes gave two major peaks, labelled (a) and (b), having a height ratio of 1:4 (Fig. 5A). Such peak splitting was also found in normal-phase HPLC of Co and Cr complexes, but has not been clearly explained [10,11]. In our previous study [2], benzene extracts of Co complexes gave only one peak in RP-HPLC. The complex dissolved in benzene has been assigned as *mer*(*S*)-$Co^{III}(qt)_3$ by ^{13}C NMR spectrometry. From the retention time, the complex for peak b in chloroform extracts is assigned as *mer*(*S*)-$Co^{III}(qt)_3$. The separation of such geometric isomers has been extensively studied for Co(III) and Cr(III) complexes with other ligands [13–16].

The absorption spectrum of peak a was almost the same as that of b in the visible region (Fig. 5B), but different in the UV region. The lower solubility in benzene and less retention in the reversed-phase HPLC together with the spectral characteristics suggest the assignment of the complex for peak a to *fac*(*S*)-$Co^{III}(qt)_3$, which is more polar than a *mer*(*S*)-isomer.

A third small peak (c) was occasionally found close to peak a. The absorption spectrum of the complex for peak c has a maximum at a shorter wavelength than those of *mer*(*S*)- and *fac*(*S*)-$Co^{III}(qt)_3$ and is close to that of $Co^{II}(mqt)_2$, for which an oxidation state of 2 is exclusively stabilized because of the steric hindrance in the tris complex [2]. This suggests the assignment of the complex for peak c as $Co^{II}(qt)_2$.

Application

This method can be applied to the separation and determination of the metals in spite of peak splitting for Co. The calibration graphs based on peak height and area were linear in the range $2.0 \cdot 10^{-5}$–$1.0 \cdot 10^{-3}$ *M* for Fe, Cu, Hg and Co [*mer*(*S*)-isomer], whereas the upper limit for Ni was restricted to $1.0 \cdot 10^{-4}$ *M* because of the limited solubility of its complex in chloroform. The detection limits of these metals (peak height-to-noise ratio = 3) are Cu 1.2, Ni 1.4, Fe 0.60, Hg 5.8 and Co 0.94 ng.

The proposed method was applied to the analysis of a standard steel sample (NBS 364) after the usual treatment [17]. The results are as follows (metal, % observed, % recommended): Co, 0.156, 0.15; Cu, 0.233, 0.249; and Ni, 0.139, 0.14.

REFERENCES

1 K. L. Cheng, K. Ueno and T. Imamura, *Handbook of Organic Analytical Reagents*, CRC Press, Boca Raton, FL, 1982, pp. 377–388; and references cited therein.
2 A. Yuchi, K. Sugiura, H. Wada and G. Nakagawa, *Bull. Chem. Soc. Jpn.*, 60 (1987) 4291.
3 Yu. A. Bankovskii, L. M. Chera and A. F. Ievin'sh, *Zh. Anal. Khim.*, 23 (1968) 1284.
4 A. T. Rane and D. R. Nepali, *J. Radioanal. Chem.*, 90 (1985) 39.
5 E. Sekido, I. Fujiwara and Y. Masuda, *Talanta*, 19 (1972) 479.
6 Y. Kidani, S. Naga and H. Koike, *Chem. Pharm. Bull.*, 23 (1975) 1652.
7 Y. Mido and E. Sekido, *Bull. Chem. Soc. Jpn.*, 44 (1971) 2130.
8 G. K. Budnikov, N. A. Ulakhovich, O. Yu. Kargina and A. P. Sturis, *Zh. Obshch. Khim.*, 51 (1981) 2588.
9 Yu. A. Bankovskii, *The Chemistry of the Mercaptoquinoline Chelates and Their Derivatives*, Zinatne, Riga, 1978.
10 K. H. König, G. Schneeweis, B. Steinbrech, P. Chaudhuri and H. U. Ehmcke, *Fresenius' Z. Anal. Chem.*, 297 (1979) 138.
11 K. H. König, H. U. Ehmcke, G. Schneeweis and B. Steinbrech, *Fresenius' Z. Anal. Chem.*, 297 (1979) 411.
12 D. Kealey and H. Freiser, *Talanta*, 13 (1966) 1381.
13 P. C. Uden, I. E. Bigley and F. H. Walters, *Anal. Chim. Acta*, 100 (1978) 555.
14 B. Wenclawiak, R. M. Barkley, E. J. Williams and R. E. Sievers, *J. Chromatogr.*, 349 (1985) 469.
15 T. Janjic, Z. Lj. Tesic, G. N. Vuckovic and M. B. Celap, *J. Chromatogr.*, 404 (1987) 307.
16 D. E. Henderson, S. J. Saltzman, P. C. Uden and Z. Cheng, *Polyhedron*, 7 (1988) 369.
17 H. Wada, T. Ishizuki, K. Kodama and G. Nakagawa, *Mikrochim. Acta*, II (1983) 139.

Journal of Chromatography, 596 (1992) 79–84
Elsevier Science Publishers B.V., Amsterdam

CHROM. 23 999

Structure–retention index relationships for derivatized monosaccharides on non-polar gas chromatography columns

Z. C. Yang and J. R. Cashman*

Department of Pharmaceutical Chemistry and Liver Center, School of Pharmacy, University of California, San Francisco, CA 94143-0446 (USA)

(Received October 25th, 1991)

ABSTRACT

A gas chromatographic method for predicting the retention index of a derivatized monosaccharide is presented. The procedures are especially useful to detect and predict minute quantities of sugars in biological or chemical samples. Monosaccharides are first converted to the alditols and then derivatized by acetylation, permethylation or silylation. The derivatized monosaccharide structure–retention index relationship that has been developed is useful in the identification of unknown monosaccharides that can be readily confirmed by gas chromatography–mass spectrometry.

INTRODUCTION

In our studies of the post-translational modification of proteins [1,2] it was necessary to develop methods to identify minute amounts of unknown oligosaccharides from a glycoprotein. The characterization of the extremely polar, non-volatile, water-soluble saccharides of unknown structure from biological samples represents a formidable challenge to biochemists and chemists. Recently, however, methods to separate oligosaccharides or monosaccharides arising from hydrolysis of oligosaccharides [3] or glycoproteins [4] in complex biological or chemical mixtures has advanced to the point where this does not represent an obstacle to separating glycans in a mixture. Even though new high-pH anion-exchange chromatography coupled with pulsed amperometric detection has been useful for correlating retention times of neutral and acidic oligosaccharides with putative structures [5], methods for definitive detection and characterization of structures of saccharides are needed. Although a number of methods for separation and detection of saccharides are available including paper chromatography [6], thin-layer chromatography [7] and high-performance liquid chromatography [8], gas chromatography [9] and gas chromatography–mass spectrometry [10] are probably the methods of choice. For derivatized saccharides that can be separated by gas chromatography, this is an extremely sensitive method of detection. To date, however, it has not been particularly useful for unknown derivatized monosaccharides because currently no monosaccharide chemical structure–retention index relationship is available in the literature. Extensive studies of the relationship between retention index (I) and chemical structure of many classes of compounds including esters [11], substituted benzenes [12], substituted [13,14] and non-substituted polycyclic aromatic hydrocarbons [15,16], amines [17], alcohols [17] and carboxylic acids [17] have been reported in the literature. It has been shown that tentative identification of organic compounds can be made from the I values on non-polar gas chromatography columns using a method where the unknown peak is compared with known standards in order to predict the structure or propose a probable structure for a compound.

0021-9673/92/$05.00

In this report we present a gas chromatography method for the prediction of the chemical structure of a monosaccharide based on the *I* value from monosaccharide chemical structure–retention index relationships of known sugars. The advantages of this method are (a) determination of putative monosaccharide structures in the low pmol level, (b) the straightforward and short derivatization and run times, (c) the lack of requirement for radioactive or difficult-to-handle materials and (d) the excellent sensitivity and separation of very similar monosaccharides.

EXPERIMENTAL

Materials

Monosaccharides were obtained from Sigma (St. Louis, MO, USA). Acetic anhydride was obtained from Supelco (Bellefonte, PA, USA). Sodium hydroxide, sodium borohydride, sodium borodeuteride, anhydrous hexane, and perchloric acid were obtained from Aldrich (Milwaukee, WI, USA). N,O-Bis(trimethylsilyl) acetamide (BSA), trimethylchlorosilane (TMCS), water and acetic acid were obtained from Pierce (Rockford, IL, USA). All other chemicals and reagents were obtained in the highest quality available from commercial sources.

Instrumental analysis

Gas chromatography

All chromatographic runs were carried out on a Hewlett-Packard Model 5890 gas chromatograph, equipped with a flame ionization detector. A fused DB-1 capillary column (30 m × 0.322 mm I.D., film thickness 1 μm) was used. Helium was used as the carrier gas at a flow-rate of 60 ml/min. The injector and detector temperatures were maintained at 300°C. Two temperature programs were used: (A) 100°C for 3 min, followed by a 8°C/min rise to 200°C and hold for 1 min, to 280°C at 5°C/min and hold for 30 min; (B) 200°C for 4 min, followed by a 5°C/min rise to 280°C and hold for 30 min. Temperature program A was used for analysis of permethylated alditols and temperature program B was used for alditol acetates, and silylated sugars and alditols.

A reference mixture of standard *n*-alkanes (C_6–C_{36}) was injected simultaneously as a marker with each derivatized monosaccharide sample to be analyzed. Peak areas and retention time values were recorded using a Hewlett-Packard Model 3394 integrator. The *I* values were calculated using the equation of Van den Dool and Kratz [18]

$$I = 100\, i \cdot \frac{X - M_{(n)}}{M_{(n+i)} - M_{(n)}} + 100\, n$$

where n is the number of carbon atoms in the *n*-alkane marker, X, $M_{(n)}$, and $M_{(n+i)}$ are the adjusted retention times of the analyte, the normal alkane marker with n carbon atoms eluting before, and the alkane with $(n + i)$ carbon atoms eluting after the analyte, respectively; i is the interval and usually has the value of 1 or 2.

Gas chromatography–mass spectrometry

Gas chromatography–mass spectra were obtained with a VG70S spectrometer fitted with a Varian Model 3600 gas chromatograph and a DB-1 capillary column (30 m × 0.25 mm I.D.). The carrier gas was helium. The linear temperature program was started at 80°C and increased to 300°C at 4°C/min. For chemical ionization mass spectrometry, ammonia was used as the reactant gas.

Chemistry

Reduction of the monosaccharide

The general procedure followed the methods previously described [19,20]. To the monosaccharide (100 μg), dried *in vacuo* by a speed-vacuo apparatus in a 0.3-ml Reacti-Vial (Pierce), a freshly prepared solution of sodium borohydride or sodium borodeuteride (100 μl of a 0.5 *M* solution) was added and allowed to stand overnight at room temperature. At the end of the reaction, acetic acid (60 μl of glacial acetic acid) was added and the entire mixture was dried *in vacuo*. At this point, the alditols resulting from the reduction of the monosaccharides were ready for derivatization.

Acetylation of alditols

The general procedure used was a modification of a method previously reported [21]. To the dried alditol, acetic anhydride (50 μl, 529 μmol), acetic acid (5 μl, 87 μmol) and perchloric acid (5 μl, 88 μmol of 60% aqueous perchloric acid) were introduced into the reaction vial. The mixture was sonicated for 2 min and allowed to stand for 8 min at room

temperature. At this point, water (200 μl, 11 mmol) was added followed by vigorous mixing. To the mixture was added dichloromethane (100 μl) and the mixture was vigorously mixed and the organic layer was separated by centrifugation. After separation, the aqueous phase was removed and the remaining dichloromethane fraction was washed with water (3 washes of 200 μl each). The alditol acetate was dried, dichloromethane (100 μl) was added and a sample (1 μl) of the acetylated alditol was directly injected onto the gas chromatograph or the gas chromatograph–mass spectrometer.

Permethylation of alditols

The general procedure used was based on previously published reports [22,23]. To the alditol or sugar, dimethylsulfoxide (300 μl) saturated with NaOH powder was added, followed by methyl-iodide (100 μl, 1.6 mmol). The mixture was vigorously mixed for 10 min. To the mixture was added water (1.0 ml), then dichloromethane (1.0 ml), and the mixture was vigorously mixed. Then the organic layer was separated from the aqueous layer by centrifugation. The aqueous fraction was removed and the remaining organic fraction was washed with water (3 washes of 3 ml each) and the organic fraction was dried with sodium sulphate, filtered, evaporated and taken up in dichloromethane (100 μl). A sample (1 μl) of the permethylated alditols was then directly injected into the gas chromatograph or the gas chromatograph–mass spectrometer.

Silylation of alditols

The general procedure for silylation of alditols was based on a previous report [24]. To the dried alditols or sugars, BSA (50 μl, 204 μmol) and TMCS (50 μl, 401 μmol) were added to the reaction vial. The reaction vial was filled with nitrogen and heated at 80°C for 30 min. During the silylation reaction, the mixture was sonicated for 5 min. After the reaction was complete, the mixture was evaporated to dryness and anhydrous hexane (100 μl) was added. A sample (1 μl) of the silylated alditol or sugar was directly injected into the gas chromatograph or the gas chromatograph–mass spectrometer. It should be noted that employing this procedure, the silylated alditols or sugars were quite stable. For analysis and sample handling, care was taken to remove traces of water by rinsing syringes and other apparatus with anhydrous hexane.

RESULTS AND DISCUSSION

The gas chromatography of a number of derivatized monosaccharide was accomplished on a DB-1 column to determine if a general monosaccharide chemical structure-retention index relationship (*I*) was present. That an apparent chemical structure–retention index relationship was observed suggested that the structure of unknown derivatized monosaccharides could be predicted from the relationship developed and ultimately assist in the identification of monosaccharides.

To prepare monosaccharides or mixtures of monosaccharides derived from biological or chemical sources of analysis by gas chromatography we developed three micro-scale monosaccharide derivatization procedures: acetylation, permethylation and silylation. While a number of methods have been previously published outlining these derivatizations of monosaccharides [20–24], our methods were especially useful for analysis of extremely low amounts of monosaccharides from biological samples. Each of the derivatization procedures was carried out in a single reaction vessel and loss of the derivatized monosaccharides was thereby minimized. Because the derivatized monosaccharides were somewhat volatile, techniques were developed to perform derivatization chemistry, evaporate the products to dryness and reconstitute in a minimal amount of solvent for analysis with a minimal loss of product. In this manner, analysis sensitivity of monosaccharides was increased to the nmol or pmol level. Thus, acetylation of monosaccharides was performed in the presence of acid- rather than base-catalyzed conditions so that removal of borate (and other salts from the reduction) and acetic acid (from the acetic anhydride) could be accomplished in the wash phase of the reaction and extractive work-up could be avoided.

To permit permethylation, care was taken when working with extremely low levels of monosaccharides because the permethylated derivatives were volatile. Using the procedure outlined under Experimental, and avoiding unnecessary sample transfer, permethylted monosaccharides (*e.g.*, glucose and others) were routinely detected by gas chromatography–mass spectrometry at the level of 50 pg primarily because of the quality of the chromatogram.

As a final method to examine monosaccharide

TABLE I

I VALUES FOR ALDITOL ACETATES

Compound	Formula[a]	*I*
L-Fucitol pentaacetate	$C_{16}H_{24}O_{10}$	1825
[^{2}H]Lyxitol pentaacetate	$C_{15}H_{21}DO_{10}$	1826
Arabitol pentaacetate	$C_{15}H_{22}O_{10}$	1823
[^{2}H]Frucitol hexaacetate	$C_{18}H_{25}DO_{12}$	2056 (2063)[b]
[^{2}H]Mannitol hexaacetate	$C_{18}H_{25}DO_{12}$	2053
[^{2}H]Glucitolamine hexaacetate	$C_{18}H_{26}DNO_{11}$	2210
[^{2}H]Ribitol pentaacetate	$C_{15}H_{21}DO_{10}$	1819
[^{2}H]Galacitol hexaacetate	$C_{18}H_{25}DO_{12}$	2069
[^{2}H]Allitol hexaacetate	$C_{18}H_{25}DO_{12}$	2025
[^{2}H]Glucitol hexaacetate	$C_{18}H_{25}DO_{12}$	2060
L-Sorbitol hexaacetate	$C_{18}H_{26}O_{12}$	2061 (2071)[b]

[a] D = Deuterium.
[b] Two peaks were observed.

TABLE III

I VALUES FOR SILYLATED ALDITOLS

Compound	Formula[a]	*I*
L-Fucitol TMS	$C_{21}H_{54}O_5Si_5$	1832
[^{2}H]Lyxitol TMS	$C_{20}H_{51}DO_5Si_5$	1749 (1753)[b]
Arabitol TMS	$C_{20}H_{52}O_5Si_5$	1748 (1756)[b]
[^{2}H]Frucitol TMS	$C_{24}H_{61}DO_6Si_6$	1989 (1995)[b]
[^{2}H]Mannitol TMS	$C_{24}H_{61}DO_6Si_6$	1988
[^{2}H]Glucitolamine TMS	$C_{24}H_{62}DNO_5Si_6$	2038 (1962)[b]
[^{2}H]Ribitol TMS	$C_{20}H_{51}DO_5Si_5$	1758
[^{2}H]Galacitol TMS	$C_{24}H_{61}DO_6Si_6$	N.R.[c]
[^{2}H]Allitol TMS	$C_{24}H_{61}DO_6Si_6$	1989
[^{2}H]Glucitol TMS	$C_{24}H_{61}DO_6Si_6$	2032
L-Sorbitol TMS	$C_{24}H_{62}O_6Si_6$	1997

[a] D = Deuterium.
[b] Two peaks were observed.
[c] N.R. = Not reported, multiple peaks were observed.

chemical structure–retention index relationships we studied silylation of monosaccharides and alditols. To permit silylation without the removal of borate and other salts we used BSA together with TMCS. Hexane was added to the reaction mixture to precipitate the salts and to extract the silylated product into the organic phase. The silylated products were much more stable in anhydrous hexane (*i.e.*, with traces of moisture removed). The excess BSA and TMCS reagents do not interfere with the analysis because these reagents decompose at high temperature.

TABLE II

I VALUES FOR PERMETHYLATED ALDITOLS

Compound	Formula[a]	*I*
L-Fucitol permethylated	$C_{11}H_{24}O_5$	1360
[^{2}H]Lyxitol permethylated	$C_{10}H_{21}DO_5$	1304
Arabitol permethylated	$C_{10}H_{22}O_5$	1304
[^{2}H]Frucitol permethylated	$C_{12}H_{25}DO_6$	1484
[^{2}H]Mannitol permethylated	$C_{12}H_{25}DO_6$	1487
[^{2}H]Ribitol permethylated	$C_{10}H_{21}DO_5$	1267
[^{2}H]Galacitol permethylated	$C_{12}H_{25}DO_6$	1507
[^{2}H]Allitol permethylated	$C_{12}H_{25}DO_6$	1422
[^{2}H]Glucitol permethylated	$C_{12}H_{25}DO_6$	1484
L-Sorbitol permethylated	$C_{12}H_{26}O_6$	1491

[a] D = Deuterium.

As shown in Table I, the alditol pentaacetates have *I* values around 1820 and the hexaacetates have *I* values around 2050. The alditolamine hexaacetate has an *I* value around 2210. As shown in Table II, the permethylated alditols have *I* values from 1267 to 1507. In the presence of borate, it was very difficult to permethylate the alditols at low level. Glucitolamine (100 μg) was resistant to permethylation. As shown in Tables III and IV, we determined

TABLE IV

I VALUES FOR SILYLATED MONOSACCHARIDES

Compound	Formula[a]	*I*
L-Fucose TMS	$C_{18}H_{44}O_5Si_4$	1751 (1708)[b]
[^{2}H]Lyxose TMS	$C_{17}H_{41}DO_5Si_4$	1685 (1641)[b]
Arabose TMS	$C_{17}H_{42}O_5Si_4$	1748 (1656)[b]
[^{2}H]Fructose TMS	$C_{21}H_{51}DO_6Si_5$	1865 (1852, 1845)[c]
[^{2}H]Mannose TMS	$C_{21}H_{51}DO_6Si_5$	1950 (1902)[b]
[^{2}H]Glucosamine TMS	$C_{21}H_{52}DNO_5Si_5$	1990 (1957)[b]
[^{2}H]Ribose TMS	$C_{17}H_{41}DO_5Si_5$	N.R.[d]
[^{2}H]Galactose TMS	$C_{21}H_{51}DO_6Si_5$	N.R.[d]
L-Glucose TMS	$C_{21}H_{52}O_6Si_5$	1930 (2009)[b]
L-Sorbose TMS	$C_{21}H_{52}O_6Si_5$	1828 (1899)[b]
Maltose TMS	$C_{36}H_{86}O_{11}Si_8$	2516 (2805)[b]
Lactose TMS	$C_{36}H_{86}O_{11}Si_8$	2852 (2720)[b]

[a] D = Deuterium.
[b] Two peaks were observed.
[c] Three peaks were observed.
[d] N.R. = Not reported, multiple peaks were observed.

TABLE V

MASS SPECTROMETRIC PROPERTIES OF DERIVATIZED MONOSACCHARIDES

Compound	Formula[a]	Mol. wt.	m/z[b]
[^{2}H]Glucitol hexaacetate	$C_{18}H_{25}DO_{12}$	435	453 (100)[c], 376 (25), 351 (4), 335 (4), 313 (5), 77 (32)
[^{2}H]Glucitolamine hexaacetate	$C_{18}H_{26}DNO_{11}$	434	435 (100), 420 (7), 375 (84), 324 (20), 141 (56), 112 (40), 97 (55), 83 (62)
Glucose permethylated	$C_{11}H_{32}O_6$	250	268 (22)[c], 236 (100), 219 (10), 187 (67), 172 (25), 157 (10), 140 (64), 88 (21)
[^{2}H]Glucitol TMS	$C_{24}H_{61}DO_6Si_6$	615	616 (66), 544 (2), 436 (2), 346 (3), 320 (11), 217 (10), 164 (18), 132 (22), 117 (11), 90 (100)
Glucose TMS[d]	$C_{21}H_{52}O_6Si_5$	540	558 (19)[c], 541 (3), 468 (5), 378 (2), 361 (73), 288 (20), 198 (52), 90 (100), 588 (76)[c], 541 (5), 468 (5), 451 (5), 378 (2), 361 (76), 288 (20), 198 (57), 90 (100)
	$C_{21}H_{52}O_6Si_5$	540	268 (12)[c], 236 (100), 219 (10), 187 (62), 172 (21), 157 (8), 140 (60), 88 (16)

[a] D = Deuterium.
[b] Determined using chemical ionization mass spectrometry. Relative intensities in parentheses.
[c] A strong ion $[M + NH_4]^+$ was observed.
[d] Two epimers were observed and mass spectral data for each are listed.

the I values for silylated alditols and monosaccharides, respectively. The silylated alditols had I values from 1748 to 2038. The silylated monosaccharides had I values from 1751 to 2852.

To confirm the structure of the derivatized monosaccharides the products were routinely subjected to gas chromatography–mass spectrometry. As shown in Table V, the derivatized monosaccharides possessed characteristic molecular ions and fragmentation patterns for the expected products.

ACKNOWLEDGEMENTS

We acknowledge the financial support from the NIH (GM 36426). We thank the generous help of the UCSF-Bioorganic Biomedical Mass Spectrometry Resource (A. L. Burlingame, Director); supported by NIADDK 26743 and the Division of Research Resources Grant RR 016614. The expert typing of Gloria Dela Cruz is gratefully aknowledged.

REFERENCES

1 S. Guan, A. M. Falick and J. R. Cashman, *Biochem. Biophys. Res. Commun.*, 170 (1990) 937.
2 S. Guan, A. M. Falick, D. E. Williams and J. R. Cashman, *Biochemistry*, 30 (1991) 9892.
3 J. D. Olechno, S. R. Carter, W. T. Edwards and D. G. Gillen, *Am. Biotechnol. Lab.*, 5 (1987) 38.
4 L.-M. Chen, M.-G. Yet and M.-C. Shao, *FASEB J.*, 2 (1988) 2819.
5 M. R. Hardy and R. R. Townsend, *Proc. Natl. Acad. Sci. U.S.A.*, 85 (1988) 3289.
6 M. D. G. Oates, A. C. Rosbottom and J. Schragen, *Carbohydr. Res.*, 34 (1974) 115.
7 A. Slomiany, E. Zdebska and B. L. Slomiany, *J. Biol. Chem.*, 259 (1984) 14743.
8 M. Bergh, P. Koppen and D. Van Den Eijnden, *Carbohydr. Res.*, 94 (1984) 225.
9 K. Stellner, H. Saito and S. Hakomori, *Arch. Biochem. Biophys.*, 155 (1973) 464.
10 G. Peterson, *Tetrahedron*, 25 (1969) 4437.
11 G. Schomburg, *J. Chromatogr.*, 14 (1964) 157.
12 F. Vernon and J. B. Suratman, *Chromatographia*, 17 (1983) 600.
13 C. M. White, A. Robbat, Jr. and R. M. Hoes, *Chromatographia*, 17 (1983) 605.
14 A. Robbat, Jr., N. P. Corso, P. J. Doherty and D. Marshall, *Anal. Chem.*, 58 (1986) 2072.
15 D. L. Vassilaros, R. C. Kong, D. W. Later and M. L. Lee, *J. Chromatogr.*, 252 (1982) 1.
16 M. L. Lee, D. L. Vassilaros, C. M. White and M. Novotry, *Anal. Chem.*, 51 (1979) 768.
17 C. T. Peng, S. F. Ding, R. L. Hua and Z. C. Yang, *J. Chromatogr.*, 436 (1988) 137.
18 H. van den Dool and P. D. Kratz, *J. Chromatogr.*, 11 (1963) 463.

19 S. J. Merllis and J. U. Baenziger, *Anal. Biochem.*, 442 (1983) 134.
20 S. C. Churms, *J. Chromatogr.*, 500 (1990) 555.
21 A. B. Blakeney, P. J. Harris, R. J. Henry and B. A. Stone, *Carbohydr. Res.*, 113 (1983) 291.
22 T. J. Waeghe, A. G. Darvill, M. McNeil and P. Albersheim, *Carbohydr. Res.*, 123 (1983) 281.
23 I. Ciucanu and F. Kerek, *Carbohydr. Res.*, 131 (1984) 209.
24 G. Petersson, *Carbohydr. Res.*, 33 (1974) 47.

Journal of Chromatography, 596 (1992) 85–90
Elsevier Science Publishers B.V., Amsterdam

CHROM. 23 975

Determination of parts per million levels of trifluoroacetic acid in ceronapril bulk substance by headspace capillary gas chromatography

Douglas A. Both* and Mohammed Jemal

Bristol-Myers Squibb Company, Bristol-Myers Squibb Pharmaceutical Research Institute, P.O. Box 191, 1 Squibb Drive, New Brunswick, NJ 08903-0191 (USA)

(First received September 16th, 1991; revised manuscript received December 17th, 1991)

ABSTRACT

A headspace capillary gas chromatographic method was developed to determine trifluoroacetic acid (TFA) in a bulk substance (ceronapril). The bulk sample is reacted in a sealed headspace vial with dimethyl sulfate in concentrated sulfuric acid to convert TFA to methyl trifluoroacetate (MTFA). A portion of the headspace of the vial containing the MTFA is chromatographed on a PoraPLOT Q 0.32 mm I.D. capillary column in the split injection mode with flame ionization detection. The limit of detection is less than 10 ppm (w/w).

INTRODUCTION

Trifluoroacetic anhydride is used as a reagent in the penultimate step in the synthesis of ceronapril (Fig. 1), a new class of angiotensin-converting enzyme inhibitor [1–3]. A sensitive analytical method was required which is capable of determining residual trifluoroacetic acid (TFA) in ceronapril bulk substance. This paper describes a headspace capillary gas chromatographic (GC) method which was developed to determine TFA down to the low ppm level. The method is based on the reaction of ceronapril with dimethyl sulfate in concentrated sulfuric acid in a sealed headspace vial, where the TFA is converted into the more volatile and more easily chromatographable derivative methyl trifluoroacetate (MTFA). A portion of the headspace gas is then chromatographed using a capillary GC system equipped with a split injector and a flame ionization detector. The limit of detection is less than 10 ppm (w/w).

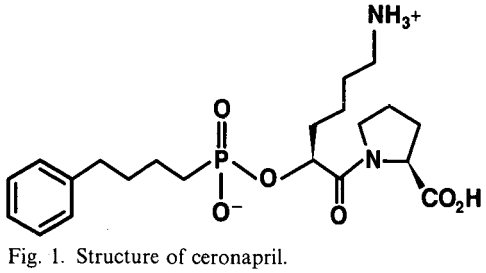

Fig. 1. Structure of ceronapril.

EXPERIMENTAL

Reagents and Chemicals

Samples of ceronapril bulk substance (powder) were obtained from the Department of Chemical Process Technology of Bristol-Myers Squibb Pharmaceutical Research Institute (New Brunswick, NJ, USA). Dimethyl sulfate (gold label, 99+%) and trifluoroacetic acid (99+%) were purchased from Aldrich (Milwaukee, WI, USA). Concentrated sulfuric acid (ACS grade) was purchased from Fisher Scientific (Pittsburgh, PA, USA).

The derivatizing solution was prepared by adding 20 ml of dimethyl sulfate to a 100-ml volumetric flask containing about 50 ml of refrigerated con-

0021-9673/92/$05.00

centrated sulfuric acid and then diluting to volume with additional refrigerated concentrated sulfuric acid. The solution was kept in a refrigerator for at least 20 min before use.

Stock TFA standard solution (0.01%, v/v) was prepared by adding 1.0 μl of TFA beneath the surface of 9 ml of cold derivatizing solution in a 10-ml volumetric flask and then diluting to volume with additional cold derivatizing solution. The solution was kept in a refrigerator until the time of use. Dilute TFA standard solution (0.001%, v/v) was prepared by diluting 1.0 ml of stock TFA standard solution to 10 ml with cold derivatizing solution. The solution was kept in a refrigerator until the time of use.

Working standard set

The working standard set consisted of a blank standard preparation and a spiked standard preparation, prepared as described below.

Blank standard preparation. A 300 ± 10-mg portion of ceronapril was weighed into a headspace vial (Hewlett-Packard No. 9301-0717). After adding 3 ml of cold derivatizing solution, the vial was capped with a Teflon-lined septum (Hewlett-Packard No. 9301-0719) and an aluminum crimp seal with pressure release (Hewlett-Packard No. 9301-0718). The ceronapril powder will float on the surface of the solution and will dissolve during the heating preceding the headspace sampling (see below). The mixture can be gently mixed to hasten the dissolution; however, it should not be allowed to come into contact with the Teflon septum to prevent contamination of the headspace sampler needle.

Spiked standard prepartion. A 300 ± 10-mg portion of the same ceronapril batch as used for the blank standard preparation was weighed into a second headspace vil. After adding 3 ml of dilute TFA standard solution, the vial was treated as described under *Blank standard prepartion.*

Sample preparation

A 300 ± 10-mg portion of the ceronapril sample to be analyzed was weighed into a headspace vial. The vial was then treated as described under *Blank standard preparation.*

Reagent blank preparation

A 3-ml portion of the derivatizing solution was added to a 10-ml headspace vial. The vial was then treated as described under *Blank standard preparation.*

Gas chromatography

A Hewlett-Packard Model 5890 capillary gas chromatograph, equipped with a split–splitless injection port and a flame ionization detector, was used in conjunction with a Hewlett-Packard Model 19395A headspace analyzer. The fused-capillary column used was PoraPLOT Q (Chrompack No. 7550) (10 m × 0.32 mm I.D.) with a 10-μm stationry phase film thickness. The oven temperature was maintained at 140°C for 5 min and then ballistically programmed at 70°C/min to 200°C and held there for 8 min. The injector and detector temperatures were maintained at 125 and 200°C, respectively. Injections were made in the split mode, with a split flow-rate of 10 ml/min. The split port liner was a 4 mm I.D. open tube packed with a short fused-silica-wool plug (Restek No. 20781) and deactivated with a solution of 5% dimethyldichlorosilane in toluene after packing. The helium carrier gas head pressure was maintained at 97 kPa (14 p.s.i.g.) and the flow-rate of the helium make-up gas for the flame ionization detector was 30 ml/min. The GC sensitivity was set at a range of 2^1 and an attenution of 2^1.

The headspace analyzer carrier gas flow-rate was set at 12 ml/min and the auxiliary flow-rate was set at 80 kPa. A 1.0-ml sample loop was used and the valve and sample loop temperature was 80°C. The heating bath temperature was set at 50°C and the equilibration time at 90 min. The headspace analyzer timing sequence was programmed so that probe insertion time was at 00:01 (0 min and 1 s) with a pressurizing start time of 00:03. The corresponding programmed times for the other parameters in the sequence were as follows: stop pressuring at 00:13; start vent/fill loop at 00:15; stop vent/fill loop at 00:25; start injection at 00:27; stop injection at 05:27; take out probe at 05:29.

After the system had equilibrated, the prepared headspace vials were placed in the headspace analyzer in the following order: reagent blank preparation, blank standard preparation, spiked standard preparation, reagent blank preparation and then the sample preparation of each of the samples to be analyzed. The starting of the headspace analyzer program will automatically allow the heating of the

headspace vials for 90 min prior to the first injection. A 1.0-ml portion of the headspace gas was transferred into the inlet of the capillary GC system via the headspace analyzer heated transfer line.

Quantification

The response due to the TFA spiked into the spiked standard preparation is calculated by the equation

$$A_s = A_2 - [A_1(W_2/W_1)]$$

where A_s is the area due to the TFA spiked into the spiked standard preparation, A_2 is the TFA peak area measured from the chromatogram of the spiked standard prepartion, A_1 is the TFA peak area measured from the chromatogram of the blank standard preparation, W_2 is the weight (g) of ceronapril in the spiked standard preparation and W_1 is the weight (g) of ceronapril in the blank standard preparation.

The amount of TFA in the sample to be analyzed is calculated by the equation

$$\text{TFA (ppm, w/w)} = \frac{C_s A_u V D \cdot 10^4}{A_s W}$$

where C_s is the concentration (%, v/v) of the spiked TFA in the spiked standard preparation, A_u is the TFA peak area measured from the chromatogram of the sample preparation, V is the volume of the sample preparation (3 ml), D is the density of TFA (1.48 g/ml), A_s is as above and W is the weight (g) of ceronapril in the sample preparation.

RESULTS AND DISCUSSION

The proposed method presented is based on the conversion of TFA in ceronapril into MTFA without prior extraction from ceronapril. The MTFA thus formed is equilibrated between the solution and headspace gas phase and then a portion of that gas is chromatographed in the capillary GC system. The headspace analyzer utilized allows the programming of the system for the automatic equilibration and sampling of the headspace.

TFA is methylated with dimethyl sulfate, which is normally used in a basic medium [4]. On the other hand, dimethyl sulfate has been used in an acidic medium for the determination of halogenated acids such as trichloroacetic acid and TFA in blood, plasma and urine [5–7]. It appears that even in strongly acidic media there is sufficient ionization of the relatively strong carboxylic acids such as TFA that the proposed mechanism [4] of methylation by dimethyl sulfate can take place with nucleophilic attack of the trifluoroacetate anion on the methyl

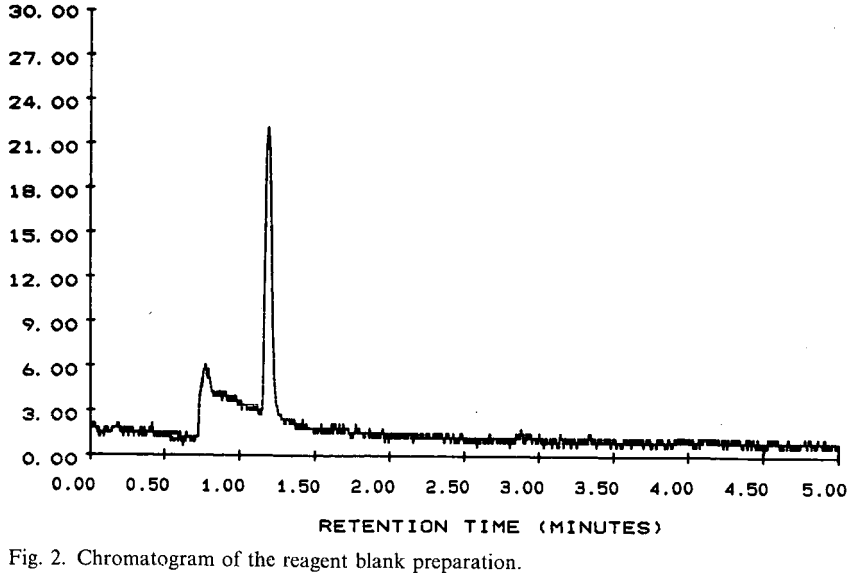

Fig. 2. Chromatogram of the reagent blank preparation.

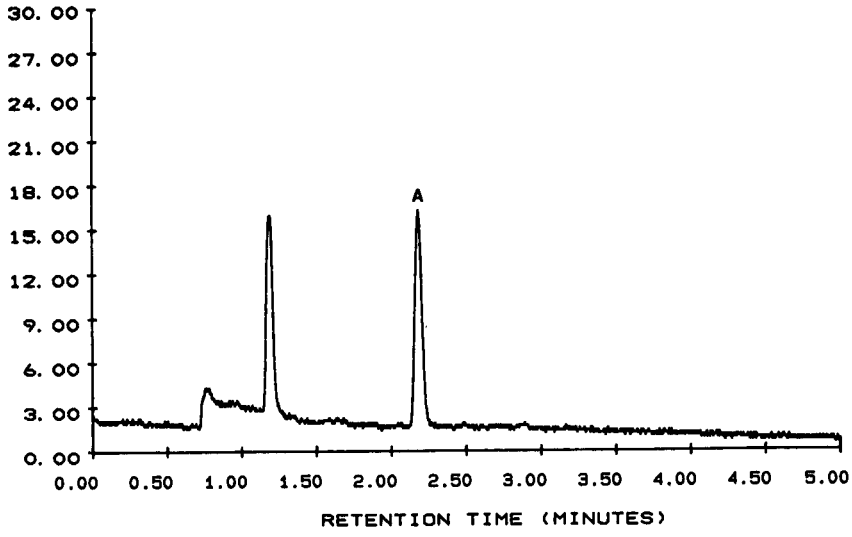

Fig. 3. Chromatogram of the spiked standard preparation corresponding to about 148 ppm (w/w). Peak A (2.2 min) is due to MTFA.

carbon of dimethyl sulfate. The reaction in concentrated sulfuric acid appears to be an ideal application for headspace GC, as the concentrated sulfuric acid will act to "salt out" the MTFA, decreasing its partition ratio and, hence, increasing the sensitivity of the method. A second advantage is that the sulfuric acid gives no solvent peak to obscure the TFA response. A third advantage is that the reaction is selective and hence gives less chemical noise as only relatively strong acids would be methylated under the strongly acidic conditions utilized here.

The dimethyl sulfate–sulfuric acid solution is added cold to the ceronapril sample in order to avoid any evaporative loss of TFA, as the dissolution of

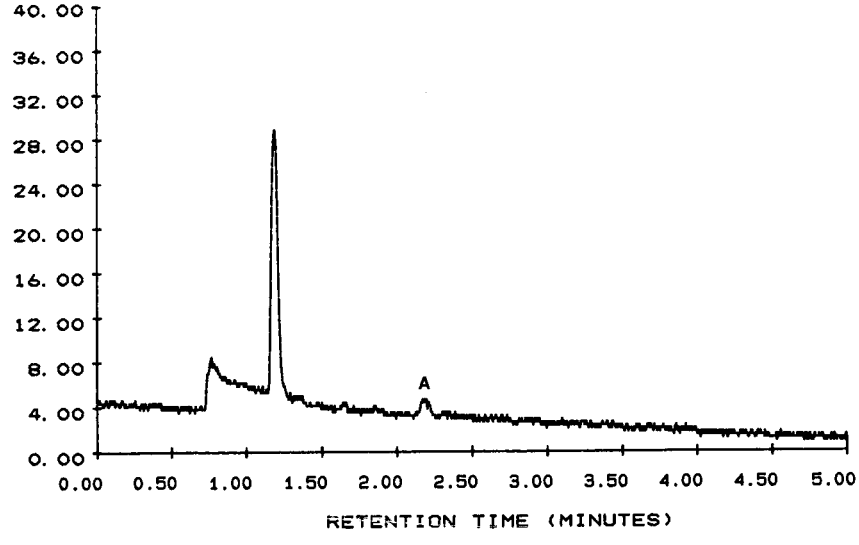

Fig. 4. Chromatogram of the sample preparation. The MTFA concentration was found to be <10 ppm (w/w) (peak A).

the ceronapril generates heat and the boiling point of TFA is only 72°C and that of MTFA is only 43°C. This reagent should be made fresh and kept refrigerated until the time of use. Some unknown non-interfering peaks were observed in the reagent blank preparation when older solutions were used. Complete reaction of the TFA was observed when the reaction mixture was heated at 50°C for 60 min. Heating the samples in the headspace analyzer for longer than 6 h showed no loss of the MTFA as long as the headspace vial was sealed airtight.

Figs. 2, 3 and 4 show chromatograms of the reagent blank preparation, spiked standard preparation and sample preparation, respectively. Note that the reagent blank is clean in the region of MTFA and the sample preparation was found to contain TFA at a level near the limit of detection.

The linearity of response was established by analyzing several 300-mg portions of a ceronapril sample spiked with various amounts of TFA and measuring the absolute peak-area response of the MTFA produced. A correlation coefficient of 0.999 and an intercept of 109 (which corresponds to about 6 ppm, w/w) were obtained (Table I).

The accuracy of the method was established by comparing the amount of TFA added to ceronapril with the amount recovered. As shown in Table II, added TFA was quantitatively recovered. Excluding the 15 ppm level, the mean recovery was 99%. This good sensitivity is achieved in spite of the split injection mode, which is required for obtaining good chromatographic peaks without cryofocusing when the headspace anlyzer is connected to the GC system through the split–splitless inlet. One approach to avoiding splitting of the sample is to connect the heated transfer line probe of the headspace sampler (which would normally enter the injection port) directly to the GC column by use of an appropriate connector (*e.g.*, Chrompack No. 4782). Another approach is to install the headspace sampler transfer line in the packed injection port of the GC system. The packed injection port is equipped with a Restek Uniliner sleeve adaptor (Restek No. 20310) and a 0.53 mm I.D. direct injection–on-column Uniliner (Restek No. 20311). In this instance a 0.53 mm I.D. column butts up to the radial taper of the head of the expansion chamber of the Uniliner. This allows the heated transfer line probe tip to enter the 0.53 mm I.D. fused-silica column so that on-column injections are achieved. The optimum carrier flow-rate of the headspace sampler necessary to sweep the sample loop and deposit the headspace sample in the injection port is about 10–20 ml/min. In spite of these high flow-rates, the utilization of the 0.53 mm I.D. capillary column affords acceptable column efficiency without having to split the sample stream. These two modes of "injection" of the headspace sample have been successfully applied in our laboratories with other methods when high sensitivity was required.

TABLE I

LINEARITY OF MTFA RESPONSE

Amount spiked (ppm, w/w)	MTFA response (area counts)
740	13196
148	2803
74	1517
14.8	224
0	0
Slope	17.7
Intercept	109
Correlation coefficient	0.999

TABLE II

RECOVERY OF TFA FROM CERONAPRIL

Added (ppm, w/w)	Found (ppm, w/w)	Recovery (%)
748	662	89
144	155	108
75	75	100
15	22	147

ACKNOWLEDGEMENT

The authors acknowledge the technical assistance provided by Mrs. Betty Fodor.

REFERENCES

1 D. S. Karanewsky, M. C. Badia, D. W. Cushman, J. M. DeForrest, T. Dejneka, M. J. Loots, M. G. Perri, E. W. Petrillo and J. R. Powell, *J. Med. Chem.*, 31 (1988) 204.
2 K. Hiwada, Y. Inoue and T. Kokubu, *Gen. Pharmacol.*, 21 (1990) 555.

3 J. M. DeForrest, T. L. Waldron, C. Harvey, R. Scalese, S. Hammerstone, J. R. Powell and D. S. Karanewsky, *J. Cardiovasc. Pharmacol.*, 16 (1990) 121.
4 J. Grundy, B. G. James and G. Pattenden, *Tetrahedron Lett.*, (1972) 757.
5 D. D. Breimer, H. C. J. Ketelaars and J. M. Van Rossum, *J. Chromatogr.*, 88 (1974) 55.
6 G. Triebig, in B. Kolb (Editor), *Applied Headspace Gas Chromatography*, Heyden, London, 1980, pp. 133–139.
7 R. M. Maiorino, A. J. Gandolfi and I. G. Sipes, *J. Anal. Toxicol.*, 4 (1980) 250.

Journal of Chromatography, 596 (1992) 91–94
Elsevier Science Publishers B.V., Amsterdam

CHROM. 23 960

Thin-layer chromatography on polyacrylonitrile

IV. Investigation of the separation mechanisms for tris-(alkylxanthato)cobalt(III) complexes

T. J. Janjić*, D. M. Milojković, G. N. Vučković and M. B. Ćelap

Faculty of Chemistry, University of Belgrade, Studentski trg 16, P.O. Box 550, 11001 Belgrade (Yugoslavia)

(First received September 24th, 1991; revised manuscript received December 16th, 1991)

ABSTRACT

The chromatographic behaviour of six tris(alkylxanthato)cobalt(III) complexes on polyacrylonitrile sorbent thin layers was investigated using four non-aqueous and two aqueous solvent systems. It was assumed that their separation under normal-phase conditions was achieved by the mechanism of hydrogen-bond formation between highly electronegative sorbate oxygen and/or sulphur atoms and sorbent methyne group hydrogens. In contrast, it was assumed that under reversed-phase conditions the separation was based on non-specific hydrophobic interactions. Finally, the linear dependence between the number of carbon atoms in the ligands and the corresponding R_M values of the investigated complexes of a homologous series was confirmed.

INTRODUCTION

A polyacrylonitrile sorbent (PANS), the preparation and characteristics of which were described in the first paper of this series [1], was subsequently applied to the separation of *cis–trans* isomeric cobalt(III) complexes [1], foodstuff dyes [2] and tris(β-diketonato) complexes of cobalt(III), chromium (III) and ruthenium(III) [3]. The separation mechanisms for these compounds were considered, and it was also shown that PANS, owing to its moderate polarity [2], can be applied to the separation of different classes of compounds by both normal- and reversed-phase chromatography.

Continuing these investigations, in this work we investigated the chromatographic behaviour of six tris(alkylxanthato)cobalt(III) complexes on thin layers of PANS with non-aqueous and aqueous solvent systems. Among other things, we wanted to check whether the earlier established rule of a linear dependence between the number of carbon atoms in the ligands and the corresponding R_M values of a homologous series of metal complexes, obtained on thin layers of silica gel [4–6], as well as in the paper chromatography [7,8], is valid for the separations on PANS. In addition, we considered the separation mechanisms for the investigated complexes.

EXPERIMENTAL

The complexes were synthesized by the procedure described previously [6]. The preparation of PANS, its application to microscope slides and the development of chromatograms by the ascending method were performed as described in Part I [1].

The chromatographic plates were spotted with 0.2-μl aliquots of freshly prepared solutions (2 mg cm^{-3}) of the complexes in acetone. Before development, the spotted plates were equilibrated for 30 min in a chromatographic chamber saturated with vapour of the solvent system being used. All solvents used were of analytical-reagent grade; the compositions of the solvent systems and development times are listed in Table I. After development,

0021-9673/92/$05.00

TABLE I

COMPOSITION OF THE CHROMATOGRAPHIC SOLVENT SYSTEMS USED AND THE CORRESPONDING DEVELOPMENT TIMES

No.	Solvent system (v/v)	Development time (min)
1	*n*-Hexane	25
2	*n*-Nonane	25
3	*n*-Hexane–carbon tetrachloride (90:10)	25
4	*n*-Hexane–benzene (90:10)	25
5	Acetone–water (80:20)	60
6	Tetrahydrofuran–water (70:30)	100

the coloured spots of the complexes were readily visible.

RESULTS AND DISCUSSION

The results of chromatographic separations are given in Table II. As can be seen from the application of two one-component and two poly-component non-aqueous solvent systems, the retention of the chelates decreased with increasing size of the *n*-alkyl chain of the ligands. However, with aqueous solvent systems the sequence of R_F values was reversed. In all instances a linear dependence of the corresponding R_M values on the number of carbon atoms in the *n*-alkyl chain of the ligands was observed (Fig. 1). As the absolute values of the slopes of these straight lines correspond to the logarithm of the separation factor [10] of two neighbouring

TABLE II

hR_F VALUES IN SOLVENTS 1–6[a] OF THE INVESTIGATED TRIS(ALKYLXANTHATO)COBALT(III) COMPLEXES AND THE CORRESPONDING TAFT'S INDUCTIVE CONSTANTS (σ^*) FOR ALKYL SUBSTITUENTS [9]

No.	Alkyl group	hR_F						σ^*
		1	2	3	4	5	6	
1	Methyl	21	18	27	47	71	60	0.000
2	Ethyl	36	27	42	67	62	51	−0.100
3	*n*-Propyl	48	41	63	84	48	42	−0.115
4	*n*-Butyl	60	57	73	93	39	34	−0.130
5	Isobutyl	62	60	78	95	37	32	−0.125
6	*sec.*-Butyl	59	55	69	93	43	43	−0.210

[a] See Table I.

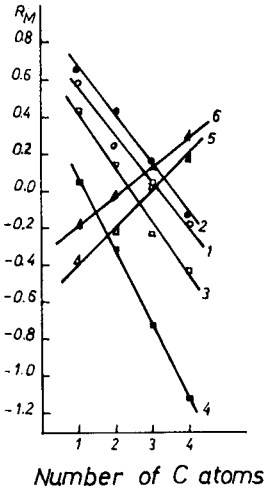

Fig. 1. Dependence of R_M values of the investigated tris(*n*-alkylxanthato)cobalt(III) complexes on the number of carbon atoms in the ligand. The numbers on the lines refer to the solvent system in Table I.

members of a series, it may be concluded that this factor was higher under normal-phase conditions when two-component solvent systems were used in comparison with the values obtained with one-component ones. Under reversed-phase conditions, this factor was the smallest. Hence it was established that the highest separation factor was obtained with solvent 4 (α = 2.5). In this connection, it is interesting that the highest α value for the same homologous series obtained on silica gel [6] was 1.6.

The R_F values of the isomeric tris(butylxanthato)cobalt(III) complexes, obtained under the conditions of normal-phase chromatography (by application of non-aqueous solvent systems) (Table II, solvents 1–4) were found to increase in the order of the corresponding Co(III) complexes: *sec*-butylxanthate < *n*-butylxanthate < isobutylxanthate, although the differences in R_F values are relatively small. When the chromatographic separations of these complexes were performed by application of aqueous solvent systems (reversed-phase chromatography), a reversed sequence for these complexes was obtained (Table II).

As reported previously [11], under conditions of normal-phase chromatography, the saturated chelates are most often adsorbed by the mechanism of hydrogen-bond formation between the solute and a

sorbent. The sorption of the investigated tris(alkylxanthato)cobalt(III) complexes under the conditions of normal-phase chromatography on thin layers of PANS may also be explained by the mechanism of hydrogen-bond formation, *i.e.*, between oxygen and/or sulphur chelate atoms [12] and methyne hydrogen atoms of the sorbent [13]. As is known, the strength of hydrogen bonds formed depends on the electron density on the corresponding electronegative atoms; in our case a positive inductive effect of alkyl groups in alkylxanthato ligands would cause a decrease in the R_F values of complexes with increasing size of the *n*-alkyl side-chain. However, the oppositie results were obtained (Table II, solvent systems 1–4), which means that in the process of chromatographic separation the mobility of the chelate depends mainly on other factors. This might be steric hindrance, as stated by Snyder [14], analogous to the results obtained in chromatographic separations of some structurally similar metal dialkyldithiophosphates on silica gel [15], or the solubilities of the investigated complexes in the corresponding solvents. In order to check which of the two mentioned effects is predominant, we plotted the R_M values obtained *versus* the steric constants of the corresponding side-chains [15,16] (Fig. 2), and also *versus* the logarithm of the complex solubilities in CCl_4 [6,17], which is the more polar component of one of the solvents used (Fig. 3). These data show in both instances a good correlation for *n*-alkylsubstituted complexes, *i.e.*, both effects probably play important roles in their separation processes.

The results obtained for the investigated *n*-alkyl-

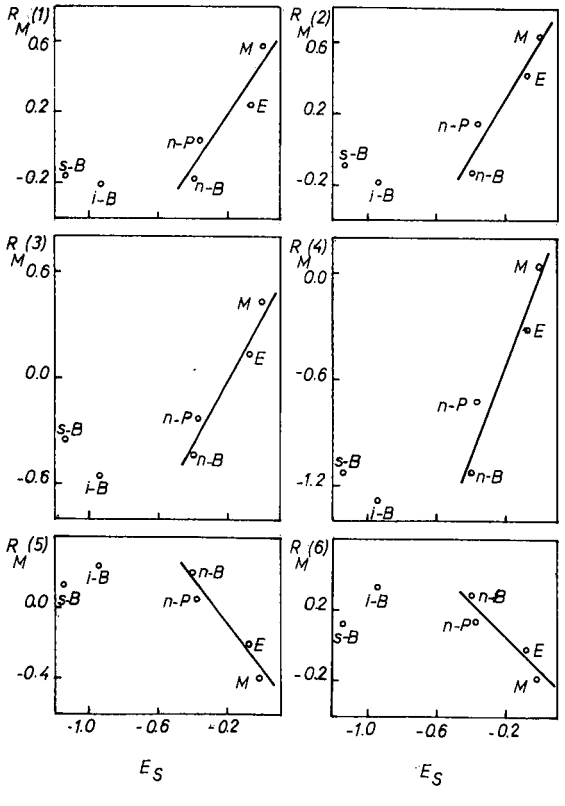

Fig. 2. Dependence of R_M values of the investigated tris(alkylxanthato)cobalt(III) complexes on the corresponding side-chain steric constants (E_S). The numbers in parentheses refer to the solvent systems in Table I. M = Methyl; E = ethyl; n-P = *n*-propyl; n-B = *n*-butyl; i-B = isobutyl; s-B = *sec.*-butyl.

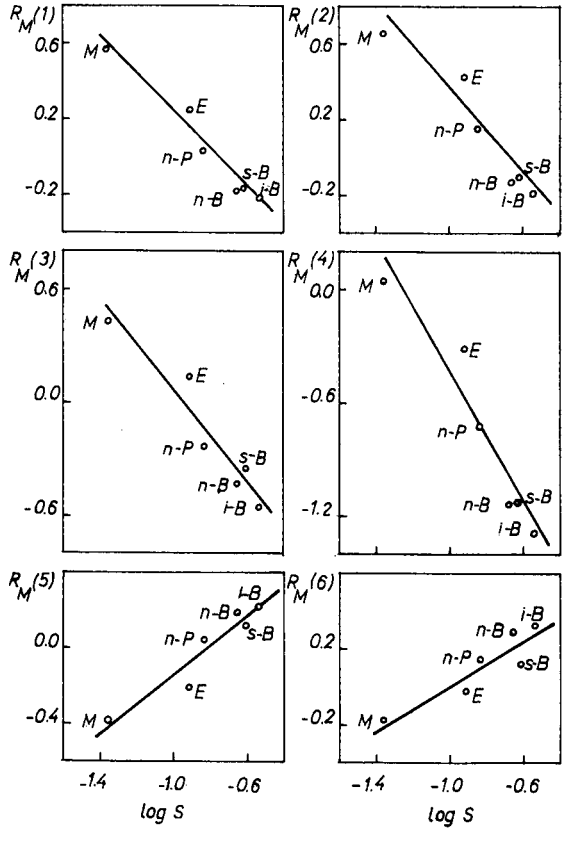

Fig. 3. Dependence of R_M values of the investigated tris(alkylxanthato)cobalt(III) complexes on the complex solubility logarithm (log *S*) in CCl_4. Numbers in parentheses and abbreviations as in Fig. 2.

xanthato chelates under conditions of reversed-phase chromatography (Table II, solvent systems 5 and 6) are in accordance with those expected, *viz.*, with an increase in the *n*-alkyl chain in the ligands, the hydrophobic moiety of a chelate acquires a greater surface area of contact with non-polar $-CH_2-CH$ segments of polyacrylonitrile, resulting in an increased retention of complexes. In addition, the order of the investigated alkylxanthato complexes under conditions of reversed-phase chromatography on PANS is analogous to that obtained by reversed-phase chromatography of a homologous series of these chelates on thin layers of some alkyl-modified silica gels [18].

As already mentioned, the isomeric tris(butylxanthato)cobalt(III) complexes, regardless of the small differences obtained in R_F values, exhibit the same sequence in normal-phase chromatography by application of all non-aqueous solvent systems used (Table II, solvent systems 1–4). This sequence is analogous to the earlier established order of the same complexes on thin layers of silica gel [6], in accord with the hydrogen bond formation hypothesis [11]. Such behaviour of the isomeric butylxanthato complexes is not in accord with steric effects of the corresponding ligand side-chains. In addition, as seen from Fig. 2, regardless of large differences in steric effects of the isomeric butyl substituents, the differences in complex R_F values obtained are very small. On the other hand, Fig. 3 shows that the order of R_M values of the isomeric butylxanthato complexes is also not in accord with their solubilities. Therefore, we assume that in this instance the inductive effects of the corresponding ligand side-chains, which influence the electron density on ligand electro-negative atoms, play a decisive role, in accordance with the corresponding inductive constants of the isomeric butyl substitutens (Table II).

The reversed order of R_F values for isomeric butylxanthato complexes obtained under reversed-phase conditions (Table II, solvent systems 5 and 6), is in accordance with that expected, because in this instance specific interactions of the sorbate are acting towards polar molecules of the mobile phase.

On the basis of the above, it may be concluded that it has been established that linear dependence between the number of carbon atoms in ligands and the corresponding R_M values of a homologous series of metal complexes is also valid on PANS, in both normal- and reversed-phase chromatography. In addition, it is obvious that the dominant separation mechanism for the investigated chelates on PANS is hydrogen bond formation between the sorbates and the sorbent under normal-phase conditions and non-specific hydrophobic interactions in reversed-phase chromatography.

ACKNOWLEDGEMENTS

The authors are grateful to the Serbian Republic Research Fund for financial support and to Mr. Žarko Arbutina for technical assistance.

REFERENCES

1 T. J. Janjić, D. M. Milojković, Ž. J. Arbutina, Ž. Lj. Tešić and M. B. Ćelap, *J. Chromatogr.*, 481 (1989) 465.
2 T. J. Janjić, D. M. Milojković, Ž. J. Arbutina and M. B. Ćelap, *J. Serb. Chem. Soc.*, 56 (1991) 33.
3 T. J. Janjić, D. M. Milojković, Ž. Lj. Tešić and M. B. Ćelap, *J. Planar Chromatogr.*, 3 (1990) 495.
4 O. Liška, J. Lehotay, E. Branšteterova and G. Guiochon, *J. Chromatogr.*, 171 (1979) 153.
5 M. B. Ćelap, G. Vučković, T. J. Janjić, M. J. Malinar and P. N. Radivojša, *J. Chromatogr.*, 196 (1980) 59.
6 G. Vučković, N. Juranić and M. B. Ćelap, *J. Chromatogr.*, 361 (1986) 217.
7 M. B. Ćelap, M. J. Malinar, S. Sarić, T. J. Janjić and P. N. Radivojša, *J. Chromatogr.*, 153 (1978) 253.
8 T. J. Janjić, Ž. Lj. Tešić, M. J. Malinar, P. N. Radivojša and M. B. Ćelap, *J. Chromatogr.*, 331 (1985) 273.
9 B. P. Nikolskii (Editor), *Spravochnik Khimika*, Vol. III, Khimiya, Moscow, 1964, p. 954.
10 K. Saitoh, M. Kobayashi and N. Suzuki, *Anal. Chem.*, 53 (1981) 2309.
11 A. R. Timerbaev and O. M. Petrukhin, *Zhidkostnaya Adsorbtsionnaya Khromatografiya Khelatov*, Nauka, Moscow, 1989, p. 26.
12 A. R. Timerbaev and O. M. Petrukkin, *Zhidkostnaya Adsorbtsionnaya Khromatografija Khelatov*, Nauka, Moscow, 1989, p. 74.
13 *Römpps Chemie-Lexikon*, Franckh'sche Verlagshandlung, Stuttgart, 6th ed., 1966, Band III, p. 5021; 8th ed., 1987, Band V, p. 3274.
14 L. R. Snyder, in E. Heftmann (Editor), *Chromatography*, Reinhold, New York, 2nd ed., 1967, p. 70.
15 A. R. Timerbaev, V. V. Salov and O. M. Petrukhin, *Zh. Anal. Khim.*, 40 (1985) 237.
16 B. P. Nikolskii (Editor), *Spravochnik Khimika*, Vol. III, Khimiya, Moscow, 1964, p. 956.
17 L. Saitoh, *Bunseki Kagaku*, 35 (1986) 895.
18 H. Eggers and H. A. Russel, *Chromatographia*, 17 (1983) 486.

Journal of Chromatography, 596 (1992) 95–100
Elsevier Science Publishers B.V., Amsterdam

CHROM. 23 933

Micellar electrokinetic chromatographic study of hydroquinone and some of its ethers

Determination of hydroquinone in skin-toning cream

Inna K. Sakodinskaya☆, Claudia Desiderio, Annalisa Nardi and Salvatore Fanali*

Istituto di Cromatografia del CNR, Area della Ricerca di Roma, P.O. Box 10, 00016 Monterotondo Scalo (Rome) (Italy)

(First received October 9th, 1991; revised manuscript received December 5th, 1991)

ABSTRACT

The separation of hydroquinone and some of its ether derivatives was studied by micellar electrokinetic chromatography with sodium dodecyl sulphate as an anionic surfactant in the background electrolyte. The optimized method was used for the determination of hydroquinone in a sample of skin-toning cream. On-column detection at 254 nm with caffeine as an internal standard gave good quantitative results.

INTRODUCTION

Hydroquinone (HQ) is used as an antioxidant, as a photographic reducer and developer, etc. HQ and some of its ethers are also used in cosmetic creams as depigmenters, the mechanism of action being the inhibition of melanin formation [1–4]. HQ is toxic at concentrations higher than 2%, causing dermatitis [1,3]. Hence a knowledge of its content in consumer products (*e.g.*, in cosmetics) is important in order to avoid health problems. Several methods have been used for the determination of hydroquinone, *e.g.*, high-performance liquid chromatography (HPLC), spectrophotometry and thin-layer chromatography (TLC) etc. [3–8].

Micellar electrokinetic capillary chromatography (MECC) [9,10] is an electrophoretic technique in which the separation is performed with the same apparatus as used for capillary zone electrophoresis (CZE). Both charged and neutral compounds have been analysed succesfully by using MECC [11–16]. Usually negative surfactants such as sodium dodecyl sulphate or sodium decyl sulphate added to the background electrolyte (BGE) will improve the selectivity of the separation. The separation mechanism is based on the partitioning of the solute between micelles, moving in the opposite direction to the electroosmotic flow, and the bulk aqueous phase.

In this work we used MECC for the determination of hydroquinone in a sample of skin-toning cream. In order to optimize the method we studied the effects of the pH of the BGE and the amount of sodium dodecyl sulphate (SDS) on the migration time (t_m) and the capacity factor (k') of hydroquinone and some of its ether derivatives.

The determination of HQ in a real sample was performed by using the internal standard method by measuring the peak-area ratio.

EXPERIMENTAL

Apparatus

Electrophoretic experiments were performed in a laboratory-made apparatus consisting of a modi-

☆ Present address: Chemical Department, Moscow State University, GSP-119899 Moscow, USSR.

0021-9673/92/$05.00

fied Varian UV 2550 detector and a Glassman LH60R power supply able to deliver either constant voltage or constant current. A fused-silica capillary tube (50 cm × 75 μm I.D., 38 cm to the detector) (SGE, Victoria, Australia) was used for the separations. The modified detector cell and the construction of the capillary connection block, the electrolyte vessel and the capillary holder have been described previously [17]. Detection was carried out at 254 nm. Electropherograms were recorded with an LKB (Bromma, Sweden) Model 2210 recorder. A Chromatopac C-R5A integrator (Shimadzu, Kyoto, Japan) was used for quantification. Sampling was done by the hydrodynamic method (6 s at a height of 10 cm). The constant-voltage mode was chosen for electrophoretic analysis.

Chemicals

The compounds investigated were hydroquinone (HQ), hydroquinone monomethyl ether (MHQ), hydroquinone dimethyl ether (DMHQQ), hydroquinone monopropyl ether (PHQ), hydroquinone monobenzyl ether (BHQ) and hydroquinone monophenyl ether (PhHQ) (all from Fluka, Buchs, Switzerland). Caffeine, used as an internal standard (I.S.), and anthracene, used to mark the maximum retention time, were obtained from Merck (Darmstadt, Germany). Sodium dodecyl sulphate (SDS) was obtained from Sigma (St. Louis, MO, USA). Methanol (Carlo Erba, Milan, Italy) was of HPLC grade. All other reagents were of analytical-reagent grade and were used as received. The water used was doubly distilled. The BGE containing methanol was prepared from stock solutions of borate buffer of adjusted pH in order to obtain a borate concentration of 0.01 *M* after the addition of methanol. The appropriate amount of SDS was added to the BGE.

Epocler skin-toning cream (Laboratory Whitehall, New York, USA), declared to contain HQ, was used as a real sample for quantitative analysis.

Standard solutions

The standard solutions used for electrophoretic experiments were prepared by dissolving the standard compounds in water–methanol (3:1, v/v). HQ standard solutions ($5 \cdot 10^{-5}$–$8 \cdot 10^{-4}$ *M*), containing a fixed concentration of caffeine (I.S.), were prepared in water–methanol (3:1) and used for calibration.

Assay of depigmenters in skin-toning cream

The extraction procedure was similar to that described by Gagliardi *et al.* [3]. A carefully weighed amount of cream (*ca.* 0.1 g) was heated in 40 ml of an aqueous solution containing 4 ml of methanol and 4 ml of caffeine ($4 \cdot 10^{-3}$ *M*) as I.S. at 50°C until it was completely dissolved. After cooling, the extract was filtered through a Millex-GS filter (Millipore) and injected for electrophoretic analysis.

RESULTS AND DISCUSSION

We first tried to separate a mixture of HQ and some of its ethers by using CZE in BGE at different pH values. CZE is a powerful analytical technique with a high resolving power and high efficiency, which is mainly used for the separation of ionic compounds even when the separation of uncharged compounds has been shown [18,19].

As expected, our attempts failed because the analyte compounds moved with similar effective mobilities under the operating conditions used. In order to modify selectively the electrophoretic mobility, it is necessary to change the composition of the BGE, *e.g.*, by adding cyclodextrins for isomer separations [20] or metal cations for peptides [21]. Therefore, considering the properties of the analyte compounds, we used SDS, added to the BGE above the critical micellar concentration (CMC) [12], as a selective agent.

Optimization of separation

Fig. 1 shows the dependence of the capacity factor (k') of HQ and its ethers on the concentration of SDS in 0.01 *M* borate buffer (pH 9.5). The k' values were calculated in accord to Terabe *et al.* [9]. In the absence of SDS all the compounds migrate with approximately the same velocity near to that of electroosmotic flow (methanol). By increasing the amount of SDS, hydrophobic compounds, such as phenyl and benzyl ether, moved with a longer migration time whereas there was no noticeable effect on methanol and only a very weak effect on HQ, which can be considered to be relatively hydrophilic compounds. This is in accord with the pK_a values of 10.35 for HQ, 10.24 for MHQ, 10.9 for BHQ, 10.7 for PrHQ and 9.9 for PhHQ [22,23], which should be neutral compounds at pH 9.5. Hence the separation achieved at high SDS concentrations is due

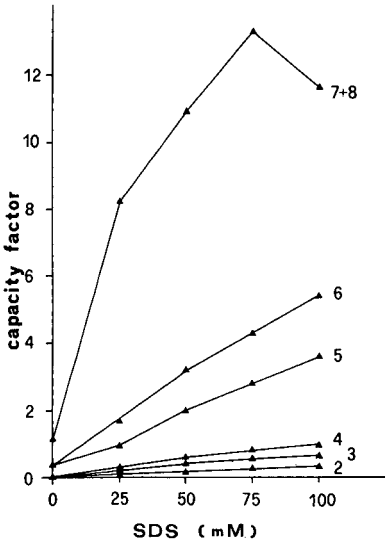

Fig. 1. Effect of SDS added to the background electrolyte [0.01 *M* borate buffer (pH 9.5)] on the capacity factor (k'). 1 = Methanol 2 = hydroquinone; 3 = caffeine (I.S.); 4 = hydroquinone monomethyl ether; 5 = hydroquinone dimethyl ether; 6 = hydroquinone monopropyl ether; 7 = hydroquinone monobenzyl ether; 8 = hydroquinone monophenyl ether. Electrophoresis, 10 kV, 20μA; sampling, hydrodynamic, 6 s per 10 cm standard mixture about 10^{-4} *M* each; volume injected, *ca.* 10 nl.

to the difference in the hydrophobicities of the analytes. The compounds investigated migrate in the same order as in reversed-phase HPLC separation [3], which is also due to the difference in their hydrophobicities.

The main criterion for the choice of the conditions was the ability to determine HQ concentration and therefore the separation of HQ from methanol and its negative peak should be carefully followed as some methanol is inevitably present in the extracts from the cream sample [3]. Experiments performed at higher voltage decreased the migration time of all the analyte compounds, owing to a higher electroosmotic flow [18]. The HQ peak was very close to the negative peak of methanol, making quantification difficult.

Several electrolyte systems containing 75 m*M* SDS at different pH values ranging from 7.5 to 11.5 were used in order to study the effect of pH on the selectivity of the separation. Increasing pH should convert HQ and its ethers into a charged form and provide separations due to the differences in the charge-to-mass ratio and differences in hydrophobicity. However, the studied compounds are unstable in basic media owing to rapid oxidation [1]. We therefore decided to select a relatively low pH value in order to ensure stability of the analytes. Fig. 2 shows the pH dependence of the capacity factors of HQ and its ethers. The influence of pH in the range 7.5–10.5 on the capacity factor of HQ seems weak, corresponding to its neutrality and hydrophilicity, whereas those compounds which are more hydrophobic are sufficiently retarded with increase in pH owing to the absorption in the negatively charged micelles of SDS. In fact, at pH 10.5 for HQ we obtained more than one peak, probably owing to decomposition of sample. Therefore, despite the availability of an additional separation mechanism at higher pH values, it is preferable to use less basic media.

All the ethers and HQ show sufficient differences in migration times at SDS concentrations above 0.05 *M* (Fig. 1). However, BHQ and PhHQ mixtures form one peak at pH 7.5–9.5 and 0.075 *M* SDS. The two compounds were partially resolved when the electrolyte at pH 10.5 containing 0.075 *M* SDS was used. The addition of an organic co-solvent has been shown to improve the selectivity of separation in MECC [24]. We therefore tried to use

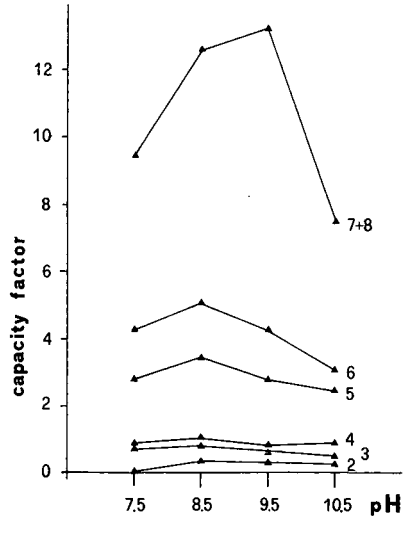

Fig. 2. Effect of carrier pH on the capacity factor of HQ and some of its ether derivatives. SDS concentration = 0.075 *M*; for experimental conditions and compounds, see Fig. 1.

a micellar buffer solution (MBS) containing different amounts of methanol ranging from 10 to 40% (v/v). The migration time of all the compounds increased with increasing amount of methanol in the MBS (results not shown); this is mainly due to the decrease in the electroosmotic flow.

The optimum buffer solution for the separation of the studied compounds was that containing 10% of methanol, which combines complete resolution with a shorter analysis time. In order to study the effect of the amount of SDS on the migration time of HQ and its ether derivatives, we performed several electrophoretic separations in borate buffer (pH 9.5) containing 10% of methanol and different amount of SDS. Table I shows the effect of SDS on the migration times when 10% methanol–borate buffer was used. There is a general increase in t_m and k' with increasing amount of SDS (except for methanol), and this effect is more evident for BHQ and PhHQ (the most hydrophobic compounds). In this electrolyte system (methanol mixture), SDS was found to be a better selective agent for the analyte compounds than in aqueous micellar solution. This may be due to the improved repartitioning of the solute between SDS and the buffer. The complete separation of BHQ and PhHQ was achieved.

Fig. 3 shows a typical electropherogram for the separation of HQ and its ether derivatives when a micellar buffer solution without and with methanol was used. Experiments performed in a micellar buffer solution containing 0.01 *M* borate buffer (pH 9.5), 10% methanol and 75 m*M* SDS in order to verify the reproducibility of the method for the analysis of HQ failed; the reproducibility of the method was poor compared with that obtained in buffer without methanol.

As in preliminary experiments carried out by analysing a sample of skin-toning cream we did not find BHQ and PhHQ, we selected a micellar buffer solution containing 0.01 *M* borate buffer (pH 9.5) and 0.075 *M* SDS for the analysis of HQ in a real sample.

Ten electrophoretic runs, performed by injecting standard solutions containing $4 \cdot 10^{-4}$ *M* caffeine (I.S.) and different amounts of HQ, were carried out and the calibration graph was found to be linear from $5 \cdot 10^{-5}$ to $8 \cdot 10^{-4}$ *M* with a correlation coefficient of 0.9997. The relative standard deviation, calculated by measuring the HQ/I.S. peak-area ratio by analysing the same sample ($2 \cdot 10^{-4}$ *M* HQ and $4 \cdot 10^{-4}$ *M* caffeine) six times, was found to be 1.8%.

TABLE I

EFFECT OF SDS CONCENTRATION IN THE BUFFER ELECTROLYTE [0.01 *M* BORATE BUFFER (pH 9.5) CONTAINING 10% (v/v) METHANOL ON THE MIGRATION TIMES (RETENTION TIMES) AND CAPACITY FACTORS OF THE STUDIED COMPOUNDS

Experimental conditions as in Fig. 1.

Compound[a]	[SDS] (m*M*)							
	25		50		75		100	
	t (min)	k'	t (min)	k'	t (min)	k'	t (min)	k'
1	4.1	0	4.5	0	4.6	0	4.6	0
2	4.5	0.2	5.0	0.2	5.0	0.2	5.5	0.3
3	4.5	0.2	5.0	0.2	5.5	0.3	6.0	0.4
4	4.7	0.2	5.8	0.5	6.2	0.6	7.0	0.8
5	5.5	0.6	7.6	1.3	9.0	2.0	10.4	3.3
6	6.0	1.0	8.8	2.3	10.4	3.2	12.2	4.5
7	8.4	2.8	12.4	8.9	14.7	15.7	17.1	24.0
8	8.7	3.2	12.7	10.2	15.0	18.4	15.5	30.0
AN	13.4	∞	15.4	∞	17.1	∞	19.3	∞
t_o/t_{mc}	0.306		0.325		0.269		0.238	

[a] Compounds 1–8 as in Fig. 1; AN = anthracene.

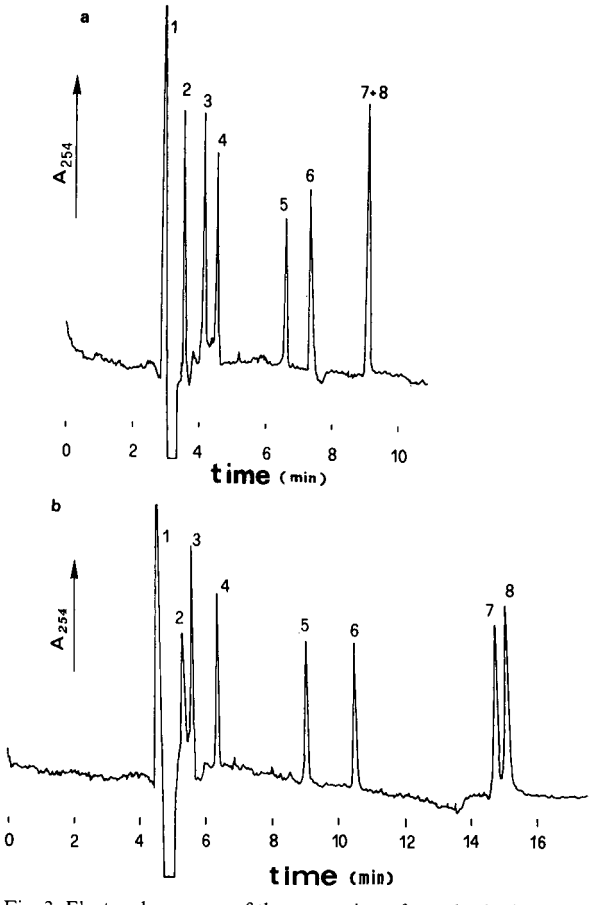

Fig. 3. Electropherogram of the separation of standard mixtures of HQ and its ether derivatives. 0.01 *M* borate buffer (pH 9.5) + 0.075 *M* SDS, (a) without methanol and (b) with 10% (v/v) methanol. Volume injected, *ca.* 10 nl.

Analysis of cream sample

Qualitative analysis of the extract of the skin-toning cream showed not only the peak corresponding to HQ but also two small peaks with migration times of 5.36 and 6.65 min corresponding to none of the studied ethers. We failed to identify the last peak, but the first has the same t_m as the positional isomer of HQ *o*-dihydroxybenzene (catechol), and when the mixture was spiked with catechol the peak with t_m = 5.36 min increased in area. Quantitative analysis of HQ showed that its content was $1.80 \pm 0.05\%$ (w/w), *i.e.*, not more than is permitted by legislation of the European Community, and almost the same as in the cream analysed by HPLC previously [3]. The presence of catechol may be due

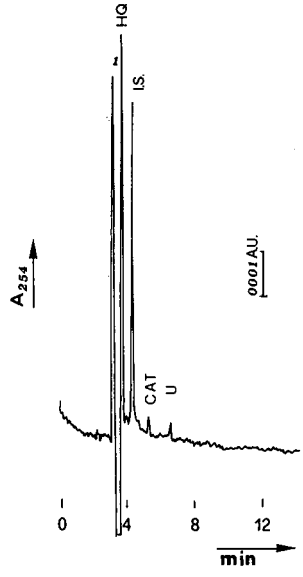

Fig. 4. Analysis of skin-toning cream. Experimental conditions as in Fig. 1. (1) methanol; (HQ) hydroquinone; (I.S.) caffeine; (CAT) catechol; (U) unknown.

to the impurities in the HQ added; this compound is known to have similar toxic effects on skin as phenol and HQ [1], but it is not claimed to be a depigmenter.

CONCLUSIONS

The separation of HQ and its ethers can be performed by using MECC. The use of an organic modifier (methanol) improved the resolution; with this electrolyte system we obtained poor reproducibility. The optimized analytical method was applied to the determination of HQ in cosmetic samples. The results showed its content to be similar to that declared by the producer. The studied method allowed the analysis to be performed in a relatively short time (less than 10 min) with good results. Further studies will be made in order to optimize the quantitative analysis with electrolyte systems containing organic modifiers.

ACKNOWLEDGEMENTS

Thanks are due to Mr. M Cristalli and G. Caponecchi for technical assistance.

REFERENCES

1 S. Budavari (Editor), *The Merck Index*, Merck, Rahway, NJ, 11th ed., 1989, pp. 762–763.
2 E. A. Swinyard, in L. S. Goodman and A. G. Gilman (Editors), *The Pharmacological Basis of Therapeutics*, Macmillan, New York, 5th ed., 1975, p. 955.
3 L. Gagliardi, A. Amato, G. Cavazzutti, F. Chimenti, A. Bolasco and D. Tonelli, *J. Chromatogr.*, 404 (1987) 267.
4 M. Motonok, *Jpn. Kokai Tokkyo Koho JP*, 01 199 916 [89 199 916], 1989; *C.A.*, 112 (1990) P223137g.
5 A. Teglia, *Cosmet. Toiletries, Ed. Ital.*, 10, No. 4 (1989) 10.
6 F. Buhl, E. Dul-Zarycta and M. Chwistek, *Chem. Anal. (Warsaw)*, 33 (1988) 819; *C.A.*, 112 (1990) 24542h.
7 P. Davidkova, J. Kopecek and J. Gasparic, *J. Inf. Rec. Mater.*, 17 (1989) 117; *C.A.* 112 (1990); 90956z.
8 W. G. Burkert, C. N. Owensby and W. L. Hinze, *J. Liq. Chromatogr.*, 4 (1981) 1065.
9 S. Terabe, K. Otsuka, K. Ichikawa, A. Tsuchiya and T. Ando, *Anal. Chem.*, 56 (1984) 111.
10 D. E. Burton, M. J. Sepaniak and M. P. Maskarimec, *J. Chromatogr. Sci.*, 24 (1986) 347.
11 R. A. Wallingford and A. G. Ewing, *J. Chromatogr.*, 441 (1988) 299.
12 H. Nishi and S. Terabe, *Electrophoresis*, 11 (1990) 691.
13 S. Fujiwara and S. Honda, *Anal. Chem.*, 59 (1987) 2773.
14 H. T. Rasmussen, L. K. Goebel and H. M. McNair, *J. High Resolut. Chromatogr.*, 14 (1991) 25.
15 S. Terabe, K. Otsuka and T. Ando, *Anal. Chem.*, 57 (1985) 834.
16 S. Terabe, *Trends Anal. Chem.*, 8 (1989) 129.
17 S. Fanali, L. Ossicini, F. Foret and P. Bocek, *J. Microcol. Sep.*, 1 (1989) 190.
18 F. Foret and P. Bocek, in A. Chrambach, M. J. Dunn and B. J. Radola (Editors), *Advances in Electrophoresis*, Vol. 3, VCH, Weinheim, 1989, p. 271.
19 A. Nardi, S. Fanali and F. Foret, *Electrophoresis*, 11 (1990) 774.
20 S. Fanali and P. Bocek, *Electrophoresis*, 11 (1990) 757.
21 R. A. Mosher, *Electrophoresis*, 11 (1990) 765.
22 R. C. Weast, S. M. Selby and C. D. Hodgman (Editors), *Handbook of Chemistry and Physics*, CRC Press, Cleveland, OH, 46th ed., 1965–66, p. D-78.
23 N. B. Chapman and J. Shorter (Editors), *Correlation Analysis in Chemistry*, Plenum Press, New York, 1978.
24 J. Corse, A. T. Balchunas, D. F. Swaile and M. J. Sepaniak, *J. High Resolut. Chromatogr. Chromatogr. Column*, 11 (1988) 554.

Journal of Chromatography, 596 (1992) 101–109
Elsevier Science Publishers B.V., Amsterdam

CHROM. 23 966

Determination of sulphonamides in pork meat extracts by capillary zone electrophoresis

M. T. Ackermans, J. L. Beckers* and F. M. Everaerts

Laboratory of Instrumental Analysis, Eindhoven University of Technology, P.O. Box 513, 5600 MB Eindhoven (Netherlands)

H. Hoogland and M. J. H. Tomassen

State Institute for Quality Control of Agricultural Products, Bornsesteeg 45, 6708 PD Wageningen (Netherlands)

(First received October 24th, 1991; revised manuscript received December 19th, 1991)

ABSTRACT

For sixteen sulphonamides the effective mobility was measured as a function of pH and from the effective mobilities determined in two different electrolyte systems the pK value and mobility at infinite dilution were calculated. A pH of 7.0 was found to be the optimum pH for the separation for both standard mixtures and mixtures of sulphonamides dissolved in pork meat extracts. For the determination of the sulphonamides in pork meat only a very simple sample pretreatment consisting of extraction with acetonitrile and centrifugation is suitable, as the matrix effects at pH 7.0 do not affect the separation. Calibration graphs for five sulphonamides were constructed, and regression coefficients of at least 0.999 were obtained. The limit of detection for the method varies from 2 to 9 ppm for a pressure injection time of 10 s (injection volume *ca.* 18 nl) using a Polymicro Technology capillary of length 116.45 cm, distance between injection and detection 109.75 cm and I.D. 50 μm.

INTRODUCTION

Many veterinary drugs in use for food-producing animals are available as injectable preparations. Depending on the formulation, the use of these preparations may give rise to residual amounts of the drug at the site of injection [1,2]. Moreover, the use of these preparations may lead to considerable local irritation of the tissue, leading to visible injection sites when treated animals are slaughtered. According to the law, visible injection sites must be removed from the carcass in Netherlands. For regulatory purposes it is often of interest to know which drug has been used, *e.g.*, when the use of an illegal drug is suspected. In order to identify the drugs present at injection sites of slaughtered animals, a selective and routinely applicable analytical method is required. As often fairly high concentrations of drugs will be found at injection sites, owing to incomplete [3] or slow [4] adsorption of the drugs, there are no special requirements regarding the sensitivity of the method. Most recently developed methods allow the selective detection of a single component, or a selected group of components, at very low concentrations [5–7], albeit that multi-screening methods have been reported [8]. Owing to this limited applicability and/or the necessary extensive purification of the samples, and sometimes derivatization, these methods are not considered suitable for our purposes.

In this paper the applicability of capillary zone electrophoresis (CZE) for the determination of sulphonamides in pork meat extracts is described. The group of sulphonamides was chosen because its members are present in injectable formulations. Moreover, this group of drugs consists of a relatively large number chemically related compounds and studies of this group will yield information concerning the applicability and the selectivity of the technique when applied to meat extracts. In the

0021-9673/92/$05.00

determination of sulphonamides in pork meat extracts using CZE, the most important questions to be answered are: (1) can the sulphonamides be separated from the matrix; (2) how can the sulphonamides be identified; and (3) are linear calibration graphs obtained and what is the limit of detection?

EXPERIMENTAL

Chemicals and reagents

The structural formulae of the compounds studied are shown in Fig. 1. Trimethoprim, sulphamethoxazole, sulphanilamide, sulphadimidine-Na, sulphathiazole, sulphamerazine, sulphadiazine, sulphadoxine, sulphamethoxypyridazine, sulphadimethoxine, sulphatroxazole, sulphaquinoxaline, sulphamethoxydiazine, sulphaguanidine, sulphachloropyrazine-Na and sulphachloropyridazine were supplied by the Netherlands State Institute for Quality Control for Agricultural Products (RIKILT). Stock solutions standard (1 mg/ml) were prepared by weighing exactly 10.0 mg of the component and dissolving it in 10.0 ml of solvent. These solutions were diluted to the desired concentrations with distilled water to give working standard solutions.

All other chemicals were of analytical-reagent grade.

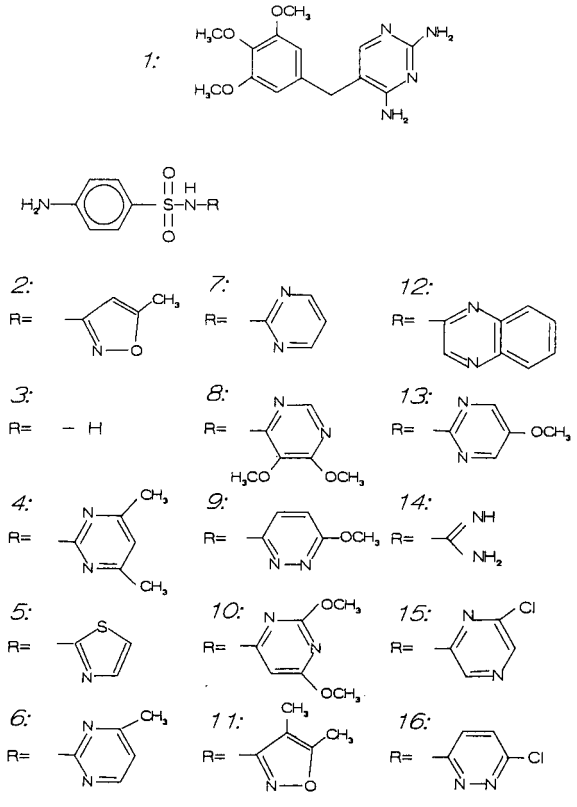

Fig. 1. Structural formulae of (1) trimethoprim, (2) sulphamethoxazole, (3) sulphanilamide, (4) sulphadimidine, (5) sulphathiazole, (6) sulphamerazine, (7) sulphadiazine, (8) sulphadoxine, (9) sulphamethoxypyridazine, (10) sulphadimethoxine, (11) sulphatroxazole, (12) sulphaquinoxaline, (13) sulphamethoxydiazine, (14) sulphaguanidine, (15) sulphachloropyrazine and (16) sulphachloropyridazine.

Instrumentation

All CZE experiments were performed using a P/ACE System 2000 HPCE instrument (Beckman Instruments, Palo Alto, CA, USA). The working temperature was 25°C. Two capillaries were used, *viz.*, an original Beckman standard capillary of length 57 cm, distance between injection and detection 50 cm, I.D. 75 μm, where a 1-s pressure injection equals an injection volume of *ca.* 19 nl, and a capillary from Polymicro Technologies (Phoenix, AZ, USA) of length 116.45 cm, distance between injection and detection 109.75 cm, I.D. 50 μm, where a 1-s pressure injection equals an injection volume of *ca.* 1.8 nl. The sample was introduced by means of pressure injection and in all experiments a constant voltage was applied. The wavelength of the UV detector was 254 nm in all experiments.

Sample pretreatment

For the pork meat extracts, 10 g of pork meat were homogenized in a household food processor and extracted in a stomacher apparatus for 5 min with 100 ml of acetonitrile. The sample was centrifuged for 10 min at 4000 *g* and filtered through a 0.45-μm filter. If the sample had to be spiked, this was done between the centrifugation and the filtration steps. The filtrate was used for injection.

RESULTS AND DISCUSSION

Determination of effective mobilities

The effective mobility is an important parameter in CZE because differences in effective mobilities determine whether components can be separated or not, and because separated components can be identified by their effective mobilities. As described

previously [9], the effective mobility m_{eff} can be calculated from the mobility of the electroosmotic flow (EOF), m_{EOF}, and the apparent mobility, m_{app}, of the component according to

$$m_{eff} = m_{app} - m_{EOF} = \frac{l_d l_c}{V}\left(\frac{1}{t_s} - \frac{1}{t_{EOF}}\right) (cm^2/V \cdot s) \quad (1)$$

where l_c and l_d are the length of the capillary and the length between injection and detection (cm), V is the applied voltage (V) and t_s and t_{EOF} are the migration times of the component and the EOF (s). As the velocity of the EOF, v_{EOF}, can vary with time, the migration time or apparent mobility of a component cannot be used for identification.

For the determination of the effective mobilities, the background electrolytes and separation conditions given in Table I were used. The effective mobilities were determined with both the Polymicro Technologies and the Beckman standard capillaries. Table II gives the effective mobilities for the sixteen sulphonamides for both capillaries at four pH values. The voltage applied in the experiments with capillary II was lower in order to avoid a large difference between the electric currents. At pH 3.2 the effective mobilities in the long Polymicro Technologies capillary could not be determined because the velocity of the EOF was so low that the analysis time became about 80 min, causing very broad peaks so that precise migration times could not be obtained. From Table II it can be concluded that the effective mobilities determined with both capillaries agree. The migration times of components not completely separated from the EOF marker are often difficult to determine, resulting in imprecise effective mobilities. In Fig. 2 the effective mobilities as a function of the pH of the background electrolyte for the Beckman standard capillary are given.

As can be seen in Fig. 2, the differences between the effective mobilities are optimum at pH 7. At this pH most of the sulphonamides can be separated from each other. Nevertheless, two pairs of sulphonamides cannot be separated, *viz.*, sulphanilamide and sulphaguanidine, which are both uncharged at this pH ($m_{eff} = 0$) and can be used as EOF markers, and sulphathiazole and sulphamethoxypyridazine, which have very similar m_{eff} values (average -6.42×10^{-5} and -6.71×10^{-5} $cm^2/V \cdot s$, respectively). Sulphadiazine, sulphadoxine and sulphadimethoxine are not completely separated, but three tops of peaks can be determined if all three are present.

As expected, the components are better separated in the Polymicro Technology capillary, which has a longer separation length. Fig. 3 shows the electropherograms obtained using the Beckman standard capillary for a mixture of twelve sulphonamides dissolved in water–acetonitrile (90:10) using a background electrolyte of (A) 0.02 *M* imidazole–acetate

TABLE I

BACKGROUND ELECTROLYTES AND SEPARATION CONDITIONS FOR THE DETERMINATION OF THE EFFECTIVE MOBILITIES OF THE SULPHONAMIDES

I, Polymicro Technologies capillary, length 116.45 cm, distance between injection and detection 109.75 cm, I.D. 50 μm. II, Beckman standard capillary, length 57 cm, distance between injection and detection 50 cm, I.D. 75 μm. The background electrolytes were prepared by adding the acid to the cationic component until the desired pH was reached, except for the phosphate–borate buffer, where KOH was added to the mixture of the acids until the desired pH was reached.

Background electrolyte[a]	pH	Applied voltage (kV) with current (μA) in parentheses		Injection time (s)	
		I	II	I	II
0.02 *M* Tris–acetate	8.2	30 (3.7)	15 (8.5)	5	2
0.01 *M* imidazole–acetate	7.0	30 (4.9)	10 (8.4)	5	2
0.02 *M* phosphate–0.02 *M* borate	7.0	30 (16.7)	10 (26.8)	5	2
0.01 *M* Tris–MES	6.5	30 (2.9)	10 (4.6)	5	2
0.01 *M* Tris–acetate	5.0	30 (3.7)	10 (5.7)	5	2
0.01 *M* Tris–formate	3.2	30 (5.2)	10 (8.1)	5	2

[a] Tris = tris(hydroxymethyl)aminomethane; MES = 2-(N-morpholino)ethanesulphonic acid.

TABLE II

EFFECTIVE MOBILITIES × 10^5 ($cm^2/V \cdot s$) FOR THE SIXTEEN SULPHONAMIDES AT DIFFERENT pH VALUES OF THE BACKGROUND ELECTROLYTES

Component	Capillary[a]	Effective mobility			
		pH 8.2	pH 7.0[b]	pH 5.0	pH 3.2
Trimethoprim	I	1.50	11.25	18.76	
	II	1.87	11.73	19.08	20.26
Sulphamethoxazole	I	−21.55	−20.48	−4.02	
	II	−21.96	−21.15	−4.30	0.00
Sulphanilamide	I	0.00	0.00	0.00	
	II	0.00	0.00	0.00	1.30
Sulphadimidine	I	−13.91	−2.92	0.00	
	II	−14.26	−2.91	0.00	1.65
Sulphathiazole	I	−19.41	−6.47	0.00	
	II	−19.67	−6.36	0.00	1.21
Sulphamerazine	I	−18.83	−9.57	−1.63	
	II	−18.98	−9.49	0.00	1.41
Sulphadiazine	I	−21.01	−16.03	−1.41	
	II	−21.29	−16.39	−0.96	0.89
Sulphadoxine	I	−18.54	−16.81	−2.43	
	II	−18.65	−17.24	−2.59	0.31
Sulphamethoxypyridazine	I	−17.77	−6.61	−0.23	
	II	−17.83	−6.81	0.00	1.05
Sulphadimethoxine	I	−19.16	−17.15	−2.19	
	II	−19.33	−17.37	−2.31	0.47
Sulphatroxazole	I	−20.31	−19.22	−3.61	
	II	−20.49	−19.65	−3.69	0.00
Sulphaquinoxaline	I	−19.49	−18.20	−2.38	
	II	−19.60	−18.59	−3.84	0.45
Sulphamethoxydiazine	I	−19.38	−12.49	−0.58	
	II	−19.35	−12.83	−0.76	0.49
Sulphaguanidine	I	0.00	0.00	0.00	
	II	0.00	0.00	0.00	2.21
Sulphachloropyrazine	I	−21.18	−21.21	−10.46	
	II	−21.36	−21.73	−9.50	0.32
Sulphachloropyridazine	I	−20.85	−20.26	−5.65	
	II	−20.89	−20.64	−4.96	0.41

[a] See Table I.
[b] For pH 7.0 the imidazole–acetate system is used.

and (B) 0.02 *M* phosphate–0.02 *M* borate and of a mixture of twelve sulphonamides dissolved in the pork meat matrix using a background electrolyte of (C) 0.02 *M* imidazole–acetate and (D) 0.02 *M* phosphate–0.02 *M* borate. As can be seen in Fig. 3A and B, the separation of the standard mixture is good in both background electrolytes. Nevertheless, the effective mobilities for some components are different in both background electrolytes (possibly owing to a slight difference in the pH and the nature of the two electrolyte solutions) but, as further experiments showed, the effective mobilities are reproducible and constant in each background electrolyte. As can be seen in Fig. 3C and D, the separation of the mixture in the matrix is much better in the phosphate–borate buffer than in the imidazole buffer, showing sharper peaks. For quantitative analysis, therefore, the 0.02 *M* phosphate–0.02 *M* borate buffer is used.

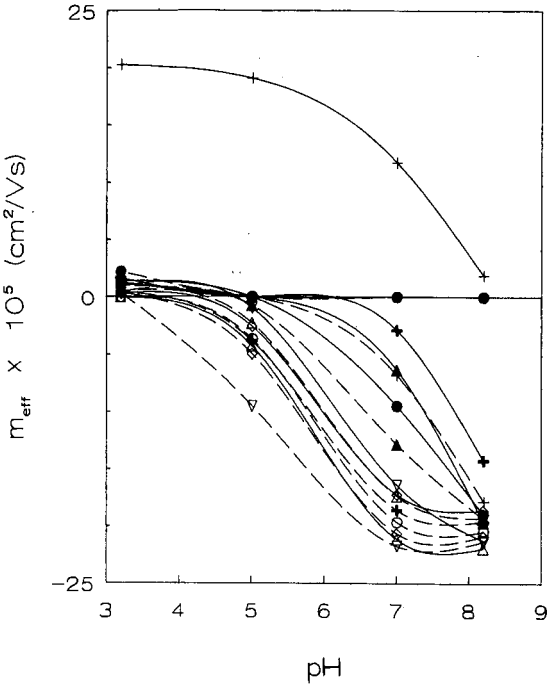

Fig. 2. Effective mobility as a function of the pH of (solid lines) (+) 1; (△) 2; (○) 3; (+) 4; (▲) 5; (●) 6; (▽) 7; (◇) 8; and (dotted lines) (+) 9; (△) 10; (○) 11; (+) 12; (▲) 13; (●) 14; (▽) 15; (◇) 16. For the names of the components, see Fig. 1.

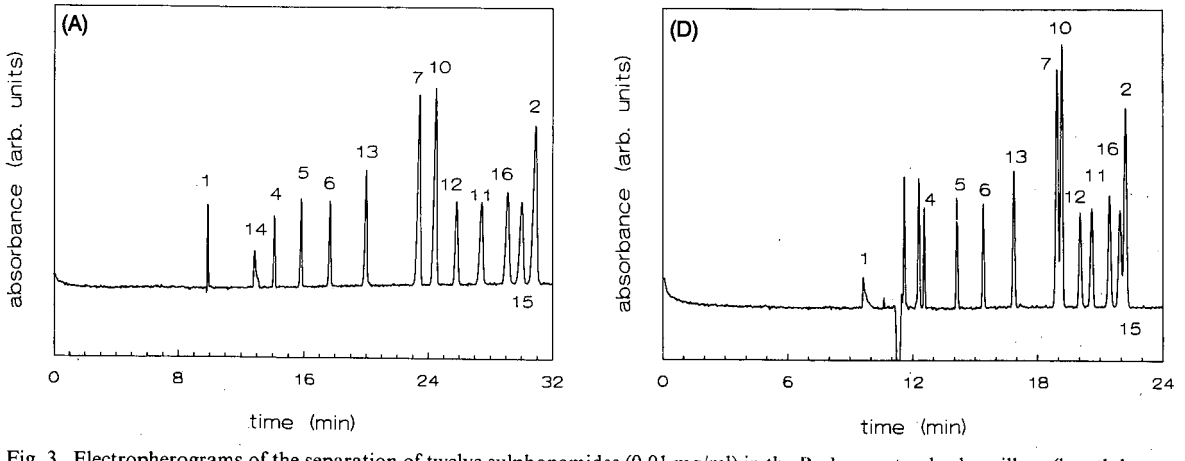

Fig. 3. Electropherograms of the separation of twelve sulphonamides (0.01 mg/ml) in the Beckman standard capillary (length between injection and detection 50 cm, pressure injection time 2 s ≈ 39 nl, applied voltage 10 kV) of standard mixture in the background electrolyte (A) 0.02 *M* imidazole–acetate at pH 7 and (B) 0.02 *M* phosphate–0.02 *M* borate at pH 7 and the standard mixture dissolved in the pork meat matrix in the background electrolyte (C) 0.02 *M* imidazole–acetate at pH 7 and (D) 0.02 *M* phosphate–0.02 *M* borate at pH 7. For the names of the components, see Fig. 1.

Calculation of pK values and mobilities at infinite dilution

If the effective mobility of a component is known for two different electrolyte systems at different pH values, at which the component shows a different degree of dissociation, both its pK value and its mobility at infinite dilution can be calculated [9]. In the calculations the best values are obtained if the pK value of the component lies between the pH values of the background electrolytes and if the effective mobilities are not too small. For components with pK values of about 7–8, background electrolytes at pH 8.2 and 7 are chosen. For components with pK values of about 5–7, both background electrolytes with pH 7 and 5 and pH 8.2 and 5 are chosen.

The pK values of sulphadiazine and sulphamethoxydiazine were calculated from the background electrolytes at pH 8.2 and 6.5. Table III gives the pK values and mobilities at infinite dilution for fourteen sulphonamides calculated from effective mobilities in the different background electrolytes, and the pK values as found in the literature [10,11]. Sulphanilamide and sulphaguanidine are not mentioned in

TABLE III

CALCULATED pK VALUES AND MOBILITIES AT INFINITE DILUTION, $m_0 \times 10^5$ ($cm^2/V \cdot s$), FOR THE SULPHONAMIDES USING THE EFFECTIVE MOBILITIES OF THE COMPONENT IN BACKGROUND ELECTROLYTES WITH THE INDICATED pH VALUES, AND LITERATURE VALUES FOR pK VALUES

Component	Capillary[a]	pK (lit.)	pH 8.2–7.0[b]		pH 8.2–5.0		pH 7.0[b]–5.0	
			pK	m_0	pK	m_0	pK	m_0
Trimethoprim	I	6.6	7.11	23.59	7.13	22.53		
	II		7.26	21.75	7.23	22.83		
Sulphamethoxazole	I				5.73	−25.40	5.72	−25.05
	II				5.70	−25.82	5.70	−25.73
Sulphadimidine	I	7.4	7.82	−22.36				
	II		7.83	−23.09				
Sulphathiazole	I	7.2	7.48	−26.25				
	II		7.50	−26.73				
Sulphamerazine	I	7.0	7.13	−23.90				
	II		7.15	−24.12				
Sulphadiazine[c]	I	6.4			6.55	−25.18		
	II				6.52	−25.45		
Sulphadoxine	I	6.1			5.91	−22.34	5.89	−21.49
	II				5.88	−22.45	5.87	−21.90
Sulphamethoxypyridazine	I	6.7	7.37	−23.81				
	II		7.39	−23.77				
Sulphadimethoxine	I	6.2			5.98	−22.99	5.95	−22.04
	II				5.96	−23.16	5.93	−22.22
Sulphatroxazole	I	5.8			5.75	−24.13	5.74	−23.76
	II				5.75	−24.32	5.74	−24.12
Sulphaquinoxaline	I	5.5			5.94	−23.32	5.94	−23.15
	II				5.70	−23.40	5.68	−22.98
Sulphamethoxydiazine[c]	I				6.75	−23.70		
	II				6.73	−23.76		
Sulphachloropyrazine	I	5.1			5.10	−24.97	5.10	−25.12
	II				5.18	−25.16	5.20	−25.72
Sulphachloropyridazine	I				5.52	−24.66	5.51	−24.47
	II				5.59	−24.71	5.60	−25.00

[a] See Table I

[b] For pH 7.0 the imidazole–acetate system is used.

[c] Calculated with background electrolyte systems at pH 8.2 and 6.5.

Table III because they have very small effective mobilities in all electrolyte systems. From Table III it can be concluded that the calculated pK values and mobilities at infinite dilution obtained from the effective mobilities of both capillaries with the same background electrolyte systems agree.

Matrix effects

Because for a routine method the pretreatment should be very simple, we studied the matrix effects for a pork meat extract where the sample pretreatment consisted only of extraction of the homogenized meat with acetonitrile and centrifugation. This acetonitrile sample was directly used for injection. In Fig. 4 the electropherograms of (a) a mixture of thirteen sulphonamides dissolved in water and (b) the pure matrix in the background electrolytes (A) 0.02 M Tris–acetate at pH 8.2, (B) 0.02 M phos-

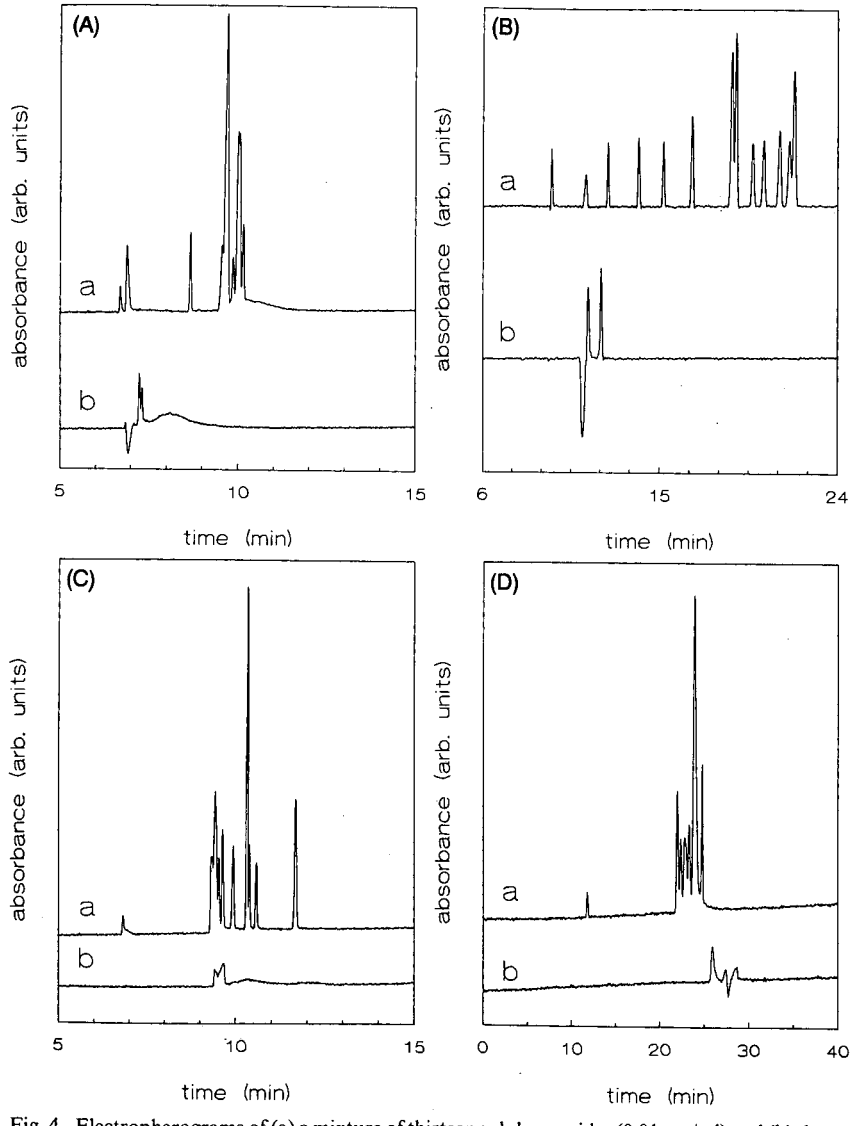

Fig. 4. Electropherograms of (a) a mixture of thirteen sulphonamides (0.01 mg/ml) and (b) the pure matrix in the background electrolytes (A) 0.02 M Tris–acetate (pH 8.2), (B) 0.02 M phosphate–0.02 M borate (pH 7.0), (C) 0.01 M Tris–acetate (pH 5.0) and (D) 0.01 M Tris–formate (pH 3.2). Beckman standard capillary, length 57 cm, distance between injection and detection 50 cm, I.D. 75 μm; applied voltage, 10 kV; pressure injection time, 2 s $\approx$ 39 nl.

TABLE IV

EFFECTIVE MOBILITIES, $m_{eff} \times 10^5$ ($cm^2/V \cdot s$) FOR TWELVE SULPHONAMIDES DETERMINED SEPARATELY, IN THE MIXTURE, AND IN THE MATRIX SPIKED WITH THE MIXTURE

Background electrolyte, 0.02 *M* imidazole–acetate at pH 7.0; Beckman standard capillary, length 57 cm, distance between injection and detection 50 cm, I.D. 75 μm; applied voltage, 10 kV.

Component	Separately	Mixture	Matrix with mixture
Trimethoprim	11.49	11.70	11.19
Sulphadimidine	−2.92	−3.01	−3.40
Sulphathiazole	−6.42	−6.35	−6.52
Sulphamerazine	−9.53	−9.38	−9.44
Sulphamethoxydiazine	−12.66	−12.45	−12.53
Sulphadiazine	−16.21	−15.88	−15.89
Sulphadimethoxine	−17.26	−16.92	−17.02
Sulphaquinoxaline	−18.40	−18.12	−18.28
Sulphatroxazole	−19.43	−19.08	−19.22
Sulphachloropyridazine	−20.45	−20.10	−20.35
Sulphamethoxazole	−20.82	−20.54	−20.70
Sulphachloropyrazine	−21.47	−21.40	−21.28

phate–0.02 *M* borate at pH 7.0, (C) 0.01 *M* Tris–acetate at pH 5.0 and (D) 0.01 *M* Tris–formate at pH 3.2 are given. It can be clearly seen that not only for the separation, but also for the matrix effects the background electrolyte at pH 7.0 gives the best results. The velocity of the EOF can vary from experiment to experiment and from this it seems that the components in Fig. 4D migrate in front of the matrix components. Further experiments showed, however, that this is only due to the change in the velocity of the EOF. The determination of sulphaguanidine and sulphanilamide in the matrix is problematic because these components are uncharged at pH 7.0 and migrate at the position of the EOF in the acetonitrile plug.

Table IV gives the effective mobilities for twelve sulphonamides determined separately, in the mixture and in the matrix spiked with the mixture, applying a background electrolyte at pH 7. For each component the effective mobilities determined in the mixture and in the matrix spiked with the mixture are comparable, and hence the effective mobility can be used for peak recognition.

Quantification

In order to evaluate the quantitative abilities of the method, calibration graphs for five sulphonamides in acetonitrile and in the matrix were constructed using the 0.02 *M* phosphate–0.02 *M* borate buffer (pH 7.0) and the Polymicro Technologies capillary. For the determination of the calibration graphs 10.0 mg of sulphadimidine-Na, sulphamerazine, sulphadoxine, sulphatroxazole and sulphamethoxazole were weighed accurately and dissolved in 10.0 ml of acetonitrile or matrix. From these solutions dilutions were made at concentrations of 0.1, 0.01 and 0.001 mg/ml. Each of the solutions was used for injection with pressure injection times of 3, 5, 10, 15, 20, 25 and 30 s (a 1-s pressure injection equals an injection volume of *ca.* 1.8 nl; sometimes the dimension $\mu g \cdot s/ml$ is used, which means the product of the pressure injection time and the concentration; 1 $\mu g \cdot s/ml$ = 1.8 pg). Peak areas were determined using the laboratory-written data analysis program CAESAR. From the calibration graphs, the limit of detection (LOD) for the method can be evaluated. For the calculation of the LOD the value $y_B + 3s_B$ is used, whereby the calculated intercept of the regression line is used as an estimate of y_B and s_B is the standard deviation in the y-direction of the regression line [12]. Table V gives the regression coefficient and LOD ($\mu g \cdot s/ml$) for the calibration graphs for the five sulphonamides. The regression coefficients were calculated with the data of the three concentration decades and for the determination of the LOD the calibration graph a sample concentration of 0.001 mg/ml was used. As can be concluded from Table V, the regression

TABLE V

REGRESSION COEFFICIENTS AND LIMITS OF DETECTION FOR THE CALIBRATION GRAPHS OF SULPHADIMIDINE, SULPHAMERAZINE, SULPHADOXINE, SULPHATROXAZOLE AND SULPHAMETOXAZOLE DISSOLVED IN (A) ACETONITRILE AND (B) THE PORK MEAT MATRIX

For the determination of the LOD the calibration graph in the lowest concentration decade was used. The regression coefficient was calculated using the data over the three concentration decades.

System	Component	Regression coefficient	LOD ($\mu g \cdot s/ml$)
A	Sulphadimidine	0.9996	4.8
	Sulphamerazine	0.9995	1.9
	Sulphadoxine	0.9994	8.8
	Sulphatroxazole	0.9993	6.3
	Sulphamethoxazole	0.9994	3.7
B	Sulphadimidine	0.9997	5.5
	Sulphamerazine	0.9994	4.4
	Sulphadoxine	0.9991	3.9
	Sulphatroxazole	0.9991	6.8
	Sulphamethoxazole	0.9991	2.8

coefficients are fairly good (>0.999) and the limit of detection for the method lies between 2 and 9 $\mu g \cdot s/ml$. For the given sample pretreatment and an injection of time of 10 s, the value of the LOD in $\mu g \cdot s/ml$ in the extract equals the value of the LOD in ppm in the meat sample, assuming 100% recovery.

CONCLUSIONS

Effective mobilities can be used for the identification of components, and they were measured for sixteen sulphonamide drugs in two different capillaries as a function of pH. From these experiments it can be concluded that a pH of the background electrolyte of 7 is the optimum pH for separation. At this pH, fourteen of the drugs can be determined and twelve of them can be identified using the effective mobilities. For some drugs, however, a further confirmation such as UV absorbance ratios or diode-array detection should be used. From the effective mobilities the pK values and the mobilities at infinite dilution for the sulphonamides were calculated.

For the determination of sulphonamides in pork meat, a very simple pretreatment consisting of an extraction with acetonitrile and centrifugation can be applied. For five sulphonamides the calibration graphs were set up both in acetonitrile and in the matrix. Linear calibration graphs were obtained with regression coefficients of at least 0.999 and limits of detection in the range 2–9 ppm in the sample for a pressure injection time of 10 s (*ca.* 18 nl) using a Polymicro Technology capillary of length 116.45 cm, distance between injection and detection 109.75 cm and I.D. 50 μm.

The applicability of this method for the determination of a variety of veterinary drugs in meat extracts and the possibilities of CZE with diode-aray detection for the peak identification are under investigation.

REFERENCES

1 J. F. M. Nouws, A. Smulders and M. Rappalini, *Vet. Q.*, 12 (1990) 129.
2 D. G. Pope, J. D. Baggot and J. Desmond, *Int. J. Pharm.*, 14 (1983) 123.
3 H. D. Mercer, J. C. Garg, J. D. Powers and T. W. Powers, *Am. J. Vet. Res.*, 38 (1977) 1353.
4 J. D. Baggot, *Principles of Drug Disposition in Domestic animals: the Basis of Veterinary Clinical Pharmacology*, Saunders, Philadelphia, 1977.
5 A. J. Manuel and W. A. Steller, *J. Assoc. Off. Anal. Chem.*, 64 (1981) 794.
6 N. Haagsma and C. van de Water, *J. Chromatogr.*, 333 (1985) 256.
7 J. D. Henion, B. A. Thomson and P. H. Dawson, *Anal. Chem.*, 54 (1982) 451.
8 R. Malish, *Z. Lebensm.-Unters.-Forsch.*, 182 (1986) 385.
9 J. L. Beckers, F. M. Everaerts and M. T. Ackermans, *J. Chromatogr.*, 537 (1991) 407.
10 *The Merck Index*, Merck, Rahway, NJ, 10th ed., 1983.
11 M. M. L. Aerts, *Thesis*, Free University of Amsterdam, Amsterdam, 1990.
12 J. C. Miller and J. N. Miller, *Statistics for Analytical Chemistry*, Ellis Horwood, Chichester, 2nd ed., 1988.

Journal of Chromatography, 596 (1992) 110–113
Elsevier Science Publishers B.V., Amsterdam

CHROM. 24 025

Short Communication

Apparent inter-channel interference in dual-electrode electrochemical detection

Charles A. Dempsey, Jan Lavicky and Adrian J. Dunn*

Department of Pharmacology and Therapeutics, Louisiana State University School of Medicine, P.O. Box 33932, Shreveport, LA 71130-3932 (USA)

(First received October 23rd, 1991; revised manuscript received January 21st, 1992)

ABSTRACT

During the course of routine high-performance liquid chromatographic analyses of brain catecholamines using dual-electrode electrochemical detection, we encountered an unusual negative peak in the lower-voltage channel. Subsequent investigations suggested that this peak was caused by tyrosine which produced a positive peak in the higher-voltage channel. Our investigations indicate that compounds that generate a peak in one channel appear to be responsible for complex peaks in a second channel set at a lower voltage, close to or below that necessary for oxidation. The complex peaks are biphasic; a sharp negative peak coinciding with the positive peak on the higher-voltage channel, followed by a positive peak. This effect was not specific for tyrosine, but was observed on the lower-voltage channel with all compounds tested that produced signals on the high-voltage channel. The cause of the problem is unknown, but it appears to be an artifact of the electrical coupling of the two electrode channels in a dual-channel system.

INTRODUCTION

We have routinely performed high-performance liquid chromatographic (HPLC) analyses of extracts of brain catecholamines and related compounds with dual-electrode electrochemical detection [1]. The dual-channel system was used because one compound (tryptophan) has a higher redox potential than the catecholamines, and use of a higher voltage on a one-channel detector obscured other peaks of interest. However, we recently encountered a negative peak on the lower-voltage channel. This negative peak caused problems for integration, and it occasionally affected peaks for compounds of interest. Therefore, we investigated the source of the negative peak. This report details our findings, which may be of general applicability to dual-electrode HPLC detection systems.

EXPERIMENTAL

Standard compounds were obtained from Sigma (St. Louis, MO, USA). Brain samples were prepared as described in previous publications [2]. Briefly, samples of frozen brain were homogenized by ultrasonication in 0.1 *M* $HClO_4$ containing 0.1 m*M* EDTA. After freezing and thawing, the precipitates were separated by centrifugation and the supernatants applied directly to the HPLC system.

The HPCL system consisted of an M-6000 dual-piston HPLC pump, WISP 712 autoinjector with the WISP cooling module (Waters, Milford, MA, USA) maintained at 4°C, a 250 × 4.5 mm Spherisorb 5-μm ODS-1 reversed-phase column (Keystone Scientific, Bellefonte, PA, USA) maintained at 35°C with an LC-23A column heater and an LC-22 temperature controller, an LC-17A electrochemical

0021-9673/92/$05.00

cell with an MF-1000 dual glassy carbon working electrode in the parallel configuration, and dual LC-4B amperometric detectors set at 0.78 and 0.95 V relative to a RE4 Ag/AgCl reference electrode (all from Bioanalytical Systems, West Lafayette, IN, USA).

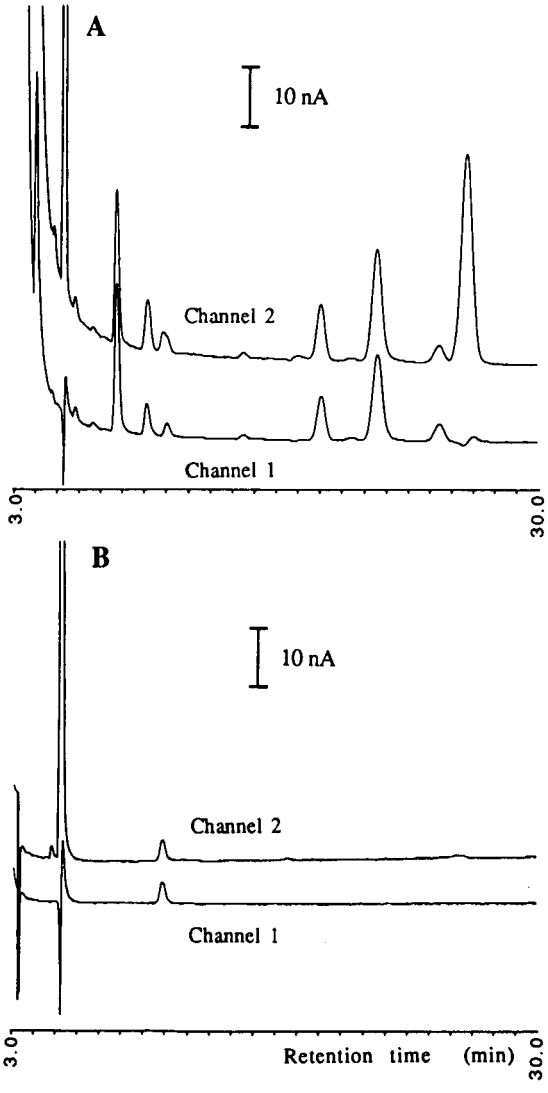

Fig. 1. HPLC chromatograms of a brain sample (A) and standard tyrosine (B) run with channel 1 of the electrochemical detector set to 0.78 V and channel 2 at 0.95 V. Detector sensitivity was set at 10 nA/V. The chromatogram started 3.0 min after sample injection. (A) A 150-ml volume of a perchloric acid extract of mouse brain stem. The retention time (5.5 min) of the sharp negative peak on channel 1 corresponded precisely with that of the large peak in channel 2. (B) A 5-ng amount of L-tyrosine–HCl. The peak at 9.9 min in all traces is the internal standard, N-methyldopamine.

The mobile phase was 0.1 *M* sodium phosphate, 0.1 m*M* EDTA, 0.45 m*M* octanesulfonic acid, pH 3.05, 3.75% acetonitrile, filtered with a 0.45-μm Vericel membrane filter (Gelman Sciences, Ann Arbor, MI, USA) and maintained under helium sparge. Flow-rate was 1.1 ml/min. Data acquisition and integration was with the Rainin (Woburn, MA, USA) Dynamax HPLC system.

RESULTS AND DISCUSSION

Fig. 1A shows the dual-electrode trace of a sample of mouse brain stem. The negative peak at about 5.5 min on channel 1 (set at 0.78 V) clearly corresponded to a large positive peak on channel 2 (set at 0.95 V). Inspection of a large number of runs indicated the consistency of this phenomenon. Therefore, we ran a number of readily oxidizable compounds the presence of which in the brain extracts was suspected. We found that tyrosine ran in approximately the same position relative to the internal standard as the unknown peak in the brain extracts (relative retention time 0.33). A 5-ng injection of tyrosine caused a biphasic peak on channel 1, a sharp negative peak followed by positive one (Fig. 1B). The negative peak exhibited the same relationship to the positive peak in channel 2 as that seen with the unknown peak in brain extracts. The positive component of the channel 1 peak was slightly delayed. Addition of various amounts of L-tyrosine to the brain samples proportionately enlarged both the negative and the positive peaks, such that the compound was indistinguishable from tyrosine.

We next compared the heights of the positive and negative peaks on channel 1 with those of the positive peak on channel 2. Fig. 2A indicates that the height of the positive peak on channel 2 was linearly related to the amount of tyrosine injected and that this amount of sample did not overload either the detector or the integrator. Fig. 2B indicates that there was also a linear relationship between the tyrosine peak on channel 2, and the negative peak on channel 1, suggesting that they were related. Fig. 2C indicates that there was also a linear relationship between the positive and negative components of the peak on channel 1.

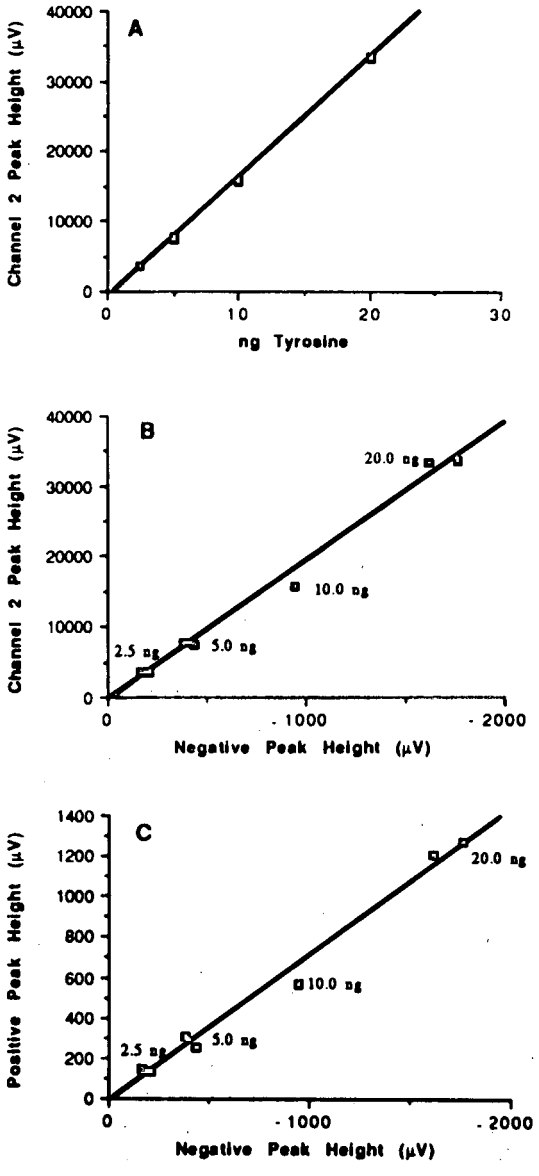

Fig. 2. Analyses of chromatograms of standard tyrosine (2.5–20 ng) run under the conditions of Fig. 1. (A) Peak height on channel 2 *vs.* ng of tyrosine injected; $y = -824.65 + 1711.9x$, $R^2 = 0.999$. (B) Peak height on channel 2 *vs.* negative component of the peak on channel 1; $y = -493.45 + 19.706x$, $R^2 = 0.989$. (C) The height of the positive *vs.* the height of the negative component on channel 1; $y = 17.037 + 0.72531x$, $R^2 = 0.988$.

Several potential artifacts were investigated: reversing the voltages on the two channels of the electrochemical detector, substituting a second set of LC4B electrochemical detectors, substituting both

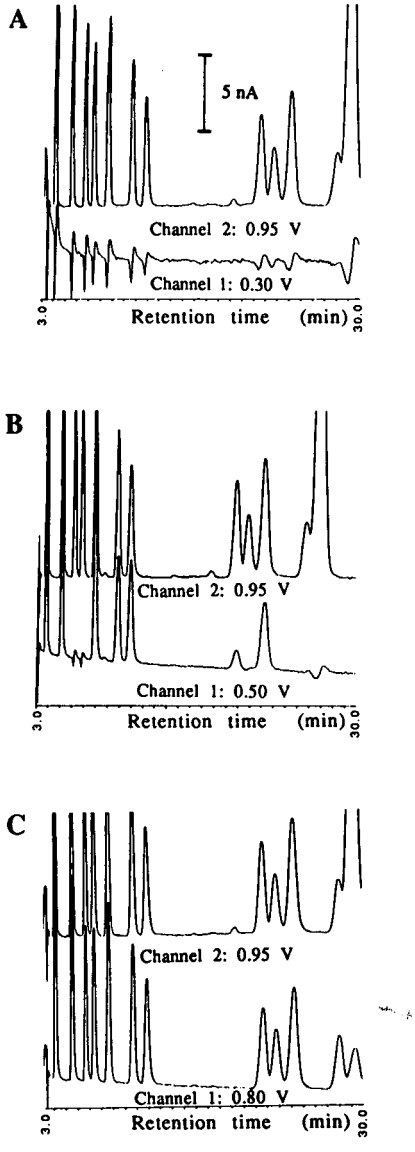

Fig. 3. HPLC chromatograms of mixed standards of catecholamines, indoleamines and related compounds. Peaks in order of elution: norepinephrine, epinephrine, 3-methoxy,4-hydroxyphenylethyleneglycol, (MHPG); normetanephrine (NM), dopamine, 3,4-dihydroxyphenylacetic acid, N-methyldopamine, 5-hydroxyindoleacetic acid, 3-methoxytyramine, 5-hydroxytryptamine, homovanillic acid (HVA), tryptophan (Trp). For all three chromatograms, the channel 2 electrode was set at 0.95 V. (A) Channel 1 at 0.30 V (below the potential necessary to oxidize any of the compounds). (B) Channel 1 at 0.50 V and showing positive peaks for the more easily oxidizable compounds, and baseline disturbances for the others (MHPG, NM, HVA and Trp). (C) Channel 1 at 0.80 V showing positive peaks for all compounds and no baseline disturbances.

working and reference electrodes, turning the MF-1000 dual glassy carbon working electrode so that the two electrodes were in series rather than in parallel [1] and the 0.95 V electrode in both the upstream and downstream positions, and substituting a different integrator. None of these changes significantly altered the presence or the magnitude of the negative peak.

We then tested whether the effect was specific for tyrosine by running our standard mixture of catecholamines, indoleamines and related compounds at different electrode potentials. Fig. 3A shows that when the voltage on the channel 1 electrode was set at 0.30 V, negative peaks appeared corresponding to each of the positive peaks on channel 2. As the voltage on channel 1 was increased, the heights of the negative peaks decreased, and they were replaced by positive peaks. Thus at 0.50 V (Fig. 3B), negative peaks appeared only for 3-methoxy,4-hydroxyphenylethyleneglycol, normetanephrine and homovanillic acid–tryptophan. When channel 1 was set at 0.80 V, close to the potential we normally use on this channel, no negative peaks were observed. The order in which the negative peaks disappeared as the voltage was increased appeared to be related to the order in which positive peaks appeared as the voltage was increased, *i.e.* in the order of their apparent redox potentials. The potential needed to oxidize tyrosine was greater than that needed for any of the other compounds in the standard mixture, except perhaps tryptophan. This may explain why we only observed the phenomenon with tyrosine in our standard runs.

Although the magnitude of the negative peak was related to the magnitude of the positive peak (Fig. 2C), the negative peak appeared with all amounts of sample in the normal range and was not related to overload of the detector or the integrator. Apparently, a negative peak appeared whenever the potential of the electrode was set below the lowest voltage necessary to oxidize the compound (Fig. 3).

We conclude that negative peaks may appear using dual-electrode electrochemical detection whenever the potential of the lower-voltage electrode is set significantly below the redox potential for that compound. The negative peak appears to be an artifact related to the electrical coupling of the two electrode detector channels. We caution chromatographers that it could appear under many different circumstances and is unlikely to be confined to the particular application where we observed it.

ACKNOWLEDGEMENT

This research was supported by grants from the National Institutes of Health (NS27283 and MH46261).

REFERENCES

1 D. A. Roston, R. E. Shoup and P. T. Kissinger, *Anal. Chem.*, 54 (1982) 1417A.
2 A. J. Dunn, *J. Neurochem.*, 51 (1988) 406.

Journal of Chromatography, 596 (1992) 114–117
Elsevier Science Publishers B.V., Amsterdam

CHROM. 23 922

Short Communication

Silica sorbents with one- and two-site attached bacitracin in affinity chromatography

Alexander Yu. Fadeev*, Pavel G. Mingalyov, Sergei M. Staroverov, Elena V. Lunina and Georgii V. Lisichkin

Chemical Department, Moscow State University, Moscow (USSR)

Anatolii V. Gaida and Vladimir A. Monastyrsky

Research Institute of Hematology and Blood Transfusion, Lvov (USSR)

(First received July 24th, 1991; revised manuscript received November 26th, 1991)

ABSTRACT

It was found that the bifunctional oligopeptide bacitracin A can be attached to a silica surface by either one or two amino groups. The latter, in contrast to the former, is active in specific binding of proteinases.

INTRODUCTION

Silicas chemically modified by organic groups are extensively used in sorption, catalysis and chromatography [1]. However, many problems with the chemically bonded compound structure and composition are unresolved because they are very complicated. Particular difficulties arise when polyfunctional molecules are immobilized. Only a few studies have been devoted to detailed investigation of the bonded layer structure of silicas chemically modified by polyfunctional molecules [2–4]. This study deals with the preparation and characterization of affinity sorbents for proteinases on silica containing covalently bound residues of bacitracin A.

The cyclic oligopeptide bacitracin A is well known as an effective ligand in affinity chromatography of proteinases [5–7]. Literature data show that the selectivity of oligopeptide-bonded sorbents depends on both the type of support and the ligand–surface binding character. Often, immobilization of ligands leads to a loss of their affinity [7,8]. Such irreproducibility, in our opinion, may be related to the complicated ligand–surface binding character. Indeed, bacitracin contains two primary amino groups, and can react with a modified silica surface by either one or both of them to yield either a one- or two-site attachment of the ligand (Fig. 1).

EXPERIMENTAL

The silica support Silokhrom S-120 has an average pore diameter at 35–40 nm, a specific surface area of 116 m^2/g and an average particle size of 0.35–0.50 mm.

Epoxy-activated silica was prepared as described elsewhere [9] by treating Silokhrom S-120 with

0021-9673/92/$05.00

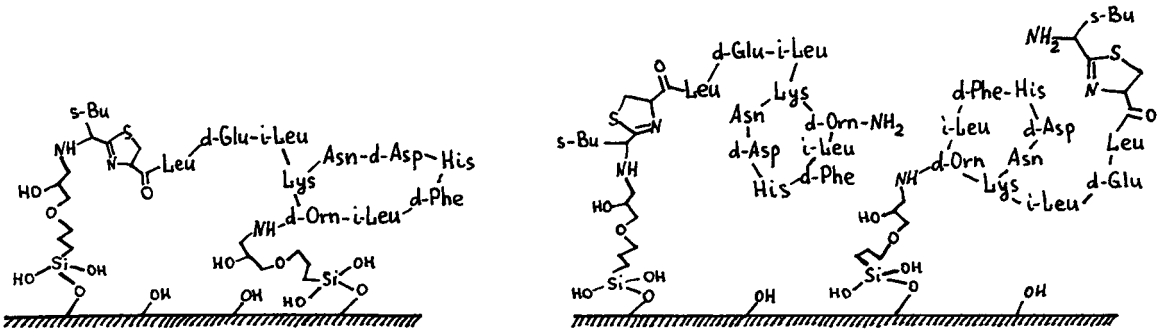

Fig. 1. Schematic representation of one-site and two-site attachment of bacitracin on the silica surface. s-Bu = *sec.*-C_4H_9; i = iso; d = optical isomer of amino acid.

γ-glycidoxypropyltriethoxysilane. Tosyl-activated silica was prepared from epoxy-activated silica by treatment with the tosyl chloride–pyridine following acidic hydrolysis of the epoxy groups [9].

Bacitracin-bonded silicas were synthesized by treating activated silicas with bacitracin (Serva) in aqueous solution (30 mg of bacitracin per gram of activated silica) for 3 days at room temperature. To remove unreacted active groups, the sorbents obtained were treated with an excess of aqueous Tris solution (pH 7.5). The characteristics of the synthesized activated silicas and affinity sorbents are given in Table I.

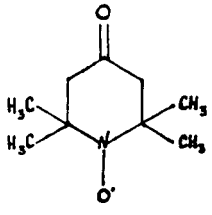

I

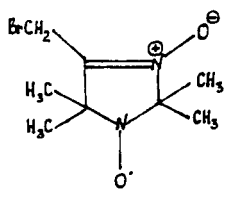

II

In order to introduce the radical **I** to bonded bacitracin molecules, the sorbent was treated with an excess of a boiling pentane solution of radical **I**. To label immobilized bacitracin with radical **II**, the sorbents were treated with a solution of **II** in acetonitrile in the presence of N,N-diisopropylethylamine. The molar amount of bonded **II** was less than the molar amount of bonded bacitracin.

Electronic reflectance spectra were obtained with a Specord M-40 UV–VIS spectrophotometer using a cuvette for solid species. ESR spectra were obtained with a model RE-1307 spectrometer (NPO EZNP, Chernogolovka, USSR). The sorbents were placed in the glass tube and evacuated to 0.01 Torr.

The bacitracin-bonded silica sorbents obtained were used in biospecific binding of human throm-

TABLE I

CHARACTERISTICS OF THE ACTIVATED SUPPORTS AND AFFINITY SORBENTS

Functional groups of the activated silica	Functional groups concentration × 10^6		$L'_{av.}$ [a] (nm)	Bonded bacitracin concentration × 10^6		Share of the one-site-bonded bacitracin (%)	Designation
	mol/g	mol/m²		mol/g	mol/m²		
Epoxy	104	0.9	1.45	6.0	0.05	100	Bc-E
Tosylate	244	2.1	0.96	6.0	0.05	22	Bc-T

[a] Average distance between functional groups of the surface, calculated from $L_{av.} = 1.075/p^{0.5}$, where p is the surface concentration of functional groups [14].

bin, pig pepsin, serine proteinase from *Thermoactinomyces vulgaris* and bovine trypsin. Sorption of proteinases was carried out under dynamic conditions. The column with sorbent was covered with the proteinase solution, which contained 0.5–3.0 mg of enzyme per millilitre of buffer solution [0.075 *M* HCl (pH 2.0) for pepsin and 0.05 *M* Tris–HCl–0.15 *M* NaCl (pH 8.0) for other enzymes].

RESULTS AND DISCUSSION

Typical chromatograms of the proteinases studied obtained on the synthesized sorbents are presented in Fig. 2. The data show that there is no binding of the studied proteinases with the Bc-E sorbent (for designations, see Table I). At the same time, there is quantitative binding of all the studied proteinases on the Bc-T sorbent (Table I). For the proteinases to be eluted one needs to change the eluent to 1 *M* NaCl solution containing 25% of isopropanol.

To investigate whether bacitracin is bound to the surface at one or two sites for the Bc-E and Bc-T sorbents, a method utilizing tetracyanoquinodimethane (TCNQ) was used. It has been shown [10,11] that reaction of TCNQ with bonded primary amino groups gives an adduct with maximum absorbance at 420–430 nm in their electronic reflectance spectra, whereas reaction with secondary or tertiary amino groups gives adducts having maximum absorbance at 340–380, 625–640 and 830–850 nm.

The electronic reflectance spectra of the Bc-E and Bc-T sorbents (before treatment with Tris treated with TCNQ are shown in Fig. 3. The presence of absorption in the 420–430 nm region for the Bc-E

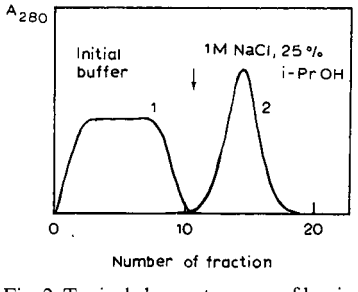

Fig. 2. Typical chromatograms of bovine trypsin on (1) Bc-E and (2) Bc-T sorbents. i-PrOH = Isopropanol.

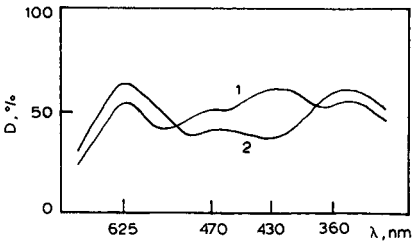

Fig. 3. Electronic reflectance spectra of the TCNQ-treated (1) Bc-E and (2) Bc-T sorbents.

sorbent indicates that one-site binding of bacitracin is predominant, whereas for the Bc-T sorbent the absence of absorption in this region indicates that binding of bacitracin occurs at two sites.

It should be noted that the method mentioned above gives only qualitative information about the ligand–surface binding character. For quantitative data relevant to one- and two-site bacitracin binding, a spin-labelling method was used. Radical **I** is known to react readily with primary amino groups to yield Schiff bases [12], whereas secondary amino groups do not react with ketones under the conditions employed. Hence the molar amount of **I** that will be immobilized on the bacitracin-bonded silica surface will be equal to the molar amount of primary amino groups of attached bacitracin. The amount of **I** that is immobilized could be exactly determined by integrating the ESR spectra.

The results obtained show that for the Bc-E sorbent, all bacitracin molecules are one-site bonded, whereas for the Bc-T sorbent about 80% of the bacitracin molecules are two-site bonded (Table I). In our opinion, this result may be related to a greater average distance between bonded epoxy groups in the epoxy-activated silica compared with the average distance between bonded tosyl groups in the tosyl-activated silica (Table I).

It was of interest to compare the one- and two-site-bonded ligand conformational mobility. To investigate the dynamic behaviour of the bonded bacitracin, the spin-labelling method was applied with radicals **I** and **II** as spin labels. Radical **II** will react with any type of amino group present in the bonded bacitracin. As a measure of the conformational mobility, the correlation time τ_c was chosen. This value

TABLE II

CHARACTERISTICS OF THE ESR SPECTRA OF THE SPIN-LABELLED Bc-E AND Bc-T SORBENTS (MEDIUM: ISOPROPANOL)

Sorbent	Spin label	τ_c ("rapid" form) (s)	Share of "rapid" radicals (%)	τ_c ("slow" form) (s)
Bc-E	I	10^{-11}	100	–
Bc-T	II	10^{-11}	15	$2 \cdot 10^{-9}$

is the reciprocal of the radical rotation frequency [13] and can be easily obtained from ESR spectra.

The τ_c values of the spin-labeled samples are given in Table II. It is clear that for the sample labelled by **I** there are components conforming to only one type of rotational motion in the ESR spectrum. For radical **II**, there is superposition of the components, conforming to two types of motion, "rapid" and "slow". The τ_c of the radical **II** "rapid" form is equal to τ_c of the radical **I** (Table II). Accordingly, we suggest that "rapid" radicals (in the case of radical **II**) are attached to primary amino groups and "slow" radicals are attached to secondary amines. In addition, the share of "rapid" radicals is approximately equal to that expected for the given amount of one-site bonded bacitracin (Tables I and II). Therefore, it is possible to say that one-site-bonded bacitracin is more mobile than two-site bonded bacitracin.

CONCLUSIONS

The cyclic oligopeptide bacitracin A, containing two primary amino groups per molecule, can be chemically attached to a silica surface by either one or both amino groups. The sorbent containing one-site-attached bacitracin does not demonstrate specific binding with proteinases. However, the sorbent containing two-site-attached bacitracin specifically binds the studied proteinases.

REFERENCES

1 G. V. Lisichkin (Editor), *Modifitsirovannye Kremnezemy v Sorbtsii, Katalize i Khromatografii* (*Modified Silica in Sorption, Catalysis and Chromatography*), Khimiya, Moscow, 1986.
2 A. Yu. Fadeev, *Ph.D. Thesis*, Moscow State University, 1990.
3 L. A. Belyakova, I. N. Polonskaya, A. Ye. Pestunovich, N. N. Vlasova and M. G. Voronkov, *Dokl. Akad. Nauk SSSR*, 299 (1988) 643.
4 M. A. Ditzler, G. Doherty, S. Sieber and R. Allston, *Anal. Chim. Acta*, 142 (1982) 305.
5 V. M. Stephanov, G. N. Rudenskaya, A. V. Gaida and A. L. Osterman, *J. Biomed. Biophys. Methods*, 5 (1981) 177.
6 A. V. Gaida, V. A. Monsatyrskii, Yu. V. Magerovskii, S. M. Staroverov and G. V. Lisichkin, *J. Chromatogr.*, 424 (1988) 385.
7 L. A. Osterman, *Khromatografiya Belkov i Nukleinovykh Kislot* (*Chromatography of Proteins and Nucleic Acids*), Moscow, 1985.
8 I. V. Berezin and K. Martinek, *Osnovy Fizicheskoi Khimii Fermentativnogo Kataliza* (*Bases of the Physical Chemistry of Fermentative Catalysis*), Vyshaya Shkola, Moscow, 1977.
9 R. R. Walters, in P. D. G. Dean, W. S. Johnson and F. A. Midle (Editors), *Affinity Chromatography*, IRL Press, Oxford, 1984, Ch. 1.
10 A. Yu. Fadeev, S. M. Staroverov and G. V. Lisichkin, *Zh. Vses. Khim. Ova*, 32 (1987) 349.
11 S. M. Staroverov, A. Yu. Fadeev, V. B. Golubev and G. V. Lisichkin, *Khim. Fiz.*, 7 (1988) 93.
12 K. Murayama, J. Suzuki and S. Amoru, *Jpn. Pat.*, 7100103 (1971).
13 A. L. Buchachenko and A. M. Vasserman, *Stabilnye Radikaly* (*Stable Radicals*), Khimiya, Moscow, 1973, Ch. 11.
14 A. Yu. Fadeev and S. M. Staroverov, *J. Chromatogr.*, 447 (1988) 103.

Journal of Chromatography, 596 (1992) 118–122
Elsevier Science Publishers B.V., Amsterdam

CHROM. 24 013

Short Communication

Counter-current chromatography of lipoproteins with a polymer phase system using the cross-axis synchronous coil planet centrifuge

Yoichi Shibusawa☆ and Yoichiro Ito*

Laboratory of Biophysical Chemistry, National Heart, Lung, and Blood Institute, Building 10, Room 7N322, Bethesda, MD 20892 (USA)

Katsunori Ikewaki☆☆, Daniel J. Rader and H. Bryan Brewer, Jr.

Molecular Disease Branch, National Heart, Lung, and Blood Institute, Building 10, Room 7N117, Bethesda, MD 20892 (USA)

(First received October 1st, 1991; revised manuscript received January 13th, 1992)

ABSTRACT

Lipoproteins were separated by counter-current chromatography using the type-XLL coil planet centrifuge. The separation was performed with a polymer phase system composed of 16% (w/w) polyethylene glycol 1000 and 12.5% (w/w) dibasic potassium phosphate by eluting the lower phase at a flow-rate of 0.5 ml/min. About 5 ml of the sample solution containing approximately 150 mg of a lipoprotein mixture were loaded. High- and low-density lipoproteins were resolved within 12 h. Each component was detected by gel electrophoresis with oil red staining.

INTRODUCTION

The chromatographic separations of lipoproteins into three main classes have been reported using several types of colum packings such as Bio-Gel [1,2], Superose [3], TSK GEL [4–6] and hydroxyapatite [7] whereas, to our knowledge, the fractionation of lipoproteins by counter-current chromatography (CCC) has not been published. Since CCC performs separations without the solid support matrix, adsorptive loss and denaturation of proteins at the liquid–solid interface are minimized [8,9].

This paper describes preliminary results of the lipoprotein separation by utilizing the cross-axis synchronous flow-through coil planet centrifuge (X-axis CPC) [10,11]. Recently, the X-axis CPC has been remarkably improved in terms of retention of the stationary phase. The apparatus is designed to accommodate a pair of small column holders each at a lateral location 7.6 cm from the center of the holder shaft. As reported elsewhere [12], this type-XLL X-axis CPC has a unique capability of retaining large amounts of stationary phase of low-interfacial-tension, viscous solvent systems effectively used for separation of polar compounds.

☆ Visiting Scientist from Tokyo College of Pharmacy, Tokyo, Japan.

☆☆ Visiting Scientist from National Defense Medical College, Saitama, Japan.

0021-9673/92/$05.00

In the present paper the performance of the type-XLL X-axis CPC is evaluated in separation of high-density (HDLs) and low-density (LDLs) lipoproteins from human plasma using an aqueous–aqueous polymer phase system. The partition coefficients (K) of the HDL and LDL fractions were optimized by choosing a polymer phase system composed of 16.0% (w/w) polyethylene glycol (PEG) 1000 and 12.5% (w/w) anhydrous dibasic potassium phosphate in distilled water. The PEG-rich upper phase was introduced into the column and phosphate-rich lower phase was used for elution of the lipoproteins. The separations were performed in a pair of multilayer coils coaxially mounted around the column holders with 3.8 cm hub diameter. The eluted HDL and LDL fractions were confirmed by agarose gel electrophoresis.

EXPERIMENTAL

Apparatus

Fig. 1 shows a photograph of the X-axis CPC used in the present study. The rotary frame of the apparatus holds a pair of horizontal rotary shafts symmetrically at 7.6 cm from the central axis of the centrifuge. Thus, each rotary shaft forms a cross to the vertical axis of the centrifuge as indicated by the name of the apparatus. A spool-shaped coil holder is mounted on each rotary shaft at a lateral position 15 cm away from its midpoint. Each coil holder measures 3.8 cm in hub diameter and 5 cm in width between the pair of flanges. A separation column was mounted on each holder by winding a 2.6 mm I.D. polytetrafluoroethylene (PTFE) tube (Zeus Industrial Products, Raritan, NJ, USA) directly onto the holder hub making multiple layers of left-handed coils. All coiled layers were connected in series by bridging each neighboring layer across the width of the column with a piece of small-bore PTFE transfer tubing (0.7 mm I.D.) using a short sheath of intermediate-size tubing (1.6 mm I.D.) as an adaptor.

Procedure

The aqueous–aqueous polymer phase system was prepared by dissolving 192 g of PEG 1000 (Sigma,

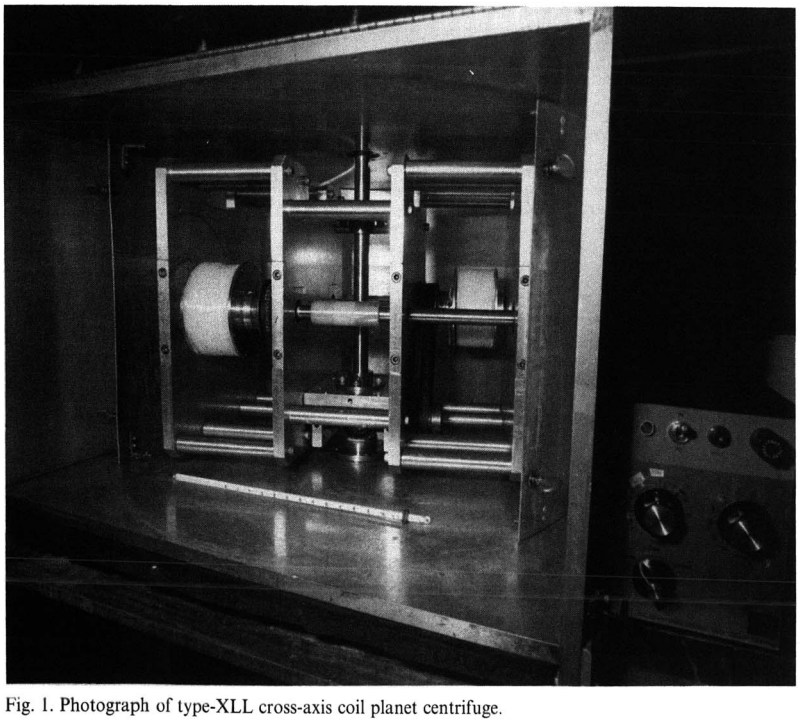

Fig. 1. Photograph of type-XLL cross-axis coil planet centrifuge.

St. Louis, MO, USA) and 150 g of anhydrous dibasic potassium phosphate (J.T. Baker, Phillipsburg, NJ, USA) in 858 g of distilled water. This composition yielded approximately equal volumes of upper and lower phases. The solvent mixture was thoroughly equilibrated in a separatory funnel at room temperature and the two phases were separated shortly before use.

The partition coefficients of the HDL annd LDL fractions and of human serum albumin and α- and γ-globulins (Sigma) were determined in the two-phase solvent system composed of PEG 1000 and dibasic potassium phosphate dissolved at various concentrations in distilled water. Human HDL and LDL fractions were isolated by ultracentrifugation [13]. A lipoprotein suspension, 0.4 ml containing 5.29 mg/ml protein for the HDL fraction and 0.76 mg/ml of protein for the LDL fraction, was partitioned in 3 ml of the aqueous polymer two-phase system (1.5 ml each of the upper and lower phases). An 0.8-ml aliquot of each phase was diluted with 2 ml of distilled water and the absorbance was measured at 280 nm with a Zeiss (Hanover, MD, USA) PM6 spectrophotometer. The partition coefficient values ($K = C_L/C_U$, where C_L and C_U are the solute concentrations in the lower and upper phases, respectively) were calculated by dividing the absorbance in the lower phase with that in the upper phase. The K values of the other plasma proteins were determined by adding about 2 mg of each sample to the solvent system.

The sample solution was prepared by adding 1 g of PEG 1000 and 0.9g of anhydrous dibasic potassium phosphate to the mixture of 3 ml HDL fraction (44.2 mg/ml protein) and 2 ml LDL fraction (11.4 mg/ml protein). Each experiment was initiated by filling the entire column with the stationary upper phase. This was followed by sample injection through the sample port. Then the apparatus was rotated at 750 rpm while the mobile lower phase was pumped into the column at a flow-rate of 0.5 ml/min in the proper elution mode [12]. The effluent from the outlet of the column was continuously monitored with an LKB (Stockholm, Sweden) Uvicord S at 280 nm and then collected into test tubes with an LKB Ultrorac fraction collector. An aliquot of each fraction was diluted with distilled water and the absorbance was determined at 280 nm with the Zeiss PM6 spectrophotometer. The peak fractions (20–50 ml) were placed into dialysis tubing (Spectro/Por, molecular weight cutoff 6000–8000; Spectrum Medical Industries, Los Angeles, CA, USA) which was immersed into an aqueous 30% (w/v) PEG 8000 solution. After 5–6 h dialysis, the fraction was concentrated to 0.2–0.3 ml. The lipoproteins in each fraction were confirmed by 0.6% agarose gel electrophoresis (Helena Labs., Beaumont, TX, USA) [14].

RESULTS AND DISCUSSION

CCC is a liquid–liquid partition method where the separation is based on the difference in the partition coefficient of solutes. For achieving efficient separation of lipoproteins from other serum proteins, it is essential to optimize the partition coefficient of each component by selecting a suitable composition of the polymer phase system. We found that a two-phase solvent system composed of 16% (w/w) PEG 1000 and 12.5% (w/w) dibasic potassium phosphate provides desired K values for the HDL fraction (3.8) and the LDL fraction (1.8) which are substantially different from those of other plasma proteins such as albumin (0.12), α-globulin (0.05) and γ-globulin (0.02).

In order to demonstrate the capability of the X-axis CPC for the separation of lipoproteins from other plasma proteins, a mixture of LDL and HDL fractions from human plasma was eluted using the polymer phase system composed of 16.0% (w/w) PEG 1000 and 12.5% (w/w) dibasic potassium phosphate. As shown in Fig. 2A, the HDL and LDL fractions were eluted from the column in the order of their partition coefficient values and also partially separated from other plasma proteins. The separation was completed within 12 h and the volume of the upper stationary phase retained in the column was 45.0% of the total column capacity (250 ml). Fig. 2B shows the agarose gel electrophoretic patterns of each peak. The lipid moiety of the lipoproteins was stained by oil red 7B. The fractions 43–50 and 60–70, corresponding to center cuts of the first and second peaks in the chromatogram, contained HDLs and LDLs, which migrated to the respective positions in lanes 1 and 2. The third peak in the chromatogram may represent plasma protein, because the fraction showed no lipid staining. No lipoprotein was detected in either the upper or

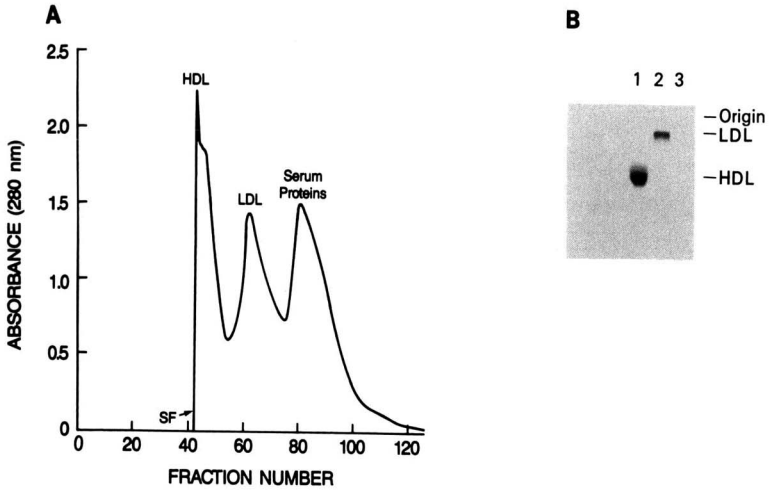

Fig. 2. Separation of lipoproteins by the X-axis CPC (A) and 0.6% agarose gel electrophoretic profile of the fractions (B). Columns: A pair of multilayer coils connected in series, 2.6 mm I.D. and 250 ml capacity; solvent system: 16.0% (w/w) PEG 1000–12.5% (w/w) dibasic potassium phosphate; mobile phase: phosphate-rich lower phase; flow-rate: 0.5 ml/min; revolution speed: 750 rpm; maximum column pressure: 20 p.s.i. SF (A) = Solvent front. Lanes (B): 1 = CCC fractions 43–50; 2 = CCC fractions 60–70; 3 = CCC fractions 80–90.

lower phase collected from the column after the completion of the separation.

From the obtained chromatogram, the partition coefficient of each peak was computed using the classical equation [8,9]. The results yielded 17.8 for the first peak, 1.8 for the second peak, and 0.86 for the third peak. Among these, the K value of the second peak agreed with the measured K value of LDLs while that of the first peak was over four times the measured K value of HDLs (3.8). As mentioned earlier, the lipoprotein sample used for determination of K values was prepared by ultracentrifugation (flotation method). Consequently, the HDL fraction contained some amounts of serum protein while the LDL fraction had much higher purity. Since the K value was determined by measuring UV absorbance, the presence of substantial amounts of serum protein in the HDL fraction resulted in an error in the K value. As of yet, we have no reasonable explanation for the discrepancy in K values between the third peak and serum protein.

The aqueous–aqueous polymer systems are useful for the partition of macromolecules including proteins, nucleic acids, polysaccharides, etc. [15]. However, high viscosity and low interfacial tension between the two phases tends to delay the phase separation, thus requiring long separation times. Although various types of counter-current chromatographs [16–19] have been introduced to overcome this problem, the amount of the stationary phase retained in the column is extremely limited unless the flow-rate of the mobile phase is reduced to a few tenths of a milliliter per minute. The type-XLL X-axis CPC provides a satisfactory retention of the stationary phase at relatively high flow-rates of 0.5–1 ml/min, thus facilitating the use of these solvent systems for the separation of various biopolymers.

ACKNOWLEDGEMENT

The authors wish to thank Dr. Henry M. Fales for his helpful advice and editing of the manuscript.

REFERENCES

1 T. Sata, D. L. Estrich, P. P. S. Wood and L. W. Kinsell, *J. Lipid Res.*, 11 (1970) 331.
2 L. L. Rudel, J. A. Lee, M. D. Morris and J. M. Felts, *Biochem. J.*, 139 (1974) 89.

3 P. M. Clifton, A. M. Mackinnon and P. J. Barter, *J. Chromatogr.*, 414 (1987) 25.
4 I. Hara, M. Okazaki and Y. Ohno, *J. Biochem.*, 87 (1980) 1863.
5 M. Okazaki, Y. Ohno and I. Hara, *J. Biochem.*, 89 (1981) 879.
6. M. Okazaki, K. Shiraishi, Y. Ohno and I. Hara, *J. Chromatogr.*, 223 (1981) 285.
7 U. Matsumoto, H. Nakayama, Y. Shibusawa and T. Niimura, *J. Chromatogr.*, 566 (1991) 67.
8 Y. Ito, in N. B. Mandava and Y. Ito (Editors), *Countercurrent Chromatography: Theory and Practice*, Marcel Dekker, New York, 1988, Ch. 3, pp. 79–442.
9 W. D. Conway, *Countercurrent Chromatography: Principle, Apparatus and Applications*, VCH, Weinheim, 1990.
10 Y. Ito, *Sep. Sci. Tech.*, 22 (1987) 1971.
11 Y. Ito, *Sep. Sci. Tech.*, 22 (1987) 1989.
12 Y. Ito, E. Kitazume, M. Bhatnagar and J. L. Slemp, *J. Chromatogr.*, 538 (1991) 59.
13 R. J. Havel, H. A. Eder and J. H. Bragdon, *J. Clin. Invest.*, 34 (1955) 1345.
14 S. A. Cobb and J. L. Sanders, *Clin. Chem.*, 24 (1978) 1116.
15 P. Å. Albertsson, *Partition of Cell Particles and Macromolecules*, Wiley-Interscience, New York, 1986.
16 Y. Ito, G. T. Bramblett, R. Bhatnagar, M. Huberman, L. Leive, L. M. Cullinane and W. Groves, *Sep. Sci. Tech.*, 18 (1983) 33.
17 W. Murayama, T. Kobayashi, Y. Kosuge, H. Yano, Y. Nunogaki and K. Nunogaki, *J.Chromatogr.*, 239 (1988) 643.
18 Y. Ito and H. Oka, *J. Chromatogr.*, 457 (1988) 393.
19 I. A. Sutherland, D. Heywood-Waddington and Y. Ito, *J. Chromatogr.*, 384 (1987) 197.

Journal of Chromatography, 596 (1992) 123–126
Elsevier Science Publishers B.V., Amsterdam

CHROM. 24 020

Short Communication

Direct high-performance liquid chromatographic separation of enantiomeric peptidoleukotriene antagonists

Ted K. Chen*

Department of Analytical Chemistry, SmithKline Beecham Pharmaceuticals, P.O. Box 1539 (UW2960), King of Prussia, PA 19406-0939 (USA)

Karl F. Erhard

Department of Medicinal Chemistry, SmithKline Beecham Pharmaceuticals, P.O. Box 1539 (UW2960), King of Prussia, PA 19406-0939 (USA)

Thomas Last

Department of Analytical Chemistry, SmithKline Beecham Pharmaceuticals, P.O. Box 1539 (UW2960), King of Prussia, PA 19406-0939 (USA)

Drake S. Eggleston

Department of Physical & Structural Chemistry, SmithKline Beecham Pharmaceuticals, P.O. Box 1539 (UW2960), King of Prussia, PA 19406-0939 (USA)

May Y. K. Ho

Department of Drug Metabolism, SmithKline Beecham Animal Health, West Chester, PA 19381 (USA)

(First received November 26th, 1991; revised manuscript received January 20th, 1992)

ABSTRACT

Enantiomeric peptidoleukotriene antagonists, SK&F *R*-106203 and SK&F *S*-106203 can be effectively separated on a cellulose tris(3,5-dimethylphenylcarbamate) chiral stationary phase. The utility of this chiral high-performance liquid chromatographic method in assigning absolute stereochemistry to SK&F *S*-106203-Z_2, a non-crystalline amorphous compound which is not amenable to single crystal X-ray analysis, is demonstrated by correlation with the absolute configuration determined crystallographically for a second salt form.

0021-9673/92/$05.00

INTRODUCTION

The peptidoleukotrienes (LTs), formed from the metabolism of arachidonic acid by 5'-lipoxygenase, have been the focus of intensive research for their possible roles in the pathophysiology of a variety of disorders [1]. To date, the disease for which the most convincing evidence exists for a primary role of LTs in its etiology is allergic asthma [2]. Most of the pharmacological effects of LTs appear to be receptor-mediated [1] and potent, specific, high-affinity LT receptor antagonists have been identified [3].

SK&F S-106203 {3(*S*)-[2-(carboxyethyl)thio]-3-[2-(8-phenyloctyl)phenyl]propanoic acid} (**1**) is a potent LT receptor antagonist currently in clinical trials. The two enantiomers of this LT receptor antagonist show markedly different pharmacological activities. The *S-enantiomer* (**1**), is more potent than its *R*-enantiomer, as with the close structural analogue, SK&F 104353 {2(*S*)-hydroxy-3(*R*)-[2-(carboxyethyl)-thio]-3-[2-(8-phenyloctyl)phenyl]-propanoic acid} (**2**) which is 100-fold more effective than its enantiomer, SK&F 104373 {2(*R*)-hydroxy-3(*S*)-[(2-carboxyethyl)thio]-3-[2-(8-phenyloctyl)-phenyl]propanoic acid} in competing for $[^3H]LTD_4$ binding sites on guinea pig lung membranes [4], or for inhibiting LTD_4-induced contractions of guinea pig trachea [5].

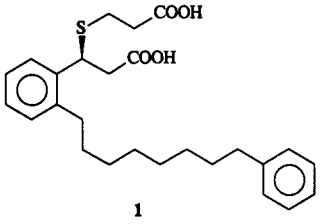

1

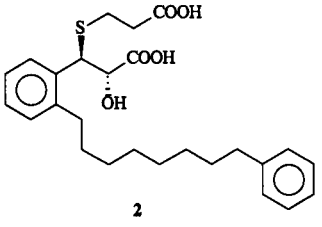

2

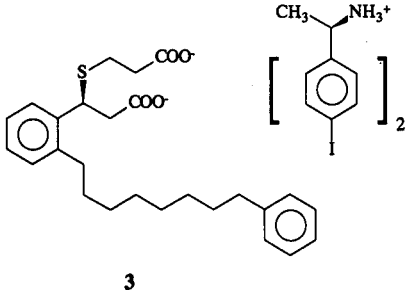

3

In order to address the structural assignment of **1** in regulatory submissions [6], and to evaluate the safety and efficacy of the single *S*-enantiomer (**1**), we required a validated stereospecific assay to determine the enantiomeric purity of the drug substance. In this communication, we describe a direct high-performance liquid chromatographic (HPLC) separation of SK&F 106203 racemates, and report on the utility of this chiral separation in assigning absolute stereochemistry to SK&F *S*-106203-Z_2, the disodium salt of **1** which is a non-crystalline amorphous compound not amenable to single crystal X-ray analysis.

EXPERIMENTAL

Solvents were of HPLC grade. All compounds used in this work were prepared in-house. Each compound was characterized by NMR, MS, IR, impurity profile by HPLC and elemental analysis.

Apparatus

The liquid chromatography system consisted of a Beckman Gold HPLC pump connected to an HP 1050 series autosampler and variable-wavelength UV detector. A 25 × 0.46 cm I.D. Chiralcel OD column (J.T. Baker, USA) with cellulose tris(3,5-dimethylphenylcarbamate) (CDMP) coated on silica gel with particle size of 10 μm was used. Data was acquired and processed using a Beckman CIS-CALS laboratory data system.

Chemicals

Racemic SK&F 106203, SK&F *S*-106203-Z_2, and the bis[(*R*)-4-iodo-α-methylbenzenemethanamine] salt of SK&F *S*-106203 **3** were synthesized in-house.

Free SK&F *S*-106203 diacid was liberated from **3** by dissolving 20 mg of the salt in 0.1 *M* hydrochlor-

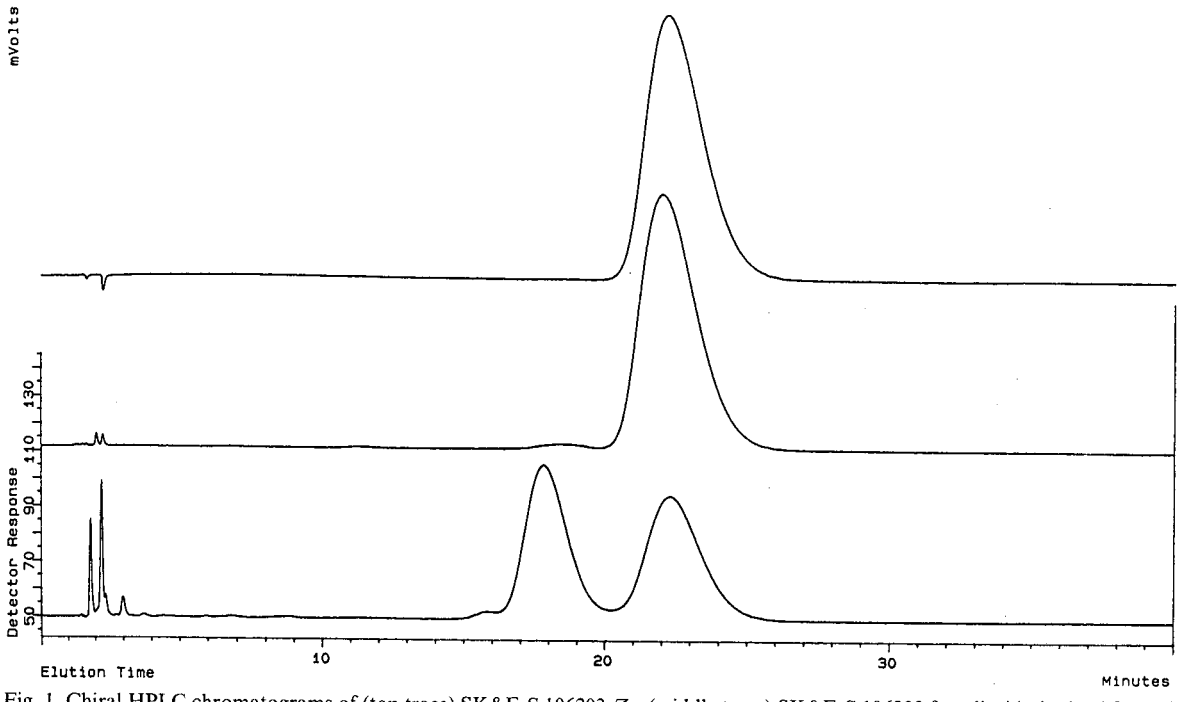

Fig. 1. Chiral HPLC chromatograms of (top trace) SK&F *S*-106203-Z_2, (middle trace) SK&F *S*-106203 free diacid obtained from the bis [(*R*)-4-iodo-α-methylbenzenemethanamine] salt of SK&F *S*-106203 (**3**) and (bottom trace) racemic (*R*/*S*) SK&F 106203.

ic acid, extracting the free diacid into ethyl acetate, drying under a gently flow of clean nitrogen and reconstitution in mobile phase.

Chromatographic conditions

The mobile phase consisted of a mixture of hexane, 2-propanol and trifluoroacetic acid (96.4:3.5:0.1). The flow-rate was 2 ml/min and UV detection was performed at 215 nm. The sample concentration was *ca.* 0.5 mg/ml in mobile phase with a 100-μl injection loop being used. The chromatography was performed at room temperature.

RESULTS AND DISCUSSION

Direct chiral separation on CDMP stationary phase has been reported for atropine, homoatropine, laudeanosine and tetrahydropalmatine [7], aminoglutethimide [8], β-lactams [9], β-adrenergic blocking alcohols [10–13], abscisic acid [14] as well as N-benzyloxycarbonyl amino acids [15]. The formation of diastereomeric solute–chiral stationary phase complexes through both hydrogen-bonding and dipole–dipole interactions is considered important, and the chiral cavity formed by the carbamate at the 6-position with that at the 2- and/or 3-positions on two neighboring glucose units is thought to play a significant role in chiral recognition [16,17]. Although successful for racemic *para*-substituted 2-arylbutyric acid, such as racemic indobufen [18] and unsubstituted 2-phenylpropionic acid, substituted racemic 2-arylpropionic acids, *e.g.*, ibuprofen, ketoprofen, flurbiprofen and tiaprofenic acid could not be resolved on CDMP stationary phase [17]. However, in the present work, good separation was obtained for racemic (*R*/*S*) SK&F 106203, a 2′,3-disubstituted arylpropionic acid. Separation of other racemic leukotriene antagonists, *e.g.*, 3-(((3-(2-(7-chloroquinolin-2-yl)-(*E*)-ethenyl)phenyl)((3-dimethylamino)-3-oxopropyl)thio)methyl)-thio)propionic acid (MK-0571) [19], or the close structural analogue, 5-[3-(2-carboxyethylthio)-1-hydroxypentadeca-3(*E*), 5(*Z*)-dienyl]-phenyl-1-H-tetrazole [20], required either prior derivatization

followed by chiral HPLC or a chiral protein column.

Fig. 1 shows the chiral separation of racemic (*R/S*) SK&F 106203. A stereochemical separation factor of 1.5 was obtained. The enantiomeric elution order was determined by performing the chromatography of the *S*-enantiomer, SK&F *S*-106203 under identical conditions. Thus, the peak that eluted with a lower capacity factor was determined as the *R*-enantiomer and the peak with a higher capacity factor, the *S*-enantiomer. The method is precise [relative standard deviation (R.S.D.) 0.28% for six replicate injections] and is linear over the range 0.1 to 4.0% of SK&F *R*-106203 in SK&F *S*-106203 ($y = 9.7910^{e-3}x - 2.9243^{e-4}$, $r = 0.998$). The limit of detection is 0.1% SK&F *R*-106203 in SK&F *S*-106203.

Since SK&F *S*-106203-Z_2 is an amorphous, non-crystalline solid, determination of its absolute stereochemistry via single crystal X-ray crystallography was not possible. However, the absolute stereochemistry of SK&F *S*-106203-Z_2 can be indirectly confirmed by using chiral HPLC to correlate the chirality of SK&F *S*-106203-Z_2 with the more crystalline bis[(*R*)-4-iodo-α-methylbenzenemethanamine] salt of SK&F S-106203 (**3**)] which was amenable to single crystal X-ray analysis. Fig. 1 shows the chiral HPLC chromatrograms of SK&F *S*-106203-Z_2 (top trace), SK&F *S*-106203 free diacid obtained from **3** (middle trace) and racemic (*R/S*) SK&F 106203 (bottom trace). As shown in Fig. 1, the chiral chromatography indicated the same absolute stereochemistry for both SK&F *S*-106203-Z_2 and **3**.

CONCLUSIONS

Racemic (*R/S*) SK&F 106203, a 2,2-disubstituted arylpropionic acid, can be effectively separated on a chiral tris-(3,5-dimethylphenylcarbamate) stationary phase. The present work also demonstrates the utility of chiral chromatography in assigning absolute stereochemistry to amorphous, non-crystalline forms which may not be amenable to single crystal X-ray analysis.

REFERENCES

1 C. D. Perchonock, T. J. Torphy and S. Mong, *Drugs Future*, 12 (1987) 871.
2 R. D. Krell, *Pulm. Pharmacol.*, 2 (1989) 27.
3 D. W. Snyder and J. H. Fleisch, *Annu. Rev. Pharmacol. Toxicol.*, 29 (1989) 123.
4 S. Mong, H. L. Wu, J. Miller, R. F. Hall, J. G. Gleason and S. T. Crooke, *Mol. Pharmacol.*, 32 (1987) 223.
5 D. W. Hay, R. M. Muccitelli, S. S. Tucker, L. M. Vickery-Clark, K. A. Wilson, J. G. Gleason, R. F. Hall, M. A. Wasserman and T. J. Torphy, *J. Pharmacol Exp. Ther.*, 243 (1987) 474.
6 W. H. De Camp, *Chirality*, 1 (1989) 2.
7 Y. Okamoto, M. Kawashima and K. Hatada, *J. Chromatogr.*, 363 (1986) 173-186.
8 H. Y. Aboul-Enein and M. R. Islam, *Chromatographia*, 30 (1990) 223.
9 Y. Okamoto, T. Senoh, H. Nakane and K. Hatada, *Chirality*, 1 (1989) 216.
10 Y. Okamoto, M. Kawashima, R. Aburatani, K. Hatada, T. Nashiyama and M. Masuda, *Chem. Lett.*, (1986) 1237.
11 H. Aboul-Enein and M. R. Islam, *Chirality*, 1 (1989) 301.
12 H. Aboul-Enein and M. R. Islam, *J. Chromatogr.*, 511 (1990) 109.
13 M. Rudolph, D. Volk and G. Schmiedel, *J. Chromatogr.*, 535 (1990) 263.
14 Y. Okamoto, R. Aburatani and K. Hatada, *J. Chromatogr.*, 488 (1988) 454.
15 Y. Okamoto, R. Aburatani, Y. Kaida and K. Hatada, *Chem. Lett.*, (1988) 1125.
16 I. W. Wainer, R. M. Stiffin and T. Shibata, *J. Chromatogr.*, 411 (1987) 139.
17 Y. Okamoto, R. Aburatani, Y. Kaida, K. Hatada, N. Inotsume and M. Nakano, *Chirality*, 1 (1989) 239.
18 G. Perrone and M. Farina, *J. Chromatogr.*, 520 (1990) 373.
19 D. L. Hughes, J. J. Bergan, J. S. Amato, M. Bhupathy, J. L. Leazer, J.M. McNamara, D. R. Sidler, P. J. Reider and E. J. J. Grabowski, *J. Org. Chem.*, 55 (1990) 6252.
20 D. M. Rackham and G. A. Harvey, *J. Chromatogr.*, 542 (1991) 189.

Journal of Chromatography, 596 (1992) 127–131
Elsevier Science Publishers B.V., Amsterdam

CHROM. 23 988

Short Communication

Studies on photoisomerization of 4,4′-diaminostilbene-2,2′-disulphonic acid for quality assurance by high-performance liquid chromatography☆

Sajid Husain*, R. Narsimha, S. N. Alvi and R. Nageswara Rao

Analytical Chemistry Division, Indian Institute of Chemical Technology, Hyderabad-7 (India)

(First received November 18th, 1991; revised manuscript received December 31st, 1991)

ABSTRACT

Studies on the photoisomerization of 4,4′-diaminostilbene-2,2′-disulphonic acid (DAST) were carried out using controlled light at 350 nm to follow the *E* to *Z* isomerization and to develop a simple and rapid stability-indicating assay using high-performance liquid chromatography. Photoisomers and process impurities, *viz.*, 4,4′-diaminodibenzyl-2,2′-disulphonic acid and 4,4′-dinitrostilbene-2,2′-disulphonic acid, were separated using a reversed-phase C_{18} column, an eluent containing aqueous ammonium sulphate and 2-propanol and a variable-wavelength UV spectrophotometric detector at 245 and 338 nm. The method was used for quality assurance and validated using several lots of industrial samples. The mean recovery of DAST from authentic samples was 99.75 ± 1.17%.

INTRODUCTION

The *E*-isomer of 4,4′-diaminostilbene-2,2′-disulphonic acid (DAST) is an important intermediate in the manufacture of dyes, optical brighteners and fluorescent whitening agents [1]. It is manufactured [2,3] generally by the reduction of 4,4′-dinitrostilbene-2,2′-disulphonic acid (DNST) using iron and hydrochloric acid. During this process, small amounts of 4,4′ diaminodibenzyl-2,2′-disulphonic acid (DADB) are obtained as a by-product [4]. Owing to the similarities in solubility characteristics and chemical properties, it is difficult to separate DADB from DAST. This is considered to be the most objectionable impurity if the material is to be used for manufacturing optical whitening agents. Further, aqueous solutions of DAST undergo rapid isomerization [5] on exposure to light or heat, yielding the *Z*-isomer. Therefore, techniques for the determination of its purity are important in determining not only the yield but also the performance of the final product.

Few methods for the quality assurance of DAST have been reported. Titrimetry and potentiometry [6,7] have been extensively used, but these methods are neither specific nor selective for DAST. Interferences from impurities and isomerization of DAST have made spectrophotometric methods [8–10] unreliable. Ion-exchange chromatography [11] has been applied but failed to separate *E*- and *Z*-isomers. Thin-layer chromatography [12] has been applied to the determination of DAST in river water. Studies on the occupational exposure of fabric brightening agents and the determination of DAST in air by ion-pair high-performance liquid chromatography [13] have been performed. However, it is

☆ IICT Communication No. 2932.

0021-9673/92/$05.00

known [14] that the use of ion-pair reagents such as tetrabutylammonium dihydrogenphosphate and cetyltrimethylammonium bromide in analyses for aromatic sulphonic acids often results in peak splitting and irreproducible peak shapes. However, this could be overcome [15–18] using solutions of inorganic salts as mobile phases.

In this investigation, studies on the photoisomerization of DAST were performed. A simple and rapid HPLC method for the quality assurance of DAST using a μBondapak C_{18} column and an eluent containing 0.15 *M* aqueous ammonium sulphate and 2-propanol at ambient temperature was developed.

EXPERIMENTAL

Materials and reagents

All reagents were of analytical-reagent grade unless stated otherwise. HPLC-grade 2-propanol was obtained from Spectrochem (Bombay, India) and ammonium sulphate from BDH (Poole, UK).

DAST was prepared by heating 4-nitrotoluene-2-sulphonic acid in sodium hydroxide solution until a deep red colour was obtained and then it was reduced with iron and hydrochloric acid [2]. Technical-grade samples of DAST were obtained from Vasant Chemicals (Hyderabad, India).

Studies on the photoisomerization of DAST were carried out by exposing aqueous solutions to UV light at 350 nm using a Raynot photochemical reactor.

Apparatus

A high-performance liquid chromatograph (Shimadzu, Kyoto, Japan) equipped with a 20-μl loop injector and a high-pressure six-way valve was used. A Shimadzu SPD-6AV variable-wavelength UV–VIS spectrophotometric detector was connected after the column. A μBondapak C_{18} (Waters Assoc., Milford, MA, USA) column (300 mm × 3.9 mm I.D.; particle size 10 μm) was used for separation. The chromatograms and the integrated data were recorded with a Chromatopac C-R3A processing system.

Chromatographic conditions

The mobile phase was 0.15 *M* aqueous ammonium sulphate–2-propanol (98:2, v/v). Samples were dissolved in small volumes of 0.02% aqueous sodium hydroxide and diluted with sufficient volumes of the mobile phase. Analyses were carried out under isocratic conditions at a flow-rate of 1 ml/min and a chart speed of 5 mm/min at room temperature (27°C). Chromatograms were recorded at 245 nm for 5 min and then at 338 nm using a wavelength-programmable UV detector.

Analytical procedure

Samples of DAST (10 mg) were dissolved in the mobile phase (25 ml) and a 20-μl volume of each sample was injected and chromatographed under the above conditions. Synthetic mixtures and commercial formulations were analysed under identical conditions. The percentage of DAST was calculated from the peak area.

RESULTS AND DISCUSSION

The HPLC separation of DAST and its impurities is shown in Fig. 1. The peaks were identified by injecting the individual compounds. It can be seen that DAST is resolved not only from the process impurities but also from its *Z*-isomer. 2-Propanol was used as an organic solvent modifier to improve

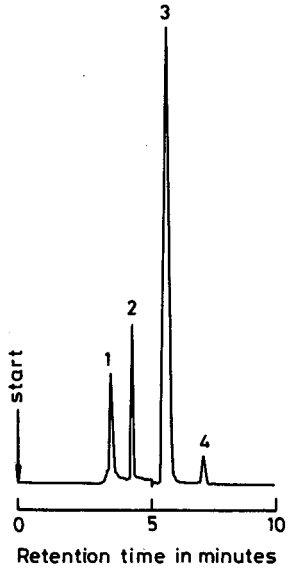

Fig. 1. HPLC profile of a typical mixture containing (1) (*Z*)-DAST (2.0 μg), (2) DADB (2.0 μg), (3) (*E*)-DAST (5.0 μg) and (4) DNST (1.0 μg). For conditions, see text.

TABLE I

RETENTION DATA

Compound	Retention time (min)	Relative retention time	λ_{max} (nm)
(*Z*)-DAST	3.67	0.52	248
DADB	4.63	0.66	245
(*E*)-DAST	5.68	0.81	338
DNST	7.03	1.00	330

TABLE II

DETECTOR RESPONSE FOR DAST AND DADB

Compound	Amount (10^{-7} g)	Area	Relative standard deviation (%)	n^a
DAST	1.57	16 272	1.89	5
DADB	1.02	11 045	2.54	5

[a] Number of measurements.

the separation. Earlier attempts using acetonitrile resulted in overlapping of the peaks of DAST and DADB.

The wavelengths of maximum absorption and retention times, for all the compounds are given in Table I. Two different wavelengths, *i.e.*, 245 nm for 5 min and then 338 nm, were used for detection not only because the detection of each component is ensured but also because good linearity between mass and integral response is obtained. The response data for DAST and DADB are given in Table II. When the UV detector is set at 0.001 a.u.f.s.

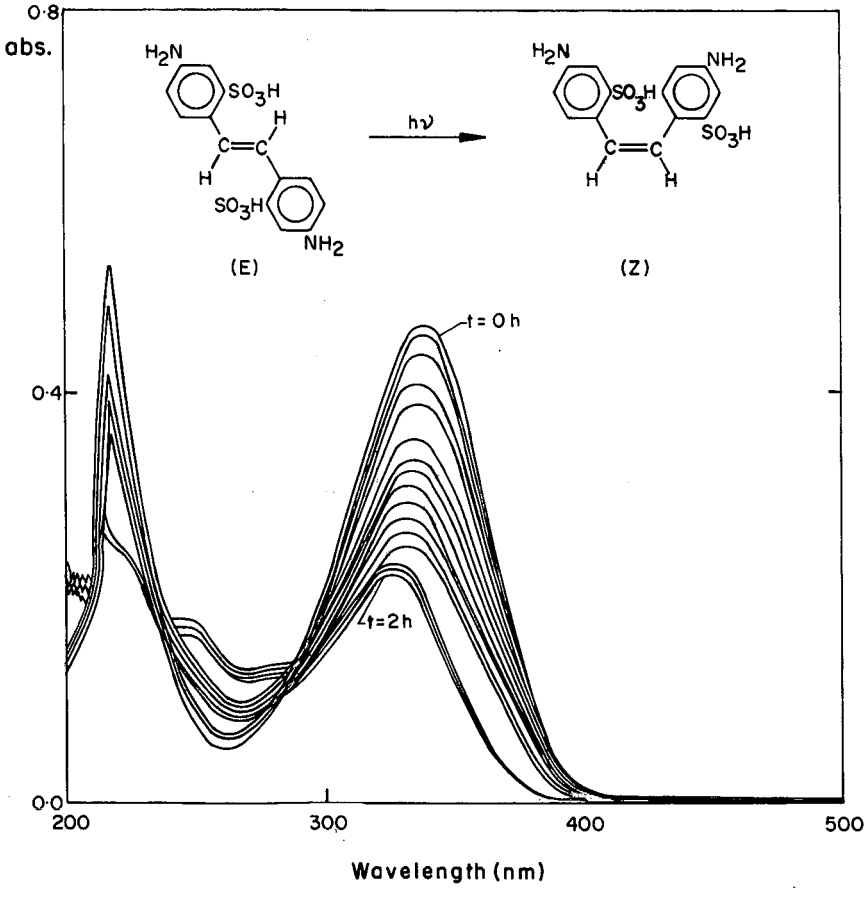

Fig. 2. Changes in the UV absorption spectrum of a $1.4 \cdot 10^{-5}$ *M* solution of DAST in NaOH on exposure to daylight.

TABLE III
UV AND ^{1}H NMR SPECTRAL DATA FOR (*E*)- AND (*Z*)-DAST

DAST	Conformation	λ_{max} (nm)	Chemical shift ppm
Before exposure to light	*E*	338	6.91, 6.93, 7.00, 7.03, 7.66, 7.71, 7.76
After exposure to light	*Z*	245	6.43, 6.46, 6.52, 6.55 6.82, 6.92, 7.03, 7.20, 7.32

TABLE IV
STABILITY-INDICATING ASSAY OF DAST

Irradiation time (h)	(*E*)-DAST (10^{-3} g)	(*Z*)-DAST (10^{-3} g)	Conversion (%)
0.00	5.18	0.00	0.00
0.25	4.37	0.84	15.63
0.50	2.14	3.04	58.68
1.00	1.90	3.28	63.32
2.00	1.83	3.35	64.67

the limit of detection for DAST is 5.0×10^{-9} g with a signal-to-noise ratio of 4.0.

Fig. 2 shows the consecutive changes in the UV absorption spectrum of DAST undergoing photochemical rearrangement. The λ_{max} was gradually shifted from 338 nm to 245 nm. The intensity of absorption also decreased significantly. These changes have been attributed to *E* to *Z* isomerization of DAST using ^{1}H NMR spectrometry. The λ_{max} and ^{1}H NMR chemical shift data of DAST before and after irradiation are given in Table III. The conversion was followed quantitatively by HPLC. The effect of light on the stability of DAST can be seen clearly from the chromatograms shown in Fig. 3. The conversion data are given in Table IV. The half-life of (*E*)-DAST is *ca.* 0.5 h on exposure to sunlight. These results indicate that aqueous solutions of DAST are highly sensitive to light, which affects the assay of DAST significantly.

Standards containing different amounts of DAST were prepared and analysed by HPLC. The measured amounts agreed well with the actual values (within 1.36%). The mean recovery of DAST was 99.75 ± 1.17%. Linear regression analysis of the data yielded the line $y = 0.9839x + 0.0658$ with a correlation coefficient of 0.9986 (y = amount of DAST found; x = amount of DAST taken). Technical and commercial preparations of DAST (Fig. 4) were analysed by the proposed method and the results, given in Table V, are in good agreement with those claimed by the manufacturer (within 1.43%).

It is concluded that the proposed method is suitable not only for the quality assurance of DAST but also to establish the proportion of each isomer resulting from photoisomerization.

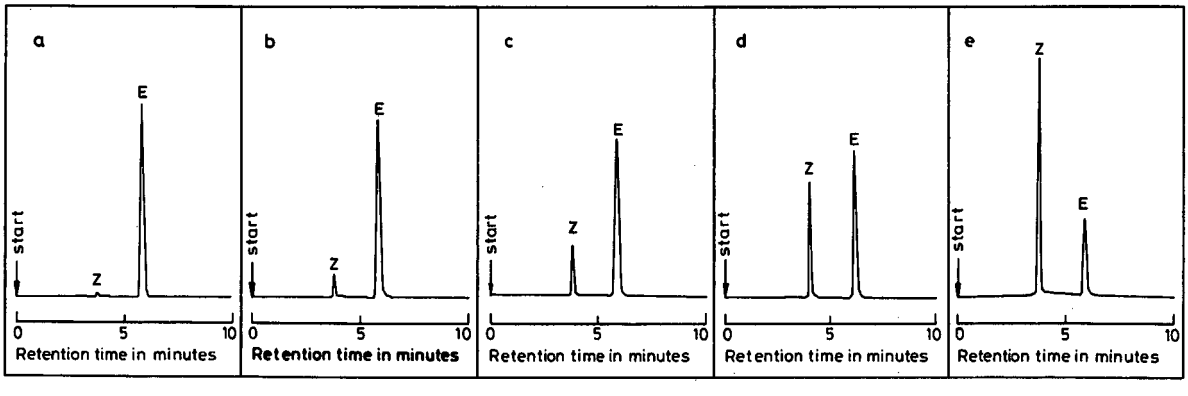

Fig. 3. Chromatograms showing the effect of light on the stability of (*E*)-DAST: (a) before irradiation; (b), (c), (d) and (e) after 0.25, 0.50, 1.00 and 2.00 h of irradation, respectively.

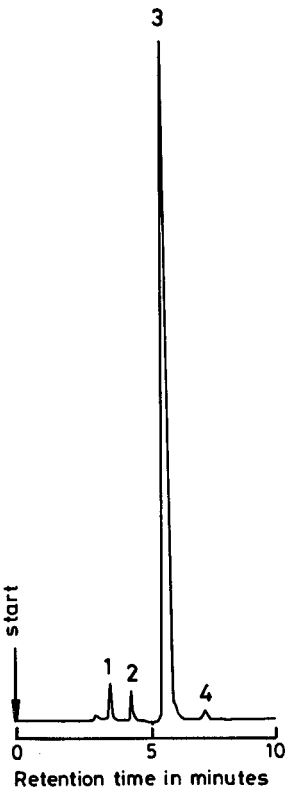

Fig. 4. Chromatogram of a commercial sample of DAST. For identification of peaks, see Fig. 1.

TABLE V

DETERMINATION OF DAST IN TECHNICAL AND COMMERCIAL PREPARATIONS

Code	Mean DAST content (%) ± R.S.D.[a] (%)		Error (%)
	Present[b]	Found[c]	
SD1	65.08 ± 2.17	65.93 ± 1.53	+ 1.31
SD2	98.62 ± 1.50	97.85 ± 1.96	− 0.78
VC1	72.57 ± 1.94	73.61 ± 1.82	+ 1.43
VC2	97.94 ± 1.08	98.58 ± 0.97	+ 0.65

[a] Relative standard deviation ($n = 5$).
[b] By UV spectrometry.
[c] By HPLC.

REFERENCES

1 S. Budavari (Editor), *The Merck Index*, Merck, Rahway, NJ, 11th ed., 1989, p. 95.
2 K. Venkatraman, in L. F. Fieser and M. Fieser (Editors), *The Chemistry of Synthetic Dyes*, Vol. 1, Academic Press, New York, 1952, pp. 628–629.
3 S. Bender, *Chem. Ber.*, 19 (1886) 3234.
4 R. E. Farris, in *Kirk-Othmer, Encyclopedia of Chemical Technology*, Vol. 21, Wiley-Interscience, New York, 1983, pp. 729–746.
5 Y. Yoshio, *Yuki Gosei Kagaku Kyokai Shi*, 30 (1972) 818.
6 *Specifications for 4,4'-Diaminostilbene-2,2'-disulphonic Acid*, IS: 4265, Indian Standards Institution, New Delhi, 1972, pp. 6–7.
7 H. Norwitz and P. N. Keliher, *Talanta*, 35 (1986) 311.
8 B. Stzeke, *Organika*, (1986) 31; *C.A.*, 101 (1984) 203641.
9 J. Barek and I. Danhel, *Collect. Czech. Chem. Commun*, 49 (1984) 2751.
10 E. J. Woodhouse, E. A. Murril, K. M. Stelting, R. D. Brown and C. W. Jameson, in C. W. Jameson and D. B. Walters (Editors), *Problems of Testing Commercial Grade Chemicals*, Butterworth, Boston, 1984, pp. 31–49.
11 D. J. Subach, *J. High Resolut. Chromatogr. Chromatogr. Commun.*, (1979) 633.
12 A. Abe and H. Yoshimi, *Water Res.*, 13 (1979) 1111.
13 S. K. Hammond, T. U. Smith and M. J. Ellenbeckee, *Am. Ind. Hyg. Assoc. J.*, 48 (1987) 117.
14 H. U. Ehmeke, H. Kelker, K. H. Konigs and H. Ullner, *Fresenius' Z. Anal. Chem.*, 294 (1979) 251.
15 P. Jandera and H. Engelhardt, *Chromatographia*, 13 (1980) 18.
16 P. Jandera, J. Churacek and B. Taraba, *J. Chromatogr.*, 262 (1983) 121.
17 A. Zein and M. Baerms, *J. Chromatogr. Sci.*, 27 (1989) 249.
18 C. D. Gaitonde and M. U. Pathak, *J. Chromatogr.*, 514 (1990) 330.

Journal of Chromatography, 596 (1992) 132–137
Elsevier Science Publishers B.V., Amsterdam

CHROM. 23 976

Short Communication

Simultaneous gas chromatographic analysis of heptyl chloride–heptanesulphonyl chloride isomeric mixtures

A. Tazerouti and S. Rahal*

Laboratoire de Synthèse Organique, Institut de Chimie, USTHB, B.P. 32, El Alia, Bab Ezzouar, Algiers (Algeria)

J. Ph. Soumillion

Laboratory of Physical Organic Chemistry, Catholic University of Louvain, Place Louis Pasteur 1, 1348 Louvain la Neuve (Belgium)

(First received July 23rd, 1991; revised manuscript received December 24th, 1991)

ABSTRACT

Gas chromatographic analyses of several sulphonyl chlorides were performed without derivatization. Optimized conditions for this analysis were selected and the results controlled by gas chromatography–mass spectrometry. The results obtained were compared with data reported for gas chromatography using derivatization. This method was extended to the simultaneous analysis of isomeric mixtures of *n*-heptyl chlorides and *n*-heptanesulphonyl chlorides obtained by the photochemical sulphochlorination of *n*-heptane.

INTRODUCTION

Photochemical sulphochlorination with sulphur dioxide–chlorine (eqn. 1) is an efficient method for the functionalization of alkanes to alkanesulphonyl chlorides [1]. This method is used on an industrial scale [2] with higher *n*-alkanes and leads, after alkaline hydrolysis, to secondary alkanesulphonate (SAS) surfactants. However, undesirable alkyl chlorides are simultaneously produced in this process, and the composition of the reaction mixture needs to be controlled at all times.

$$RH \xrightarrow[(R = \text{alkyl})]{h\nu, SO_2, Cl_2} RSO_2Cl + RCl + HCl \quad (1)$$

Gas chromatographic (GC) analysis of the distribution of the sulphochlorinated isomers (C_5–C_{16} saturated hydrocarbons) has been reported [3,4]. Packed silicone grease columns were used and the alkanesulphonyl chlorides were derivatized to the corresponding fluorides, esters or amides. The amides were recommended as being the most convenient derivatives. The distribution of the alkanesulphonyl chloride isomers was established. The chloroalkane content was not measured in the same photolysis mixture. Kirkland [5] had previously reported the GC analysis of sulphonyl chlorides or ester derivatives of the sulphonic acids (or acid salts) of aliphatic, aromatic and alkylaryl hydrocarbons. The chromatographic separation was carried out under reduced pressure in order to prevent sample decomposition. The esterification approach was used in the analysis of toluene–sulphonic acid isomers on short columns made of glass or stainless steel [6]. Aliphatic sulphonyl chlorides were also converted into their *tert.*-butyldimethylsilyl derivatives, in order to avoid their decomposition to alkyl

0021-9673/92/$05.00

halides in the injection port [7,8]. The sulphonamide method seems to be the most convenient when compared with other more time-consuming derivatizations [9].

In the frame of our work, devoted to the study of a new sulphochlorination process, we were interested in optimizing a method for the complete and quantitative analysis of the reaction mixture. In this work, the direct GC analysis of sulphonyl chlorides was studied and conditions were defined for the simultaneous analysis of chlorides and sulphonyl chlorides of *n*-heptane.

EXPERIMENTAL

Sulphochlorination of N-heptane

A 50-ml volume of *n*-heptane was photolysed at 360 nm for 90 min with continuous bubbling of sulphur dioxide and chlorine in a 2:1 flow-rate ratio. Two samples of 5 ml were removed. The first sample, used in the direct GC analysis, was washed with water until neutral. The volume was adjusted to 5 ml with heptane. Standards were added to 100 μl of this sample, making it ready for injection. The second sample was derivatized to the corresponding amide by addition of diethylamine, using the Berthold method [3]. After the reaction, the volume was again adjusted to its initial value, and standards were added to 100 μl of this solution.

Synthesis of 1-heptanesulphonyl chloride

Grignard reagent, prepared from 1 mol of 1-chloroheptane and 1.1 mol of magnesium [10], was added at 0°C to 2 mol of sulphuryl chloride dissolved in *n*-hexane. After hydrolysis with sodium hydrogencarbonate solution, the mixture was extracted with diethyl ether. The organic phase was dried and filtered and the solvent evaporated, yielding a yellow oil. Distillation (80°C, 0.3 mmHg) gave 1-heptanesulphonyl chloride as a colourless oil (65% yield). IR (film): 1360, 1160 cm^{-1}. ^1H NMR ($CC:_4$):δ (ppm) 3.67 (t, 2H), 2.04 (q, 2H), 1.5 (m, 8H), 0.9 (t, 3H). ^{13}C NMR (CCl_4):δ (ppm) 65.5 (C-1), 31.36 (C-2), 28.57, 27.53, 24.31, 22.48 (C-3–C-6), 13.98 (C-7).

Synthesis of cyclohexanesulphonyl chloride

The same method as above yielded cyclohexanesulphonyl chloride as a colourless oil. Boiling point: 134°C (1 mmHg). IR (film): 1370, 1170 cm^{-1}. ^1H NMR (CCl_4):δ (ppm) 3.5 (m, 1H), 2.6–0.87 (m, 1-OH). ^{13}C NMR (CCl_4):δ (ppm) 74.9, 27.2, 24.95, 24.7.

Reagents

Methane-, trichloromethane-, 1-naphthalene-, 2-naphthalene-, 1-octane- and benzenesulphonyl chlorides, 1-chloroheptane and dibenzyl were purchased from Janssen, *p*-toluenesulphonyl chloride, *tert.*-butylbenzene and dimethoxynaphthalene from Aldrich and methoxynaphthalene from Fluka.

Gas chromatography

Analyses were performed using either an Intersmat IGC 120 or Hewlett-Pckard 5730 A gas chromatograph equipped with a flame ionization detector. The injector and detector temperatures were 270°C unless specified otherwise. The carrier gas was nitrogen at a flow-rate of 0.7 ml/min. The columns used were as follows: SE-54, 5% diphenyl–95% dimethylsiloxane bonded DB-5 stationary phase, 30 m × 0.25 mm I.D., 0.25 μm film thickness, fused-quartz capillary column; OV-1, 100% polydimethylsiloxane (gum) bonded DB-1 stationary phase, 30 m × 0.32 mm I.D., 0.25 μm film thickness, fused-quartz capillary column; OV-101, 100% polydimethylsiloxane (fluid) with a bonded DB-1 stationary phase, 25 m × 0.32 mm I.D., 0.25 μm film thickness, fused-quartz capillary column; Carbowax 20M, 100% poly(ethylene glycol) with a bonded DW-Wax stationary phase, 30 m × 0.32 mm I.D., 0.25 μm film thickness, fused-quartz capillary column; and SE-30, 100% methylsilicone (gum) on Chromosorb P AW, 80–100 mesh, 2 m × 2 mm I.D. packed column.

Gas chromatography–mass spectrometry (GC–MS)

A Finnigan MAT TSQ 70 mass spectrometer was used with a Varian 3400 gas chromatograph equipped with an SE-54 column. The conditions were trap current 200 μA, ionizing voltage 70 eV, ion-source temperature 150°C, helium flow-rate 1.5 ml/min, and vacuum 10^{-7} mmHg.

IR and NMR

A Perkin-Elmer Model 457 IR spectrophotometer was used and ^1H and ^{13}C NMR analyses were performed on a Varian Gemini 200 spectrometer at

200 MHz. Tetramethylsilane (TMS) was used as an internal standard.

RESULTS AND DISCUSSION

Direct gas chromatographic analysis of sulphonyl chlorides

Table I gives the retention time of 1-heptanesulphonyl chloride, showing that this isomer may be analysed on several capillary or packed non-polar columns. With the polar Carbowax columns, the sulphonyl chloride was no longer detected. This is probably due to on-column reaction between the sulphonyl chloride and the hydroxyl groups of the stationary phase.

On the other hand, comparison between the retention times given in Table I shows that the direct analysis is time saving when compared with the sulfonamides analysis.

For the remainder of this work, an OV-1 column was used. Direct and isothermal (180°C) GC analysis of the heptanesulphonyl chloride isomers (prepared by photolysis of *n*-heptane with SO_2–Cl_2) shows four peaks in the following order: 8.4 min (isomer 4), 8.6 min (isomer 3), 8.9 min (isomer 2), 9.5 min (isomer 1). Peak attribution for isomer 1 of heptanesulphonyl chloride was established by crossed injection. Analyses were also made after conversion to sulphonamide derivatives (see below). The elution order is well known for these compounds [3]. A quantitative comparison between the direct sulphonyl chloride analysis and indirect sulphonamide analysis allowed us to establish the identity of isomers 2, 3 and 4. GC–MS with electron impact ionization showed for each of the four isomers the fragment at *m/z* 163 corresponding to chlorine loss $[C_7H_{15}SO_2]^+$. The moleculr ions t *m/z* 199 and 201 $[MH]^+$ with the characteristic chlorine isotopic ratio were observed using GC–MS with chemical ionization.

These results show that under the conditions used, heptanesulphonyl chlorides are not decomposed into the corresponding chlorides, as stated by some workers [6,7].

The linearity of the detection was measured with the help of commercial 1-octanesulphonyl chloride and dibenzyl as a standard. No significant deviation from linearity was found in the concentration range examined (the injected solutions had concentrations between 0.1 and $5 \cdot 10^{-4}$ *M*).

The scope of the method was examined with the help of several other aliphatic and aromatic sulphonyl chlorides (Table II).

Sulphonyl chlorides were easily detected with reasonable retention times. However, with benzenesulphonyl chloride, two peaks were observed, with a ratio depending on the injector temperature. The first peak (t_R = 6.8 min) was identified as benzyl chloride, as shown by crossed injection. The second peak was benzenesulphonyl chloride, as demonstrated by GC–MS. Trace amounts of dibenzyl were also found, showing that an increase in the temperature favoured a radical bond rupture, leading to a stable benzyl radical, precursor of benzyl chloride and dibenzyl:

$$C_6H_5CH_2SO_2Cl \xrightarrow{T \text{ increasing}}$$

$$Cl^{\cdot} + C_6H_5CH_2^{\cdot} + SO_2 \begin{cases} \longrightarrow C_6H_5CH_2Cl \\ \longrightarrow (C_6H_5CH_2)_2 \end{cases}$$

TABLE I

RETENTION TIMES OF 1-HEPTANESULPHONYL CHLORIDE AND 1-HEPTANESULPHONIC ACID DIETHYLAMIDE ON VARIOUS STATIONARY PHASES

Compound	Retention time (min)				
	SE-54[a]	SE-30[b]	OV-101[a]	Carbowax 20 M[a]	OV-1[a]
$C_7H_{15}SO_2Cl$	9.8	4	10		9.5
$C_7H_{15}SO_2NEt_2$	15	13	21	35	20

[a] Injector 270°C; column 180°C.
[b] Injector 210°C; column 160°C.

TABLE II

RETENTION TIMES (t_R) OF SULPHONYL CHLORIDES (RSO_2Cl)

Parameter	R						
	CH_3	CCl_3	*p*-Tolyl	1-Naphthyl	2-Naphthyl	Cyclohexyl	Benzyl
t_R (min)	5	6.7	6.7	10.9	11.2	7.7	7.3
T (°C)[a]	130	130	220	220	220	180	140

[a] Column temperature.

These results demonstrate that direct GC analysis is suitable for sulphonyl chlorides. However, compounds leading to stable radicals may decompose in the injector (and not in the column). In that event, the method needs to be standardized, taking into account the decomposition products.

Gas chromatographic identification of N-heptyl chloride isomers

The isomeric mixture of *n*-heptyl chlorides obtained as side-products in the photochemical sulphochlorination of *n*-heptane was analysed by GC using the same column at 70°C. The added standard was *tert.*-butylbenzene (t_R = 19.6 min).

Three peaks were observed on the chromatogram. Isomer 4 (11.5 min), isomers 3 nd 2 (12 min) and isomer 1 (15 min) were identified by crossed injection with authentic samples prepared by an already published method [11].

Comparison between amide derivatization and direct analysis of heptanesulphonyl chlorides

An isomeric mixture of *n*-heptanesulphonyl chlorides prepared by the photochemical sulphochlorination of *n*-heptane was analysed by GC and the results were compared with those obtained after derivatization (Table III).

Considering the results obtained previously with

TABLE III

DISTRIBUTION (%) AND CONCENTRATIONS [C (mmol/l)] OF UNDERIVATIZED AND DERIVATIZED HEPTANESULPHONYL CHLORIDE ISOMERS AT DIFFERENT INJECTION TEMPERATURES

Compounds	Injector temperature (°C)	Isomer 1		Isomer 2		Isomer 3		Isomer 4	
		%	C^a	%	C^a	%	C^a	%	C^a
Heptanesulphonyl chlorides	180	19.5	91	34.9	162	30.2	140	15.4	71
	210	20.2	89	34.1	160	31.1	138	14.6	69
	240	20.2	91	34.5	155	30.8	138	14.5	65
	270	20.4	90	33.9	149	30.9	136	14.8	64
	300	25.1	80	35.5	114	26.4	85	13.0	41
Heptanesulphonyl diethylamides	180	22.9	94	32.8	135	30.3	125	14.0	57
	210	23.9	100	32.6	136	29.6	123	13.9	58
	240	23.6	99	32.4	139	30.1	130	13.9	59
	270	23.2	99	32.9	140	29.8	127	14.1	60
	300	24.3	111	32.8	137	29.3	122	13.6	57
Heptanesulphonyl diethylamides (from ref. 3)	—[b]	20.4–21.7		31.8–33.2		45.4–47.3[c]			

[a] Relative accuracy and reproducibility between measurements made on different samples are ±2%.
[b] Not mentioned.
[c] Isomers 3 and 4 were unresolved.

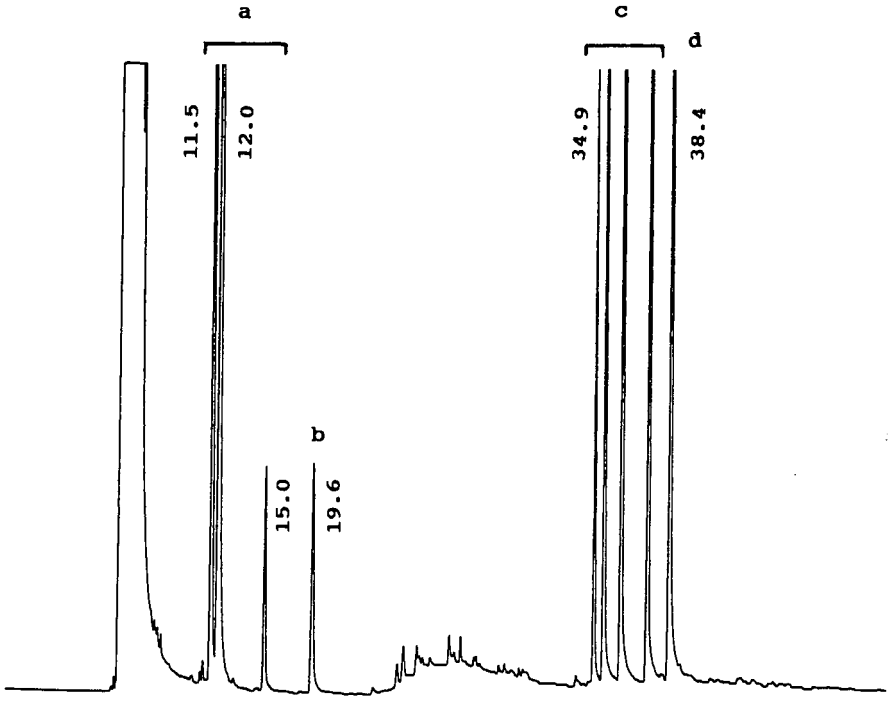

Fig. 1. GC analysis of heptyl chloride–heptanesulphonyl chloride mixtures. (a) Heptyl chloride isomers; (b) *tert.*-butylbenzene as standard; (c) heptanesulphonyl chloride isomers; (d) dimethoxynaphthalene as standard. Numbers at peaks indicate retention times in min.

benzenesulphonyl chloride, the influence of injector temperature was studied in the range 180–300°C. Methoxynaphthalene and dibenzyl were used as added standards for *n*-heptanesulphonyl chlorides and dimethoxynaphthalene for the corresponding *n*-heptanesulphonic acid diethylamides. The same temperature was used in the two analyses (180°C).

The isomeric distribution results given in Table III do not show any influence of the injection temperature for diethylamide derivatives and this was also the case for the sulphonyl chlorides between 180 and 270°C. However, at 300°C, some degradation of sulphonyl chlorides takes place. This degradation is less important for isomer 1 than for the others.

Good agreement with the literature results was observed with injection temperatures between 180 and 270°C. Below 180°C, the *n*-heptanesulphonic acid diethylamides are not efficiently vaporized in the injector. It is worth mentioning that the separation between isomers 3 and 4 of the sulphonamide was not reported in the derivatization method [3].

The GC conditions for the simultaneous analysis of the heptanesulphonyl chlorides and heptyl chlorides are a column temperature of 70°C (isothermal) for 19 min (in order to observe the *n*-heptyl chlorides), then increased at 10°C/min to 180°C, and isothermal detection of *n*-heptanesulphonyl chlorides. The injector temperature is fixed at 270°C. A typical chromatogram is shown in Fig. 1.

The determination of the heptyl chlorides was unaffected by the method used for the sulphonyl chlorides.

As shown by the concentrations obtained with the two methods, the direct analysis of sulphonyl chlorides is in very good agreement with the sulphonamide analysis. The comparison between the two procedures indicates that the direct technique is a valuable, convenient and simple method for a complete analysis of this type of reaction mixture.

ACKNOWLEDGEMENTS

We thank the Algerian Government and the Belgian French Community for financial support and Professor De Hoffmann for GC–MS analyses.

REFERENCES

1 C. F. Reed, *US Pat.*, 2 046 090 (1936).
2 J. M. Quacq and M. Trautmann, *Ann. Chim. (Rome)*, 77 (1987) 245.
3 H. Berthold, C. Braünig, S. Grosse, M. Hampel, F. D. Kopinke, W. Pritzkow and G. Stachowski, *J. Prakt. Chem.*, 318 (1976) 1019.
4 D. Burghardt, M. Hampel, D. Helwig, F. D. Kopinke, H. Niegel, W. Pritzkow, J. Ziegler and J. Zipfel, *J. Prakt. Chem.*, 321 (1979) 279.
5 J. J. Kirkland, *Anal. Chem.*, 32 (1960) 1388.
6 K. M. Baker and G. E. Boyce, *J. Chromatogr.*, 117 (1976) 471.
7 W. T. Smith and J. M. Patterson, *Anal. Chem.*, 62 (1990) 70R.
8 N. G. Lay-Keow and M. Hüppé, *J. Chromatogr.*, 513 (1990) 61.
9 H. Kataoka, T. Okazaki and M. Matika, *J. Chromatogr.*, 473 (1989) 276.
10 S. N. Bhattacharya, C. Earbon and D. R. M. Walton, *J. Chem. Soc. C*, (1968) 1261.
11 W. Pritzkow and K. A. Müller, *Justus Liebigs Ann. Chem.*, 597 (1956) 167.

Journal of Chromatography, 596 (1992) 138–140
Elsevier Science Publishers B.V., Amsterdam

CHROM. 23 980

Short Communication

Direct aqueous injection gas chromatography on a potassium fluoride crystal hydrate-containing sorbent

Determination of volatile organic solvents in the fermentation broth of *Clostridium* strains

Boris M. Polanuer

Institute for Genetics of Industrial Microorganisms, 1 Dorozny pr. 1, Moscow 113545 (Russia)

(First received October 9th, 1991; revised manuscript received December 30th, 1991)

ABSTRACT

For the direct aqueous injection gas chromatographic determination of volatile organic solvents (acetone, ethanol, butanol) in culture spent media of *Clostridium acetobutilicum*, a sorbent which contains potassium fluoride crystal hydrate and a conventional stationary phase, Triton X-305, is used. Analysis is carried out using a stainless-steel column packed with the developed sorbent. The total time of analysis is less than 5 minutes at a column temperature of 65°. The column is stable for at least 1 year.

INTRODUCTION

The biotechnological production of volatile organic solvents, such as acetone, ethanol, isopropanol and butanol, is based on anaerobic fermentation of different strains of *Clostridium* on carbohydrate-rich media, such as molasses, starch, hydrolysed wood, straw and corn. Solvents such as acetone and butanol can be obtained at concentrations up to 20 g/l [1–4].

For the selection of suitable strains of microorganisms and optimization of the fermentation conditions, fast and convenient analytical methods are necessary. Usually gas chromatography (GC) is used for this purpose. The samples are aqueous systems which consist of the different components, including microbial cells, high-molecular-mass compounds such as proteins and nucleic acids, low-molecular-mass, non-volatile compounds including amino acids, sugars and salts and volatile organic compounds such as aldehydes, alcohols and lower carboxylic acids. Quantitative isolation of the volatile fraction from such matrix is complex and time consuming [5–7]. The preferred method of analysis is based on the direct injection of aqueous samples into the chromatographic column. When the direct injection of aqueous solutions is necessary, columns packed with porous polymeric sorbents (*e.g.*, Porapak, Chromosorb "Century" series, Tenax GC) are mostly used [8,9].

The utilization of such sorbents leads to specific problems. Owing to the very high tendency for dispersive interactions, the determination of organic solvents in *Clostridium* spent media on porous poly-

0021-9673/92/$05.00

mers is usually carried out at relatively high temperatures (120–200°C) [1–4]. At these temperatures thermolabile compounds in samples of natural origin may degrade, with the formation of volatile products.

Recently, we demonstrated the possibility of using sorbents that contain potassium fluoride crystal hydrate (m.p. 42°C) and conventional stationary phases for the direct aqueous injection GC of polar compounds such as alcohols and amines [10]. With such columns it was possible to determine polar compounds in aqueous solutions with high sensitivity and under mild analytical conditions.

The aim of this work was to use these sorbents for the rapid analysis of the production of the volatile organic solvents acetone, ethanol and butanol by *Clostridium* strains.

EXPERIMENTAL

A stainless-steel column (200 cm × 3 mm I.D.) with a sorbent which contains 5% of Triton X-305 and 5% of KF · $2H_2O$ (per unit weight of solid support) on Chromosorb W AW (60–80 mesh) was packed and conditioned as described previously [10].

A Varian Model 3600 gas chromatograph with a flame ionization detector was used for the measurements. The incorporated data handling system with a thermal printer–plotter served as a recorder–integrator. The temperatures of the column, injector and detector were 65, 120 and 250°C, respectively, the flow-rate of helium carrier gas was 30 ml/min and the flow-rates of hydrogen and air were 30 and 300 ml/min, respectively.

C_2–C_4 alcohols and acetone were obtained from Merck or Aldrich and used as received. The test compounds were injected as aqueous solutions using 10- and 50-μl microsyringes (Hamilton).

Different strains of *Clostridium* were cultivated as described previously [1]. Samples of fermentation media were centrifuged using a Model 5414S microfuge (Eppendorf). The volume of sample injected was usually 1 μl. Quantification of samples was effected using the external standard method. A standard mixture was injected at the start and end of the working day.

RESULTS AND DISCUSSION

Preliminary experience with model mixtures demonstrated that the developed sorbent is suitable for the separation of volatile compounds produced by *Clostridium* strains. On a 2-m column packed with Triton X-305–KF · $2H_2O$, up to a baseline separation of solutes of interest (acetone, ethanol and butanol) is obtained within 5 min at a column temperature of 65°C, which is about 100°C lower than when polymeric sorbents are used (Fig. 1). A linear dependence between concentration of volatile compounds and peak areas was achieved in the range 0.1–20 g/l. Therefore, it is possible to exclude the stage of sample dilution and inject the samples directly. With this direct injection of supernatants of centrifuged samples, the total time of analysis is decreased and the precision increases.

Fermentation media of different strains of *Clostridium acetobutilicum* were used to test the ability of the studied columns for direct aqueous injection GC of biotechnological samples (Fig. 2). Usually 1-μl samples were injected but it was possible to inject up to 50 μl of fermentation broth without any visible change in the properties of the column.

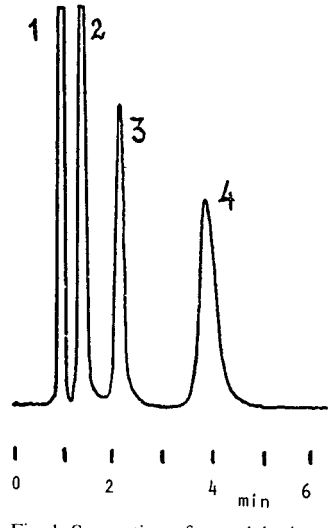

Fig. 1. Separation of a model mixture. Column: 200 cm × 3 mm I.D. stainless steel. Sorbent: 5% Triton X-305 and 5% KF · $2H_2O$ on Chromosorb W AW (60–80 mesh). Column temperature: 65°C. Sample: 1 ml of aqueous solution containing *ca.* 1 g/l of each of the test compounds. Total analysis time: 5 min. Peaks: 1 = acetone; 2 = ethanol; 3 = propanol; 4 = butanol.

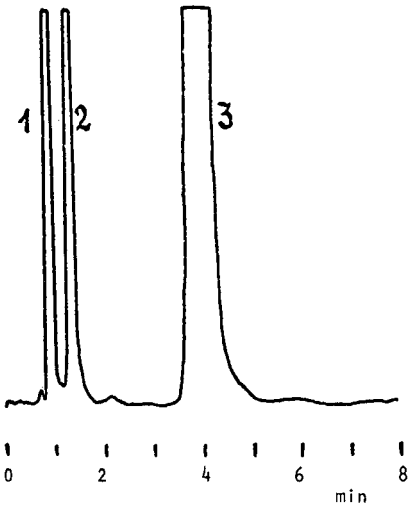

Fig. 2. Analysis of samples of fermentation broth of an industrially used *Clostridium* strain. Column and temperature as in Fig. 1. Sample: 1 ml of fermentation broth. Peaks: 1 = acetone; 2 = ethanol; 3 = butanol.

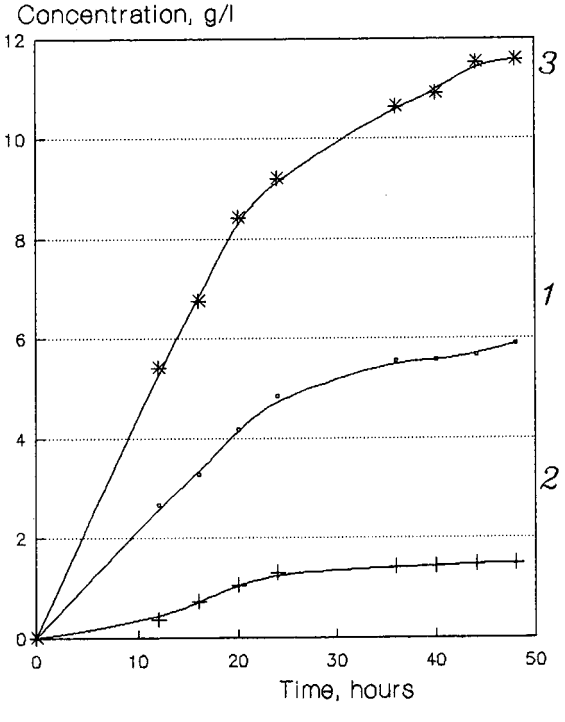

Fig. 3. Kinetics of the accumulation of organic solvents by *Clostridium acetobutilicum*. 1, Acetone; 2, ethanol; 3, butanol.

With this column about 50 strains of *Clostridium* obtained from soil samples were tested. Among these, strains producing up to 10 g/l of butanol were found. This column also was used to test the influence of fermentation conditions on the production of volatile solvents by industrially used strains of *Clostridium acetobutilicum*. The kinetics of the production of organic solvents with these strains were studied (Fig. 3). It was found that tested strains produce most of the organic solvents during first 36 h of fermentation.

During a 1-year period about 500 samples of fermentation media were analysed on a column packed with Triton X-305–KF · $2H_2O$ without visible deterioration of the peak shape or symmetry.

CONCLUSIONS

A direct aqueous injection GC method for polar volatile solvents in fermentation media of *Clostridium* strains using a sorbent which contains potassium fluoride crystal hydrate and Triton X-305 has been developed. A rigid stainless-steel column was used instead a fragile glass column. Considering the possibility of injecting samples of fermentation broth directly and carrying out GC under relatively gentle conditions, this sorbent may be recommended for the determination of volatile polar compounds in different biotechnological samples. Such columns may also be useful in environmental pollution control, forensic studies and other tasks connected with the GC analysis of aqueous samples.

REFERENCES

1 A. S. Afschar and K. Schaller, *J. Biotechnol.*, 18 (1991) 255.
2 G. Godin and J.- M. Engasser, *Appl. Microbiol. Biotechnol.*, 33 (1990) 269.
3 F. Monot, J.-M. Engasser and H. Petitdemange, *Biotechnol. Bioeng. Symp.*, 13 (1983) 207.
4 B. M. Ennis and I. S. Maddox, *Biotechnol. Lett.*, 7 (1985) 601.
5 R. D. McDowall, *J. Chromatogr.*, 492 (1989) 3.
6 I. Liska, J. Krupcik and P. A,. Leclercq, *J. High Resolut. Chromatogr.*, 12 (1989) 577.
7 J. L. Hedrick and L. T. Taylor, *J. High Resolut. Chromatogr.*, 13 (1990) 312.
8 S.-T. Cheung and W.-N. Lin, *J. Chromatogr.*, 414 (1987) 248.
9 J. Peinado, F. J. Lopez-Soriano and J. M. Argiles, *J. Chromatogr.*, 415 (1987) 372.
10 B. M. Polanuer, *Chromatographia*, in press.

Journal of Chromatography, 596 (1992) 141–149
Elsevier Science Publishers B.V., Amsterdam

CHROM. 24 021

Short Communication

DNA electrophoresis in uncross-linked polyacrylamide solution, studied by epifluorescence microscopy

Nicholas J. Rampino* and Andreas Chrambach

Section on Macromolecular Analysis, Laboratory of Theoretical and Physical Biology, National Institute of Child Health and Human Development, National Institutes of Health, Bethesda, MD 20892-0001 (USA)

(First received October 29th, 1991; revised manuscript received January 20th, 1992)

ABSTRACT

Electrophoresis of human DNA fragments (approximately $1 \cdot 10^5$ to $1 \cdot 10^7$ bases in size) was conducted in a solution of uncross-linked polyacrylamide contained in a horizontally mounted 1 mm diameter glass tube and monitored by epifluorescence microscopy. In presence of the polymer, molecular conformations described as a "trailing network" of DNA and a globular "head" were observed. The migration velocity varies between species differing in the size of the "head", and in the ratio between the size of the "head" and that of the trailing "network". By contrast, in pure buffer, λ phage DNA migrates in a globular form at a mobility consistent with known macroscopic data. When electrophoresis in the polymer solution of an agarose plug preparation of *Schizosaccharomyces pombe* DNA was carried out after melting at 70°C, a migrating DNA-agarose complex was observed. The complex was not fully dissociated by an agarose-hydrolyzing enzyme (Gelase).

INTRODUCTION

DNA electrophoresis in capillaries filled with polymer solutions providing size separation based on molecular sieving was pioneered by Heiger *et al.* [1]. Using uncross-linked polyacrylamide solutions, these authors separated DNA fragments up to 23 kilobase pairs (kb) in size. Schwartz *et al.* [2] have separated DNA in this size range by electrophoresis in 0.5% methyl-hydroxypropyl-cellulose. Recently, Boček and Chrambach [3] have demonstrated size separations of DNA up to 12 kb by capillary electrophoresis in solutions of agarose above its gelling temperature. The application of polymer-coated capillaries of narrow diameter to polystyrene separations [4] may also be considered in this context.

Electrophoresis in agarose gel slabs with continuous monitoring by epifluorescence microscopy [5–10] has been applied to the study of individual DNA molecules larger than 50 kb in size. This technique has yielded data concerning the relation between DNA conformation and mobility operative in electrophoretic size separations of DNA [11,12].

The work reported here combines the capillary technique of electrophoresis in polymer solution with the capacity of microscopic monitoring for relating DNA conformation with mobility.

MATERIALS AND METHODS

DNA

Human genomic DNA [MCF7 breast cancer cells (ATCC, Rockville, MD, USA)] were cultured in the Roswell Park Memorial Institute (RPMI) 1640 medium with 10% fetal bovine serum. They were harvested and washed with 100 m*M* NaCl, 50 m*M*

0021-9673/92/$05.00

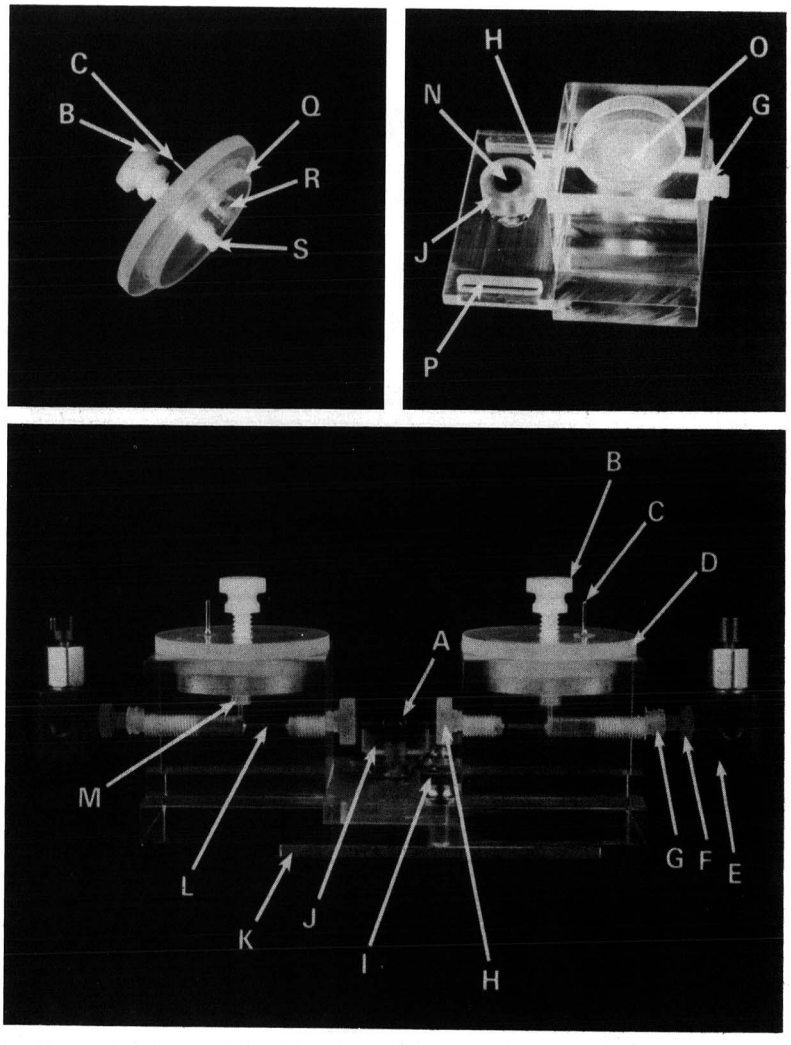

Fig. 1. Horizontal tube electrophoresis apparatus, allowing for the detection of macromolecules by microscopy. A = point of detection for oil immersion microscope objective (oil drop surrounding electrophoresis tube was shown); B = screw regulating the size of the connection between buffer chamber and electrophoresis tube; C = male pin (gold) connector to electrode; D = buffer chamber lid with air-outlet pinhole; E = four-post 90°C Hamilton HV valve; F = male Luer connector; G = female Luer connector; H = perforated screw serving as an electrophoresis tube (I.D. range 1.1 to 0.05 mm) guide; the screw makes contact with a silicone rubber "doughnut" seal; I = lock screw regulating the distance of the buffer chambers from one another; J = support plate of adjustable height for the electrophoresis tube and immersion oil drop; K = base plate (90 mm length) allowing the calipers on the microscope stage to hold the apparatus; L = channel connection between electrophoresis tube and buffer chamber; the length of the electrophoresis tube between the two channel connections and supported at A was 100 mm; M = seat for B; N = light trap blackening below the capillary at the top of J); O = buffer chamber; P = slot allowing distance of the buffer chambers along the base plate; Q = threads on D regulating the electrode position and sealing the buffer chamber; R = platinum electrode; S = sealing flat bottom of B.

Tris–HCl, 3 m*M* $MgCl_2$, pH 8, then in the same buffer containing 0.2% Triton *X*-100. The washed nuclei were incubated in phosphate-buffered saline (PBS), 0.01 *M* disodium ethylenediaminetetraacetate (Na_2, EDTA), 50 μg/ml proteinase K, 1.5 *M* lithium acetate, 0.2% sodium dodecyl sulfate (SDS) at 37°C for 24 h. DNA was extracted 3 times with phenol–chloroform and dialyzed against 0.25 m*M* Na_2EDTA (Fig. 5) or 50 m*M* Tris–Hcl, 10 m*M* Na_2EDTA, 10 m*M* NaCl (Fig. 3). The procedure was a modification of that given by McGhee *et al.* [13].

Yeast chromosomal DNA (*Schizosaccharomyces pombe*) was obtained encased in an agarose plug (melting point 65°C) from Bio-Rad Labs (Richmond, CA, USA). The plug was heated to 70°C for 15–20 min prior to loading and, in the cases indicated, cooled to 40°C and incubated with Gelase (0.5 U/ml, Epicentre Technologies [14]) for 1 h.

Lambda phage DNA was obtained from Gibco BRL (Gaithersburg, MD, USA).

Polyacrylamide

Uncross-linked polyacrylamide was obtained from Polysciences (Warrington, PA, USA) as a 1% (w/v) aqueous solution, weight-average molecular weight $5.5 \cdot 10^6$, intrinsic viscosity 10.835 $(dl/mol)^{1/3}$. The solution was diluted with TBE buffer (89 m*M* Tris, 89 m*M* boric acid, 2 m*M* Na_2EDTA) to yield 0.9% (w/v) polyacrylamide in 0.5 × TBE buffer, pH 8.3. This will be referred to as "PA buffer".

Electrophoresis apparatus

Horizontal glass tube apparatus suitable for microscopic monitoring of electrophoresis at room temperature is depicted in Fig. 1. A central point of detection on the tube connects to the oil immersion microscope objective via an oil drop. The microscopic setup was similar to the one described previously [8]. Applicable tube diameters range from the 1 mm used in this study to 50 μm (not reported here).

Procedure of electrophoresis monitored by microscopy

Tubes (1 mm I.D.) coated internally with linear polyacrylamide [15] were filled with PA buffer, uncoated tubes were filled with 0.5 × TBE buffer, as specified in the figure legends. A solution of human DNA or melted DNA–agarose plug (70°C) was injected by Hamilton syringe (25 μl) into the tube through port G (Fig. 1). Electrophoresis was conducted at 2 V/cm. Fluorescent labeling with 4′,6-diamidino-2-phenylindole (DAPI), microscopic detection, acquisition of the image and measurements were carried out as previously described [8]. Images shown in the figures were photographed as displayed on the computer monitor at high contrast.

RESULTS

Microscopic data on fluorophore-labelled DNA during and prior to electrophoresis in 0.5 × TBE buffer in presence of uncross-linked polyacrylamide

λ Phage DNA, fluorophore labeled by DAPI, when placed into a solution of 0.5 × TBE buffer (in the absence of uncross-linked polyacrylamide) appears spherical under microscopic observation (Fig. 2A). It maintains its spherical appearance and exhibits a constant average velocity during electrophoretic migration (Fig. 2B), consistent with the previous macroscopic findings and the notion of a common charge density for DNA of all sizes [16]. During migration, the globular λ-DNA molecules were not displaced linearly but at variable angles to the orientation of the electrodes. The migrating molecules appear to move into and out of the confocal plane of the microscope in time. Such a mode of migration appears consistent with the previously noted the three-dimensional migration behavior of individual DNA molecules during electrophoresis in agarose gels [11].

By contrast, when electrophoresis of human DNA was carried out in PA buffer, microscopy reveals three types of conformational features, designated descriptively as (a) a globular "head"; (b) an apparent DNA boundary emanating from the "head" and comigrating at 69.5°C (standard error, S.E. = 0.5, $n = 3$) to the direction of electrophoresis; and (c) a comigrating trailing and widely spatially spread DNA trailing "network" (Fig. 3). The area ratio between "head" and "network" varies among the various migrating DNA molecules observed microscopically (Fig. 3A, B). Such DNA trailing "networks", observed in the presence of polyacrylamide, are not observed during electrophoresis either in TBE buffer [17] or in agarose gels [11]. Large

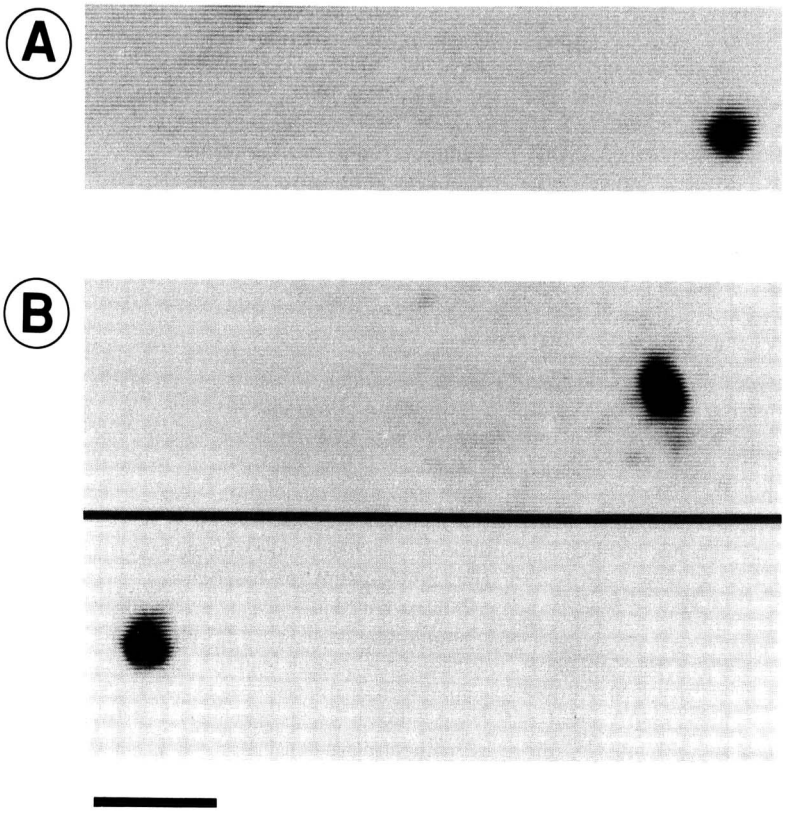

Fig. 2. Epifluorescence videomicrograph of λ-DNA in 0.5 × TBE buffer, uncoated soda glass tube, 1 mm I.D., and at room temperature. (A) Prior to electrophoresis; molecule was positioned at the tube wall and not undergoing Brownian motion; (B) during electrophoresis (from right to left), 1.8 V/cm (minimal field strength for distancing the molecule from the wall), 6 μm/s migration rate. The black line in panel B separates the videomicrograph taken at 0 time (top of the line) from that taken after 4 s of migration (below the line). Fluorescent area 3.0 μm^2. Bar = 5 μm. Anode was on the left.

DNA in buffer is deformed rather than perfectly spherical under the conditions used.

Different migration velocities for human DNA fragments exhibiting condensed "heads" of differing fluorescent areas

When the migration rates of the "head" portions of human DNA exhibiting different fluorescent areas, interpreted as a measure of DNA size (Fig. 2 in ref. 18), were compared, differences in migration rates by a factor of more than two were observed, as well as the absence of a correlation between size and migration rate (Fig. 4).

Microscopic data on fluorophore labeled DNA contained in a solution of 0.25 mM Na_2EDTA and 0.9% uncrosslinked polyacrylamide

When the human DNA configuration was spread by placing the molecule into a milieu of low ionic strength (0.25 m*M* Na_2EDTA), electrophoresis results in progressive deceleration of migration and ultimate arrest. The arrested DNA molecule can exhibit, in addition to a globular "head", a trailing DNA network (Fig. 5A). [The strands in the 2-dimensional projection of the microscope appear linked at a 30° (S.E. = 1.5, $n = 20$) angle, with a node density of 25 per 1000 μm^2]. Arrest can also be ac-

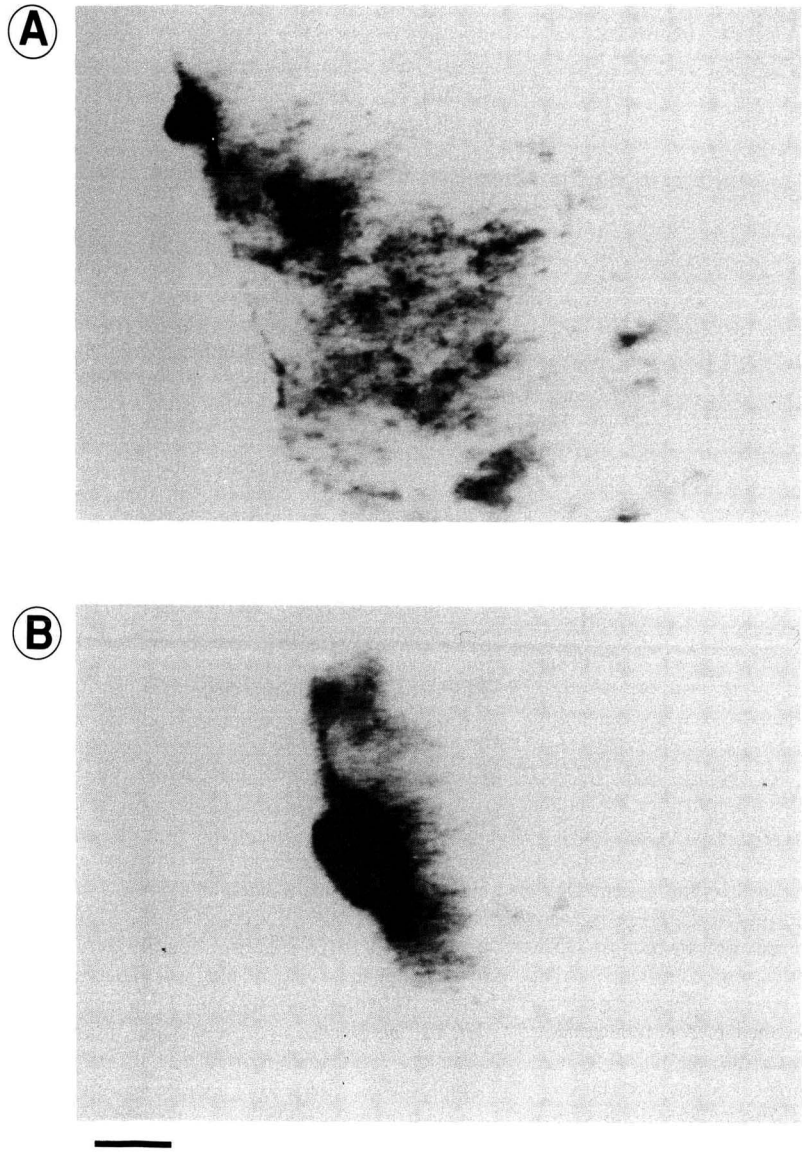

Fig. 3. Epifluorescence videomicrograph of human genomic DNA fragments in 0.5 × TBE buffer containing 0.9% uncross-linked polyacrylamide with a weight-average molecular weight of $5.5 \cdot 10^6$. Tube internally coated with uncross-linked polyacrylamide [15]; field strength 2 V/cm; temperature 24°C. (A) Representative DNA molecule with small "head", large trailing "network", 2.3 μm/s, 45 μm^2. (B) Representative DNA molecule with large "head", small trailing "network", migration rate 3.25 μm/s, 117 μm^2 fluorescent area. Bar = 10 μm. Anode was on the left.

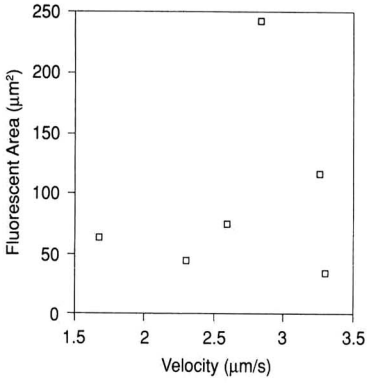

Fig. 4. Differences in migration rate between human genomic DNA fragments during electrophoresis in 0.5 × TBE buffer containing 0.9% uncross-linked polyacrylamide with a weight-average molecular weight of $5.5 \cdot 10^6$. Conditions as in Fig. 3. The migration rate of the DNA depicted in Fig. 3 was plotted in Fig. 4 in addition to four other data points.

companied by nodulated structures connected by branches (Fig. 5B).

An electrophoretically migrating agarose-DNA complex

Fluorophore labeled yeast chromosomal (*S. pombe*) DNA, loaded as an agarose plug [19] melted at 70°C, when monitored by epifluorescence microscopy (Fig. 6A) during electrophoresis in PA-buffer was seen to comigrate with a cluster of agarose molecules which were detected by light microscopy (Fig. 6B). The area occupied by fluorescent DNA (Fig. 6A) is smaller than that of the DNA–agarose complex viewed by light microscopy because DNA is contained within the agarose. The evidence that the comigrating material in Fig. 6B was agarose derives from a comparison of its micrograph with that of an unmelted agarose sample gel plug (Fig. 6C). The DNA-agarose complex was not dissociated by the action of agarase at 40°C under conditions under which free agarose was hydrolyzed.

DISCUSSION

We cannot as yet account in physical terms for the observed "head", emanating boundary and trailing "network" of DNA electrophoresed in a solution of polyacrylamide. It appears likely, however, that an originally globular DNA molecule —as it exists in buffer— through an interaction with the surrounding polyacrylamide was stretched so as to give rise to an open trailing network of DNA strands. The observed angles between DNA strands of the arrested "network" (Fig. 5B) may possibly relate to the intramolecular angles between DNA strands previously measured during agarose gel electrophoresis [11,12]. The observed DNA boundary emanating from the "head" may be due to the progressive resistance of the polymer network, that through its interaction with the traversing DNA gives rise to a steady state between the electrophoretic pull and the polymer induced drag. Since neither the trailing DNA "network" nor the boundary emanating from the "head" is observed during electrophoresis in either TBE buffer or agarose gel, it appears highly likely that the conformational interactions are due to interaction with linear polyacrylamide in solution.

Although physico-chemical evidence exists which suggests a DNA–agarose interaction [20], the migrating agarose–DNA complex has not been previously documented. We infer its existence from viewing the migrating species by light and fluorescent microscopy in alternating fashion. It appears that the migrating agarose complexed to DNA is similar in appearance to the agarose gel plug containing *S. pombe* DNA (Fig. 6C). This suggests that the agarose within the DNA complex was not in solution, and would explain why the DNA in the migrating complex remains localized (Fig. 6A), and why during electrophoresis the embedded DNA was not displaced to the front of the complex. It is also evident from Fig. 6A that a concentration of DNA present in the commercial agarose plug was capable of propelling the entire agarose–DNA complex. The notion that complexed agarose was not in a solubilized state was also supported by the fact that the complex when subjected to agarase (Gelase [14]) in a heat-solubilized bulk phase fails to dissociate or digest its agarose gel moiety. One corollary of these findings was that a previously reported separation of DNA species from a yeast chromosomal (*S. pombe*) agarose plug [21] refers to DNA-agarose complexes, not to DNA. These complexes also appeared white and were resistant to Gelase treatment. It is not as yet known whether any DNA–agarose association is maintained under the conditions of agarose gel electrophoresis.

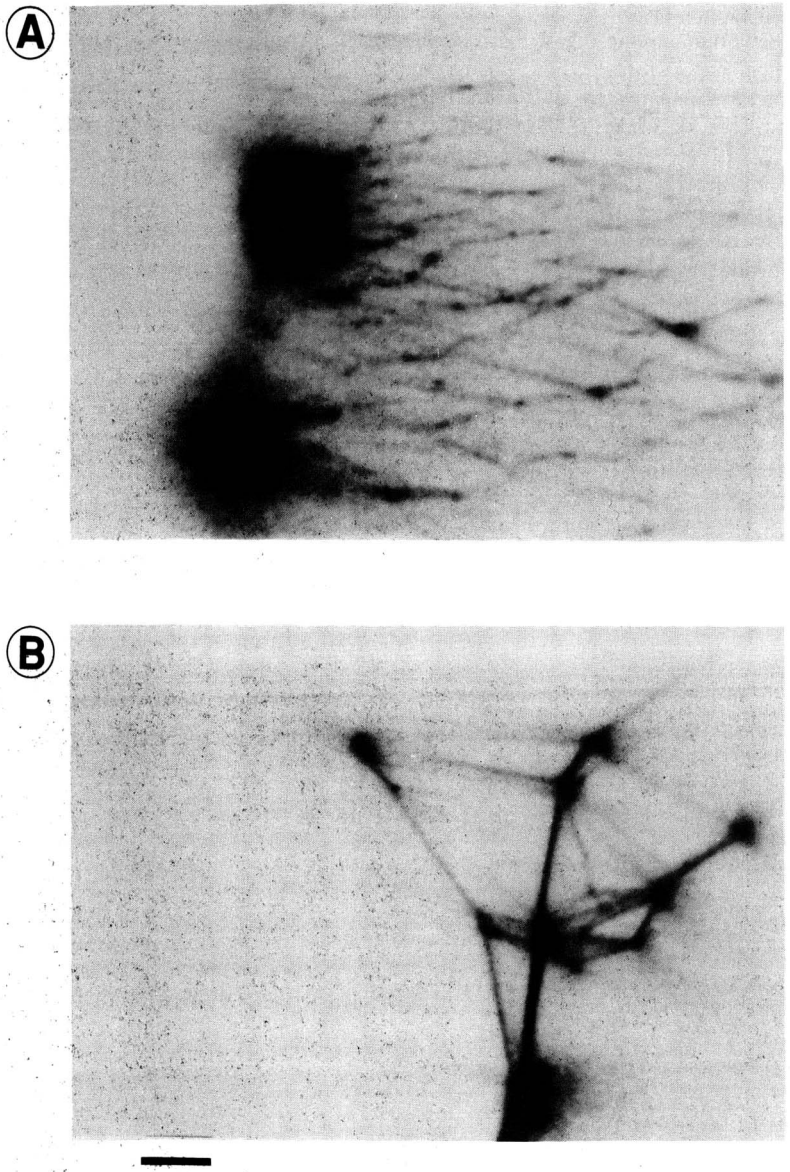

Fig. 5. Two forms of human genomic DNA fragments arrested during electrophoresis in 0.25 m*M* Na_2EDTA containing 0.9% uncross-linked polyacrylamide. The arrested state after 30 s of electrophoresis was depicted. (A) "Heads" with trailing networks; (B) DNA nodes linking the branches of a "network". Bar = 10 μm.

There were limitations regarding the interpretation of the migration velocity (mobility) in Fig. 4. (i) The ordinate in this figure refers to the DNA "head", neglecting the presence and relative size contribution of the trailing network, while the abscissa refers to the velocity of both —the "head" with its comigrating trailing network. Therefore, the measured velocities may equally pertain to a large "head" with small "network" as to a small "head" and a large "network". (ii) The polymer used in this study, polyacrylamide with a weight-average molecular weight of $5.5 \cdot 10^6$, when compared to methyl-hydroxypropyl-cellulose, agarose and polyvinyl alcohol solutions, has been found to be relatively ineffective in retarding the migration of model polystyrene sulfates of diameters comparable to large DNA [22]. It does not seem surprising, therefore, that no dependence of mobility on size could be demonstrated in Fig. 4. Nonetheless, the data indicate that the free mobility of DNA, equal

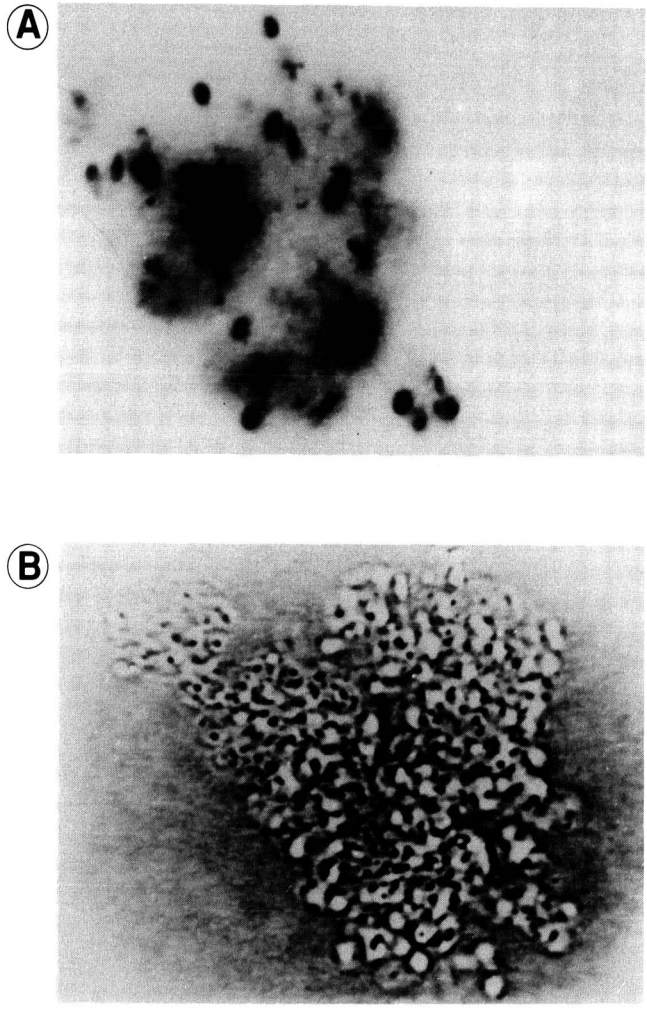

Fig. 6.

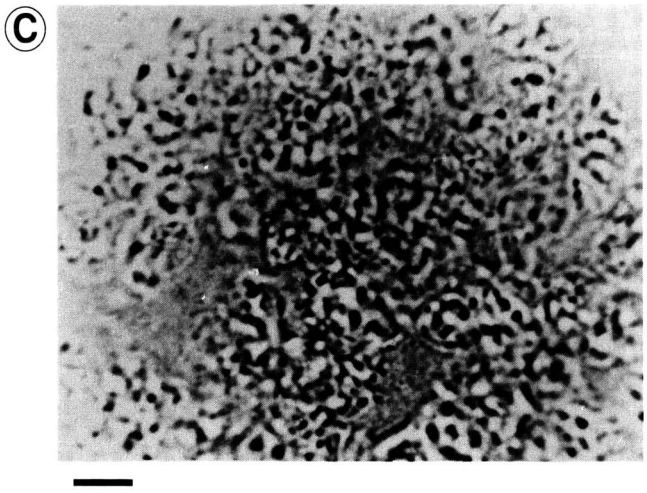

Fig. 6. Light and epifluorescence micrographs of agarose and agarose-DNA complex during electrophoresis in PA buffer. (A) Epifluorescence micrograph of yeast chromosomal DNA (*S. pombe*) loaded as an agarose gel plug (Bio-Rad) melted at 70°C; 2 s migration time; (B) light micrograph of A at 0 s; (C) light micrograph of agarose gel plug of yeast chromosomal DNA (*S. pombe*, Bio-Rad). Bar = 10 μm. Anode was on the left.

for all DNA sizes in the absence of polymer [16], was unequal in the polymer solution. This fact raises the possibility that under other conditions large DNA of different sizes may be separated by electrophoresis in a constant electric field using polymer solutions.

REFERENCES

1 D. N. Heiger, A. S. Cohen and B. L. Karger, *J. Chromatogr.*, 516 (1990) 33.
2 H. E. Schwartz, K. Ulfelder, F. J. Sunzeri, M. P. Busch and R. G. Brownlee, *J. Chromatogr.*, 559 (1991) 267.
3 P. Boček and A. Chrambach, *Electrophoresis*, in press.
4 B. B. VanOrman and G. L. McIntire, *J. MicroColumn Sep.*, 1 (1989) 289.
5 S. B. Smith, P. K. Aldridge and J. B. Callis, *Science (Washington, D.C.)*, 243 (1989) 203.
6 D. C. Schwartz and M. Koval, *Nature (London)*, 338 (1989) 520.
7 N. J. Rampino, *Doctoral Thesis*, University of California at Berkeley, Berkeley, CA, 1989.
8 N. J. Rampino and A. Chrambach, *Anal. Biochem.*, 194 (1991) 278.
9 S. B. Smith, in G. C. Salzman (Editor), *Proceedings of the International Society for Optical Engineering (SPIE), Los Angeles, CA, January 1990*, SPIE, Bellingham, WA, 1990, p. 90.
10 S. Guirreri, E. Rizzarelli, D. Beach and C. Bustamante, *Biochemistry*, 29 (1990) 3396.
11 N. J. Rampino, *Biopolymers*, 31 (1991) 1009.
12 N. J. Rampino and A. Chrambach, *Biopolymers*, 31 (1991) 1297.
13 J. D. McGhee, J. M. Nickol, G. Felsenfeld and D. C. Rau, *Nucl. Acids Res.*, 11 (1983) 4065.
14 *Gelase Worksheet*, Epicentre Technologies, Madison, WI, 1991.
15 S. Hjertén, *J. Chromatogr.*, 347 (1985) 191.
16 B. M. Olivera, P. Baine and N. Davidson, *Biopolymers*, 2 (1964) 245.
17 N. J. Rampino, unpublished results.
18 N. J. Rampino and P. G. Johnston, *Biochem. Biophys. Res. Commun.*, 179 (1991) 1344.
19 D. C. Schwartz and C. R. Cantor, *Cell*, 37 (1984) 67.
20 S. S. Smith, T. E. Gilroy and F. A. Ferrari, *Anal. Biochem.*, 128 (1983) 138.
21 T. Guszczynski and A. Chrambach, *Biochem. Biophys. Res. Commun.*, 179 (1991) 482.
22 A. Chrambach, P. Bocek, T. Guszczynski, M. M. Garner and M. Deml, in B. J. Radola (Editor), *Elektrophorese '91*, Technical University Munich Publ., Munich, 1991, p. 35.

Chromatography, 5th edition

Fundamentals and Applications of Chromatography and Related Differential Migration Methods

edited by **E. Heftmann**, *Orinda, CA, USA*

These are completely new books, organized according to the successful plan of the previous four editions. While avoiding repetition of material covered in the previous editions, the authors have succeeded in presenting a coherent and comprehensive picture of the state of each topic. The books provide beginners as well as experienced researchers with a key to understanding current activities in various separation methods. They will also serve as textbooks for graduate courses in technical, medical and engineering schools as well as all universities offering science courses.

Part A: Fundamentals and Techniques

Journal of Chromatography Library Volume 51A

Part A covers the theory and fundamentals of such methods as column and planar chromatography, countercurrent chromatography, field-flow fractionation, and electrophoresis. Affinity chromatography and supercritical-fluid chromatography are covered for the first time. Each topic is treated by one of the most eminent authorities in the field.

Contents Part A: 1. Theory of chromatography *(L.R. Snyder)*. 2. Countercurrent chromatography *(Y. Ito)*. 3. Planar chromatography *(S. Nyiredy)*. 4. Column liquid chromatography *(H. Poppe)*. 5. Ion-exchange chromatography *(H.F. Walton)*. 6. Size-exclusion chromatography *(L. Hagel and J.-C. Janson)*. 7. Affinity chromatography *(T.M. Phillips)*. 8. Supercritical-fluid chromatography *(P.J. Schoenmakers and L.G.M. Uunk)*. 9. Gas chromatography *(C.F. Poole and S.K. Poole)*. 10. Field-flow fractionation *(J. Janca)*. 11. Electrophoresis *(P.G. Righetti)*. Manufacturers and dealers of chromatography and electrophoresis supplies. Subject Index.

1992 xxxvi + 552 pages
Price: US $ 179.50 / Dfl. 350.00
ISBN 0-444-88236-7

Parts A & B Set
Set price: US $ 333.50 / Dfl. 650.00
ISBN 0-444-88404-1

Part B: Applications

Journal of Chromatography Library Volume 51B

Part B presents various applications of these methods. New developments are reviewed and summarized. Important topics such as environmental analysis and the determination of synthetic polymers and fossil fuels, are covered for the first time.

Contents Part B: 12. Inorganic species *(P.R. Haddad and E. Patsalides)*. 13. Amino acids and peptides *(C.T. Mant, N.E. Zhou and R.S. Hodges)*. 14. Proteins *(F.E. Regnier and K.M. Gooding)*. 15. Lipids *(A. Kuksis)*. 16. Carbohydrates *(S.C. Churms)*. 17. Nucleic acids, their constituents and analogs *(N-I Jang and P.R. Brown)*. 18. Porphyrins *(K. Jacob)*. 19. Phenolic compounds *(J.B. Harborne)*. 20. Drugs *(K. Macek and J. Macek)*. 21. Fossil fuels *(R.P. Philp and F.X. de las Heras)*. 22. Synthetic polymers *(T.H. Moury and T.C. Schunk)*. 23. Pesticides *(J. Sherma)*. 24. Environmental analysis *(K.P. Naikwadi and F.W. Karasek)*. 25. Amines from environmental sources *(H.A.H. Billiet)*. Manufacturers and dealers of chromatography and electrophoresis supplies. Subject Index.

1992 xxxii + 630 pages
Price: US $ 189.50 / Dfl. 370.00
ISBN 0-444-88237-5

Elsevier Science Publishers

P.O. Box 211, 1000 AE Amsterdam, The Netherlands
P.O. Box 882, Madison Square Station, New York, NY 10159, USA

Chemically Modified Surfaces

Proceedings of the Fourth Symposium on Chemically Modified Surfaces, Chadds Ford, PA, July 31-August 2, 1991

edited by **H.A. Mottola,** Oklahoma State University, Stillwater, OK, USA and **J.R. Steinmetz,** Hüls America Inc., Bristol, PA, USA

This volume contains the papers presented at the Fourth Symposium on Chemically Modified Surfaces which provided a forum for the presentation of new scientific contributions on chemical modification of different materials, surface characterization, and ancillary topics. Particular attention was paid to the external structure of solids as addressed by fractal considerations, the expanding field of polymer modification, and the chemical modification of membranes and films. Traditional topics in this series of symposia (e.g. different modification of silica surfaces, especially via silane modification and the different analytical techniques to assess the degree and characteristics of the modification) have also received considerable coverage. The book presents the latest developments on surface modification and characterization of polymers, membranes as well as inorganic surfaces.

1992 xiv + 400 pages
US$ 197.00 / Dfl. 345.00
ISBN 0-444-89305-9

Elsevier Science Publishers
P.O. Box 211, 1000 AE Amsterdam, The Netherlands
P.O. Box 882, Madison Square Station, New York, NY 10159, USA

PUBLICATION SCHEDULE FOR 1992

Journal of Chromatography and *Journal of Chromatography, Biomedical Applications*

MONTH	O 1991	N 1991	D 1991	J	F	M	A	
Journal of Chromatography	585/1	585/2 586/1 586/2 587/1	587/2 588/1 + 2	589/1 + 2 590/1 590/2	591/1 + 2 592/1 + 2 593/1 + 2	594/1 + 2 595/1 + 2	596/1 596/2 597/1 + 2	The publication schedule for further issues will be published later.
Cumulative Indexes, Vols. 551–600								
Bibliography Section						610/1		
Biomedical Applications				573/1 573/2	574/1 574/2	575/1 575/2	576/1	

INFORMATION FOR AUTHORS

(Detailed *Instructions to Authors* were published in Vol. 558, pp. 469–472. A free reprint can be obtained by application to the publisher, Elsevier Science Publishers B.V., P.O. Box 330, 1000 AH Amsterdam, The Netherlands.)

Types of Contributions. The following types of papers are published in the *Journal of Chromatography* and the section on *Biomedical Applications:* Regular research papers (Full-length papers), Review articles and Short Communications. Short Communications are usually descriptions of short investigations, or they can report minor technical improvements of previously published procedures; they reflect the same quality of research as Full-length papers, but should preferably not exceed five printed pages. For Review articles, see inside front cover under Submission of Papers.

Submission. Every paper must be accompanied by a letter from the senior author, stating that he/she is submitting the paper for publication in the *Journal of Chromatography*.

Manuscripts. Manuscripts should be typed in double spacing on consecutively numbered pages of uniform size. The manuscript should be preceded by a sheet of manuscript paper carrying the title of the paper and the name and full postal address of the person to whom the proofs are to be sent. As a rule, papers should be divided into sections, headed by a caption (*e.g.*, Abstract, Introduction, Experimental, Results, Discussion, etc.). All illustrations, photographs, tables, etc., should be on separate sheets.

Introduction. Every paper must have a concise introduction mentioning what has been done before on the topic described, and stating clearly what is new in the paper now submitted.

Abstract. All articles should have an abstract of 50–100 words which clearly and briefly indicates what is new, different and significant.

Illustrations. The figures should be submitted in a form suitable for reproduction, drawn in Indian ink on drawing or tracing paper. Each illustration should have a legend, all the *legends* being typed (with double spacing) together on a *separate sheet.* If structures are given in the text, the original drawings should be supplied. Coloured illustrations are reproduced at the author's expense, the cost being determined by the number of pages and by the number of colours needed. The written permission of the author and publisher must be obtained for the use of any figure already published. Its source must be indicated in the legend.

References. References should be numbered in the order in which they are cited in the text, and listed in numerical sequence on a separate sheet at the end of the article. Please check a recent issue for the layout of the reference list. Abbreviations for the titles of journals should follow the system used by *Chemical Abstracts.* Articles not yet published should be given as "in press" (journal should be specified), "submitted for publication" (journal should be specified), "in preparation" or "personal communication".

Dispatch. Before sending the manuscript to the Editor please check that the envelope contains four copies of the paper complete with references, legends and figures. One of the sets of figures must be the originals suitable for direct reproduction. Please also ensure that permission to publish has been obtained from your institute.

Proofs. One set of proofs will be sent to the author to be carefully checked for printer's errors. Corrections must be restricted to instances in which the proof is at variance with the manuscript. "Extra corrections" will be inserted at the author's expense.

Reprints. Fifty reprints of Full-length papers and Short Communications will be supplied free of charge. Additional reprints can be ordered by the authors. An order form containing price quotations will be sent to the authors together with the proofs of their article.

For Superior Chiral Separation From Analytical To Preparative.

The finest from DAICEL……

Why look beyond DAICEL? We have developed the finest CHIRALCEL, CHIRALPAK and CROWNPAK with up to 17 types of HPLC columns, all providing superior resolution of racemic compounds.

NEW CHIRALPAK AS

● CHIRALPAK AS

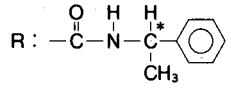

for β-Lactam antibiotics

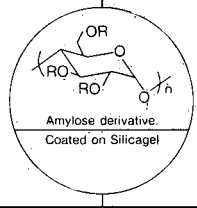

NEW CHIRALPAK AD

● CHIRALPAK AD

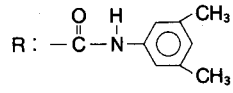

4-Acetoxy-2-azetidine

Eluent : Hexane/Ethanol = 8/2
Flow rate : 1.0mℓ/min
Temperature : r.t.
Detection : UV254nm

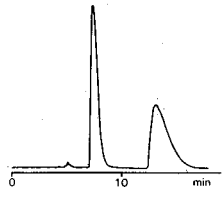

Oxyphencyclimine

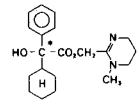

Eluent : Hexane/2-Propanol = 9/1
Flow rate : 1.0mℓ/min
Temperature : r.t.
Detection : UV254nm

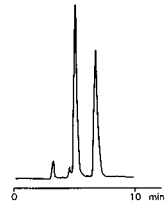

Ofloxacine methyl ester

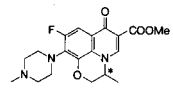

Eluent : Hexane/EtOH = 8/2
Flow rate : 1.2mℓ/min
Temperature : 40°C
Detection : UV254nm

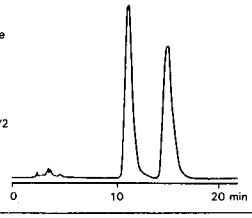

Verapamil

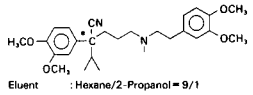

Eluent : Hexane/2-Propanol = 9/1
Flow rate : 1.0mℓ/min
Temperature : r.t.
Detection : UV254nm

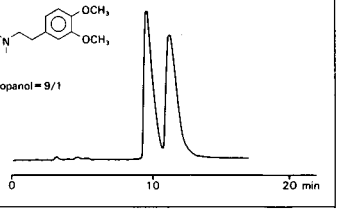

Analytical column 0.46cm × 25cm(10μm)
CHIRALCEL OA
OB
OC
OD
OJ
OF
OG
OK
CHIRALPAK AS
AD

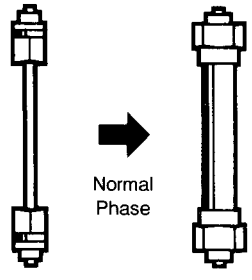

Semi-preparative column 2cm × 25cm(10μm)

You can have Pure enantiomer quickly!!

■Separation Service

- A pure enantiomer separation in the amount of 100g~10kg is now available.
- Please contact us for additional information regarding the manner of use and application of our chiral columns and how to procure our separation service.

DAICEL CHEMICAL INDUSTRIES, LTD.

chiral chemicals division.
8-1, Kasumigaseki 3-chome, Chiyoda-ku, Tokyo 100, Japan Phone: 03 (507) 3151 FAX: 03 (507) 3193

DAICEL(U.S.A.), INC.
Fort Lee Executive Park
Two Executive Drive, Fort Lee,
New Jersey 07024
Phone: (201) 461-4466
FAX: (201) 461-2776

DAICEL(U.S.A.), INC.
23456 Hawthorne Blvd.
Bldg. 5, Suit 130
Torrance, CA 90505
Phone: (213) 791-2030
FAX: (213) 791-2031

DAICEL(EUROPA)GmbH
Oststr. 22
4000 Düsseldorf 1, F.R. Germany
Phone: (211) 369848
Telex: (41) 8588042 DCEL D
FAX: (211) 364429

DAICEL CHEMICAL(ASIA)PTE. LTD.
65 Chulia Street #40-07
OCBC Centre, Singapore 0104
Phone: 5332511
FAX: 5326454